MycoKeys 79: 1–16 (2021)
doi: 10.3897/mycokeys.79.65221
https://mycokeys.pensoft.net

RESEARCH ARTICLE

A peer-reviewed open-access journal
MycoKeys
Launched to accelerate biodiversity research

Micromelanconis kaihuiae gen. et sp. nov., a new diaporthalean fungus from Chinese chestnut branches in southern China

Ning Jiang[1], Qin Yang[2], Xin-Lei Fan[1], Cheng-Ming Tian[1]

1 *The Key Laboratory for Silviculture and Conservation of the Ministry of Education, Beijing Forestry University, Beijing 100083, China* **2** *Forestry Biotechnology Hunan Key Laboratories, Central South University of Forestry and Technology, Changsha 410004, China*

Corresponding author: Cheng-Ming Tian (chengmt@bjfu.edu.cn)

Academic editor: A.K. Gautam | Received 1 March 2021 | Accepted 3 April 2021 | Published 16 April 2021

Citation: Jiang N, Yang Q, Fan X-L, Tian C-M (2021) *Micromelanconis kaihuiae* gen. et sp. nov., a new diaporthalean fungus from Chinese chestnut branches in southern China. MycoKeys 79: 1–16. https://doi.org/10.3897/mycokeys.79.65221

Abstract

Melanconis-like fungi are distributed in several families of Diaporthales, mainly Juglanconidaceae, Melanconidaceae, Melanconiellaceae and Pseudomelanconidaceae. A new *Melanconis*-like genus of Pseudomelanconidaceae was discovered on branches of Chinese chestnut (*Castanea mollissima*) in southern China, which was confirmed by both morphology and phylogenetic analysis of combined ITS, LSU, *tef1a* and *rpb2* sequences. The new genus *Micromelanconis* is characterized by two types of conidia from natural substrate and manual media of PDA, respectively. Conidia from Chinese chestnut branches are pale brown, ellipsoid, multiguttulate, aseptate with hyaline sheath. While conidia from PDA plates are pale brown, long dumbbell-shaped, narrow at the middle and wide at both ends, multiguttulate, aseptate, and also with hyaline sheath. All Pseudomelanconidaceae species were only reported on tree branches in China until now. More interesting taxa may be discovered if detailed surveys on tree-inhabiting fungi are carried out in East Asia in the future.

Keywords

Castanea mollissima, Diaporthales, DNA phylogeny, *Melanconis*, systematics

Introduction

Diaporthales, a species-rich order within Sordariomycetes of Ascomycota, is characterized by perithecia with elongate beaks, often forming within stromatic tissues, deliquescent paraphyses, and asci that have a refractive apical annulus (Barr 1978; Rossman et al. 2007; Senanayake et al. 2017, 2018; Fan et al. 2018a; Jiang et al. 2020a). Species of this order inhabit a variety of substrates, including plants, soil, even living animal tissues (Barr 1978; Castlebury et al. 2002; Sogonov et al. 2008; Yang et al. 2020). Most of them are pathogens associated with plant diseases, and the rest are endophytes in healthy plants or saprobes on dead tissues (Crous et al. 2012a; Chen et al. 2016; Norphanphoun et al. 2018; Jiang et al. 2019d; Xavier et al. 2019; Zhu et al. 2020; Yang et al. 2021). Some diaporthalean fungi cause severe forest diseases, so gained attention in forest pathological studies in recent years. For example, *Cryphonectria parasitica* (Cryphonectriaceae) causes chestnut blight worldwide (Rigling and Prospero 2018; Jiang et al. 2019b); *Cytospora chrysosperma* (Cytosporaceae) causes common polar and willow cankers in China (Fan et al. 2020); *Gnomoniopsis smithogilvyi* (Gnomoniaceae) results in European chestnut fruit rot and branch canker (Shuttleworth et al. 2016; Shuttleworth and Guest 2017; Jiang and Tian 2019; Jiang et al. 2020b).

Diaporthales is well classified into families based on morphological and phylogenetic studies (Voglmayr and Jaklitsch 2014; Norphanphoun et al. 2016; Voglmayr et al. 2017; Fan et al. 2018a; Senanayake et al. 2018; Yang et al. 2018a), and up to 32 families were accepted in the order Diaporthales (Jiang et al. 2021). Specimens can be identified to specific level by morphological characters, such as transversely distoseptate brown conidia of *Coryneum* (Jiang et al. 2018b, 2019c; Senwanna et al. 2018); allantoid ascospores and conidia of *Cytospora* (Fan et al. 2020); two-guttulate fusiform conidia of *Diaporthe*-like taxa (Fan et al. 2018a; Yang et al. 2018a, b); stromatic tissues turning to purple in 3% KOH of Cryphonectriaceae species (Chen et al. 2013, 2018); dark acervular conidiomata with conspicuous central column of *Melanconis*-like taxa (Fan et al. 2016; Jaklitsch and Voglmayr 2020).

Melanconis-like taxa are distributed in several families of Diaporthales, mainly Juglanconidaceae, Melanconidaceae, Melanconiellaceae and Pseudomelanconidaceae, which are four morphologically similar clades in distinct phylogenetic clades within this order (Fan et al. 2018b). Species of these four families are usually discovered on branches of Betulaceae, Juglandaceae and Fagaceae, but they are not strong pathogens (Wehmeyer 1937; Du et al. 2017; Voglmayr et al. 2019).

Castanea, commonly known as chestnut trees, is a worldwide genus containing several economic species. Chinese chestnut (*C. mollissima*), is widely cultivated in most of the provinces in China. Previous studies have revealed that seven families (Coryneaceae, Cryphonectriaceae, Cytosporaceae, Diaporthaceae, Erythrogloeaceae, Gnomoniaceae and Pseudomelanconidaceae) of Diaporthales have been reported on branches of *Castanea*. *Coryneum castaneicola*, *C. gigasporum* and *C. suttonii* of Coryneaceae were reported on dead and diseased *Castanea mollissima* branches (Jiang et al. 2018b). *Aurantiosacculus castaneae*, *Cryphonectria neoparasitica*, *C. parasitica* and

Endothia chinensis of Cryphonectriaceae were confirmed to be *Castanea mollissima* canker pathogens (Jiang et al. 2019b). *Cytospora ceratospermopsis*, *C. kuanchengensis*, *C. leucostoma*, *C. myrtagena*, *C. schulzeri* and *C. xinglongensis* of Cytosporaceae were reported to be associated with *Castanea mollissima* branch cankers (Jiang et al. 2020c). *Diaporthe eres* of Diaporthaceae was discovered on dead branches of *Castanea mollissima* in Beijing (Yang 2018). *Dendrostoma aurorae*, *D. castaneae*, *D. castaneicola*, *D. chinense*, *D. parasiticum*, *D. shaanxiense* and *D. shandongense* of Erythrogloeaceae were associated with *Castanea mollissima* stem, branch and twig cankers (Jiang et al. 2019a). *Gnomoniopsis chinensis* of Gnomoniaceae caused severe stem and branch cankers only in Hebei Province (Jiang and Tian 2019; Jiang et al. 2020b). *Neopseudomelanconis castaneae* of Pseudomelanconidaceae was discovered on *Castanea mollissima* branches in Shaanxi Province (Jiang et al. 2018a).

In the present study, investigations were conducted in *Castanea mollissima* plantations in Hunan Province of south China. Two *Melanconis*-like specimens were collected on a cultivated chestnut tree. The aim of the present study was to identify the fresh collections and confirm their phylogenetic positions.

Materials and methods

Collection, examination and isolation

The fresh specimens of diseased and dead chestnut branches were collected in a *Castanea mollissima* plantation in Hunan Province of south China. Morphological characteristics of the conidiomata were determined under a Nikon AZ100 dissecting stereomicroscope. More than 20 fruiting bodies were sectioned, and 50 conidia were selected randomly for measurement using a Leica compound microscope (LM, DM 2500). Isolates were obtained by removing a mucoid conidial mass from conidiomata, spreading the suspension onto the surface of 1.8% potato dextrose agar (PDA), and incubated at 25 °C for up to 24 h. Single germinating conidium was removed and plated onto fresh PDA plates. Cultural characteristics of isolates incubated on PDA in the dark at 25 °C were recorded, including the colony color and conidiomata structures. Specimens were deposited in the Museum of the Beijing Forestry University (**BJFC**). Axenic cultures were maintained in the China Forestry Culture Collection Centre (**CFCC**).

DNA extraction, PCR amplification and phylogenetic analyses

Genomic DNA was extracted from colonies grown on cellophane-covered PDA, using a cetyltrimethylammonium bromide (CTAB) method (Doyle and Doyle 1990). DNA was estimated by electrophoresis in 1% agarose gel and the quality was measured using the NanoDrop 2000 (Thermo Scientific, Waltham, MA, USA). Four partial loci, including the 5.8S nuclear ribosomal DNA gene with the two flanking internally tran-

scribed spacer (ITS) regions, the large subunit of the nrDNA (LSU), and the translation elongation factor 1-alpha (*tef1a*) and DNA-directed RNA polymerase II second largest subunit (rpb2) genes, were amplified by the following primer pairs: ITS1 and ITS4 for ITS (White et al. 1990), LR0R and LR5 for LSU (Vilgalys and Hester 1990), EF1-728F and EF2 for *tef1a* (O'Donnell et al. 1998; Carbone and Kohn 1999), and RPB2-5F and fRPB2-7cR for *rpb2* (Liu et al. 1999). The polymerase chain reaction (PCR) conditions were as follows: an initial denaturation step of 5 min at 94 °C, followed by 35 cycles of 30 s at 94 °C, 50 s at 48 °C (ITS, LSU) or 54 °C (*tef1a*) or 55 °C (*rpb2*), and 1 min at 72 °C, and a final elongation step of 7 min at 72 °C. PCR products were assayed via electrophoresis in 2% agarose gels. DNA sequencing was performed using an ABI PRISM 3730XL DNA Analyser with a BigDye Terminater Kit v.3.1 (Invitrogen, USA) at the Shanghai Invitrogen Biological Technology Company Limited (Beijing, China).

For phylogenetic reconstruction, newly-generated sequences of ITS, LSU, *tef1a* and *rpb2* were initially subjected to BLAST search (BLASTn) in NCBI website (https://www.ncbi.nlm.nih.gov). Then species and their sequences from recently published articles were selected and listed in Table 1 (Crous et al. 2012b; Alvarez et al. 2016; Senanayake et al. 2017; Braun et al. 2018; Fan et al. 2018a; Jiang et al. 2020a; Wang et al. 2020). The sequence alignments of the four individual loci (ITS, LSU, *tef1a* and *rpb2*) were conducted using MAFFT 7 (http://mafft.cbrc.jp/alignment/server/index.html), manually edited in MEGA 7.0.21, and then assembled as a dataset of ITS-LSU-*tef1a*-*rpb2* to infer the phylogenetic placement of our new isolates.

ML and Bayesian analysis were implemented on the CIPRES Science Gateway portal (https://www.phylo.org) using RAxML-HPC BlackBox 8.2.10 (Stamatakis 2014) and MrBayes 3.1.2 (Ronquist and Huelsenbeck 2003), respectively. For ML analyses, a GTR+GAMMA substitution model with 1000 bootstrap iterations was set. MrModeltest 2.3 was used to estimate the best nucleotide substitution model settings for each gene. Bayesian inference (BI) was performed based on the DNA data set from the results of the MrModeltest, using a Markov chain Monte Carlo (MCMC) algorithm in MrBayes 3.1.2. Two MCMC chains were run from random trees for 1000 million generations and stopped when the average standard deviation of split frequencies fell below 0.01. Trees were saved each 1000 generations. The first 25% of trees were discarded as the burn-in phase of each analysis, and the Bayesian posterior probabilities (BPPs) were calculated from the remaining trees. Phylogenetic trees were viewed with FigTree v.1.3.1 and processed by Adobe Illustrator CS5. The nucleotide sequence data of the new taxon have been deposited in GenBank (Table 1).

Results

The ITS, LSU, *tef1a* and *rpb2*, and combined data matrices contained 624, 867, 513, 865, and 2869 characters with gaps, respectively. The alignment comprised 92 strains, with *Nakataea oryzae* (CBS 243.76) and *Pyricularia grisea* (Ina168) from Magna-

Table 1. Details of the isolates included for molecular study used in this study.

Species	Isolates	GenBank accession numbers			
		ITS	LSU	*tef1a*	*rpb2*
Apiognomonia errabunda	AR 2813	DQ313525	NG027592	DQ313565	DQ862014
Apiosporopsis carpinea	CBS 771.79	NA	AF277130	NA	NA
Apoharknessia insueta	CBS 111377*	JQ706083	AY720814	MN271820	NA
	CBS 114575	MN172402	MN172370	MN271821	NA
Asterosporium asterospermum	MFLU 15-3555	NA	MF190062	NA	NA
Auratiopycnidiella tristaniopsis	CBS 132180*	JQ685516	JQ685522	MN271825	NA
	CPC 16371	MN172405	MN172374	MN271826	NA
Aurifilum marmelostoma	CBS 124928*	FJ890495	MH874934	MN271827	MN271788
Celoporthe eucalypti	CBS 127190*	HQ730837	HQ730863	HQ730850	MN271790
Celoporthe woodiana	CBS 118785*	DQ267131	MN172375	JQ824071	MN271791
Chiangraiomyces bauhiniae	MFLUCC 17-1669	MF190119	MF190064	MF377598	MF377603
Coniella africana	CBS 114133*	AY339344	AY339293	KX833600	KX833421
Coniella eucalyptorum	CBS 112640*	AY339338	AY339290	KX833637	KX833452
Coniella fusiformis	CBS 141596*	KX833576	KX833397	KX833674	KX833481
Coniella javanica	CBS 455.68*	KX833583	KX833403	KX833683	KX833489
Coryneum gigasporum	CFCC 52319*	MH683565	MH683557	MH685737	MH685729
Coryneum umbonatum	D201	MH674329	MH674329	MH674337	MH674333
Cryphonectria decipens	CBS 129353	EU442655	MN172386	MN271845	MN271797
Cryptometrion aestuescens	CBS 124007*	GQ369457	MN172387	MN271851	MN271798
Cytospora chrysosperma	CFCC 89982	KP281261	KP310805	KP310848	KU710952
Cytospora elaeagni	CFCC 89633	KF765677	KF765693	KU710919	KU710956
Dendrostoma aurorae	CFCC 52753*	MH542498	MH542646	MH545447	MH545405
Dendrostoma castaneae	CFCC 52745*	MH542488	MH542644	MH545437	MH545395
Dendrostoma chinense	CFCC 52755*	MH542500	MH542648	MH545449	MH545407
Dendrostoma dispersum	CFCC 52730*	MH542467	MH542629	MH545416	MH545374
Dendrostoma mali	CFCC 52102*	MG682072	MG682012	MG682052	MG682032
Dendrostoma osmanthi	CFCC 52106*	MG682073	MG682013	MG682053	MG682033
Dendrostoma parasiticum	CFCC 52762*	MH542482	MH542638	MH545431	MH545389
Dendrostoma qinlingense	CFCC 52732*	MH542471	MH542633	MH545420	MH545378
Dendrostoma quercinum	CFCC 52103*	MG682077	MG682017	MG682057	MG682037
Dendrostoma quercus	CFCC 52739*	MH542476	MH542635	MH545425	MH545383
Dendrostoma shaanxiense	CFCC 52741*	MH542486	MH542642	MH545435	MH545393
Dendrostoma shandongense	CFCC 52759*	MH542504	MH542652	MH545453	MH545411
Diaporthosporella cercidicola	CFCC 51994*	KY852492	KY852515	MN271855	NA
Diaporthostoma machili	CFCC 52100*	MG682080	MG682020	MG682060	MG682040
	CFCC 52101	MG682081	MG682021	MG682061	MG682041
Dwiroopa lythri	CBS 109755*	MN172410	MN172389	MN271859	MN271801
Dwiroopa punicae	CBS 143163*	MK510676	MK510686	NA	MK510692
Foliocryphia eucalypti	CBS 124779*	GQ303276	GQ303307	MN271861	MN271802
Foliocryphia eucalyptorum	CBS 142536*	KY979772	KY979827	MN271862	MN271803
Gnomonia gnomon	CBS 199.53	DQ491518	AF408361	EU221885	EU219295
Harknessia australiensis	CBS 132119*	JQ706085	JQ706211	MN271863	NA
Harknessia capensis	CBS 111829*	AY720719	AY720816	MN271864	NA
Harknessia ellipsoidea	CBS 132121*	JQ706087	JQ706213	MN271865	NA
Harknessia eucalypti	CBS 342.97	AY720745	AF408363	MN271866	NA
Holocryphia eucalypti	CBS 115842*	MN172411	MN172391	MN271882	MN271804
Immersiporthe knoxdaviesiana	CBS 132862*	JQ862765	JQ862755	MN271886	MN271805
Juglanconis juglandina	CBS 121083	KY427148	KY427148	KY427217	KY427198
Juglanconis oblonga	MAFF 410216	KY427153	KY427153	KY427222	KY427203
Juglanconis pterocaryae	MAFF 410079	KY427155	KY427155	KY427224	KY427205
Lamproconium desmazieri	MFLUCC 15-0870	KX430134	KX430135	MF377591	MF377605
	MFLUCC 15-0872	KX430138	KX430139	MF377593	MF377606
Macrohilum eucalypti	CPC 10945	DQ195781	DQ195793	NA	MN271809
	CPC 19421	KR873244	KR873275	NA	MN271810
Mastigosporella anisophylleae	CBS 136421*	KF779492	KF777221	MN271892	NA

Species	Isolates	GenBank accession numbers			
		ITS	LSU	*tef1a*	*rpb2*
Mastigosporella pigmentata	COAD 2370*	MG587929	MG587928	NA	NA
Melanconiella ellisii	BPI 878343	JQ926271	JQ926271	JQ926406	JQ926339
Melanconiella spodiaea	MSH	JQ926298	JQ926298	JQ926431	JQ926364
Melanconis betulae	CFCC 50471	KT732952	KT732971	KT733001	KT732984
Melanconis itoana	CFCC 50474	KT732955	KT732974	KT733004	KT732987
Melanconis stilbostoma	CFCC 50475	KT732956	KT732975	KT733005	KT732988
Micromelanconis kaihuiae	**CFCC 54572***	**MW414473**	**MW414373**	**MW419880**	**MW419878**
	KH5-4	**MW414474**	**MW414374**	**MW419881**	**MW419879**
Nakataea oryzae	CBS 243.76	KM484861	DQ341498	NA	NA
Neopseudomelanconis castaneae	CFCC 52787*	MH469162	MH469164	NA	NA
Phaeoappendicospora thailandensis	MFLU 12-2131	MF190157	MF190102	NA	NA
Prosopidicola albizziae	CPC 27478	KX228274	KX228325	NA	NA
Prosopidicola mexicana	CBS 113529	AY720709	NA	NA	NA
Pseudomelanconis caryae	CFCC 52110*	MG682082	MG682022	MG682062	MG682042
Pseudoplagiostoma corymbiae	CPC 14161	GU973510	GU973604	GU973540	NA
Pseudoplagiostoma oldii	CBS 115722	GU973535	GU973610	GU973565	NA
Pseudoplagiostoma variabile	CBS 113067	GU973536	GU973611	GU973566	NA
Pyricularia grisea	Ina168	NA	AB026819	NA	NA
Pyrispora castaneae	CFCC 54349	MW208108	MW208105	MW227340	MW218535
	CFCC 54351	MW208110	MW208107	MW227342	MW218537
Sillia karstenii	MFLU 16-2864	KY523482	KY523500	NA	KY501636
Sirococcus tsugae	CBS 119626	EU199203	EU199136	EF512534	EU199159
Stegonsporium acerophilum	CBS 117025	EU039982	EU039993	EU040027	KF570173
Stilbospora longicornuta	CBS 122529*	KF570164	KF570164	KF570232	KF570194
Synnemasporella aculeans	CFCC 52094	MG682086	MG682026	MG682066	MG682046
Synnemasporella toxicodendri	CFCC 52097*	MG682089	MG682029	MG682069	MG682049
Thailandiomyces bisetulosus	BCC 00018	NA	EF622230	NA	NA
Tirisporella beccariana	BCC 38312	NA	JQ655449	NA	NA
Tubakia seoraksanensis	CBS 127490*	MG591907	KP260499	MG592094	NA
Tubakia iowensis	CBS 129012*	MG591879	MG591971	MG592064	NA
Ursicollum fallax	CBS 118663*	DQ368755	EF392860	MN271897	MN271816

Ex-type strains are marked by an asterisk (*) and the strains from this study are in bold.

porthales as outgroup taxa. The ML analysis yielded a tree with a ln likelihood value of –45806.266577 and the following model parameters: alpha = 0.298226, ∏(A) = 0.241173, ∏(C) = 0.258552, ∏(G) = 0.275145, and ∏(T) = 0.225130. For BI analyses, the general time reversible model, additionally assuming a proportion of invariant sites with gamma-distributed substitution rates of the remaining sites (GTR+I+G), was determined to be the best for the ITS, LSU, and *tef1a* loci by MrModeltest, whereas the most appropriate model for the *rpb2* locus was the Tamura-Nei model, additionally assuming a proportion of invariant sites with gamma-distributed substitution rates of the remaining sites (TrN+I+G). The phylogeny resulting from the RAxML maximum likelihood analysis of the combined gene sequence data is shown in Fig. 1. Overall, the topologies obtained from the different phylogenetic analyses were similar, and the best scoring RAxML tree is illustrated here. The bootstrap support values above 50% of maximum likelihood analysis (ML) and Bayesian posterior probability scores (≥0.90) are noted at the nodes.

The *Diaporthales* separates into 32 clades, representing 32 families, and the new isolates were clustered with a well-supported clade (ML/BI = 100/1) in Pseudomelanconidaceae. The two new isolates were different from any known genera in Pseudomelanconidaceae, and represented a new genus (Fig. 1).

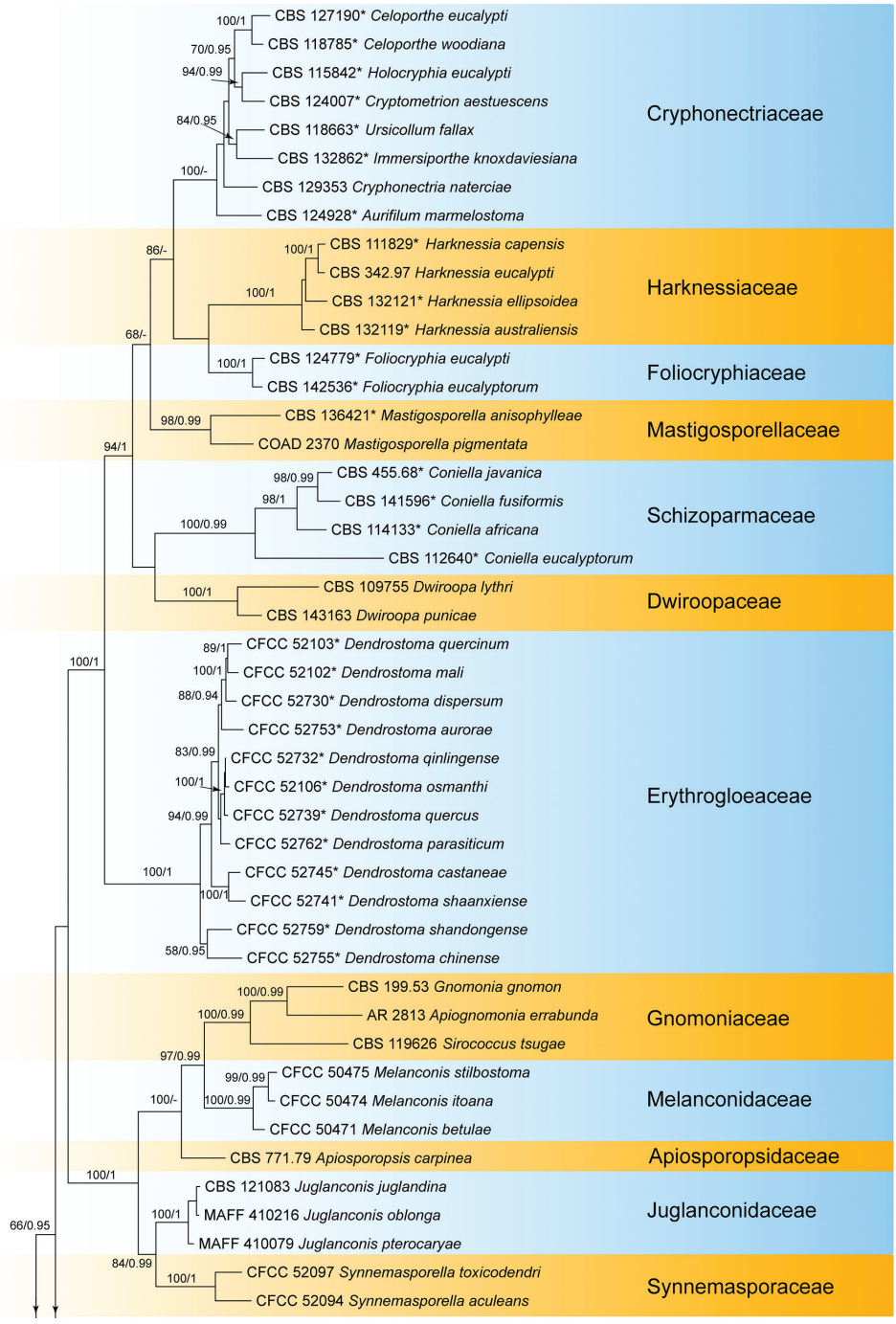

Figure 1. Phylogram of Diaporthales from a maximum likelihood analysis based on combined ITS, LSU, *tef1a* and *rpb2*. Values above the branches indicate maximum likelihood bootstrap (left, ML BP ≥ 50%) and Bayesian probabilities (right, BI PP ≥ 0.90). The tree is rooted with *Nakataea oryzae* (CBS 243.76) and *Pyricularia grisea* (Ina168). New species proposed in the current study is in blue and the ex-type strains are marked with *.

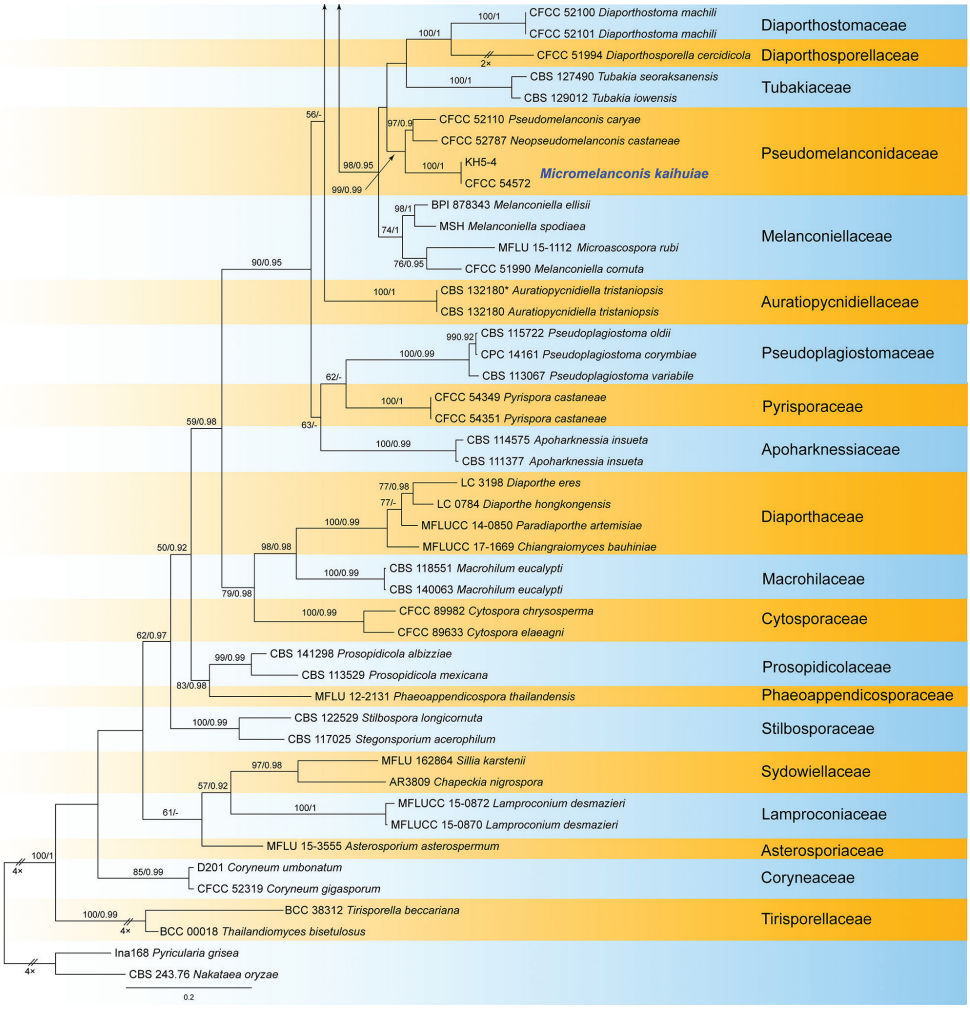

Figure 111. Continued.

Taxonomy

Micromelanconis **C.M. Tian & N. Jiang, gen. nov.**
MycoBank No: 838927

Etymology. Name derived from micro- and the genus name *Melanconis*.

Type species. *Micromelanconis kaihuiae* C.M. Tian & N. Jiang.

Description. ***Sexual morph*****:** not observed. ***Asexual morph*****:** Conidiomata acervular, conspicuous, immersed in host bark to erumpent, covered by brown to blackish exuding conidial masses at maturity. Central column beneath the disc more or less conical. Conidiophores unbranched, aseptate, cylindrical, pale brown, smooth-walled. Conidiogenous cells annellidic, occasionally with distinct annellations and collarettes.

Conidia hyaline when immature, becoming pale brown, ellipsoid, multiguttulate, aseptate, with hyaline sheath. Conidiomata formed on PDA after three weeks, randomly distributed, and black. Conidiophores unbranched, septate, cylindrical, pale brown, smooth-walled. Conidiogenous cells annellidic. Conidia pale brown, long dumbbell-shaped, narrow at the middle and wide at both ends, multiguttulate, aseptate, with hyaline sheath.

Notes. *Micromelanconis* is the third genus after *Neopseudomelanconis* and *Pseudomelanconis* in the family Pseudomelanconidaceae (Fig. 1). *Micromelanconis* is united in this family based on the *Melanconis*-like conidiomata, and pale brown conidia with conspicuous hyaline sheath. *Micromelanconis* produces two types of conidia from natural branches and manual media respectively, which differs from *Neopseudomelanconis* and *Pseudomelanconis* (Fan et al. 2018a; Jiang et al. 2018a). Additionally, *Neopseudomelanconis* is characterized by its septate conidia (Jiang et al. 2018a).

***Micromelanconis kaihuiae* C.M. Tian & N. Jiang, sp. nov.**
MycoBank No: 838928
Figures 2, 3

Etymology. Named after Kaihui Yang, a Chinese heroine; Kaihui is also the name of the town where holotype was collected.

Description. ***Sexual morph*:** not observed. ***Asexual morph*:** Conidiomata acervular, 350–800 μm diam., conspicuous, immersed in host bark to erumpent, covered by brown to blackish exuding conidial masses at maturity. Central column beneath the disc more or less conical. Conidiophores unbranched, aseptate, cylindrical, pale brown, smooth-walled. Conidiogenous cells annellidic, occasionally with distinct annellations and collarettes, 12.4–47.1 × 1.2–3.8 μm. Conidia hyaline when immature, becoming pale brown, ellipsoid, multiguttulate, aseptate, 7.6–10.3 × 3.1–4.1 μm, L/W = 2–3.2, with hyaline sheath, 1 μm.

Culture characters. Colony on PDA at 25 °C irregular, grey olivaceous, margin becoming diffuse, aerial hyphae short, dense, surface becoming imbricate, growth limited and ceasing after two weeks. Conidiomata formed after three weeks, randomly distributed, black. Conidiophores unbranched, septate, cylindrical, pale brown, smooth-walled. Conidiogenous cells annellidic, 9.1–18.5 × 2.5–5.3 μm. Conidia pale brown, long dumbbell-shaped, narrow at the middle and wide at both ends, multiguttulate, aseptate, 10.4–13.5 × 4–5 μm, L/W = 2.3–3.3, with hyaline sheath, 1.5 μm.

Specimens examined. China, Hunan Province, Changsha City, Changsha County, Kaihui Town, chestnut plantation, 40°24'32.16"N, 117°28'56.24"E, 262 m asl, on stems and branches of *Castanea mollissima*, Tian Chengming and Ning Jiang, 10 November 2020 (BJFC-S1831, holotype; ex-type culture, CFCC 54572 = KH5-3). *Ibid.* (BJFC-S1832, KH5-4).

Notes. *Micromelanconis kaihuiae* on *Castanea mollissima* (Fagaceae, Fagales) is phylogenetically close to *Neopseudomelanconis castaneae* on *Castanea mollissima* and

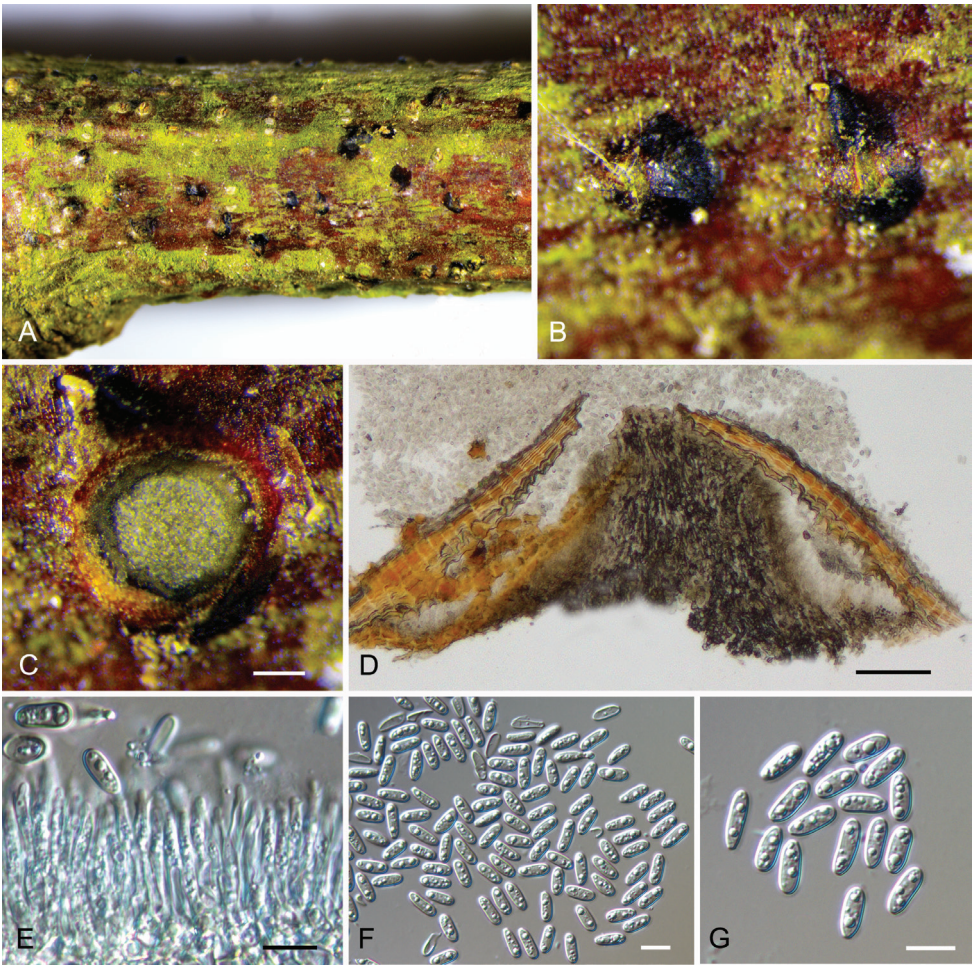

Figure 2. Morphology of *Micromelanconis kaihuiae* on branches of *Castanea mollissima* (BJFC-S1831) **A, B** habit of conidiomata on a branch **C** transverse section of conidiomata **D** longitudinal section through conidiomata **E** conidiogenous cells attached with conidia **F, G** conidia. Scale bars: 100 μm (**C, D**); 10 μm (**E–G**).

Pseudomelanconis caryae on *Carya cathayensis* (Juglandaceae, Juglandales) (Fig. 1). All these three species are discovered on tree branches in China, and share similar morphological characters in having pale brown conidia with conspicuous hyaline sheath. *Micromelanconis kaihuiae* and *Neopseudomelanconis castaneae* even share the same host. However, they can be easily distinguished based on conidia shape, color and overall size of conidia (*M. kaihuiae*, pale brown, ellipsoid and aseptate conidia, 7.6–10.3 × 3.1–4.1 μm; pale brown, long dumbbell-shaped and aseptate conidia, 10.4–13.5 × 4–5 μm ***vs.*** *N. castaneae*, brown, ellipsoid to oblong and septate conidia, 18–21.5 × 4.8–7 μm ***vs.*** *P. caryae*, pale brown, ellipsoid to oblong and aseptate conidia, 12.5–16 × 4–5 μm) (Fan et al. 2018a; Jiang et al. 2018a). Furthermore, *M. kaihuiae* is separated

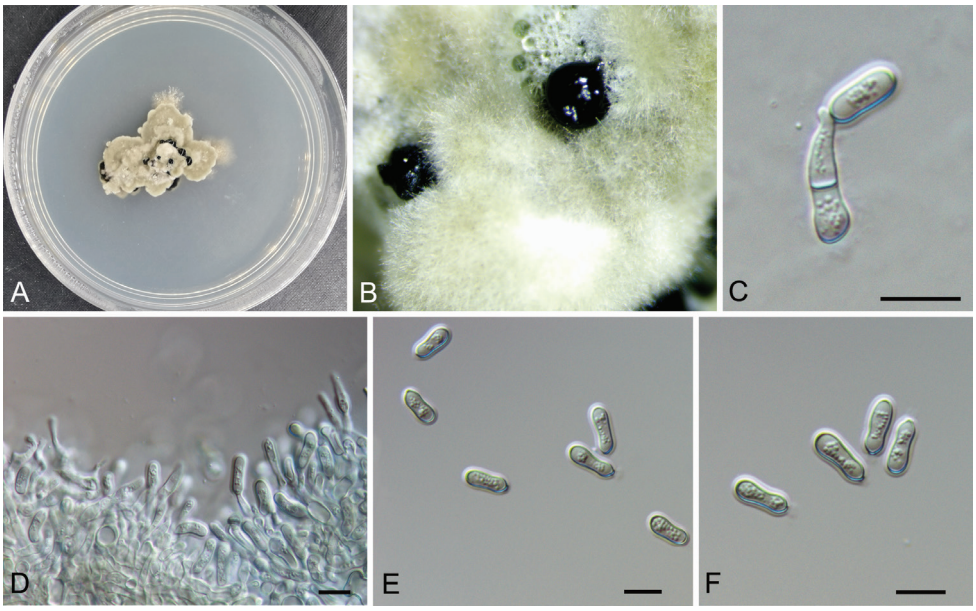

Figure 3. Morphology of *Micromelanconis kaihuiae* on the PDA plate (CFCC 54572) **A** colony on PDA **B** habit of conidiomata formed on PDA **C, D** conidiogenous cells attached with conidia **E, F** conidia. Scale bars: 10 μm (**C–F**).

from *N. castaneae* by 51/490 bp (10.4%) differences in ITS and 12/563 bp (2.1%) differences in LSU, and from *P. caryae* by 56/490 bp (11.4%) differences in ITS and 6/563 bp (1.1%) differences in LSU.

Key to Pseudomelanconidaceae genera and species

1	On *Carya* of Juglandaceae, conidia ellipsoid to oblong and aseptate..... ..... ***Pseudomelanconis caryae***
–	On *Castanea* of Fagaceae..... **2**
2	Conidia aseptate ..... ***Micromelanconis kaihuiae***
–	Conidia septate..... ***Neopseudomelanconis castaneae***

Discussion

Diaporthales is a well-studied order based on integrated approaches of morphology and phylogeny in recent years (Castlebury et al. 2002; Rossman et al. 2007; Voglmayr and Jaklitsch 2014; Alvarez et al. 2016; Senanayake et al. 2017, 2018; Voglmayr et al. 2017; Braun et al. 2018; Fan et al. 2018a; Jiang et al. 2020a). Thirty-two accepted families are monophyletic and supported by morphological characters; four of them

contain *Melanconis*-like fungi, namely Juglanconidaceae, Melanconidaceae, Melanconiellaceae and Pseudomelanconidaceae (Fan et al. 2018a). The *Melanconis*-like fungi were similar in their asexual morph, but well-separated in the phylogeny and their hosts (Voglmayr et al. 2012, 2017, 2019; Fan et al. 2018a, b; Jaklitsch and Voglmayr 2020). In the present study, a new genus and species were clustered in the family Pseudomelanconidaceae (Fig. 1), and differed from the other *Melanconis*-like genera by its long dumbbell-shaped conidia formed on PDA plates.

Hosts are useful taxonomic information in some families of Diaporthales, such as Coryneaceae, Cryphonectriaceae, Erythrogloeaceae and Gnomoniaceae (Voglmayr et al. 2012; Jaklitsch and Voglmayr 2019; Roux et al. 2020; Wang et al. 2020; Yang et al. 2020). Hosts are important to separate *Melanconis*-like genera, *Juglanconis* inhabit *Juglans* and *Pterocarya* of Juglandaceae, *Melanconiella* and *Melanconis* occur only on the plant family Betulaceae (Voglmayr et al. 2012, 2017, 2019; Fan et al. 2018b; Jaklitsch and Voglmayr 2020). *Melanconis* species are discovered only on *Alnus* and *Betula*, while *Melanconiella* occurs in the subfamily Coryloideae with the exception of *M. betulae* and *M. decorahensis* on *Betula* (Voglmayr et al. 2012; Du et al. 2017; Fan et al. 2018a). Species of Pseudomelanconidaceae inhabit *Carya* of Juglandaceae, and *Castanea* of Fagaceae (Fan et al. 2018a; Jiang et al. 2021). More interesting *Melanconis*-like may be revealed by more detailed surveys on tree-inhabiting fungi in the future.

Acknowledgements

This study is financed by the National Natural Science Foundation of China (Project No.: 31670647). We are grateful to Chungen Piao and Minwei Guo (China Forestry Culture Collection Center, Chinese Academy of Forestry, Beijing) for support of strain preservation during this study.

References

Alvarez LV, Groenewald JZ, Crous PW (2016) Revising the Schizoparmaceae: *Coniella* and its synonyms *Pilidiella* and *Schizoparme*. Studies in Mycology 85: 1–34. https://doi.org/10.1016/j.simyco.2016.09.001

Barr ME (1978) The Diaporthales in North America with emphasis on *Gnomonia* and its segregates. Mycologia Memoir 7: 1–232.

Braun U, Nakashima C, Crous PW, Groenewald JZ, Moreno-Rico O, Rooney-Latham S, Blomquist CL, Haas J, Marmolejo J (2018) Phylogeny and taxonomy of the genus *Tubakia* s. lat. Fungal Systematics and Evolution 1: 41–99. https://doi.org/10.3114/fuse.2018.01.04

Carbone I, Kohn LM (1999) A method for designing primer sets for speciation studies in filamentous ascomycetes. Mycologia 91: 553–556. https://doi.org/10.1080/00275514.1999.12061051

Castlebury LA, Rossman AY, Jaklitsch WJ, Vasilyeva LN (2002) A preliminary overview of the Diaporthales based on large subunit nuclear ribosomal DNA sequences. Mycologia 94: 1017–1031. https://doi.org/10.1080/15572536.2003.11833157

Chen SF, Liu QL, Li GQ, Wingfield MJ, Roux J (2018) A new genus of Cryphonectriaceae isolated from *Lagerstroemia speciosa* in southern China. Plant Pathology 67: 107–123. https://doi.org/10.1111/ppa.12723

Chen SF, Wingfield MJ, Li GQ, Liu FF (2016) *Corticimorbus sinomyrti* gen. et sp. nov. (Cryphonectriaceae) pathogenic to native *Rhodomyrtus tomentosa* (Myrtaceae) in South China. Plant Pathology 65: 1254–1266. https://doi.org/10.1111/ppa.12507

Chen SF, Wingfield MJ, Roets F, Roux J (2013) A serious canker disease caused by *Immersiporthe knoxdaviesiana* gen. et sp. nov. (Cryphonectriaceae) on native *Rapanea melanophloeos* in South Africa. Plant Pathology 62: 667–678. https://doi.org/10.1111/j.1365-3059.2012.02671.x

Crous PW, Summerell BA, Alfenas AC, Edwards J, Pascoe IG, Porter IJ, Groenewald JZ (2012a) Genera of diaporthalean coelomycetes associated with leaf spots of tree hosts. Persoonia 28: 66–75. https://doi.org/10.3767/003158512X642030

Crous PW, Summerell BA, Shivas RG, Carnegie AJ, Groenewald JZ (2012b) A re-appraisal of *Harknessia* (Diaporthales), and the introduction of Harknessiaceae fam. nov. Persoonia 28: 49–65. https://doi.org/10.3767/003158512X639791

Doyle JJ, Doyle JL (1990) Isolation of plant DNA from fresh tissue. Focus 12: 39–40.

Du Z, Fan XL, Yang Q, Tian CM (2017) Host and geographic range extensions of *Melanconiella*, with a new species *M. cornuta* in China. Phytotaxa 327: 252–260. https://doi.org/10.11646/phytotaxa.327.3.4

Fan XL, Bezerra JDP, Tian CM, Crous PW (2018a) Families and genera of diaporthalean fungi associated with canker and dieback of tree hosts. Persoonia 40: 119–134. https://doi.org/10.3767/persoonia.2018.40.05

Fan XL, Bezerra JDP, Tian CM, Crous PW (2020) *Cytospora* (Diaporthales) in China. Persoonia 45: 1–45. https://doi.org/10.3767/persoonia.2020.45.01

Fan XL, Du Z, Bezerra JDP, Tian CM (2018b) Taxonomic circumscription of melanconis-like fungi causing canker disease in China. MycoKeys 42: 89–124. https://doi.org/10.3897/mycokeys.42.29634

Fan XL, Du Z, Liang YM, Tian CM (2016) *Melanconis* (Melanconidaceae) associated with *Betula* spp. in China. Mycological Progress 15: 1–40. https://doi.org/10.1007/s11557-016-1163-2

Jaklitsch WM, Voglmayr H (2019) European species of *Dendrostoma* (Diaporthales). MycoKeys 59: 1–26. https://doi.org/10.3897/mycokeys.59.37966

Jaklitsch WM, Voglmayr H (2020) The genus *Melanconis* (Diaporthales). MycoKeys 63: 69–117. https://doi.org/10.3897/mycokeys.63.49054

Jiang N, Fan XL, Crous PW, Tian CM (2019a) Species of *Dendrostoma* (Erythrogloeaceae, Diaporthales) associated with chestnut and oak canker diseases in China. MycoKeys 48: 67–96. https://doi.org/10.3897/mycokeys.48.31715

Jiang N, Fan XL, Tian CM (2019b) Identification and pathogenicity of Cryphonectriaceae species associated with chestnut canker in China. Plant Pathology 68: 1132–1145. https://doi.org/10.1111/ppa.13033

Jiang N, Fan XL, Tian CM (2021) Identification and characterization of leaf-inhabiting fungi from *Castanea* plantations in China. Journal of Fungi 7: e64. https://doi.org/10.3390/jof7010064

Jiang N, Fan XL, Tian CM, Crous PW (2020a) Reevaluating Cryphonectriaceae and allied families in Diaporthales. Mycologia 112: 267–292. https://doi.org/10.1080/00275514.2019.1698925

Jiang N, Li J, Piao CG, Guo MW, Tian CM (2018a) Identification and characterization of chestnut branch-inhabiting melanocratic fungi in China. Mycosphere 9: 1268–1289. https://doi.org/10.5943/mycosphere/9/6/14

Jiang N, Liang LY, Tian CM (2020b) *Gnomoniopsis chinensis* (Gnomoniaceae, Diaporthales), a new fungus causing canker of Chinese chestnut in Hebei Province, China. MycoKeys 67: 19–32. https://doi.org/10.3897/mycokeys.67.51133

Jiang N, Tian CM (2019) An emerging pathogen from rotted chestnut in China: *Gnomoniopsis daii* sp. nov. Forests 10: e1016. https://doi.org/10.3390/f10111016

Jiang N, Voglmayr H, Tian CM (2018b) New species and records of *Coryneum* from China. Mycologia 110: 1172–1188. https://doi.org/10.1080/00275514.2018.1516969

Jiang N, Voglmayr H, Tian CM (2019c) Morphology and phylogeny reveal two novel *Coryneum* species from China. MycoKeys 56: 67–80. https://doi.org/10.3897/mycokeys.56.35554

Jiang N, Yang Q, Fan XL, Tian CM (2020c) Identification of six *Cytospora* species on Chinese chestnut in China. MycoKeys 62: 1–25. https://doi.org/10.3897/mycokeys.62.47425

Jiang N, Yang Q, Liang YM, Tian CM (2019d) Taxonomy of two synnematal fungal species from Rhus chinensis, with *Flavignomonia* gen. nov. described. MycoKeys 60: 17–29. https://doi.org/10.3897/mycokeys.60.46395

Liu YJ, Whelen S, Hall BD (1999) Phylogenetic relationships among ascomycetes: evidence from an RNA polymerse II subunit. Molecular Biology and Evolution 16: 1799–1808. https://doi.org/10.1093/bioinformatics/btq224

Norphanphoun C, Hongsanan S, Doilom M, Bhat DJ, Wen T-C, Senanayake IC, Bulgakov TS, Hyde KD (2016) Lamproconiaceae fam. nov. to accommodate *Lamproconium desmazieri*. Phytotaxa 270: 89–102. https://doi.org/10.11646/phytotaxa.270.2.2

Norphanphoun C, Raspé O, Jeewon R, Wen TC, Hyde KD (2018) Morphological and phylogenetic characterisation of novel *Cytospora* species associated with mangroves. MycoKeys 38: 93–120. https://doi.org/10.3897/mycokeys.38.28011

O'Donnell K, Kistler HC, Cigelnik E, Ploetz RC (1998) Multiple evolutionary origins of the fungus causing *Panama* disease of banana: concordant evidence from nuclear and mitochondrial gene genealogies. Proceedings of the National Academy of Sciences 95: 2044–2049. https://doi.org/10.1073/pnas.95.5.2044

Rigling D, Prospero S (2018) *Cryphonectria parasitica*, the causal agent of chestnut blight: invasion history, population biology and disease control. Molecular Plant Pathology 19: 7–20. https://doi.org/10.1111/mpp.12542

Ronquist F, Huelsenbeck JP (2003) MrBayes 3: Bayesian phylogenetic inference under mixed models. Bioinformatics 19: 1572–1574. https://doi.org/10.1093/bioinformatics/btg180

Rossman AY, Farr DF, Castlebury LA (2007) A review of the phylogeny and biology of the Diaporthales. Mycoscience 48: 135–144. https://doi.org/10.1007/S10267-007-0347-7

Roux J, Nkuekam GK, Marincowitz S, van der Merwe NA, Uchida J, Wingfield MJ, Chen SF (2020) Cryphonectriaceae associated with rust-infected *Syzygium jambos* in Hawaii. MycoKeys 76: 49–79. https://doi.org/10.3897/mycokeys.76.58406

Senanayake IC, Crous PW, Groenewald JZ, Maharachchikumbura SSN, Jeewon R, Phillips AJL, Bhat JD, Perera RH, Li QR, Li WJ, Tangthirasunun N, Norphanphoun C, Karunarathna SC, Camporesi E, Manawasighe IS, Al-Sadi AM, Hyde KD (2017) Families of Diaporthales based on morphological and phylogenetic evidence. Studies in Mycology 86: 217–296. https://doi.org/10.1016/j.simyco.2017.07.003

Senanayake IC, Jeewon R, Chomnunti P, Wanasinghe DN, Norphanphoun C, Karunarathna A, Pem D, Perera RH, Camporesi E, McKenzie EHC, Hyde KD, Karunarathna SC (2018) Taxonomic circumscription of Diaporthales based on multigene phylogeny and morphology. Fungal Diversity 93: 241–443. https://doi.org/10.1007/s13225-018-0410-z

Senwanna C, Hyde KD, Phookamsak R, Jones EG, Cheewangkoon R (2018) *Coryneum heveanum* sp. nov.(Coryneaceae, Diaporthales) on twigs of Para rubber in Thailand. MycoKeys 43: 75–90. https://doi.org/10.3897/mycokeys.43.29365

Shuttleworth LA, Guest DI (2017) The infection process of chestnut rot, an important disease caused by *Gnomoniopsis smithogilvyi* (Gnomoniaceae, Diaporthales) in Oceania and Europe. Australasian Plant Pathology 46: 397–405. https://doi.org/10.1007/s13313-017-0502-3

Shuttleworth LA, Walker DM, Guest DI (2016) The chestnut pathogen *Gnomoniopsis smithogilvyi* (Gnomoniaceae, Diaporthales) and its synonyms. Mycotaxon 130: 929–940. https://doi.org/10.5248/130.929

Sogonov MV, Castlebury LA, Rossman AY, Mejía LC, White JF (2008) Leaf-inhabiting genera of the Gnomoniaceae, Diaporthales. Studies in Mycology 62: 1–77. https://doi.org/10.3114/sim.2008.62.01

Stamatakis A (2014) RAxML version 8: a tool for phylogenetic analysis and post-analysis of large phylogenies. Bioinformatics 30: 1312–1313. https://doi.org/10.1093/bioinformatics/btu033

Vilgalys R, Hester M (1990) Rapid genetic identification and mapping of enzymatically amplified ribosomal DNA from several *Cryptococcus* species. Journal of Bacteriology 172: 4238–4246. https://doi.org/10.1128/JB.172.8.4238-4246.1990

Voglmayr H, Castlebury LA, Jaklitsch WM (2017) *Juglanconis* gen. nov. on Juglandaceae, and the new family Juglanconidaceae (Diaporthales). Persoonia 38: 136–155. https://doi.org/10.3767/003158517X694768

Voglmayr H, Jaklitsch WM (2014) Stilbosporaceae resurrected: generic reclassification and speciation. Persoonia 33: 61–82. https://doi.org/10.3767/003158514X684212

Voglmayr H, Jaklitsch WM, Mohammadi H, Chakusary MK (2019) The genus *Juglanconis* (Diaporthales) on *Pterocarya*. Mycological Progress 18: 425–437. https://doi.org/10.1007/s11557-018-01464-0

Voglmayr H, Rossman AY, Castlebury LA, Jaklitsch WM (2012) Multigene phylogeny and taxonomy of the genus *Melanconiella* (Diaporthales). Fungal Diversity 57: 1–44. https://doi.org/10.1007/s13225-012-0175-8

Wang W, Li GQ, Liu QL, Chen SF (2020) Cryphonectriaceae on *Myrtales* in China: phylogeny, host range, and pathogenicity. Persoonia 45: 101–131. https://doi.org/10.3767/persoonia.2020.45.04

Wehmeyer LE (1937) Studies of certain species of *Melanconis* on *Carpinus*, *Ostrya* and *Corylus*. Mycologia 29: 599–617. https://doi.org/10.2307/3754513

White TJ, Bruns T, Lee S, Taylor J (1990) Amplification and direct sequencing of fungal ribosomal RNA genes for phylogenetics. PCR protocols: a guide to methods and applications 18: 315–322. https://doi.org/10.1016/B978-0-12-372180-8.50042-1

Xavier KV, Kc AN, Crous PW, Groenewald JZ, Vallad GE (2019) *Dwiroopa punicae* sp. nov. (Dwiroopaceae fam. nov., Diaporthales), associated with leaf spot and fruit rot of pomegranate (*Punica granatum*). Fungal Systematics and Evolution 4: 33–41. https://doi.org/10.3114/fuse.2019.04.04

Yang Q (2018) Taxonomy and phylogeny of *Diaporthe* in China. Doctor, Beijing Foresty University.

Yang Q, Fan XL, Du Z, Tian CM (2018a) Diaporthosporellaceae, a novel family of Diaporthales (Sordariomycetes, Ascomycota). Mycoscience 59: 229–235. https://doi.org/10.1016/j.myc.2017.11.005

Yang Q, Fan XL, Guarnaccia V, Tian CM (2018b) High diversity of *Diaporthe* species associated with dieback diseases in China, with twelve new species described. MycoKeys 39: 97–149. https://doi.org/10.3897/mycokeys.39.26914

Yang Q, Jiang N, Tian CM (2020) Tree inhabiting gnomoniaceous species from China, with *Cryphogonomonia* gen. nov. proposed. MycoKeys 69: 71–89. https://doi.org/10.3897/mycokeys.69.54012

Yang Q, Jiang N, Tian CM (2021) New species and records of *Diaporthe* from Jiangxi Province, China. MycoKeys 77: 41–64. https://doi.org/10.3897/mycokeys.77.59999

Zhu HY, Pan M, Bezerra JDP, Tian CM, Fan XL (2020) Discovery of *Cytospora* species associated with canker disease of tree hosts from Mount Dongling of China. MycoKeys 62: 97–121. https://doi.org/10.3897/mycokeys.62.47854

MycoKeys 79: 17–118 (2021)
doi: 10.3897/mycokeys.79.63363
https://mycokeys.pensoft.net

MONOGRAPH

A peer-reviewed open-access journal
MycoKeys
Launched to accelerate biodiversity research

A survey of *Hebeloma* (Hymenogastraceae) in Greenland

Ursula Eberhardt[1], Henry J. Beker[2,3,4], Torbjørn Borgen[5], Henning Knudsen[6], Nicole Schütz[1], Steen A. Elborne[7]

1 *Staatliches Museum für Naturkunde Stuttgart, Rosenstein 1, D-70191 Stuttgart, Germany* **2** *Rue Pére de Deken 19, B-1040 Bruxelles, Belgium* **3** *Royal Holloway College, University of London, Egham, UK* **4** *Plantentuin Meise, Nieuwelaan 38, B-1860 Meise, Belgium* **5** *Sensommervej 142, 8600 Silkeborg, Denmark* **6** *Hauchsvej 15, 1825 Frederiksberg, Denmark* **7** *Frederik VII´s Vej 29, 3450 Allerød, Denmark*

Corresponding author: Ursula Eberhardt (ursula.eberhardt@smns-bw.de)

Academic editor: M. P. Martín | Received 19 January 2021 | Accepted 25 February 2021 | Published 19 April 2021

Citation: Eberhardt U, Beker HJ, Borgen T, Knudsen H, Schütz N, Elborne SA (2021) A survey of *Hebeloma* (Hymenogastraceae) in Greenland. MycoKeys 79: 17–118. https://doi.org/10.3897/mycokeys.79.63363

Abstract

This is the first study exclusively dedicated to the study of *Hebeloma* in Greenland. It is based on almost 400 collections, the great majority of which were collected by three of the co-authors over a period of 40 years and were lodged in the fungarium of the Natural History Museum in Copenhagen. The material was identified using molecular and morphological methods. In total, 28 species were recognized, 27 belonging to three sections, *H.* sects *Hebeloma*, *Denudata* and *Velutipes*. One species sampled was new to science and is here described as *H. arcticum*. For all species, a description, a distribution map within Greenland and macro and microphotographs are presented. A key is provided for the 28 species. The distribution of species within Greenland is discussed. The findings are placed in the context of studies of arctic and alpine *Hebeloma* from other parts of the world where comparable data exist. Notably, *H. grandisporum*, *H. louiseae* and *H. islandicum*, previously only known from Romania, Svalbard, Iceland or Norway, respectively, have been found in Greenland. The latter is also the only species encountered that does not belong to any of the above sections. *Hebeloma excedens* and *H. colvinii* – for the latter we here publish the first modern description – are to date only known from continental North America and now Greenland.

Keywords

Arctic distribution, High Arctic, Low Arctic, mycorrhizal hosts, new species, pruned median joining networks

Table of contents

Introduction

Hebeloma are notoriously difficult to identify to species. The genus is very common in arctic habitats and plays an important role as a mycorrhizal symbiont in arctic scrubland for plants like *Salix*, *Betula* and *Dryas* and thus for the turnover of nutrients in these harsh environments. In spite of their frequency and abundance in arctic areas, the alpha taxonomy of the genus was confused until the work of Beker and colleagues (Eberhardt et al. 2015a, b, 2016; Beker et al. 2016; Grilli et al. 2016) who described a number of new species from Europe, including the arctic and alpine regions of Europe, and reappraised the delimitation of known taxa.

Here we provide a review of *Hebeloma* spp. collected in Greenland and verified by molecular and morphological analysis. These encompass 378 of the 405 collection from Greenland that were digitized in the fungarium C of the Natural History Museum in Copenhagen, and represent 28 species. The great majority of this material was collected by three of the authors (T.B., S.A.E. and H.K.) over a period of 40 years in preparation for a forthcoming "Funga Arctica & Alpina" of basidiomycetes. The material presented here is a part of the 15.000 collections for the funga.

Each of the 28 species is presented with a morphological description, a photo of the macroscopic characters, photos of spores and cystidia as well as a distribution map of the collection sites in Greenland. Characters of each species are discussed and compared to related and similar species. Species ecology and distribution in Greenland and other regions (as appropriate) are discussed. Among these species is one species that is new to science

and here described as *H. arcticum*. For another species, *H. colvinii*, originally described by Peck (1875; effectively published 1876), the first modern description is provided.

In spite of the amount of study that went into the genus, species identification, also by molecular data, remains challenging. Beker and co-workers used several loci (ITS, partial *RPB2*, partial *Tef1*a, partial *MCM7*, and the variable regions V6 and V9 of the mitochondrial genes). The sections mainly encountered in Greenland (*H.* sects. *Denudata*, *Hebeloma* and *Velutipes*) include a number of species that can only be distinguished by one of these loci, or by a combination of two loci or by combining molecular results and morphology. Also, a number of species are not monophyletic, even if all loci are concatenated. Although many species cannot be distinguished by ITS alone, the combination of ITS and morphology normally allows species identification (Beker et al. 2016).

Pruned median joining networks (Ayling and Brown 2008) are calculated to analyze the ITS results. Networks rather than trees are used to visualize DNA sequence variation when evolution has not been unidirectional. No assumptions are made with regard to which evolutionary mechanisms have been responsible for the observed variation. As in Cripps et al. (2019), it is not possible to unambiguously determine haplotypes from many sequences, i.e. when PCR was only successful in two fragments or when ambiguity in more than one single base pair position existed that was not accompanied by length variation. Therefore, we used as input for the network analysis what we refer to as "ITS variants", for each collection, a consensus sequence of the ITS, whether or not intragenomic variation occurred. In the case of length variation, indels were treated as insertions.

Hebeloma in Greenland and similar arctic (and alpine) areas

Lange (Lange 1957) collected in Greenland in 1946 and recorded four species: *Hebeloma mesophaeum*, *H. longicaudum*, *H. pusillum* and *H. strophosum*. His material has not been revised for this study, which is solely based on sequenced samples. Of his four species, we confirmed the presence of *H. mesophaeum*, but the three other named species are open to interpretation. *Hebeloma longicaudum* (Pers.) P. Kumm. is considered to be impossible to typify in accordance with the diagnosis. *Hebeloma pusillum* J.E. Lange is a species forming small basidiomes and was described from *Salix* scrublands in Denmark. According to Beker et al. (2016) this species does not occur in arctic and subarctic areas of northern Europe; the symbiont is not dwarf *Salix*, but rather larger *Salix* in bogs and fens, such as *S. aurita* L., *S. atrocinerea* Brot. and *S. cinerea* L. *Hebeloma strophosum* (Fr.) Sacc. is now (Beker et al. 2016) considered to be a synonym of *H. mesophaeum*.

Petersen (1977) also reported *H. mesophaeum* and *H. pusillum*, referring to Gulden and Lange (1971), and he added *H. crustuliniforme*, material, which is more likely to have represented *H. alpinum* or *H. velutipes*. Lamoure et al. (1982) reported *H. kuehneri* (= *H. nigellum*) from Disko Island, from where we have later also recorded it.

Watling (1977) reported *H. marginatulum* and *H. versipelle*, noting that the latter was probably included in Lange's (1957) concept of *H. mesophaeum*. According

to Beker et al. (2016), *H. versipelle* is probably synonymous with *H. mesophaeum*, although synonymy with *H. dunense* cannot be excluded. Watling (1983) reported *H.* aff. *leucosarx*, *H. marginatulum* and *H. mesophaeum*, revising collections from A. Erskine (NE Greenland, in the surroundings of Mestersvig airstrip) and A. Fox (Eqalummiut Nunaat). All of these species are here confirmed for Greenland, although *H. populinum* Romagn., mentioned by Watling as similar to his *H.* aff. *leucosarx*, is not and in fact is not known to occur north of the southern part of the British Isles. According to modern taxonomy, *H. populinum* is a member of *H.* sect. *Denudata*, and not a close relative of *H. leucosarx* which is a member of *H.* sect. *Velutipes* (Beker et al. 2016).

When Vesterholt (1989) revised the veiled species of *Hebeloma* in the Nordic countries, he included material from Greenland of *H. helodes*, *H. leucosarx* and *H. marginatulum*. Later Vesterholt (2005) added *H. alpinum*, *H. nigellum* (as *H. kuehneri*), *H. subconcolor* and *H. vaccinum* in his book "The Genus *Hebeloma*" and finally he added *H. dunense* (as *H. collariatum*). Two species reported in Borgen et al. (2006), *H. sinapizans* and *H. monticola*, are not among the material in this survey, and at least *H. sinapizans* is unlikely to be found. The collections ascribed to *H. sinapizans* may have represented *H. alpinum* or *H. geminatum*, the former in at least one case. Some, at least, of the collections of *H. monticola*, are now known to represent either *H. nigellum* or *H. oreophilum*, although it is likely that *H. monticola* may indeed be present in Greenland, particularly in the southern, subarctic areas.

Given the problems with interpretation of *Hebeloma* species names, in particular from the pre-molecular era, and therefore the application of taxon names, we will not make further reference to these studies. A small number of studies of other alpine or arctic regions have been published which use names in the same manner as here. Recently, Eberhardt et al. (2015a) described new species of *Hebeloma* from the alpine belt of the Carpathians. Beker et al. (2016) dedicated part of a chapter to alpine/arctic *Hebeloma*, identifying 17 species as 'specialists' and 8 species as 'opportunists' in these habitats in Europe. Beker et al. (2018) reviewed *Hebeloma* in Svalbard and recorded 17 species, of which five were only known from Svalbard. Cripps et al. (2019) described *Hebeloma* from the alpine Rocky Mountains in USA and found 16 species, of which one was subalpine and connected to conifers. Most recently, Grilli et al. (2020) presented seven species of *Hebeloma* from the Alps. This does not mean that, for example, we consider reports of *H. alpinum*, *H. marginatulum* or *H. mesophaeum* from various parts of the Russian Arctic or Alaska (Nezdoiminogo 1994; Miller 1998; Karatygin et al. 1999; Shiryaev et al. 2018; Gorbunova 2019) as unlikely, but we prefer to be consistent in referring only to material we have been able to validate.

Bioclimatic zones and the collecting sites in Greenland

Greenland is an island, which for the greater part is covered by an ice cap, the Inland Ice. The island is biogeographically divided into four parts. South Greenland is the area south of 62.20°N. West Greenland is the area from 62.20°N to 74°N on the western

side of the island. North Greenland is the area north of 74°N, and East Greenland the area on the eastern side between 74°N and 62.20°N.

The length of the island is ca. 2000 km, but only two bioclimatic zones are present, the Subarctic zone and the Arctic (or Polar) zone (Fredskild 1996). The Subarctic zone has a climate where the warmest month has an average temperature above 10 °C. This area is very small and restricted to the bottom of some of the fjords in South Greenland around Narsarsuaq. The outer part of the fjords is moist and cool, but in the protected inner parts, the temperature may rise during the summer to reach an average 10 °C for July. Botanically, this Subarctic zone is defined by the coincident occurrence of the two plants, *Sagina nodosa* and *Eleocharis quinqueflora*. The interest for *Hebeloma* lies in the occurrence of woodland with large specimens of *Betula pubescens* var. *pumila* (L.) Govaerts in a few valleys (Feilberg 1984), associated with a number of subarctic fungi (Elborne and Knudsen 1990). All other parts of Greenland are arctic. This is separated into the Low Arctic zone and the High Arctic zone. This separation (Fig. 1A) is important for the distribution of many organisms including fungi. The dividing line runs from the central part of Disko Island in the West across the Inland Ice to Blosseville Coast in the East, i.e. approximately along 70°N. The High Arctic zone has four months with an average temperature above 0 °C, whereas the Low Arctic zone has six months above 0 °C.

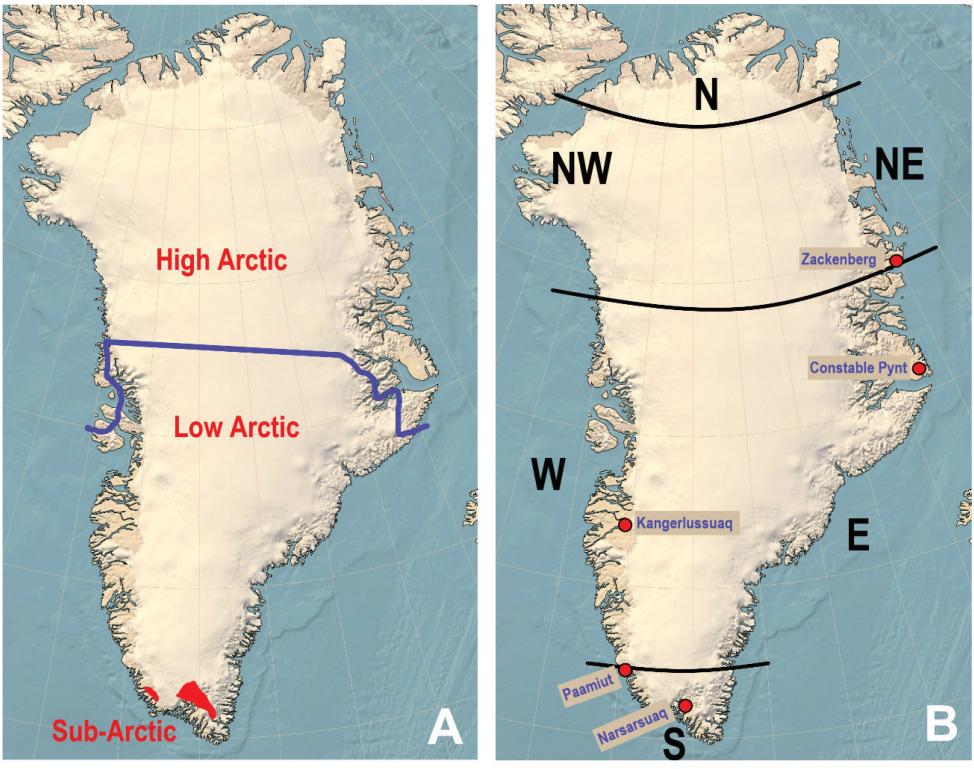

Figure 1. A Demarcation of Low and High Arctic, and **B** limits of North, East, West and South Greenland and location important collection sites.

Collection sites are not distributed uniformly throughout Greenland since many areas are difficult to access. Collecting activities were concentrated on a few localities scattered over the accessible part of Greenland (Fig. 1B), taking into account the variation in the climate, soil and vegetation that defines the funga on this big island. A reflection of this is seen in the maps, where dots are always absent from some parts of Greenland, due to inaccessibility. This is especially true for NW Greenland (Melville Bay), where the Inland Ice comes out to the sea, leaving little opportunity for fungal life. The other area where records are generally missing is the southern half of the east coast, i.e. from the southernmost point in Greenland and up to Jameson Land on the East side. This is generally inaccessible, or extremely difficult to access, but a few collections were made by T.B. at Tasiilaq/Ammassalik. Finally, northernmost Greenland is an arctic desert, where the snowfall is generally too low to support fungi. Thus, our five main localities are Narsarsuaq, Paamiut, Kangerlussuaq, Zackenberg and Jameson Land.

Narsarsuaq at 60°N

A well-investigated area housing one of the two airports, which receives regular air traffic from Copenhagen. Generally a Low Arctic area, but at the bottom of some of the fjords the climate is Subarctic, and scrubland of *Betula pubescens* var. *pumila* occurs. The trunks attain heights up to 7–8 m and diameters to ca. 30 cm. Apart from these scrublands, occurring in a very restricted area, *Betula glandulosa* Michaux is widespread and common in the area. *Salix glauca* L. is ubiquitous, forming 1–3 m high shrubs, *S. arctophila* Cockerell and *S. herbacea* L. are common, while *S. uva-ursi* Pursh is rare and scattered. *Dryas integrifolia* M. Vahl is scattered. The soil is mixed, but generally rich in the valleys.

Paamiut at 62°N

This is the best studied area in Greenland for fungi as T.B. lived here for 20 years. The bedrock is acidic gneiss, in places with weathered basaltic dykes, and areas with less acid, syanitic "rotten" mountains. The climate is Low Arctic and hyper oceanic along the coast with heaths and snowbeds with *Salix herbacea*. Inland, *Betula glandulosa* heaths and copses of *Salix glauca* dominate. In addition to these widespread and common types of vegetation, a few scrubland areas of *Alnus alnobetula* subsp. *crispa* (Aiton) Raus. as well as *Dryas integrifolia* occur. *Betula pubescens* Erh. also grow here rarely, close to its northern limit.

Kangerlussuaq at 67°N

A well-studied area for the same reason as Narsarsuaq, in that the presence of an airport implies regular air traffic from Copenhagen. The area is Low Arctic and the bottom of the Kangerlussuaq Fjord (formerly Søndre Strømfjord) is the most continental area in Greenland, warm and dry in the summertime and even with salt lakes. The vegetation consists of low shrubs of *Betula nana* L., *Salix glauca*, *S. herbacea* and *S. arctophila*.

Dryas integrifolia is common. The soil along the river and fjord is generally very rich due to loess coming from the Inland Ice with the rivers and with the wind, but the surrounding bedrock is acidic gneiss.

Zackenberg at 74.5°N

This area has been studied over the last 25 years, since the establishment of a field station in this High Arctic part of the Greenland National Park. Fungi were studied during two seasons by T.B. The shrub vegetation is *Betula nana*, *Salix arctica* Pall., *S. herbacea*, *Dryas integrifolia* and *D. octopetala* ssp. *punctata* (Juz.) Hult. The bedrock is gneissic or sedimental, mixed on the plains.

Constable Pynt, Jameson Land at 70.8°N

The area is situated on the border between Low Arctic and High Arctic and is accessible during summertime from Iceland. We studied the area in 1989 and in 2017. The bedrock is calcareous and the soil is generally nutrient rich. The vegetation is shrubs of *Betula nana*, *Salix arctica*, *S. glauca* and *Dryas octopetala* L.

Materials and methods

Collections

This study is based on 378 collections of *Hebeloma* from Greenland, which yielded (at least) ITS sequence data. Collections, which did not produce a sequence, are not considered further in this paper.

T.B., S.A.E. and H.K. collected 325 of the included collections over a period of 40 years. The remaining 56 collections were collected by Erik Rald (21), David Boertmann (9), Esteri Ohenoja (5, Herb. OULU), H.J.B. (4, HJB), Bent Fredskild (4), Egon Horak (2, Herb. ZT), Christian Bay (2), T.T. Elkington (2), Børge Lauritsen (2), Thomas Læssøe (2), Jens H. Petersen (1), Kuulo Kalamees (1) and Birger Knudsen (1). Many collections are provided with notes and photos. Unless otherwise mentioned, all material is kept at the Fungarium at the Natural History Museum of Denmark (C) in Copenhagen.

Photos were taken in the field with a camera or with an iphone, and T.B. also often took a laboratory photo of the fresh specimens. Collections were dried on an electrical heater whenever possible. In uninhabited areas without access to electricity, a system was used with three sieves fastened on aluminium “legs” and surrounded by a cylinder of wax cloth, creating a closed column. The “legs” were fastened to the ground, and beneath the sieves, a small kerosene lamp was placed to dry the material overnight.

Molecular analyses

Dried collections were used as the source for genomic DNA. DNA extraction followed Cripps et al. (2019), with more recent material (i.e. younger than 20 years) omitting the pre-lysis incubation with lytic enzyme and omitting the lysis step overnight at 37 °C. Also, the time for DNA precipitation was shortened to 15–60 min.

PCR followed Cripps et al. (2019), but using the standard primer combination of ITS1F and ITS4 (White et al. 1990; Gardes and Bruns 1993) for more recent material. Partial *RPB2* PCR products (encoding the second largest subunit of RNA polymerase II; forward primer bRPB2-6f 'TGG GGY ATG GTN TGY CCY GC', Matheny 2005; and reverse fRPB2-7cr 'CCC ATR GCT TGY TTR CCC AT', Liu et al. 1999) were generated in 25 µl PCR reactions, using hotstart Taq polymerase, i.e. 1.25u Bioline (London, UK) MyTaq HS DNA Polymerase, 5 µl of 5× buffer, 20 pmol of each primer and 10% (2.5 µl) of 1:25 diluted DNA extract. PCRs were run with 5 min 95 °C, 40 cycles of 1 min 95 °C, 1 min 50 °C, 2 min 72 °C, and a final elongation of 5 min at 72 °C. The PCR cocktail for partial *Tef1*a, other than primers (translation elongation factor 1-α; forward primer elo31m 'TTC ATC AAG AAC ATG ATC AC' and reverse elo33R_A 'GAC GTT GAA ACC RAC RTT GTC', modified from Stielow et al. 2015) and Taq (MyTaq DNA polymerase, Bioline) was the same as for *RPB2*; PCRs were run as follows: 5 min 95 °C, 10 cycles of 45 sec 95 °C, 45 sec 58 °C, 1 min 72 °C, 35 cycles of 45 sec 95 °C, 45 sec 48 °C, 1 min 72 °C, and a final elongation of 5 min at 72 °C.

Sequencing was done by LGC Genomics (Berlin, Germany), using the PCR primers as sequencing primers. Sequences were edited using Sequencher (vs. 4.2 or 4.8). Newly generated sequences were submitted to GenBank (accession nos MW357874–MW357877, MW357892–MW357897, MW445544–MW445902, MW452577–MW452595, MW465762, MW465838 and MW465839). Other sequences used were previously published by Eberhardt et al. (2009, 2015a, b, 2016, 2018), Beker et al. (2010, 2013, 2016), Schoch et al. (2012), Grilli et al. (2016) and Cripps et al. 2019). Table 1 lists the GenBank accession numbers for the Greenland material treated in this paper.

Sequences were aligned in Mafft v. 7 online (https://mafft.cbrc.jp/alignment/server/, Katoh et al. 2019), using the G-INS-i method for ITS sequences for networks and the E-INS-i for ITS, *RPB2* and *Tef1*a data for the tree analysis.

Following Cripps et al. (2019), pruned quasi-median joining networks (Ayling and Brown 2008) were used to visualize the biological diversity of ITS sequences generated from Greenland collections. In the networks, observed sequence variants are shown as circles and the size of each circle gives some indication of the number of times the respective sequence variant has been retrieved. Two circles connected by an unsegmented line differ in 1 bp. So-called quasimedians, a kind of placeholder for unobserved sequence variants depicted as small squares, are placed between observed sequence variants that each differ from the quasi-median by 1 bp. The number of

Table 1. *Hebeloma* database references (see Beker et al. 2016), voucher information and Genbank accession numbers of Greenland collections considered in this study. For details, see Materials and Methods. Vouchers are from the fungal collection of the Herbarium of the University of Copenhagen (C), of the University of Oulu (OULU) or the collection of E. Horak at the herbarium of the Eidgenössische Technische Hochschule Zürich (ZT) or from the private collection of H.J. Beker.

Hebeloma Database reference	Voucher	Other Number	Genbank acc. no. ITS
Hebeloma alpinicola			
HJB15784	C-F-119805	TB99.238	MW445632
HJB16321	C-F-5081	TB85.071	MW445633
HJB16322	C-F-5082	TB85.099	MW445634
HJB16580	C-F-103554	TB81.111	MW445635
HJB16585	C-F-103532	TB85.218	MW445636
HJB16605	C-F-103516	TB00.049	MW445637
HJB16664	C-F-103534	TB84.063	MW445638
HJB16688	C-F-103559	TB84.028	MW445639
HJB17503	C-F-101623	TB08.039	MW445640
HJB17505	C-F-101621	TB08.037	MW445641
HJB17669	C-F-108401	HK16.165	MW445642
HJB18928	C-F-111109	HK18.010	MW445643
HJB18935	C-F-111116	HK18.322	MW445644
Hebeloma alpinum			
HJB11887	C-F-103458	TB86.115	MW445593
HJB12191	C-F-119742	TB99.027	MW445594
HJB12194	C-F-119744	TB99.023	KM390632, KM390633
HJB12204	C-F-104294	TB99.199	KM390685
HJB15711	C-F-119763	TB06.034	MW445544
HJB15714	C-F-119766	TB06.137	MW445545
HJB15785	C-F-119806	TB99.115	MW445548
HJB15786	C-F-119807	TB99.159	MW445549
HJB15787	C-F-119808	TB99.283	MW445550
HJB16276	C-F-101230	TB86.153	MW445551
HJB16581	C-F-103537	TB84.148	MW445552
HJB16591	C-F-103507	TB97.153a	MW445554
HJB16594	C-F-103506	TB97.152	MW445555
HJB16631	C-F-103565	TB86.141	MW445559
HJB16638	C-F-103503	TB95.004	MW445560
HJB17442	C-F-106779	TB17C.089	MW445564
HJB17445	C-F-106775	TB17C.053	MW445565
HJB17455	C-F-106784	TB17C.134	MW445566
HJB17458	C-F-105185	HK17.278	MW445567
HJB17459	C-F-104889	HK17.001	MW445568
HJB17461	C-F-105024	HK17.123	MW445569
HJB17467	C-F-104893	HK17.005	MW445570
HJB17470	C-F-105050	HK17.148	MW445571
HJB17475	C-F-104938	HK17.049	MW445595
HJB17476	C-F-104912	HK17.023	MW445572
HJB17477	C-F-104894	HK17.006	MW445573
HJB17482	C-F-104895	HK17.007	MW445575
HJB17486	C-F-104943	HK17.054	MW445576
HJB17491	C-F-106759	SAE-2017.014	MW445577
HJB17498	C-F-106758	SAE-2017.008	MW445579
HJB17509	C-F-106757	SAE-2017.006	MW445581
HJB17510	C-F-106766	SAE-2017.188	MW445582
HJB17663	C-F-104951	HK17.062	MW445586
HJB17687	C-F-5180	BF 90 loc. 6	MW445584
HJB18934	C-F-111115	HK18.308	MW445589
HJB18938	C-F-111119	HK18.390D	MW445591

Hebeloma Database reference	Voucher	Other Number	Genbank acc. no. ITS
Hebeloma arcticum			
HJB16618	C-F-103571	TB86.277A	MW445558
HJB16673	C-F-103555	TB90.083	MW445561
HJB16676	C-F-103483	TB90.071	MW445562
HJB16687	C-F-103584	TB16.095	MW445563
HJB17506	C-F-106751	TB08.153	MW445580
HJB17662	C-F-108472	SAE-2000.021-GR	MW445585
HJB17673	C-F-104149	HK16.119	MW445587
HJB17680	C-F-104080	HK16.044	MW445588
Hebeloma aurantioumbrinum			
HJB11884	C-F-119737	TB84.112	MW445897
HJB11885	C-F-2309	HK89.366	MW445896
HJB12189	C-F-119741	TB06.091	MW445899
HJB12205	C-F-119751	TB99.044	MW445898
HJB15716	C-F-119768	TB06.150	MW445858
HJB15719	C-F-119771	TB06.259	MW445859
HJB15740	C-F-119784	DB 85-17	MW357875†
HJB15741	C-F-119785	DB 85-28	MW357892‡
HJB15742	C-F-103459	TB85.239	MW445861
HJB15751	C-F-2327	SAE-89.121	MW445863
HJB15752	C-F-2424	SAE-89.430	MW445864
HJB15753	C-F-119787	DB GR88-22	MW445865
HJB15756	C-F-1461	SAE-88.149-GR	MW445866
HJB15757	C-F-119788	HK87.218	MW445867
HJB15758	C-F-119789	SAE-87.113-GR	MW445868
HJB15759	C-F-119790	HK87.004	MW445869
HJB15766	C-F-103462	TB84.135	MW445870
HJB15767	C-F-119792	TB84.150	MW445871
HJB15771	C-F-3637		MW445872
HJB15775	C-F-119797		MW445874
HJB16578	C-F-103461	TB84.132	MW445875
HJB16624	C-F-103502	TB93.070	MW445876
HJB16633	C-F-103570	TB86.251	MW445878
HJB16671	C-F-103484	TB90.072	MW445879
HJB16672	C-F-103546	TB90.039	MW445880
HJB16678	C-F-103481	TB90.041	MW445881
HJB16680	C-F-103545	TB90.029	MW445882
HJB16681	C-F-103482	TB90.057	MW445883
HJB16683	C-F-103547	TB90.012	MW445884
HJB16684	C-F-103548	TB90.011	MW445885
HJB16686	C-F-103485	TB90.133	MW445886
HJB16697	C-F-103526	TB85.217	MW445894
HJB17060	C-F-6992		MW445888
HJB17061	C-F-6993		MW445889
HJB17078	C-F-104315	ER93.262	MW445890
HJB17083	C-F-104321	ER93.091	MW445891
HJB17521	C-F-106745	SAE-2016.146	MW445892
HJB17674	C-F-104118	HK16.089	MW445893
HJB18933	C-F-111114	HK18.296	MW445895
HJB19596	C-F-103570	TB86.277B	MW445900
Hebeloma clavulipes			
HJB12316	C-F-119760	TB 90.100	MW357874†
Hebeloma colvinii			
HJB16630	C-F-103585	TB16.075	MW445745
HJB17502	C-F-106756	TB02.166	MW445746
HJB17684	C-F-104038	HK16.008	MW445747
HJB17685	C-F-104035	HK16.005	MW445748
HJB19653	C-F-107346	SAE-2016.188-GR	MW445749

Hebeloma Database reference	Voucher	Other Number	Genbank acc. no. ITS
Hebeloma dunense			
HJB12196	C-F-119746	TB99.114	MW445645
HJB12198	C-F-119748	TB99.411	MW445646
HJB12206	C-F-119752	TB99.219	MW445647
HJB15722	C-F-119774	TB06.159	MW445648
HJB15724	C-F-119776	TB06.263	MW445649
HJB16324	C-F-5087	TB86.159	MW445650
HJB16584	C-F-103530	TB85.200	MW445651
HJB16590	C-F-103486	TB91.045	MW445652
HJB16595	C-F-103536	TB84.114	MW445653
HJB16635	C-F-103563	TB86.177	MW445654
HJB16639	C-F-103589	TB85.183	MW445655
HJB16650	C-F-103527	TB85.186	MW445656
HJB16651	C-F-103535	TB84.090	MW445657
HJB17057	C-F-2561	JHP 89.259	MW445658
HJB17058	C-F-4216		MW445659
HJB17062	C-F-7017		MW445660
HJB17064	C-F-8231	HK15.078	MW445661
HJB17066	C-F-104293	TB16.076	MW445662
HJB17444	C-F-106782	TB17C.118	MW445663
HJB17449	C-F-106771	TB17C.010	MW445664
HJB17450	C-F-106770	TB17C.006	MW445665
HJB17452	C-F-106780	TB17C.094	MW445666
HJB17453	C-F-106773	TB17C.037	MW445667
HJB17456	C-F-106772	TB17C.030	MW445668
HJB17462	C-F-104959	HK17.070	MW445669
HJB17463	C-F-104932	HK17.043	MW445670
HJB17465	C-F-105171	HK17.265B	MW445671
HJB17466	C-F-105189	HK17.282	MW445672
HJB17471	C-F-104984	HK17.088	MW445673
HJB17474	C-F-104934	HK17.045	MW445674
HJB17481	C-F-105049	HK17.147	MW445675
HJB17483	C-F-105170	HK17.265A	MW445676
HJB17484	C-F-105108	HK17.203	MW445677
HJB17485	C-F-104941	HK17.052	MW445678
HJB17487	C-F-105028	HK17.127	MW445679
HJB17488	C-F-104945	HK17.056	MW445680
HJB17497	C-F-106765	SAE-2017.186	MW445681
HJB17507	C-F-106761	SAE-2017.103	MW445682
HJB17508	C-F-106769	SAE-2017.219	MW445683
HJB17678	C-F-104045	HK16.015	MW445684
HJB17688	C-F-6994		MW445685
HJB19155	C-F-7881	HK00-032	MW445686
Hebeloma excedens			
HJB13537	OULU F051033	EO19.8.00	MW445687
HJB16320	C-F-5073	TB85.238	MW445688
HJB16604	C-F-103517	TB00.086	MW445689
Hebeloma fuscatum			
HJB15739	C-F-119783	DB 85-21	MW445760
HJB17454	C-F-106783	TB17C.129	MW445787
HJB17473	C-F-104987	HK17.091	MW445789
HJB17478	C-F-104897	HK17.009A	MW445790
HJB17494	C-F-106768	SAE-2017.215	MW445791
HJB17517	C-F-106737	SAE-2016.072	MW445797
HJB18945	C-F-112530	TB18.243	MW445819
HJB18946	C-F-115623	DB 12.047	MW445820
Hebeloma geminatum			
HJB16588	C-F-103508	TB97.154a	MW445553
HJB16596	C-F-103514	TB00.065	MW445556

***Hebeloma* Database reference**	**Voucher**	**Other Number**	**Genbank acc. no. ITS**
HJB18936	C-F-111117	HK18.379B	MW445590
Hebeloma grandisporum			
HJB17067	C-F-104295	TB99.376	MW445784
HJB17460	C-F-104997	HK17.101	MW445788
Hebeloma helodes			
HJB15747	C-F-103460	TB85.072	MW445862
HJB15748	C-F-103476	TB85.090	MW357894‡
HJB15780	C-F-4003	TB88.114	MW445873
HJB16627	C-F-103525	TB85.065	MW445877
HJB17044	C-F-104317	ER93.153	MW445887
Hebeloma hiemale			
HJB12193	C-F-119743	TB06.067	GQ869517
HJB12195	C-F-119745	TB99.258	GQ869515
HJB12200	C-F-104296	TB99.146	GQ869524
HJB12202	C-F-119777,	TB06.081	GQ869518
HJB12210	C-F-119756	TB99.118	GQ869516
HJB12544	Coll. E. Horak at ZT 8901		GQ869527
HJB13538	OULU F050202	EO12.8.00	MW445631
HJB15712	C-F-119764	TB06.250	MW445596
HJB15713	C-F-119765	TB06.120	MW445597
HJB15715	C-F-119767	TB06.128	MW445598
HJB15717	C-F-119769	TB06.061	MW445599
HJB15718	C-F-119770	TB06.033	MW445600
HJB15736	C-F-103465	TB91.136	MW445601
HJB15737	C-F-119782	TB91.112	MW445602
HJB15743	C-F-103466	TB85.182	MW445603
HJB15746	C-F-119786	TB85.250	MW357893‡
HJB15770	C-F-119794	TL 84.608	MW357895‡
HJB15781	C-F-119802	TB99.280	MW445604
HJB15782	C-F-119803	TB99.304	MW445605
HJB15788	C-F-119809	TB99.160	MW445606
HJB16600	C-F-103515	TB00.069	MW445607
HJB16616	C-F-103497	TB93.183	MW445608
HJB16619	C-F-103499	TB93.210	MW445609
HJB16621	C-F-103498	TB93.187	MW445610
HJB16622	C-F-103500	TB93.155	MW445611
HJB16628	C-F-103552	TB81.112	MW445612
HJB16636	C-F-103496	TB93.159	MW445613
HJB16659	C-F-103543	TB90.032	MW445614
HJB16666	C-F-103540	TB90.087	MW445615
HJB16667	C-F-103549	TB90.084	MW445616
HJB16674	C-F-103544	TB90.019	MW445617
HJB16675	C-F-103568	TB86.203	MW445618
HJB16685	C-F-103550	TB90.104a	MW445619
HJB16692	C-F-103504	TB95.114	MW445620
HJB17042	C-F-104550	ER93.330	MW445621
HJB17043	C-F-104292	TB98.201	MW445622
HJB17045	C-F-104551	ER93.302	MW445623
HJB17080	C-F-104318	ER93.152	MW445624
HJB17443	C-F-106776	TB17C.072	MW445625
HJB17446	C-F-106777	TB17C.078	MW445626
HJB17501	C-F-106752	TB08.157	MW445627
HJB18931	C-F-111112	HK18.269	MW445628
HJB18941	C-F-112771	SAE-2018.225-GR	MW445629
HJB18942	C-F-112904	SAE-2018.357-GR	MW445630
Hebeloma hygrophilum			
HJB16647	C-F-103511	TB98.234	MW357897‡
HJB17041	C-F-104549	ER93.425	MW445783
HJB17516	C-F-106736	SAE-2016.022	MW445796

Hebeloma Database reference	Voucher	Other Number	Genbank acc. no. ITS
HJB17520	C-F-106735	SAE-2016.005	MW445799
HJB17522	C-F-106741	SAE-2016.105	MW445800
HJB17523	C-F-106746	SAE-2016.168	MW445801
HJB17524	C-F-106742	SAE-2016.116	MW445802
HJB17661	C-F-108600	SAE-2000.148-GR	MW445803
HJB17667	C-F-108446	HK16.195	MW445804
HJB17681	C-F-104093	HK16.064	MW445811
HJB18937	C-F-111118	HK18.390A	MW445815
HJB18943	C-F-115622	SAE-2018.429-GR	MW445817
HJB18944	C-F-112528	TB18.236	MW445818
HJB19151	C-F-105494	ER93.519	MW445813
HJB19710	C-F-137115	TB19.052	MW445821
Hebeloma ingratum			
HJB10797	C-F-119732	HK87.262	KT217437
HJB13546	OULU F050503	EO18.8.00.36	MW445837
HJB16620	C-F-103501	TB93.205	MW445826
HJB17513	C-F-106748	SAE-2016.208	MW445831
Hebeloma islandicum			
HJB16632	C-F-103573	TB86.291	MW445901
Hebeloma leucosarx			
HJB16656	C-F-103513	TB98.119	MW445844
HJB16658	C-F-103551	TB81.211	MW445845
Hebeloma louiseae			
HJB16602	C-F-103518	TB00.061	MW445557
HJB17479	C-F-105029	HK17.128	MW445574
HJB17493	C-F-106763	SAE-2017.125A	MW445578
HJB17519	C-F-106747	SAE-2016.197	MW445583
HJB19601	C-F-106763	SAE-2017.125B	MW445592
Hebeloma marginatulum			
HJB10730	Priv. coll. HJB10730		MW445690
HJB10732	Priv. coll. HJB10732		MW445691
HJB10739	Priv. coll. HJB10739		MW445692
HJB10742	Priv. coll. HJB10742		MW445693
HJB12197	C-F-119747	TB06.090	MW445694
HJB15723	C-F-119775	TB06.158	MW445695
HJB15727	C-F-119779	TB06.090	MW445696
HJB15762	C-F-103467	TB86.247	MW445697
HJB16323	C-F-5085	TB85.036	MW445698
HJB16327	C-F-5090	TB86.072	MW445699
HJB16612	C-F-103489	TB91.198	MW445700
HJB16623	C-F-103495	TB93.139	MW445701
HJB16646	C-F-103566	TB86.119	MW445702
HJB16652	C-F-103493	TB92.027	MW445703
HJB16654	C-F-103492	TB92.028	MW445704
HJB16663	C-F-103553	TB81.109	MW445705
HJB16665	C-F-103538	TB84.151	MW445706
HJB16691	C-F-103505	TB95.068	MW445707
HJB17049	C-F-104552	ER93.320	MW445708
HJB17050	C-F-104300	TB86.299	MW445709
HJB17051	C-F-104306	ER92.181	MW445710
HJB17052	C-F-104314	ER93.181	MW445711
HJB17059	C-F-6922	TB86.060	MW445712
HJB17070	C-F-104304	ER92.109	MW445713
HJB17071	C-F-104305	ER92.180	MW445714
HJB17077	C-F-104312	ER93.111	MW445715
HJB17081	C-F-104319	ER93.021	MW445716
HJB17086	C-F-104554	ER93.589	MW445717
HJB17457	C-F-106421	ER93.112	MW445718

Hebeloma Database reference	Voucher	Other Number	Genbank acc. no. ITS
HJB17489	C-F-105051	HK17.149	MW445719
HJB17490	C-F-106738	SAE-2016.085	MW445720
HJB17499	C-F-106749	TB08.126	MW445721
HJB17500	C-F-106753	TB09K017	MW445722
HJB17525	C-F-101622	TB08.035	MW445723
HJB17526	C-F-106750	TB08.146	MW445724
HJB17658	C-F-108419	HK16.181	MW445725
HJB17666	C-F-108418	HK16.180	MW445726
HJB17677	C-F-104164	HK16.134	MW445727
HJB17683	C-F-104111	HK16.082	MW445728
HJB17686	C-F-5113	BF 90 loc. 5	MW445729
HJB17689	C-F-5147	BF 90 loc. 8	MW445730
HJB18932	C-F-111113	HK18.288	MW445731
Hebeloma mesophaeum			
HJB12213	C-F-104297	TB99.264	MW445735
HJB12313	C-F-119759	TB90.040	MW465762
HJB13560	OULU F050224	EO12.8.00.1	MW445736
HJB16348	C-F-76757	TB90.086	MW445732
HJB16598	C-F-103521	TB00.093	MW445737
HJB16601	C-F-103522	TB00.094	MW445738
HJB16603	C-F-103520	TB00.091	MW445739
HJB16629	C-F-103578	TB16.040G	MW445740
HJB17068	C-F-104301	TB16.038	MW445741
HJB17464	C-F-104908	HK17.020	MW445733
HJB19682	C-F-137116	TB00.088	MW445734
Hebeloma minus			
HJB15745	C-F-104302	TB86.085	MW445546
HJB15769	C-F-119793	TL 84.041	MW445547
Hebeloma nigellum			
HJB10957	C-F-119734	DB GR83-80	MW445750
HJB11874	C-F-103468	TB84.183	MW445752
HJB11888	C-F-119739	TB86.052	MW445751
HJB12545	Coll. E. Horak at ZT 9139		MW445756
HJB13559	OULU F050653	EO19.8.00.20	MW445758
HJB15761	C-F-119791	TB86.065	MW445761
HJB16592	C-F-103577	TB16.035G	MW445764
HJB16606	C-F-103490	TB91.080	MW445766
HJB16634	C-F-103572	TB86.276	MW445769
HJB16657	C-F-103529	TB85.249	MW445773
HJB16670	C-F-103479	TB90.035	MW445776
HJB16677	C-F-103541	TB90.073	MW445777
HJB16679	C-F-103542	TB90.056	MW445778
HJB16694	C-F-103583	TB16.086G	MW445781
HJB16696	C-F-103580	TB16.060G	MW445782
HJB17518	C-F-106743	SAE-2016.131	MW445798
HJB17670	C-F-108402	HK16.165A	MW445805
HJB17675	C-F-104140	HK16.110	MW445808
HJB17676	C-F-104163	HK16.133	MW445809
HJB17679	C-F-104063	HK16.033	MW445810
HJB18929	C-F-111110	HK18.199	MW445814
Hebeloma oreophilum			
HJB11889	C-F-119740	TB85.180	MW445755
HJB12199	C-F-119772	TB06.225	MW445757
HJB12212	C-F-119758	TB99.374	MW445753
HJB15721	C-F-119773	TB06.098	MW445759
HJB15768	C-F-104298	TB84.215	MW445762
HJB16589	C-F-103539	TB84.184	MW445763
HJB16599	C-F-103576	TB16.017G	MW445765

Hebeloma Database reference	Voucher	Other Number	Genbank acc. no. ITS
HJB16611	C-F-103487	TB91.233	MW445767
HJB16613	C-F-103588	TB86.292	MW445768
HJB16644	C-F-103510	TB98.120	MW445770
HJB16645	C-F-103509	TB98.073	MW445771
HJB16648	C-F-103590	TB85.061	MW445772
HJB16668	C-F-103472	TB83.035	MW445774
HJB16669	C-F-103558	TB90.010	MW445775
HJB16682	C-F-103480	TB90.036	MW445779
HJB17515	C-F-106744	SAE-2016.134	MW445795
HJB17672	C-F-104120	HK16.091	MW445807
HJB18939	C-F-111120	HK18.401	MW445816
Hebeloma pubescens			
HJB12203	C-F-119750	TB99.194	MW445742
HJB12207	C-F-119753	TB99.305	MW445743
HJB16326	C-F-5089	TB86.128	MW445744
Hebeloma spetsbergense			
HJB10869	C-F-119733	SAE-1986.135-GR	MW445822
HJB12211	C-F-119757	TB99.256	MW445754
HJB15763	C-F-103478	TB86.121	MW357896‡
HJB15779	C-F-119801	DB 83-62	MW357877†
HJB16693	C-F-103579	TB16.056G	MW445780
HJB17447	C-F-106781	TB17C.113	MW445785
HJB17448	C-F-106774	TB17C.050	MW445786
HJB17495	C-F-106764	SAE-2017.174	MW445792
HJB17496	C-F-106760	SAE-2017.043	MW445793
HJB17514	C-F-106740	SAE-2016.102	MW445794
HJB17671	C-F-108450		MW445806
HJB17682	C-F-104100	HK16.071	MW445812
Hebeloma subconcolor			
HJB12413	C-F-119761	TB90.018	KT218391
HJB15750	C-F-2195	HK89.302	MW445840
HJB15760	C-F-4002	TB87.117	MW445841
HJB16579	C-F-103587	TB86.122	MW445902
HJB17055	C-F-104299	TB90.033	MW445848
HJB17056	C-F-104313	ER93.168	MW445849
HJB17065	C-F-8242	HK15.089	MW445847
HJB17512	C-F-106739	SAE-2016.090	MW445852
HJB18930	C-F-111111	HK18.232	MW445855
Hebeloma vaccinum			
HJB12190	C-F-119780,	TB06.246	KT217493
HJB12209	C-F-119755	TB99.109	KT217494
HJB15749	C-F-103477	TB85.045	MW357876†
HJB15783	C-F-119804	TB99.008	MW445838
HJB17063	C-F-8222	HK15.069	MW445833
HJB17073	C-F-104308	ER92.038	MW445834
HJB17076	C-F-104311	ER92.323	MW445835
HJB17082	C-F-104320	ER93.022	MW445836
HJB17451	C-F-106778	TB17C.073	MW445827
HJB17469	C-F-104909	HK17.021	MW445828
HJB17472	C-F-104910	HK17.022A	MW445829
HJB17492	C-F-106767	SAE-2017.194	MW445830
HJB17664	C-F-104911	HK17.022B	MW445832
Hebeloma velutipes			
HJB12201	C-F-119749	TB99.336	MW445857
HJB12208	C-F-119754	TB99.309	MW445856
HJB15730	C-F-103557	TB86.179	MW445839
HJB16597	C-F-103519	TB00.073	MW445842
HJB16655	C-F-103512	TB98.158	MW445843
HJB16689	C-F-103582	TB16.087G	MW445846

Hebeloma Database reference	Voucher	Other Number	Genbank acc. no. ITS
HJB17468	C-F-105090	HK17.186	MW445850
HJB17511	C-F-106762	SAE-2017.110	MW445851
HJB17659	C-F-108492	SAE-2000.041-GR	MW445853
HJB17660	C-F-108502	SAE-2000.051-GR	MW445854

† ITS1 only; ‡ ITS2 only.

segments to a line represents the number of base pair changes between two sequence variants or a sequence variant and a quasi-median. A pruning mechanism is applied to reduce the complexity of the networks while depicting at least one shortest path between all pairs of sequence variants (Ayling and Brown 2008).

Only complete ITS sequences were considered. The Greenland sequences were incorporated in alignments previously published by Cripps et al. (2019). *Hebeloma ingratum* was not encountered by Cripps et al. (2019), but is present in the Greenland sample. Thus the *H. cavipes*/*H. vaccinum* dataset was extended by 10 randomly selected *H. ingratum* sequences from Europe. Because of the large number of sequences, and because there was no overlap between *H. marginatulum* and the other members of the species group around *H. mesophaeum*, *H. marginatulum* sequences were analyzed in a separate analysis. *Hebeloma incarnatulum*, a boreal species included by Cripps et al. (2019) in the *H.* sect. *Velutipes* network, was excluded from the analysis as it had no corresponding data in the Greenland sample. Alignments are published in TreeBase (Study ID TB2:S27569), where GenBank acc. numbers for all sequences used are given.

Networks were calculated in SplitsTree (version 4.15.1, Huson and Bryant 2006) with the default options other than activating the 'scale nodes by taxa' and 'subdivide edges' options. Nodes representing different classes of sequences (differentiated by species and origin, 'Greenland' versus 'outside Greenland') were replaced in Adobe Illustrator CS6 by pie charts of corresponding diameters, showing the relative numbers of sequences for each class.

For showing the phylogenetic placement of the newly described species *H. arcticum*, a tree analysis of members of *H.* subsect. *Crustuliniformia* was included, based on concatenated data of ITS, *RPB2* and *Tef1*a. Table 2 lists the respective GenBank asscion numbers. Tree analyses were done locally in RAxML (Stamatakis 2014) using raxmlGUI v. 2.0 (Edler et al. 2020), using the "ML + rapid bootstrap" option, determining the number of bootstrap replicates by the autoMRE method. Prior to concatenation, single locus trees (see Treebase submission) were generated. No conflicts were detected using the principle by Kauff and Lutzoni (2002), assuming a conflict to be significant if two different relationships for the same set of taxa, one being monophyletic and the other non-monophyletic, are supported by bootstrap with more than 70% in ML analyses. Based on the results of Eberhardt et al. (2015b), the data were analyzed unpartitioned. *Hebeloma louiseae* was used for rooting following Beker et al. (2016).

Morphological methods

All microscopical analysis was carried out on dried material, using a Leica DMRZA2 microscope with a Leica DFC495 camera connected to a computer running Leica

Table 2. *Hebeloma* database references (see Beker et al. 2016), country, voucher and GenBank accession numbers of sequences used for the ML analysis (Fig. 5B). BR-MYCO, C-F and L refer to the fungal collections of the Meise Botanic Garden (BR), the Herbarium of the University of Copenhagen (C), or Naturalis, Leiden (L), respectively. Vouchers with numbers starting with AdH, AT, or HJB are from the private collections of A.F.S. Taylor, A. de Haan or H.J. Beker.

Hebeloma database reference	Country	Voucher	ITS GenBank acc. no.	*Tef1a* GenBank acc. no.	*Rpb2* GenBank acc. no.
Hebeloma aanenii					
HJB10282	Belgium	HJB10282	JN943877	KT216789	KF309471
HJB10670	Sweden	AT2003063	KM390550	KT216808	KM390126
HJB12630 holotype	Poland	BR-MYCO 173987-66	KM390723	KT216852	KM390169
Hebeloma alpinum					
HJB11051	Iceland	HJB11051	JN943865	MW452578	KF309496
HJB11094	Switzerland	HJB11051	KM390594 KM390595	KT216817	KM390142
HJB11117	Switzerland	HJB11051	KM390593	KT216819	KM390141
Hebeloma arcticum					
HJB16687	Greenland	C-F-103584	MW445563	MW452581	MW452590
HJB17506	Greenland	C-F-106751	MW445580	MW452583	MW452592
HJB17673 holotype	Greenland	C-F-104149	MW445587	MW452584	MW452593
HJB17680	Greenland	C-F-104080	MW445588	MW452585	MW452594
Hebeloma aurantioumbrinum					
HJB12058 holotype	Norway, Svalbard	BR-MYCO 173985-64	KM390686 KM390687	KT216845	KM390158
HJB12445	U.S.A.	HJB12445	KM390714 KM390715	KT216851	KM390166
HJB12451	U.S.A.	HJB12451	KM390720 KM390721	MW452577	KM390168
Hebeloma crustuliniforme					
HJB11237	Spain		JN943870	KT216824	KF309480
HJB12807	Netherlands	L WBS 9581	KF309415	KT216854	KF309492
HJB13713 epitype	France	BR-MYCO 173989-68	KF309424	KT216860	KF309495
Hebeloma eburneum					
HJB9267	U.K., England	HJB9267	JN943880	KT216777	KF309468
HJB10290	Belgium	HJB10290	KM390533 KM390534	KT216792	KM390113
HJB12670	Poland	HJB12670	KM390727 KM390728	KT216853	KM390171
Hebeloma geminatum					
HJB8633	Belgium	HJB8633	KM390526	KT216769	KM390109
HJB10384	U.K., England	HJB10384	KF309400	KT216794	KF309472
HJB10833 holotype	Denmark	C-F-90152	KF309405	KT216815	KF309478
Hebeloma helodes					
HJB8115	U.K., Wales	HJB8115	KM390527	KT216768	KM390110
HJB10680	U.K., England	HJB10680	KM390548	KT216810	KM390124
HJB11698	France	HJB11698	KM390622	KT216831	KM390151
Hebeloma louiseae					
HJB11984	Norway, Svalbard	HJB11984	KM390705	KT216839	KM390164
HJB16602	Greenland	C-F-103518	MW445557	MW452580	MW452589
HJB19601	Greenland	C-F-106763	MW445592	MW452586	MW452595
Hebeloma luteicystidiatum					
HJB11837 holotype	Belgium	BR-MYCO 166233-72	KM390624	KT216837	KM390152
HJB12174	Belgium	HJB12174	KM390710		KT216978
HJB16715	France	HJB EG-151028.02	MW465839	MW452582	MW452591
Hebeloma lutense					
HJB 9819	U.K., Scotland		JN943871	KT216783	KF309479
HJB 10523	Belgium	AdH04059	KM390541	KT216798	KM390119
HJB11328	France	HJB11328	JN943864	KT216825	KF309486

Hebeloma database reference	Country	Voucher	ITS GenBank acc. no.	*Tef1a* GenBank acc. no.	*Rpb2* GenBank acc. no.
Hebeloma matritense					
HJB9485 holotype	Spain	BR-MYCO 174910-19	KT217364	KT216781	KT216879
HJB9486	Spain	HJB9486	KT217365	KT216782	KT216880
Hebeloma minus					
HJB11079	Iceland	HJB11079	JN943866	KT216816	KF309481
HJB11107	Switzerland	HJB11107	JN943868	KT216818	KF309483
HJB12007	Norway, Svalbard	HJB12007	JN943857	KT216842	KF309488
Hebeloma pallidolabiatum					
HJB11992 holotype	Norway, Svalbard	BR-MYCO 174908-17	KM390702 KM390703	KT216840	KM390163
HJB12059	Norway, Svalbard	HJB12059	KM390713	KT216846	MW452587
Hebeloma perexiguum					
HJB12038 holotype	Norway, Svalbard	BR-MYCO 173979-58	KM390689	KT216844	KM390160
Hebeloma pusillum					
HJB9494	U.K., Wales	HJB9494	KM390530		KM390111
HJB11728	Belgium	HJB11728	JN943862	KT216835	KF309497
HJB14747	U.K., Isle of Man	HJB14747	MW465838	MW452579	MW452588
Hebeloma salicicola					
HJB10260	Belgium	HJB10260	KF309403	KT216788	KF309470
HJB10422	Belgium	HJB10422	JN943878	KT216795	KF309473
HJB 13302 holotype	Belgium	BR-MYCO 173977-56	KM390683	KT216857	KM390177

Application Suite (LAS) V4 software. The spores were first studied in Melzer's reagent to assess the shape, degree of dextrinoidity, ornamentation and the degree of loosening of the perispore. For the assessment of the degrees of ornamentation (O0, O1, O2, O3, O4), of the loosening perispore (P0, P1, P2, P3) and for the dextrinoidity (D0, D1, D2, D3, D4), we used Beker et al. (2016), where more details can be found.

A number of photographs were taken of the spores at x500 and x1600, which were then measured using the LAS software. Wherever possible, for each collection at least 50 spores were measured in Melzer's reagent, excluding the apiculi. The maximum length and width of each spore was measured, and its Q value (ratio of length to width) calculated. Average length, width, and Q value were calculated and recorded, as well as the median, standard deviation, and 5% and 95% percentiles. Photographs were also taken of the cheilocystidia on the lamella edge at x500 and of individual cystidia and basidia at x1000. The material was then examined in 5% KOH. Again, photographs were taken of the spores at x500 and x1600 and of the cheilocystidia (and pleurocystidia if any were present) and basidia at x500 and x1000.

For the cheilocystidia, the average width of the widest part of the cheilocystidium in the vicinity of the apex appears to be an important character in the separation of species within *Hebeloma* (Vesterholt 2005). It is also important, when determining this average width near the apex, not to be selective with regard to the cystidia chosen for measurement. To determine the average width at the apex about 100 cheilocystidia were measured on the lamellae edge. For other measurements, at least 20 cheilocystidia, wherever possible, separated from the lamella edge, were measured from each collection. Because of the complex shapes of the cheilocystidia four measurements were made: length, width at apex (A), width at narrowest point in central region (M), and maximum width in lower half (B). The measurements were given in this order, and an

average value was calculated for each of these measurements. For each cheilocystidium the ratios A/M, A/B, and B/M were calculated and averaged across all cheilocystidia measured. Separate mountings of the material were used, where possible, to examine the caulocystidia and pileipellis.

Morphological terms, including colors, are as in Beker et al. (2016), which we have used as the basis for the descriptions, emending some of them where new data from new collections became available.

Results

Of the 405 collections studied, sequence data was generated from 378, which formed the basis of this study. The overall distribution of the sample is shown in Fig. 2A, but the main collection sites starting with the most southerly were Narsarsuaq, Paamiut, Kangerlussuaq, Zackenberg and Jameson Land.

The combined morphological and molecular analysis determined the presence of 28 species, of which one, *H. arcticum*, is described as new to science. For another, *H. colvinii*, the first modern description is provided. The others are *H. alpinicola*, *H. alpinum*, *H. aurantioumbrinum*, *H. clavulipes*, *H. dunense*, *H. excedens*, *H. fuscatum*, *H. geminatum*, *H. grandisporum*, *H. helodes*, *H. hiemale*, *H. hygrophilum*, *H. ingratum*, *H. islandicum*, *H. leucosarx*, *H. louiseae*, *H. marginatulum*, *H. mesophaeum*, *H. minus*, *H. nigellum*, *H. oreophilum*, *H. pubescens*, *H. spetsbergense*, *H. subconcolor*, *H. vaccinum* and *H. velutipes*. Nineteen of these taxa are new records for Greenland and six are new records for the North American continent: *H. clavulipes*, *H. grandisporum*, *H. islandicum*, *H. louiseae*, *H. minus* and *H. pubescens*. Three species, *H. arcticum*, *H. colvinii* and *H. excedens* have not been recorded from Europe.

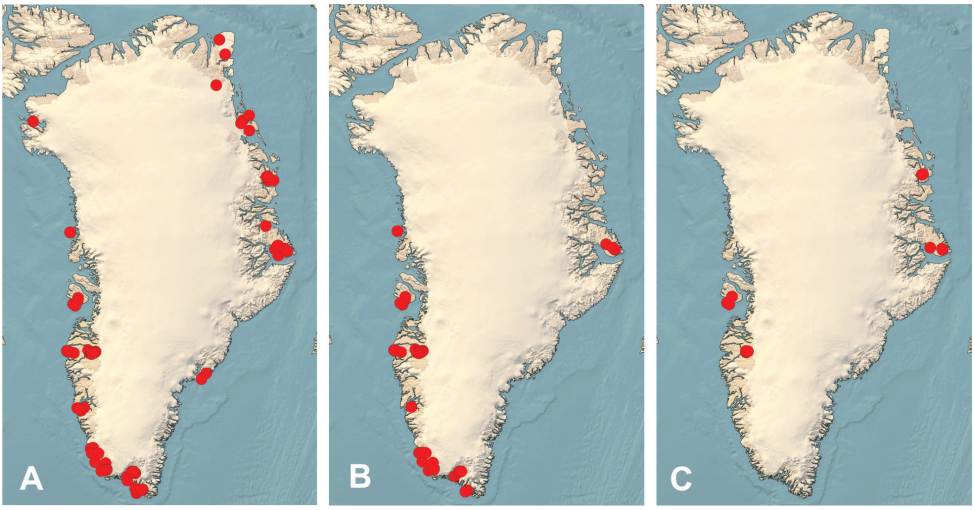

Figure 2. *Hebeloma* species collecting sites in Greenland **A** all **B** collection sites in the Low Arctic, encompassing groups 1–3, and **C** in the High Arctic, encompassing group 5.

Geographical distribution of *Hebeloma* species in the sample

The 28 species all occur in the Arctic zone. In the small Subarctic zone in southernmost Greenland (< 61.25°N), 13 species were recorded, but they also occurred in the Arctic zone. Below, the species are grouped according to the regions within which they occur; Table 3 lists the species in each group.

- Group 1. Four species appear to have a southerly distribution and are only known from South Greenland (< 62.2°N): *H. clavulipes*, *H. helodes*, *H. islandicum* and *H. leucosarx*.
- Group 2. Seven species appear to have a southwesterly distribution, i.e. are known from just southern and western Greenland (< 69.25°N): *H. arcticum*, *H. colvinii*, *H. excedens*, *H. ingratum*, *H. geminatum*, *H. hygrophilum* and *H. minus*.
- Group 3. Only three species have been collected in southwestern and southeastern Greenland but not northern Greenland (< 67°N): *H. fuscatum*, *H. nigellum* and *H. subconcolor*.
- Group 4. Ten species have been collected all over Greenland in Subarctic, Low Arctic and High Arctic zones: *H. alpinicola*, *H. alpinum*, *H. aurantioumbrinum*, *H. dunense*, *H. hiemale*, *H. marginatulum*, *H. mesophaeum*, *H. oreophilum* (not collected in east Greenland), *H. vaccinum* (not collected in west Greenland), and *H. velutipes.*
- Group 5. Four species are northern and have never been collected in south Greenland (> 67°N). They have only been verified for the High Arctic zone: *H. grandisporum*, *H. louiseae*, *H. pubescens* and *H. spetsbergense*.

Fourteen species are only found in the southern half of Greenland (groups 1, 2 and 3; Table 3 and Fig. 2B, the Subarctic and Low Arctic zones defined by at least six months with an average temperature above zero: *H. arcticum*, *H. clavulipes*, *H. colvinii*, *H. excedens*, *H. fuscatum*, *H. geminatum*, *H. helodes*, *H. hygrophilum*, *H. ingratum*, *H. islandicum*, *H. leucosarx*, *H. minus*, *H. nigellum* and *H. subconcolor.* Four species have never been recorded from south Greenland. This is Group 5, above and see also Table 3 and Fig. 2C.

Molecular results

Full ITS sequence data was obtained from 367 Greenland collections; 10 collections, indicated in Table 1, only yielded either ITS1 or ITS2 sequences. These sequences were compared to existing sequence data and supported the morphological identifications. They are not included in the molecular analyses.

The data was divided into seven datasets for the network analyses and are depicted in Figs 3–7: Three networks for *H.* sect. *Hebeloma*, three networks for *H.* sect. *Denudata* and one for *H.* sect. *Velutipes*. The molecular result for the Greenland *H. islandicum* collection is treated in the Taxonomy part where the species is discussed.

The *H. mesophaeum* complex network (Fig. 3A) includes 124 sequences of which 76 are from Greenland material. The only species which has 'private' ITS variants, i.e. not mixing with other species' sequences, is *H. colvinii*. Fourteen collections of

Table 3. *Hebeloma* species composition of the Greenland sample by species distribution groups (see main text). Classification into "specialist" and "opportunist" taxa follows Beker et al. (2016).

Species by region	No. of collections	Specialist (S) or opportunist (O)
Group 1 – South Greenland (60.9–62°N)		
H. clavulipes	1	O
H. helodes	5	O
H. islandicum	1	S
H. leucosarx	2	O
Group 2 – South & West Greenland (60.2–69.3°N)		
H. arcticum	8	S
H. colvinii	5	O
H. excedens	3	O
H. geminatum	3	O
H. hygrophilum	15	O
H. ingratum	4	O
H. minus	2	S
Group 3 – South, West & East Greenland (60.1–72.8°N)		
H. fuscatum	8	S
H. nigellum	21	S
H. subconcolor	9	S
Group 4 – All of Greenland (60.1–81.6°N)		
H. alpinicola	13	S
H. alpinum	36	S
H. aurantioumbrinum	40	S
H. dunense	42	S
H. hiemale	44	O
H. marginatulum	42	S
H. mesophaeum	11	S
H. oreophilum	18	S
H. vaccinum	13	O
H. velutipes	10	O
Group 5 – Never collected in South Greenland (67–74.5°N)		
H. grandisporum	2	S
H. louiseae	5	S
H. pubescens	3	S
H. spetsbergense	12	S
Total	**378**	

H. alpinicola and six of *H. dunense* have ITS variants that occur in both species. The overlap concerns only Greenland collections of *H. alpinicola*, although Greenland collections do not generally appear to be segregated from non-Greenland collections. Some (5) *H. mesophaeum* ITS variants coincide with *H. excedens* (7) and others (11) with *H. pubescens* (6), irrespective of geographical origin.

No overlap was observed between *H. marginatulum* ITS variants and those of other species. The network (Fig. 3B) gives evidence of the ITS sequence diversity of the species. The network includes 92 sequences, of which 42 were from Greenland. The circles representing only non-Greenland collections in the upper part of the network only include North American sequence variants, but other North American collections are also represented by circles in the lower part of the diagram. The ITS of the Greenland collections do not appear to stand out in this circumpolar sample.

Fig. 4A shows the network of the *H. nigellum* complex and *H. grandisporum.* The analysis included 144 sequences of which 73 stemmed from Greenland material. Only a partial ITS sequence of the single collection of *H. clavulipes* from Greenland could

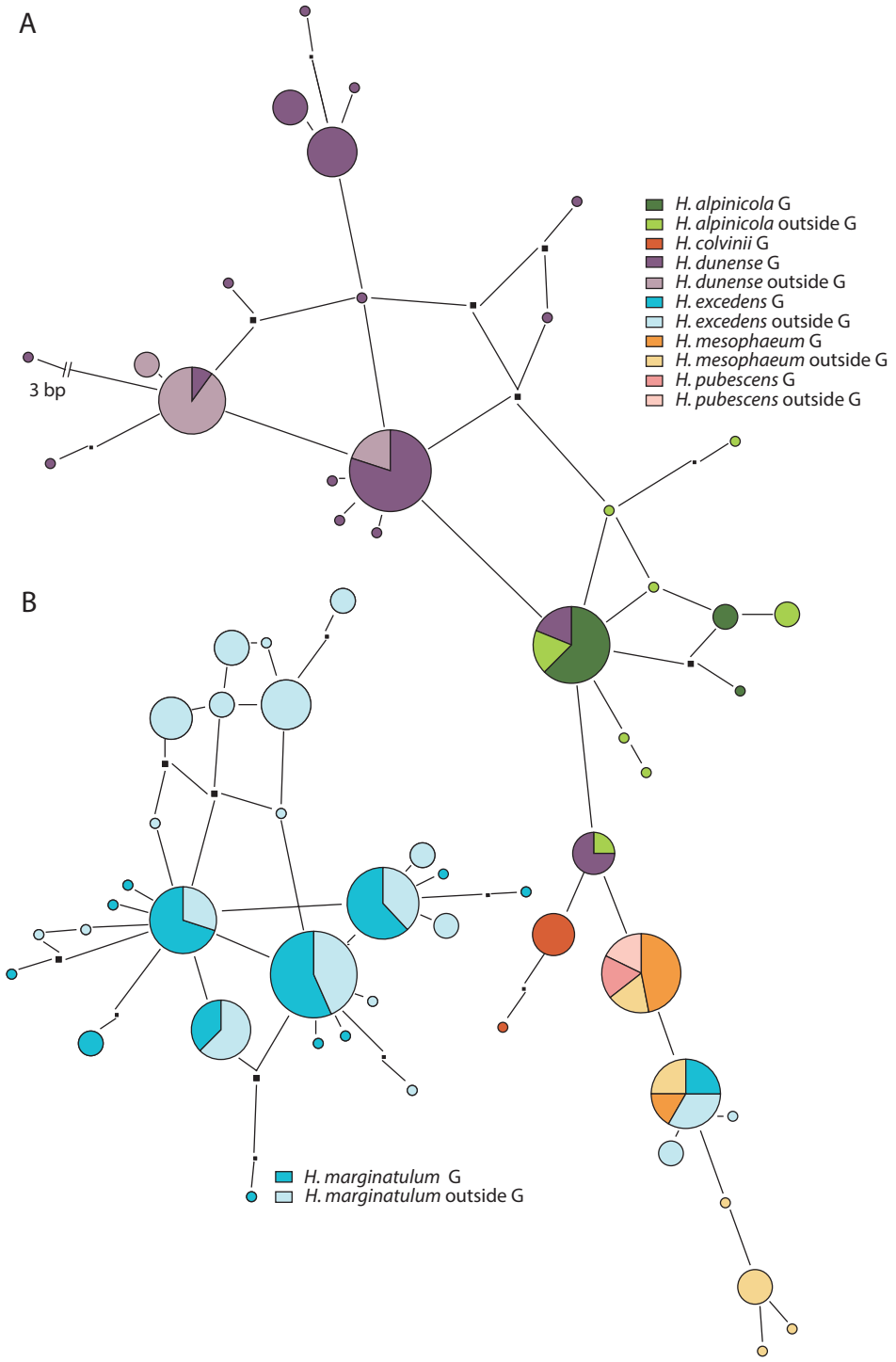

Figure 3. Pruned quasi-median networks of **A** the *Hebeloma mesophaeum* complex and **B** *Hebeloma marginatulum*. Circles shared by two or more taxa or collections from two regions, from Greenland (G) or collected elsewhere, are divided according to the number of representatives for each class.

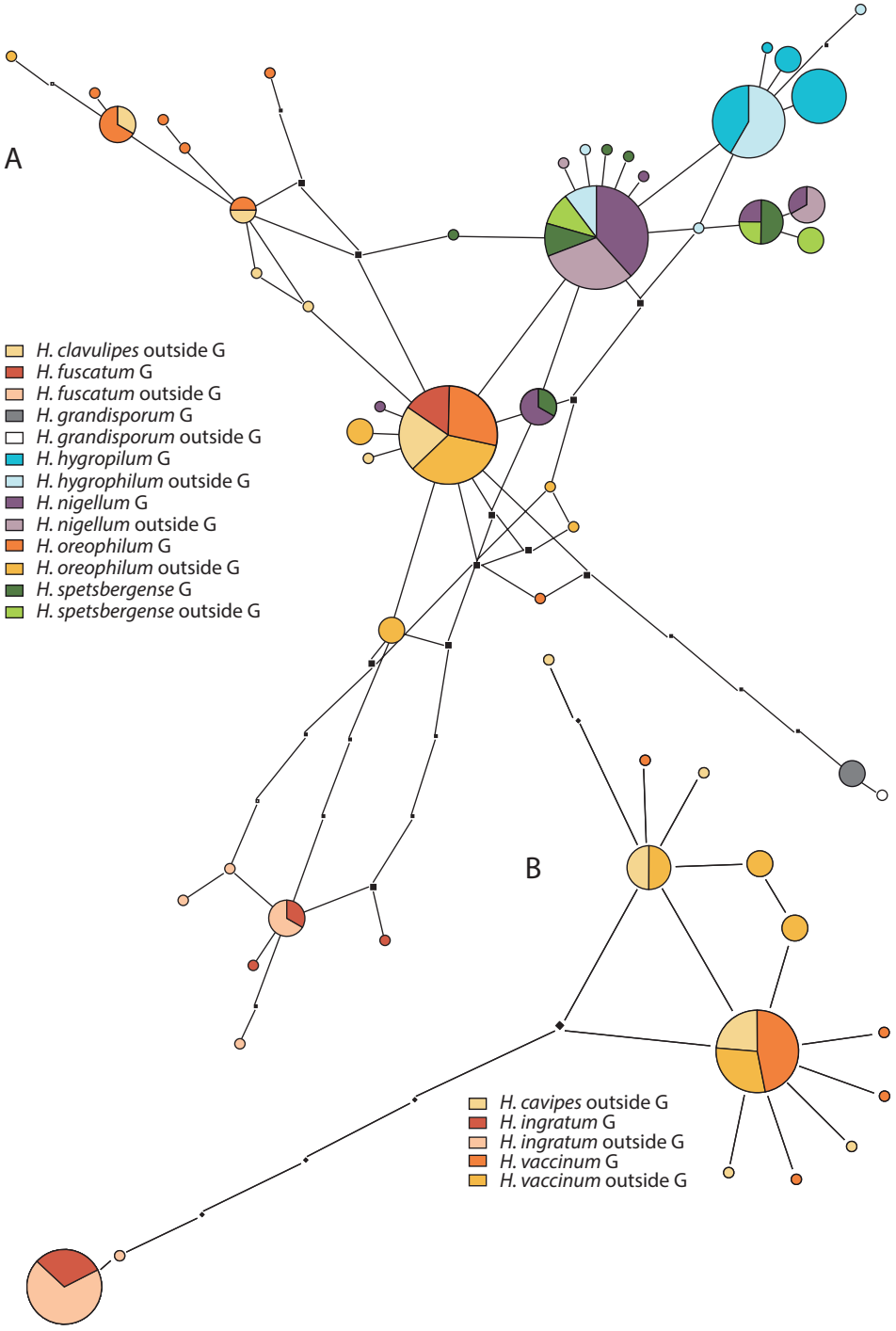

Figure 4. Pruned quasi-median network of **A** the *Hebeloma nigellum* complex and *H. grandisporum* and **B** *Hebeloma cavipes*, *H. ingratum* and *H. vaccinum*. Circles shared by two or more taxa or collections from two regions, from Greenland (G) or collected elsewhere, are divided according to the number of representatives for each class.

be generated and was thus not included in the analysis. *Hebeloma grandisporum* is the only species in this network that is distinct; it is separated by at least 5 alignment positions from the sequences of the members of the *H. nigellum* complex. The ITS of *H. fuscatum* is split between one group of sequences that differs in at least 3 alignment positions from all other sequences in the analyses and a number (5) of Greenland collections that group together with sequences of *H. oreophilum* (20) and *H. clavulipes* (7). The latter two species are not separable by ITS. Similarly, *H. nigellum* cannot be separated from *H. spetsbergense*; 29 collections of *H. nigellum* and 12 of *H. spetsbergense* are represented in the shared circles. Some collections of *H. hygrophilum* (4) mix with *H. nigellum* and *H. spetsbergense* in the network.

Fig. 5A shows the ITS network of the *H. alpinum* complex in a broad sense, including *H. minus* and *H. pallidolabiatum*, as well as *H. louiseae* and *H. arcticum*. The latter species is described as new in this paper. The network includes 109 sequences, of which 54 are from Greenland material. Eight species are included in the network; five of these have been collected in Greenland and *H. arcticum* is represented exclusively by Greenland material. *Hebeloma louiseae* and *H. arcticum* are clearly distinct and do not share any ITS variants with other species. All member species of the *H. alpinum* complex, in this broad sense, either have some members that are represented in the central circle of the network or are linked through it (*H. pallidolabiatum*). All members of *H. geminatum* (12) and the majority of collections of *H. alpinum* (35), irrespective of origin, are represented in the central circle. Additional information on the results referring to *H. arcticum* are given in the context of the species description below.

In Fig. 5B the position of *H. arcticum* within *H.* subsect. *Crustuliniformia* is shown in the result of the ML analysis. The species clade of *Hebeloma arcticum* received full bootstrap support (100%) and formed a highly supported clade (99%) with the species clades of *H. aurantioumbrinum*, *H. helodes*, *H. luteicystidiatum*, *H. lutense*, *H. matritense*, *H. perexiguum* and *H. pusillum* all of which are also fully supported, apart from *H. perexiguum* which is only known from the type.

The networks relating to other members of *H.* sect. *Denudata* are depicted in Figs 4B, 6A and 6C. The network of members of *H.* subsect. *Clepsydroida* (Fig. 4B) includes 47 sequences (16 from Greenland) from three species. *Hebeloma ingratum* is distinct from the other two species in the network, separated by at least 5 alignment positions.

Sequences from Europe and Greenland are represented in the same circle. *Hebeloma cavipes* (4 sequences), not present in Greenland and *H. vaccinum* (13 sequences) share one ITS variant; there is no taxonomic or geographical structure apparent in the *H. cavipes*/*H. vaccinum* part of the network.

Hebeloma hiemale (Fig.6A), not unlike *H. marginatulum*, is a species that is distinct from its relatives based on ITS, but with a high intraspecific variation in the ITS. Greenland collections (42 out of a total of 86 sequences in the analysis) are concentrated in the upper part of the network, but the circles that only include non-Greenland collections include European as well as North American collections.

The network of *H. aurantioumbrinum* and *H. helodes* (Fig. 6C) shows that in Greenland *H. helodes* cannot be distinguished based on ITS (the mixed circle represents three sequences of *H. helodes* and one of *H. aurantioumbrinum*, all from Greenland), although

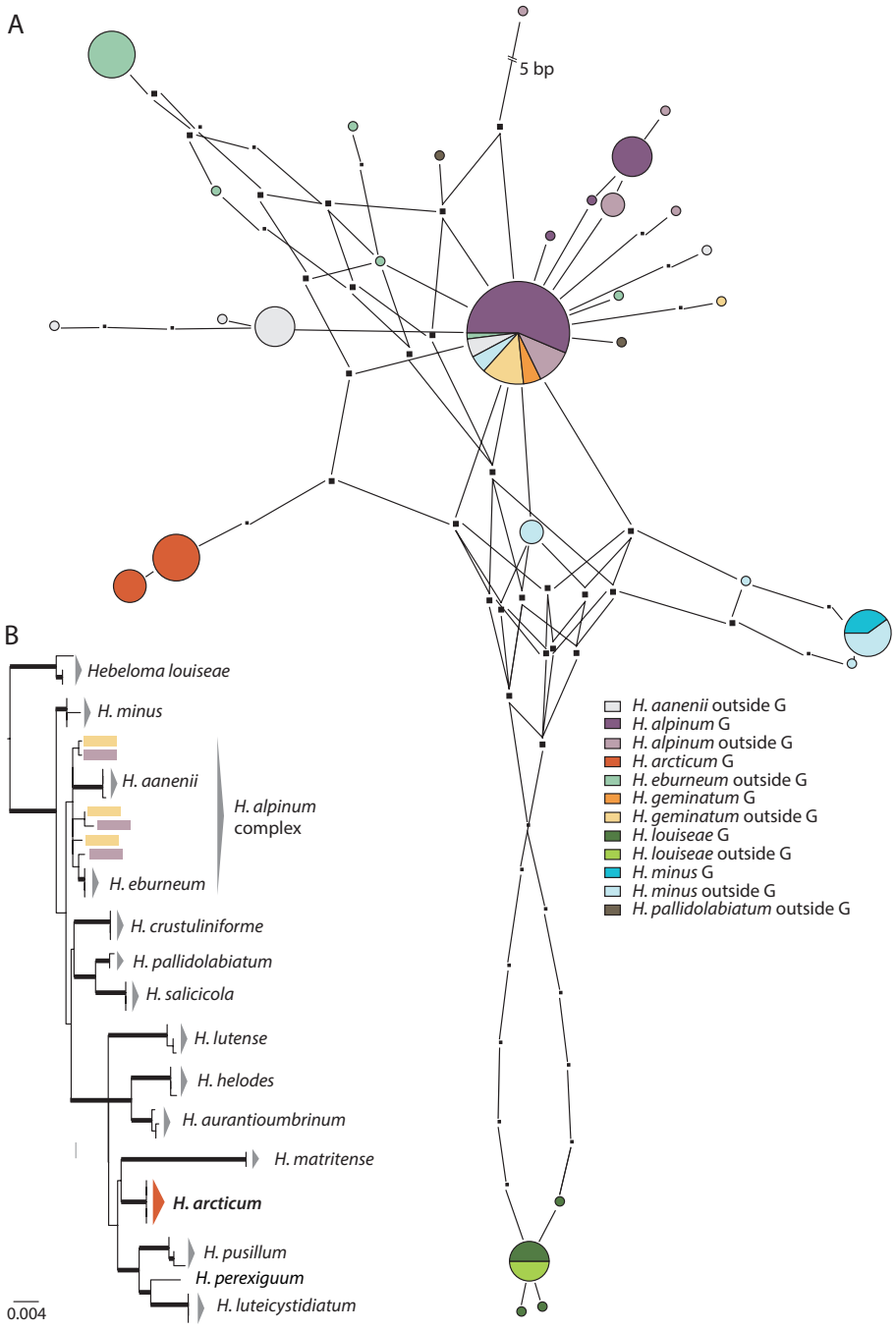

Figure 5. A Pruned quasi-median network of the *Hebeloma alpinum* complex, *H. arcticum* and *H. louiseae*. Circles shared by two or more taxa or collections from two regions, from Greenland (G) or collected elsewhere, are divided according to the number of representatives for each class **B** ML result for *Hebeloma* subsect. *Crustuliniforme*, based on concatenated ITS, *RPB2* and *Tef1*a data, rooted with *H. louiseae*. Thick branches indicate bootstrap support of at least 80% (450 bootstrap replicates). Species are represented by three collections (if available); *Hebeloma arcticum* by four collections including the holotype.

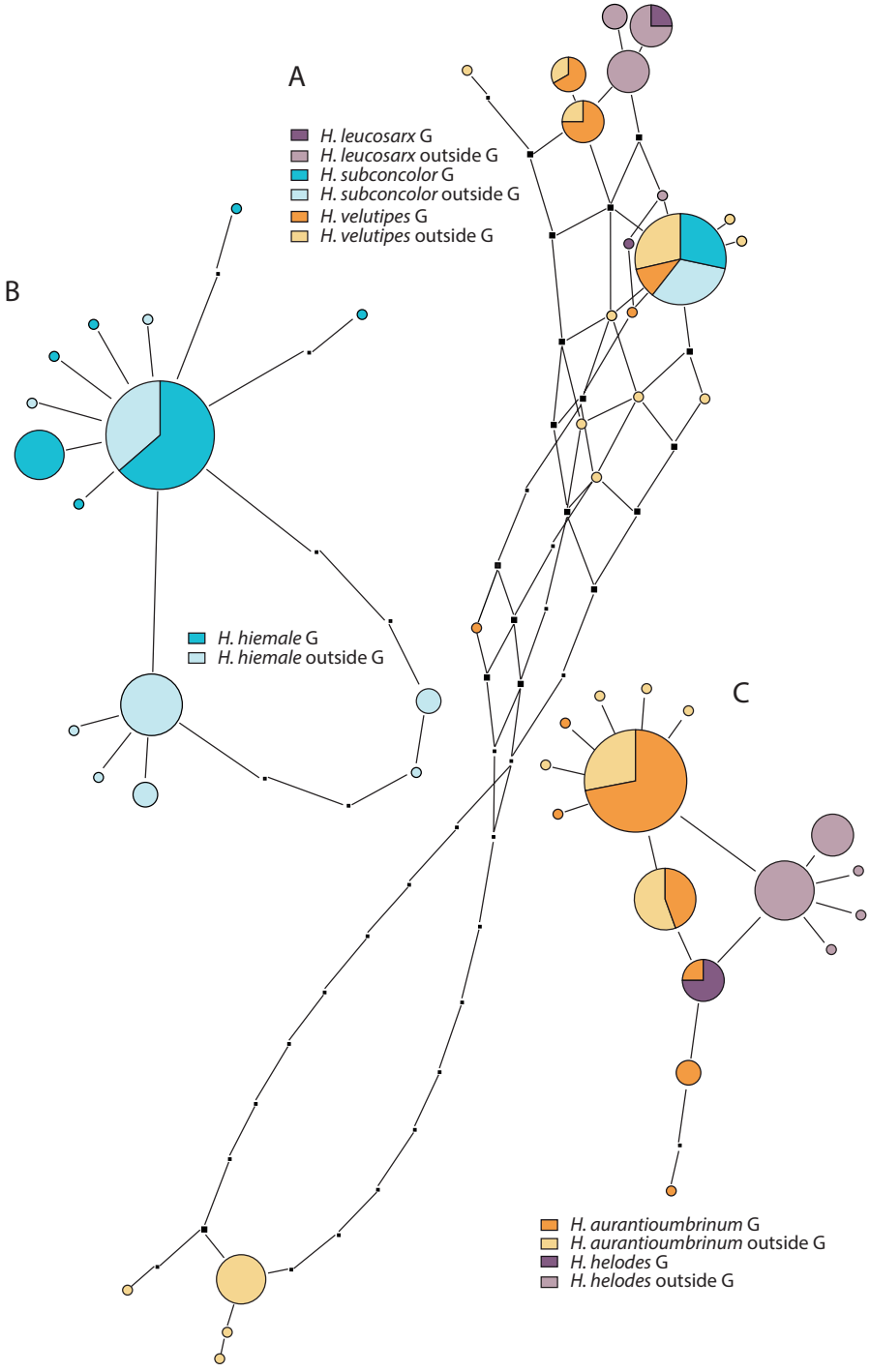

Figure 6. Pruned quasi-median networks of **A** the *Hebeloma velutipes* complex **B** *H. hiemale* and **C** *H. aurantioumbrinum* and *H. helodes*. Circles shared by two or more taxa or collections from two regions, from Greenland (G) or collected elsewhere, are divided according to the number of representatives for each class.

outside Greenland *H. helodes* appears to be better distinct from *H. aurantioumbrinum*. The network is based on 80 sequences, of which 43 are of Greenland origin.

Three species of *H.* sect. *Velutipes* have been collected in Greenland. The respective network is depicted in Fig. 6B and is based on 65 sequences of which 20 were from Greenland collections. *Hebeloma leucosarx* differs by at least one alignment position from the other two species; *H. subconcolor* and *H. velutipes* sequences are represented by the biggest circle (28 sequences) of the network. Neither in the Greenland sample nor in the US sample, did *H. velutipes* ITS variants occur that were more similar to *H. incarnatulum* (at the bottom of the network; see figure 5 of Cripps et al. (2019) for the placement of *H. incarnatulum*) than to *H. leucosarx*. The circle representing *H. subconcolor* and *H. velutipes* includes 17 sequences from the former and 11 from the latter.

Taxonomic treatment

Hebeloma (Fr.) P. Kumm.

General description. Cap 0.9–21 cm, convex or more rarely campanulate or applanate, rarely depressed at center, dry, in wet weather viscid in some species, or tacky, smooth or rarely scaly, margin even or undulate, smooth, rarely hygrophanous, rarely striate, several shades of brown, from whitish to pale beige to dark brown, occasionally orange-brown, rarely reddish brown, along margin with or without remnants of universal veil, floccose or velutinate. Lamellae emarginate to adnate, thin, unicolored, at first pale, at maturity browner, in some groups with hyaline or brown droplets along margin. Stem 2.0–14.0 × 0.1–2.0 cm, cylindrical or bulbous at base, occasionally rooting, at first white, whitish or cream, becoming pale ochraceous to brown or even black, white tomentose, floccose or pruinose, rarely velutinate, some groups with partial veil, rarely with a membranous ring. Flesh color resembling the color of the stem, often discoloring brownish from stem base when bruised or old. Smell often radish-like, in one section sweetish, in some species insignificant. Taste mild to bitter, rarely significant. Spore deposit umber to dark cinnamon or dark brick red.

Spores most often amygdaloid, also ellipsoid or limoniform, rarely fusoid or navicular, in some species distinctly papillate, from pale yellow to dark brown, almost smooth to distinctly verrucose and ornamented with separate or coherent irregular warts, in some groups with ± loosening perispore, in Melzers solution from indextrinoid to distinctly and strongly dextrinoid. Cheilocystidia present in all species, variable but distinctive, cylindrical, lageniform, slenderly clavate, spheropedunculate, ventricose or balloon-shaped or variations thereof, rarely forked, in some species partially thick-walled, straight, sinuate or geniculate, hyaline or pale brown. Pleurocystidia rarely present, when present usually similar to cheilocystidia. Caulocystidia present in all species, similar to cheilocystidia, often fasciculate. Basidia cylindrical to slenderly clavate, 4-spored, rarely also 2-spored, in one arctic species only 2-spored. Pileipellis an ixocutis, a thin layer of narrow, hyaline hyphae, smooth or encrusted, 30–250 μm thick.

Comments. *Hebeloma* is a genus of ectomycorrhizal fungi. The symbionts belong to a wide variety of families of dicotyledons. In Greenland, according to the observations of T.B., S.A.E. and H.K. symbionts appear to belong to the families: Salicaceae, Betulaceae, Polygonaceae and Rosaceae. The total list consists of only 11 species: *Salix glauca*, *S. herbacea*, *S. arctica* Pall., *S. arctophila*, *Betula pubescens* var. *pumila*, *B. nana.*, *B. glandulosa*, *Alnus alnobetula* subsp. *crispa*, *Bistorta vivipara*, *Dryas octopetala* and *D. integrifolia*.

Bistorta vivipara (L.) Delarbre (≡ *Polygonum viviparum* L., Polygonaceae) has often been observed close to species of *Hebeloma* and Brevik et al. (2010) isolated sequences of *Hebeloma* spp. from its roots in Spitsbergen, which is normally considered as a strong indication that this plant associates with the respective fungus. In a few cases, T.B. found rhizoids from *Hebeloma* attached to the roots of *Bistorta*, but found it difficult to rate the importance of these observations, since there have often been other possible hosts observed nearby. For *Alnus*, there is no evidence that it is a host; for the few records from *Alnus*-shrubs, it is not possible to rule out nearby willows or birches. The remaining perennial shrubs in Greenland, *Sorbus groenlandica* (C.K. Schneid.) Á. Löve & D. Löve and *Juniperus communis* L. do not form ectomycorrhiza. This is also the case for members of the heather family (Ericaceae) that occur in Greenland, with the rare exception of *Arctostaphylos alpina*.

Key to sections and subsections of *Hebeloma* in Greenland, (including *H. islandicum*)

Spore character measures (O1–O4; P0–P3 and D0–D4) are explained in Beker et al. (2016: 22ff and figure 6A–G (color)).

1 Veil present, either on the cap margin or from the margin to the stem or both; margin of lamellae rarely exuding small drops; most cheilocystidia distinctly ventricose..... ***H.* sect. *Hebeloma***

– Veil absent (except in primordia); margin of lamellae when fresh usually exuding droplets; most cheilocystidia distinctly swollen at apex..... **2**

2 Cheilocystidia at apex and base enlarged (hourglass-shaped), apically or in the middle sometimes with thickened walls **3**

– Cheilocystidia distinctly enlarged at apex, below ± cylindrical, walls rarely thickened..... **5**

3 Spores O2 and not O3 and many spores D3, found in alpine-arctic habitats ..... ***H. islandicum***

– Above conditions not satisfied..... **4**

4 Many spores O1 or O2 and many spores D0 or D1 and spores not P2 or if spores are P2 then pileus is not yellow or cream in the center but with brown or buff tones ..... ***H. hiemale* (*H.* subsect. *Hiemalia*)**

– The above conditions not satisfied..... ***H.* subsect. *Clepsydroida***

5 Cheilocystidia distinctly restricted below apex, hardly swollen in lower third ..... ***H.* subsect. *Crustuliniformia***
– Cheilocystidia more gently tapering downwards, some ventricose cystidia present ..... ***H.* sect. *Velutipes***

Key to species of *Hebeloma* section *Hebeloma* in Greenland

1 Spores mainly ellipsoid, indextrinoid to weakly dextrinoid **2**
– Spores mainly amygdaloid, usually rather strongly to strongly dextrinoid **8**
2 Number of full-length lamellae (L) < 32 and pileus with a matting of short soft hairs ..... ***H. pubescens***
– Number of full-length lamellae ≥ 32 or if < 32 then pileus with at most a few fibrils at margin **3**
3 Spores on ave. at least 12.5 × 7.5 µm ..... ***H. colvinii***
– Spores smaller **4**
4 Cap distinctly bicolored, at least in mature specimens ..... ***H. mesophaeum***
– Cap mainly unicolored, at most indistinctly bicolored **5**
5 Spores clearly ellipsoid to ovoid, very rarely amygdaloid, ave. size rarely exceeding 10 × 6 µm **6**
– Ave. spore length > 10 µm and ave. spore width ≥ 6 µm or if spores smaller, then most spores ellipsoid, but many amygdaloid, almost always with Salicaceae 7
6 Stem relatively narrow, usually 0.2–0.6 cm thick, cap often overhanging lamellae ..... ***H. excedens***
– Stem relatively robust, usually 0.5–1 cm thick, cap not overhanging lamellae ..... ***H. alpinicola***
7 Spores with some clear ornamentation (O1,O2) and an indistinct but clear reaction in Melzer's reagent (D1) ..... ***H. dunense***
– Spores showing almost no ornamentation, even under immersion (O1) or completely indextrinoid (D0) ..... ***H. marginatulum***
8 Number of full-length lamellae (L) ≥ 40 ..... **9**
– Number of full-length lamellae (L) < 40 ..... **10**
9 Spores, on ave. ≥ 6.7 µm wide ..... ***H. oreophilum***
– Spores, on ave. < 6.7 µm wide ..... ***H. clavulipes***
10 Ave. spore length ≥ 15 µm ..... ***H. grandisporum***
– Ave. spore length < 15 µm **11**
11 Spore papilla distinctly present and many spores limoniform .... ***H. fuscatum***
– Spore papilla at most indistinctly present and spores rarely limoniform **12**
12 Ave. spore width > 7.5 µm ..... ***H. spetsbergense***
– Spores amygdaloid **13**
13 Spores < 7 µm wide ..... ***H. hygrophilum***
– Spores ≥ 7 µm wide ..... ***H. nigellum***

Key to species of *Hebeloma* section *Denudata* in Greenland

1 Cheilocystidia at apex and base enlarged (hourglass-shaped), apically or in the middle sometimes with thickened wall.....**2**
– Cheilocystidia distinctly enlarged at apex, below ± cylindrical, walls rarely thickened.....**4**
2 Spores on ave. 12–14.5 µm long, rather strongly dextrinoid (D3); cap at center rust brown to reddish brown ..... ***H. vaccinum***
– Spores on ave. 10–12.5 µm long, less dextrinoid (D2); cap at center paler....**3**
3 Spores on ave. 10–11 µm long, O2 to O3, D1 to D2.....***H. ingratum***
– Spores on ave. 10–12.5 µm long, O1 to O2, Do to D1 ..... ***H. hiemale***
4 Number of full-length lamellae (L) ≥ 60 and ave. spore length < 11 µm .... ***H. geminatum***
– Number of full-length lamellae (L) < 60 or ave. spore length ≥ 11 µm.....**5**
5 Spores O2 to O3 and D2 to D3, many D3..... ***H. arcticum***
– Spores at most D2 .....**6**
6 Number of full-length lamellae (L) ≥ 40, spore length ≥ 11 µm, spores with distinct papilla ..... ***H. alpinum***
– Any of the above conditions not satisfied **7**
7 Ave. spore length < 11 µm **8**
– Ave. spore length ≥ 11 µm **9**
8 Cheilocystidia without consistent and distinct apical thickening..... ..... ***H. aurantioumbrinum***
– Cheilocystidia with consistent and distinct apical thickening..... ***H. belodes***
9 Spores O1 or O2, few if any spores O3..... ***H. louiseae***
– A large number of spores O3 ..... ***H. minus***

Key to species of *Hebeloma* section *Velutipes* in Greenland

1 No. of full-length lamellae < 35 ..... ***H. subconcolor***
– No. of full-length lamellae > 35; stem base ± bulbose.....**2**
2 Cap distinctly colored, often quite dark with reddish tones, umbonate..... ..... ***H. leucosarx***
– Cap pale colored, whitish to beige or buff, convex, sometimes umbonate .... ***H. velutipes***

Hebeloma* sect. *Hebeloma

Veil present, often along cap margin. Cap uniformly colored or bicolored, with a paler margin. Lamellae without droplets. Stem fibrillose, often browning from base. Spores ellipsoid, ovoid, amygdaloid or limoniform, ornamentation weak, dextrinoid or non-dextrinoid, perispore not or only very slightly loosening.

***Hebeloma alpinicola* A.H. Sm., V. S. Evenson & Mitchel; Veiled species of *Hebeloma* in the western United States (Ann Arbor): 48, 1983.**
Fig. 7

Macroscopic description. Cap 1.2–4.5 cm in diameter, robust, fleshy, irregularly hemispherical to convex, somewhat domed or not, almost unicolored, center cinnamon to dark pinkish buff, dark olive buff or rarely umber, sometimes with grayish tones, outwards ocher and lighter buff not white towards margin, sometimes with hoary canescent coating that dries shiny, with weakly hygrophanous spots, dry, margin inrolled at first, and then turned down, partial veil present. Lamellae narrowly attached, slightly emarginate, or with a tooth, or pulling away, somewhat broad (2−5 mm), pale gray brown to milky coffee, number of lamellae {L} 30–44, edges white floccose, without watery droplets. Stem 1.5–7.0 × 0.2–0.8 cm, cylindrical, whitish pruinose at apex, often with a whitish ring zone, dingy ocher to sordid yellowish or fairly dark brown, longitudinally strongly fibrillose and striate in lower part, often darkening when bruised, base sometimes encrusted with sand or earth, solid or slightly hollow. Context dingy whitish, darker below, unchanging or flesh staining brown. Smell weakly raphanoid. Taste almost insipid to slightly bitter. Spore deposit near fulvous.

Microscopic description. Spores ellipsoid or some slightly amygdaliform or ovoid, with rounded end, apiculus small, on ave. 8–10.5 × 5–6 µm, ave. Q = 1.55–1.85, smooth to slightly rough (O1), not guttulate, not or very slightly dextrinoid (D0 D1), perispore not loosening (P0). Basidia clavate, mostly four-spored, 20–35 × 6–8 µm. Cheilocystidia lageniform or ventricose, on ave. 35–55 × 5–6.5 (apex) × 4.5–6.5 (middle) × 6.5–10 (base) µm, occasionally geniculate or bifurcate, sometimes septate. Ratios A/M = 0.95−1.24, A/B = 0.54−0.88, B/M = 1.43−2.17. Epicutis an ixocutis, up to 200 µm thick, maximum hyphae width to 8 µm, encrusted hyphae not seen, shape of trama elements beneath subcutis cylindrical. Caulocystidia similar to cheilocystidia, but generally larger.

Collections examined. S-Greenland: Kangilinnguit, 61.23°N, 48.07°W, 12 Aug 1985, T. Borgen (TB85.099, C-F-5082), 95 m, with *Salix glauca* and *Chamaenerion latifolium* in heathland. Kangilinnguit, 61.23°N, 48.10°W, 6 Aug 1984, T. Borgen (TB84.063, C-F-103534), 25 m, with *Salix glauca* in scrubland. Kangilinnguit, 61.23°N, 48.07°W, 17 Aug 1985, T. Borgen (TB85.071, C-F-5081), 95 m, with *Alnus alnobetulae*. Narsarsuaq, 61.15°N, 45.42°W, 9 Aug 2018, H. Knudsen (HK18.010, C-F-111109), 185 m, with *Salix glauca* and *Betula pubescens* in scrubland. Narsarsuaq, airport area, 61.08°N, 45.26°W, 3 Aug 1984, T. Borgen (TB84.028, C-F-103559), 20 m, with *Salix glauca* and *Betula glandulosa* in scrubland. Paamiut, 62.01°N, 49.4°W, 1 Aug 2000, T. Borgen (TB00.049, C-F-103516), 10 m, with *Salix herbacea* in snowbed. Paamiut, 62.01°N, 49.4°W, 8 Aug 1981, T. Borgen TB81.111, C-F-103554), 25 m. Paamiut, 62.01°N, 49.4°W, 20 Aug 1985, T. Borgen (TB85.218, C-F-103532), 30 m, with *Salix herbacea* and *Bistorta vivipara* in snowbed. **W-Greenland:** Kobbefjord, NuukBasic Station, 64.078°N, 51.23°W, 25 Aug 2018, H. Knudsen (HK18.322, C-F-111116), 5 m, with *Salix herbacea* in tundra. Sisimiut, Kællinge-

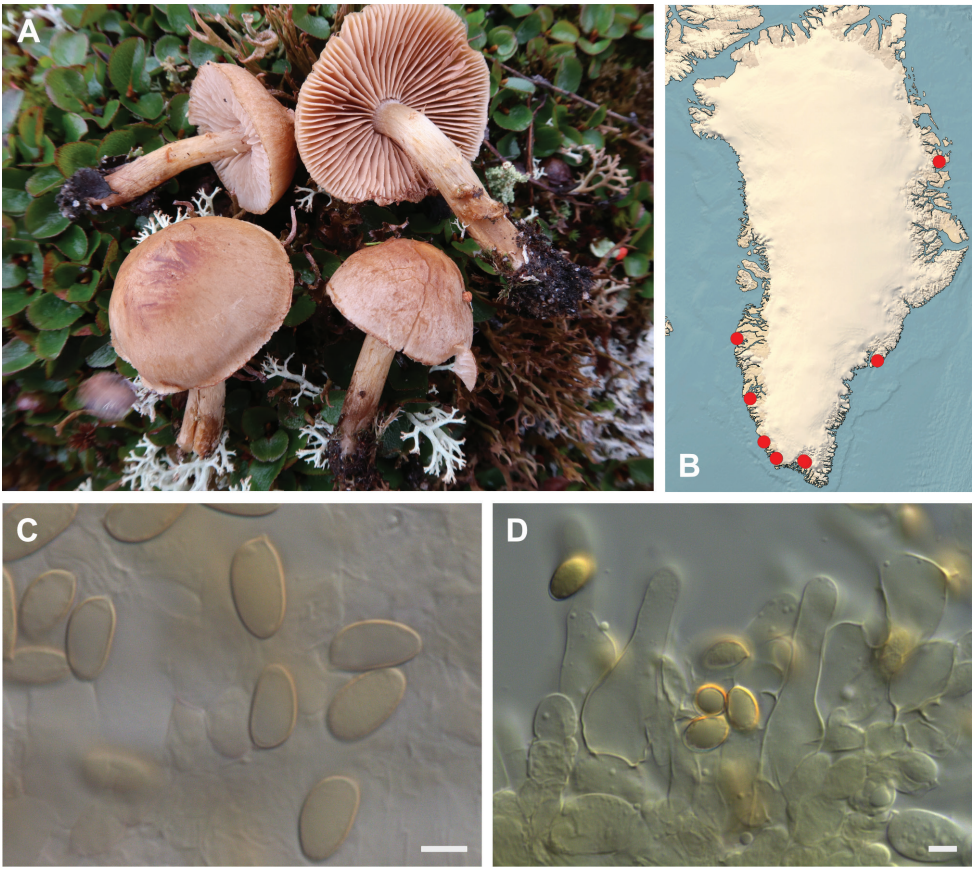

Figure 7. *Hebeloma alpinicola* **A** HK18.322, photograph H. Knudsen **B** distribution of cited collections **C** spores ×1600 and **D** cheilocystidia ×1000 of HK18.322 in Melzer's reagent. Scale bars: 5 µm; microphotographs H.J. Beker.

hætten, 66.93°N, 53.59°W, 16 Aug 2016, H. Knudsen (HK16.165, C-F-108401), 400 m. **N-Greenland:** Zackenberg, Ulvehøj, 74.47°N, 21°W, 7 Aug 1999, T. Borgen (TB99.238, C-F-119805), 40 m, with *Salix arctica* and *Bistorta vivipara*. **E-Greenland:** Kuummiut, Torsukattak, 65.87°N, 37.01°W, 2 Aug 2008, T. Borgen (TB08.039, C-F-101623), 35 m; with *Salix glauca* in heathland. Kuummiut, Torsukattak, 65.87°N, 37.01°W, 2 Aug 2008, T. Borgen (TB08.037, C-F-101621), 35 m.

Distribution. Widely distributed in Greenland, only missing in Constable Pynt. Originally described from the Seven Devils Mountains in Idaho, North America by Smith et al. (1983), more recently from the Rocky Mountains by Cripps et al. (2019) and from the European Alps by Grilli et al. (2020). This species appears to favor both boreal and arctic or alpine habitats. Most collections from Rocky Mountains were from subalpine areas. In Greenland, it occurs from the Subarctic zone to the High Arctic zone, and the Greenland collections from Zackenberg are the northernmost known (74.47°N). Circumpolar, arctic-alpine.

Habitat and ecology. Thirteen collections in all, mainly with *Salix glauca* in scrubs and heathland, three collections in snowbeds with *S. herbacea*, one collection with *S. arctica*, and one collection with *Alnus alnobetulae* ssp. *crispa*, but the presence of other possible associates should not be ruled out. In the Rocky Mountains, Cripps et al. (2019) found two collections, one with *Dryas*, *Salix planifolia* Pursh. and *S. reticulata* L., the other subalpine record with dwarf willows only. *Hebeloma alpinicola* seems not to be specific regarding soil conditions.

***Hebeloma clavulipes* Romagn.; Bull. trimest. Soc. mycol. Fr. 81(3): 326, 1965.**
Fig. 8

Macroscopic description. Cap 1.0–4.1 cm in diameter, convex, sometimes umbonate, margin involute, rarely sulcate, tacky when moist, sometimes hygrophanous, uniformly colored or variably bicolored, at center umber to sepia (6E6, 6E7, 6F6, 6F7), margin cream to pinkish-buff to ochraceous or dark olive buff (4A2, 4A3, 5A3, 5B3, 5B5, 5C5); remains of universal veil sometimes present; partial veil present. Lamellae adnate or adnexed to emarginate, pale brown, maximum depth 3–5 mm, number of lamellae {L} 40–48, droplets usually absent, but occasionally visible with × 10 lens, white fimbriate edge usually present, but sometimes indistinctly. Stem 1.3–7.0 × 0.3–0.6 cm, 4.5–7.3(–8) cm at base, stem Q 3.3–15.5(–18), at first whitish fibrillose becoming pale brown, base cylindrical to clavate or bulbous, usually pruinose or floccose at apex. Context firm, stem inside stuffed, later hollow, stem flesh discoloring from base, sometimes weakly. Smell raphanoid, sometimes with hints of cocoa. Taste mild to bitter, usually raphanoid. Spore deposit brownish olive (5E5).

Microscopic description. Spores amygdaloid or limoniform, occasionally appearing ovoid or fusoid, on ave. 10.5–12.5 × 6.0–6.5 µm, ave. Q 1.6–2.1, very weakly ornamented (O1 O2), perispore not or somewhat loosening (P0 P1), rather strongly dextrinoid (D2 D3), yellow to yellow brown, ± guttulate, papillate. Basidia 23–32(–36) × 7–10 µm, ave. Q = 2.6–4.4, mostly four-spored. Cheilocystidia lageniform to ventricose, occasionally cylindrical, occasionally with a characteristic thickening, apically, basically or medially, sometimes geniculate or septate, on ave. 41–60 × 4.5–6 (apex) × 4–5.5 (middle) × 7.5–12 (base) µm, ratios A/M = 0.93–1.25, A/B = 0.45–0.76, B/M = 1.58–2.31. Epicutis an ixocutis, 125–170 µm thick (measured from exsiccata), maximum hyphae width 3.5–7 µm, sometimes encrusted, shape of trama elements beneath subcutis sausage-shaped, up to 14 µm wide. Caulocystidia similar to cheilocystidia, but usually less ventricose, up to 120 µm long.

Collections examined. S-Greenland: Paamiut, W of the Navigation School area, 62°N, 49.67°W, 7 Sep 1990, T. Borgen (TB90.100, C-F-119760), 20 m, with *Salix herbacea*.

Distribution. Only one record and apparently a very rare species in Greenland recorded only once during the 20 years when Borgen regularly collected in Paamiut. The general distribution in Europe (Beker et al. 2016) is from the Temperate zone

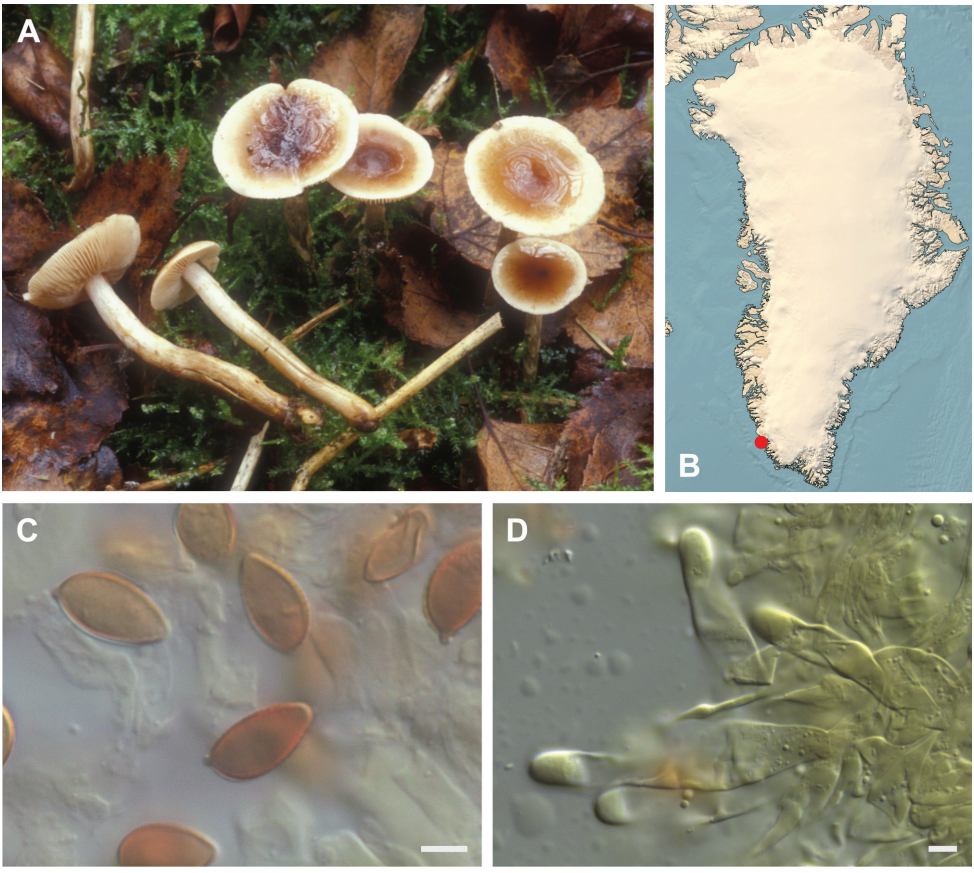

Figure 8. *Hebeloma clavulipes* **A** JV02-517 (from Denmark), photo J. Vesterholt, reproduced by kind permission from Beker et al. (2016) **B** distribution of cited collections **C** spores ×1600 and **D** cheilocystidia ×1000 of TB90.100 in Melzer's reagent. Scale bars: 5 µm; microphotographs H.J. Beker.

to southern Boreal and Subalpine zone up to 1700 m. The Greenland record is the northernmost known (62.00°N). Temperate, boreal, subarctic, and now also from Low Arctic zone.

Habitat and ecology. Only one collection, with *Salix herbacea*. In Europe, the hosts are *Betula*, *Picea* and *Salix* (Beker et al. 2016), but the associated *Salix* species are of the shrub-like kind, like *S. aurita.*

***Hebeloma colvinii* (Peck) Sacc.; Syll. fung. (Abellini) 5: 805, 1887.**
Fig. 9

Macroscopic description. Cap 2.5–7.5 cm, convex to irregularly gibbous, sometimes broadly umbonate, with incurved later straight, opaque margin, occasionally appendiculate, dry and dull, unicolored mainly sepia, sometimes with light grayish adpressed

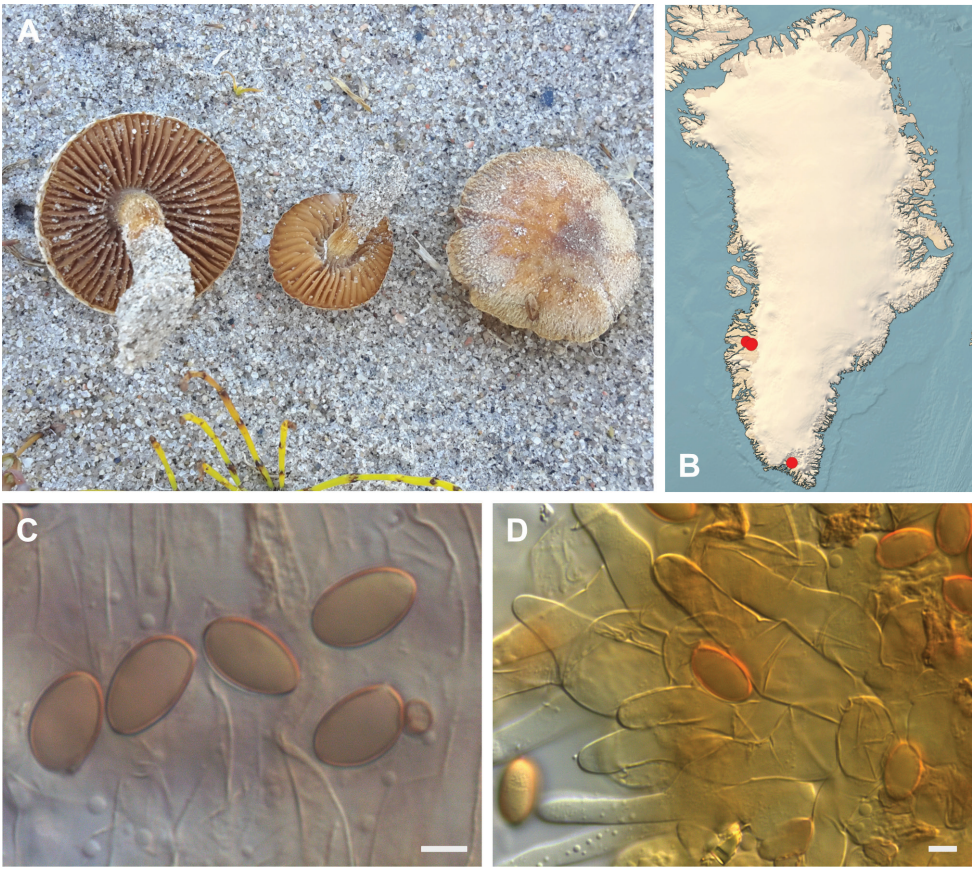

Figure 9. *Hebeloma colvinii* **A** HK16.005, photograph H. Knudsen **B** distribution of cited collections; **C** spores ×1600 and **D** cheilocystidia ×1000 of HK16.005 in Melzer's reagent. Scale bars: 5 µm; microphotographs H.J. Beker.

covering. Lamellae almost free to emarginate gray (olive) brown, edge entire, slightly tomentose, number of lamellae {L} 45–58. Stem whitish pale fibrillose, sordid gray-brown, often more or less buried in sand with a sand bulb around the base, cortina pale. Context initially fairly thick, with cavity, firm watery grayish in pileus, pale brownish in stipe to near buff, towards base dark, sordid brown. Smell weakly and indistinctly raphanoid. Taste similar, mild. Spore deposit color not recorded.

Microscopic description. Spores ellipsoid, often ovoid or amygdaloid on ave. 12.0–14.5 × 7.5–8.5 µm, ave. Q 1.5–1.9, very weakly ornamented (O1 O2), perispore not noticeably loosening (P0), indistinctly dextrinoid (D0 D1), yellow brown, ± guttulate, not papillate. Basidia 26–42 × 7–11 µm, ave. Q = 3.0–4.2, mostly four-spored. Cheilocystidia lageniform to ventricose, occasionally cylindrical or clavate-ventricose, occasionally with a characteristic wall thickening, apically, basically, sometimes septate, on ave. 40–50 × 5.5–8 (apex) × 5–9 (middle) × 10–13 (base) µm, ratios A/M = 0.90–1.26, A/B = 0.46–0.77, B/M = 1.40–2.45. Epicutis an ixocutis, up to 120 µm

thick (measured from exsiccata), maximum hyphae width 10 µm, sometimes encrusted, shape of trama elements beneath subcutis sausage-shaped, cylindrical or ellipsoid. Caulocystidia similar to cheilocystidia, but usually less ventricose, up to 130 µm long.

Collections examined. S-Greenland: Narsarsuaq, 61.16°N, 45.43°W, 31 Aug 2002, T. Borgen (TB02.166, C-F-106756), 30 m, with *Salix glauca* in riverbed. **W-Greenland:** Kangerlussuaq, Sandflugtsdalen, 67.13°N, 51.16°W, 7 Aug 2016, T. Borgen (TB16.075, C-F-103585), 50 m, with *Salix glauca* at riverside dune. Kangerlussuaq, Sandflugtsdalen, 67.06°N, 50.46°W, 7 Aug 2016, H. Knudsen (HK16.008, C-F-104038), 200 m, with *Salix glauca*. Kangerlussuaq, Sandflugtsdalen, 67.06°N, 50.46°W, 7 Aug 2016, H. Knudsen (HK16.005, C-F-104035), 200 m, with *Salix glauca*. Kangerlussuaq, southeast of Sugar Loaf, 66.989438°N, 50.548760°W, 25 Aug 2015, S.A. Elborne (SAE-2016.188GR, C-F-107346), 50 m with *Salix glauca* at riverside dune.

Distribution. Known from a few collections from three localities in southwestern Greenland. *H. colvinii* was described by Peck (1875; effectively published 1876) from West Albany in North America. He found it in drifting sand in West Albany near Albany, N.Y. State. Later Kauffman (1918) reported this or a very similar species from New Richmond in Michigan, as did Ritchie (1946) from Lewes, Delaware Bay. Neither of these two collections has been examined as part of this study.

Habitat and ecology. Five collections, all with *Salix glauca* in pure sand along a river. In one of the localities, Sandflugtsdalen ("valley of driftsand") at Kangerlussuaq, it was very common and scattered over a large area. The sand is mineral-rich due to mixing with loess.

Note. *Hebeloma colvinii* was originally described as "Agaricus colvini" (Peck 1875). The name is currently not in use, e.g. there are no records on Mushroom Observer (https://mushroomobserver.org/, accessed 23 Sept 2020) and while Mycoportal (https://mycoportal.org/portal/collections/list.php, accessed 2 Dec 2020) has 63 records, the most recent is from 1972. The identification of the Greenland collections is supported by unpublished studies of type material. It appears that exposed expanses of sandy soil are the characteristic habitat for the species, which is morphologically similar to a number of species of the difficult group around *H. dunense* and *H. mesophaeum*. *Hebeloma colvinii* can be recognized by its large ellipsoid spores, reminiscent of *Hebeloma psammophilum*, which is currently known only from western Europe (Beker et al. 2016).

***Hebeloma dunense* L. Corb. & R. Heim; Mém. Soc. natn. Sci. nat. Cherbourg 40 (2): 166, 1929.**
Fig. 10

Macroscopic description. Cap 1.0–7.0 cm in diameter, convex to umbonate, sometimes papillate, sometimes umbilicate, margin often involute when young, sometimes scalloped or serrate, becoming wavy or upturned with age, sometimes fibrillose along margin, tacky when moist, sometimes but not consistently hygrophanous, uniformly colored or variably bicolored, at center clay buff, dark olive buff, ochraceous or

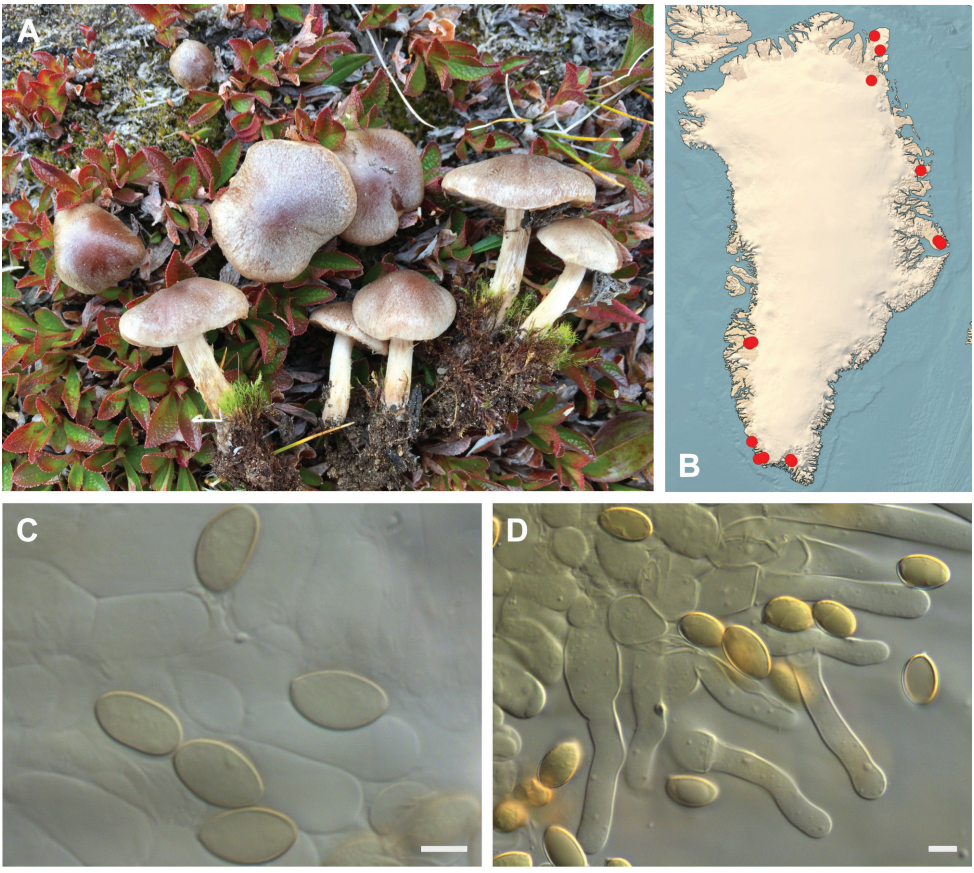

Figure 10. *Hebeloma dunense* **A** SAE-2017.103, photograph S.A. Elborne **B** distribution of cited collections **C** spores ×1600 and **D** cheilocystidia ×1000 of SAE-2017.103 in Melzer's reagent. Scale bars: 5 µm; microphotographs H.J. Beker.

yellowish brown to brownish olive or umber or sepia to dark brick or orange brown or fuscous, at margin cream to buff or honey to pinkish buff to dark olive buff or yellowish brown to umber or sepia, sometimes with remains of universal veil, partial veil present. Lamellae light gray brown or very pale clay, later brownish clay, adnexed to adnate, usually emarginate, sometimes with decurrent tooth and occasionally decurrent, maximum depth 2.5–9 mm, number of lamellae {L} 20–48, droplets usually absent, but occasionally visible with ×10 lens, white fimbriate edge usually present, but often weak. Stem (1.0–)1.4–8.0 × (0.2–)0.3–1.2 cm, at base 0.2–1.0(–1.2) cm, stem Q = 3.5–15, base cylindrical, sometimes slenderly clavate, occasionally with sand bulb, fibrillose, pruinose or floccose at apex. Context firm, stem interior stuffed, later hollow, occasionally with superior wick, flesh usually discoloring from base, sometimes very strongly. Smell raphanoid, rarely without smell, occasionally hints of cocoa; taste mild to raphanoid to bitter. Spore deposit dark olive buff to brownish olive to umber to fuscous or sepia.

Microscopic description. Spores mainly ellipsoid, some amygdaloid or ovoid, not papillate, 10.0–12.5 × 6.0–7.5 µm, ave. Q 1.5–1.9, very weakly ornamented (O1 O2), perispore not or somewhat loosening (P0 P1), indistinctly dextrinoid (D0 D1), yellow through yellow brown to brown, ± guttulate. Basidia 20–33 × 7–9 µm, ave. Q = 2.8–4, mostly four-spored. Cheilocystidia usually lageniform or ventricose, sometimes cylindrical, occasionally with characteristic wall thickenings, apically, medially or basically, occasionally bifurcate, geniculate, septate (sometimes clamped), subcapitate, 34–57 × 4.5–8 (apex) × 4–7 (middle) × 7–12 (base) µm, with yellow contents, ratios A/M = 0.82–1.43, A/B = 0.42–0.89, B/M = 1.4–2.14. Epicutis an ixocutis, 25–75 µm thick (measured from exsiccata), ixocutis maximum hyphae width 4–8 µm, hyphae occasionally encrusted, shape of trama elements beneath subcutis angular, ellipsoid, isodiametric, spherical or sausage-shaped up to 20 µm wide. Caulocystidia similar to cheilocystidia, but usually more irregular and often multi-septate.

Collections examined. S-Greenland: Kangilinnguit, 61.14°N, 48.6°W, 15 Aug 1985, T. Borgen (TB85.200, C-F-103530), 400 m, with *Salix herbacea* and *Dryas integrifolia* in snowbed. Kangilinnguit, 61.23°N, 48.10°W, 8 Aug 1984, T. Borgen (TB84.090, C-F-103535), 25 m, with *Salix herbacea* along streamside. Kangilinnguit, at Grønnedal Hut, 61.23°N, 48.08°W, 15 Aug 1985, T. Borgen (TB85.183, C-F-103589), 180 m. Kangilinnguit, near Grønnedal Hut, 61.23°N, 48.08°W, 15 Aug 1985, T. Borgen (TB85.186, C-F-103527), 350 m, with *Salix arctophila* in streamside. Narsarsuaq, 61.08°N, 45.26°W, 1 Aug 1991, T. Borgen (TB91.045, C-F-103486), 100 m, with *Salix glauca*. Narsarsuaq, 61.17°N, 45.41°W, 17 Aug 2015, H. Knudsen (HK15.078, C-F-8231), 60 m, with *Dryas* sp. along pathside. Paamiut, 62.01°N, 49.4°W, 12 Aug 1984, T. Borgen (TB84.114, C-F-103536), 10 m, with *Salix glauca* and *Salix herbacea*. **W-Greenland:** Kangerlussuaq, airport area, 67.02°N, 50.72°W, 10 Aug 1986, T. Borgen (TB86.177, C-F-103563), 30 m, with *Salix glauca*. Kangerlussuaq, near the inland ice, 67.09°N, 50.25°W, 12 Aug 2000, K. Kalamees (HK00.032, C-F-7881), 200 m, in tundra. Kangerlussuaq, Sandflugtsdalen, 67.06°N, 50.46°W, 7 Aug 2016, H. Knudsen (HK16.015, C-F-104045), 200 m, with *Salix glauca*. Kangerlussuaq, Sandflugtsdalen, c. 15 km E of Base, 67.04°N, 50.53°W, 7 Aug 2016, T. Borgen (TB16.076, C-F-104293), 50 m, with *Salix glauca*. Kangerlussuaq, Store Saltsø, 66.98°N, 50.6°W, 8 Aug 1986, T. Borgen (TB86.159, C-F-5087), 200 m, with *Salix glauca*. **N-Greenland:** Amdrup Land, 80.81°N, 17.32°W, 19 Jul 1993, B. Fredskild (s.n., C-F-7017), 225 m, with *Salix arctica* in tundra. Blåsø, Kronprins Christians Land, 79.62°N, 23.33°W, 4 Aug 1987, C. Bay (s.n., C-F-6994), 100 m. Prinsesse Dagmars Halvø, Knuths Fjeld, 81.58°N, 16.77°W, 6 Aug 1986, C. Bay (s.n., C-F-4216), 15 m. Zackenberg, at the S bank of Kærelv, 74.5°N, 21°W, 27 Jul 1999, T. Borgen (TB99.114, C-F-119746), 50 m, with *Dryas* sp. and *Salix arctica* in scrubland. Zackenberg, in the new delta, 74.5°N, 21°W, 22 Aug 1999, T. Borgen (TB99.411, C-F-119748), 20 m, with *Salix arctica* in scrubland. Zackenberg, just N of Gadekæret, 74.5°N, 21°W, 5 Aug 1999, T. Borgen (TB99.219, C-F-119752), 20 m, with *Dryas* sp. and *Salix arctica* in scrubland. Zackenberg, S of E part of airstrip, 74.5°N, 21°W, 12 Aug 2006, T. Borgen (TB06.159, C-F-119774), 30 m, with *Salix arctica* in snowbed.

Zackenberg, Zackenberg River, 74.5°N, 21°W, 23 Aug 2006, T. Borgen (TB06.263, C-F-119776), 20 m, with *Salix arctica* in riverbed. **E-Greenland:** Jameson Land, Constable Pynt, camp N of Katedralen, S of Ugleelv, 70.9°N, 22.92°W, 25 Jul 1989, J.H. Petersen (JHP 89.259, C-F-2561), 170 m. Jameson Land, Nerlerit Inaat/Constable Pynt, delta of Gåseelv valley, 70.76°N, 22.65°W, 12 Aug 2017, T. Borgen (TB17C.118, C-F-106782), 40 m, with *Bistorta vivipara* and *Salix arctica*. Jameson Land, Nerlerit Inaat/Constable Pynt, delta of Gåseelv valley, 70.76 22.65°W, 4 Aug 2017, T. Borgen (TB17C.037, C-F-106773), 40 m, with *Salix* sp. Jameson Land, Nerlerit Inaat/Constable Pynt, delta of Gåseelv valley, 70.76°N, 22.65°W, 12 Aug 2017, H. Knudsen (HK17.265B, C-F-105171), 40 m. Jameson Land, Nerlerit Inaat/Constable Pynt, delta of Gåseelv valley, 70.76°N, 22.65°W, 7 Aug 2017, H. Knudsen (HK17.147, C-F-105049), 40 m. Jameson Land, Nerlerit Inaat/Constable Pynt, delta of Gåseelv valley, 70.76°N, 22.65°W, 12 Aug 2017, H. Knudsen (HK17.265A, C-F-105170), 40 m. Jameson Land, Nerlerit Inaat/Constable Pynt, delta of Gåseelv valley, 70.76°N, 22.65°W, 6 Aug 2017, H. Knudsen (HK17.127, C-F-105028), 40 m. Jameson Land, Nerlerit Inaat/Constable Pynt, delta of Gåseelv valley, 70.77°N, 22.67°W, 5 Aug 2017, S.A. Elborne (SAE-2017.103-GR, C-F-106761), 40 m, with *Arctostaphylos alpina*. Jameson Land, Nerlerit Inaat/Constable Pynt, delta of Gåseelv valley, 70.77°N, 22.73°W, 11 Aug 2017, S.A. Elborne (SAE-2017.219-GR, C-F-106769), 40 m, with *Salix arctica* at riverside. Jameson Land, Nerlerit Inaat/Constable Pynt, delta of Gåseelv, Harris fjeld, 70.75°N, 22.68°W, 31 Jul 2017, T. Borgen (TB17C.006, C-F-106770), 100 m, with *Dryas* sp. in heathland. Jameson Land, Nerlerit Inaat/Constable Pynt, delta of Gåseelv, Harris fjeld, 70.75°N, 22.68°W, 3 Aug 2017, H. Knudsen (HK17.070, C-F-1049599, 100 m. Jameson Land, Nerlerit Inaat/Constable Pynt, Gåseelv valley, north side, 70.76°N, 22.69°W, 4 Aug 2017, H. Knudsen (HK17.088, C-F-104984), 160 m. Jameson Land, Nerlerit Inaat/Constable Pynt, Hareelv, 70.7°N, 22.68°W, 10 Aug 2017, T. Borgen (TB17C.094, C-F-106780), 200 m, with *Salix arctica* in snowbed. Jameson Land, Nerlerit Inaat/Constable Pynt, Hareelv, 70.7°N, 22.68°W, 2 Aug 2017, T. Borgen (TB17C.030, C-F-106772), 200 m, with *Salix arctica*. Jameson Land, Nerlerit Inaat/Constable Pynt, Hareelv, 70.7°N, 22.68°W, 2 Aug 2017, H. Knudsen (HK17.043, C-F-104932), 200 m. Jameson Land, Nerlerit Inaat/Constable Pynt, Hareelv, 70.7°N, 22.68°W, 2 Aug 2017, H. Knudsen (HK17.045, C-F-104934), 200 m. Jameson Land, Nerlerit Inaat/Constable Pynt, Hareelv, 70.7°N, 22.68°W, 2 Aug 2017, H. Knudsen (HK17.052, C-F-104941), 200 m. Jameson Land, Nerlerit Inaat/Constable Pynt, Hareelv, 70.7°N, 22.68°W, 2 Aug 2017, H. Knudsen (HK17.056, C-F-104945), 200 m. Jameson Land, Nerlerit Inaat/Constable Pynt, Hareelv, 70.71°N, 22.68°W, 10 Aug 2017, S.A. Elborne (SAE-2017.186-GR, C-F-106765), 200 m, with *Salix arctica* along streamside. Jameson Land, Nerlerit Inaat/Constable Pynt, middle of Hareelv valley, N side, 70.71°N, 22.73°W, 10 Aug 2017, H. Knudsen (HK17.203, C-F-105108), 320 m. Jameson Land, Nerlerit Inaat/Constable Pynt, Primulaelv, 70.74°N, 22.67°W, 1 Aug 2017, T. Borgen (TB17C.010, C-F-106771), 180 m, with *Salix arctica* and *Bistorta vivipara*. Jameson Land, Nerlerit Inaat/Constable Pynt, Primulaelv, 70.74°N, 22.67°W, 13 Aug 2017, H. Knudsen (HK17.282, C-F-105189), 180 m.

Distribution. *Hebeloma dunense* is a common and widespread *Hebeloma* distributed throughout Mediterranean, Temperate, Boreal, Arctic and Alpine areas. It has been recorded in arctic and alpine areas of North America, Europe and Asia (Russia) (Beker et al. 2016). It has one of the most northern records for a *Hebeloma* at 81.58° in Greenland (Beker et al. 2016). It appears to be one of the most common and widespread of all *Hebeloma* species in arctic or alpine regions. Circumpolar, Temperate, Boreal, Subarctic and Arctic-Alpine.

Habitat and ecology. Forty-two collections and one of the five most often collected species in Greenland with 11% of the collections. Most are with *Salix arctica* (10), *S. glauca* (6), *S. herbacea* (2), *S. arctophila* (1) or unspecified *Salix* in more or less calcareous habitats. The collection from Paamiut was from a man-made area, in this otherwise acid soil locality. Four collections were recorded with *Dryas integrifolia* and *D. octopetala* and one with *Arctostaphylos alpina* (L.) Spreng., although it is possible that some *Salix* was present. *Arctostaphylos alpina* is known as a likely mycorrhizal partner for *Hebeloma*, and has been recorded as the only possible mycorrhizal partner on several occasions (see for example Grilli et al. 2020). In the Rocky Mountains, *Hebeloma dunense* was recorded as mycorrhizal with *S. arctica*, *S. planifolia* and *S. reticulata* (Cripps et al. 2019). Beker et al. (2016) found the same pattern for hosts; practically all collections were connected to *Salix* or *Populus* (Salicaceae), and a few with *Dryas* in arctic areas. In Beker et al. (2018), reporting on collections from Svalbard, *H. dunense* was recorded with *Salix* 91% of the time, with *Dryas* 16%, with *Bistorta* 7% (note that more than one possible host was often recorded).

***Hebeloma excedens* (Peck) Sacc.; Syll. fung. (Abellini) 5: 806, 1887.**
Fig. 11

Macroscopic description. Cap 1.0–4.0 cm in diameter, shallowly convex, campanulate, then almost applanate, broadly umbonate or not, viscid or greasy, with hygrophanous spots, cinnamon to orange-brown or dark brick in center and pale brown on most of the cap, almost unicolored, with or without velar remnants at margin, or with whitish rim, margin originally described as extending beyond the lamellae, thin-fleshed, universal veil sometimes visible on margin edge, partial veil present. Lamellae sinuate, subdecurrent, narrow, becoming broader and eroded, 3.5–5.5 mm broad, without droplets, very pale, cream with pinkish buff tint, number of lamellae {L} 36–48. Stem 1.5–5.0 × 0.2–0.4 cm, equal, slightly curved, pale cream, silky, pruinose above ring zone, dingier to dark brown below, but still pale with golden brown fibrils in zones, blackening towards base, tough, rubbery. Context whitish in cap and stem apex and yellowish brown in lower stem down to blackish at base. Smell raphanoid, rarely odorless. Spore deposit brownish olive.

Microscopic description. Spores ellipsoid, a few slightly ovoid, not papillate, 8.5–10.5 × 5–6 µm, ave. Q 1.5–2.0, very weakly ornamented (O1 O2), perispore not noticeably loosening (P0), indistinctly dextrinoid (D0 D1), pale yellow, rarely yellow brown, ± guttulate. Basidia 20–33 × 6–8 µm, ave. Q = 3.2–4, clavate, mostly

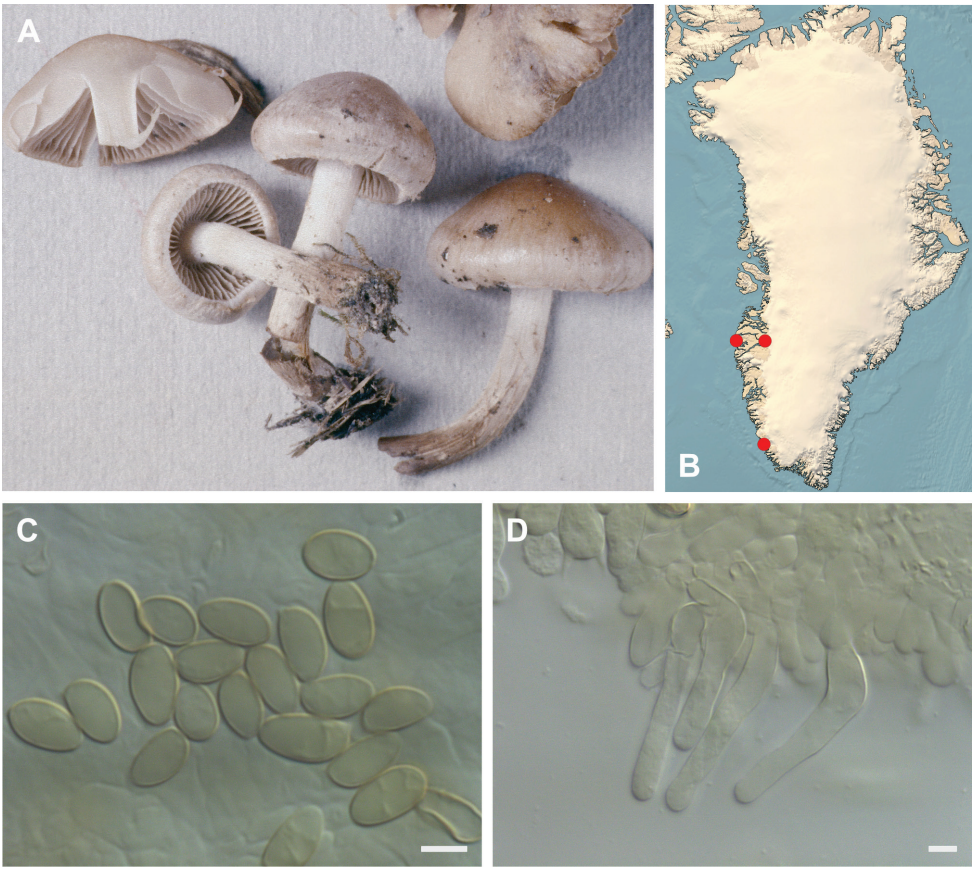

Figure 11. *Hebeloma excedens* **A** TB85.238, photograph T. Borgen **B** distribution of cited collections **C** spores ×1600 and **D** cheilocystidia ×1000 of TB85.238 in Melzer's reagent. Scale bars: 5 µm; microphotographs H.J. Beker.

four-spored. Cheilocystidia usually lageniform or ventricose, sometimes cylindrical, occasionally geniculate or septate, subcapitate, on ave. 30–55 × 4–6 (apex) × 4–5 (middle) × 7–9 (base) µm, ratios A/M = 0.96–1.23, A/B = 0.60–0.71, B/M = 1.60–1.82. Epicutis an ixocutis, up to 90 µm thick (measured from exsiccata), ixocutis maximum hyphae width up to 6 µm, hyphae rarely encrusted, shape of trama elements beneath subcutis ellipsoid. Caulocystidia similar to cheilocystidia, but usually larger.

Collections examined. S-Greenland: Paamiut, 62.01°N, 49.4°W, 23 Aug 1985, T. Borgen (TB85.238, C-F-5073), 10 m, with *Salix glauca*. **W-Greenland:** Kangerlussuaq near the Ice cap, 67.10°N, 50.23°W, 12 Aug 2000, A-M. Larsen, T. Borgen (TB00.086, C-F-103517), 40 m, with *Salix glauca* in a copse. Sisimiut, 1 km N of the village, 66.94°N, 53.67°W, 19 Aug 2000, E. Ohenoja (EO19.8.00.20, OULU F050653), 0 m, in heathland.

Distribution. Known from three localities in southwestern Greenland. Originally described from New York State under *Pinus* and widespread across North America

(Cripps et al. 2019). Similar to *H. mesophaeum* and therefore likely to be confused and overlooked. Cripps et al. also describe recent records from alpine Rocky Mountains in Colorado and Montana.

Habitat and ecology. Three collections, two of them with *Salix glauca*. In the Rocky Mountains, *S. planifolia* was the dominant host (Cripps et al. 2019). Two of the localities are on acid soil.

***Hebeloma fuscatum* Beker & U. Eberh.; Beker, Eberhardt & Vesterholt, Fungi Europ. (Alassio) 14: 133, 2016.**
Fig. 12

Macroscopic description. Cap 0.7–2.5 cm in diameter, convex to umbonate, margin smooth, tacky when moist, not hygrophanous, uniformly colored or more often bicolored, at center sepia to fuscous or dark brick, sometimes with a thin tomentum, at margin dark olive buff to cinnamon or umber; sometimes with remains of universal veil, partial veil present. Lamellae yellowish ochre then brown, emarginate, maximum depth 4 mm, number of lamellae {L} 24–32, droplets absent, white fimbriate edge usually present, but weak. Stem 0.8–7.0 × 0.15–0.5 {median} cm, whitish or pale grayish then browner to gray brown, not darker towards the base, cylindrical, stem Q 4–13, fibrillose, pruinose at apex. Context firm, stem interior stuffed, later hollow, flesh usually discoloring from base. Smell usually raphanoid but sometimes without smell; taste not recorded. Spore deposit color not recorded.

Microscopic description. Spores amygdaloid, limoniform, occasionally ovoid, papillate, on ave. 12.5–13.5 × 7.0–7.5 µm, ave. Q = 1.6–1.9, brown, guttulate, almost smooth to weakly ornamented (O1 O2), perispore not or hardly loosening (P0 (P1)), weakly to rather strongly dextrinoid (D2 D3). Basidia 27–33(-36) × 8–9 µm, ave. Q = 3.0–4.1, mostly four-spored. Cheilocystidia usually lageniform or ventricose, occasionally cylindrical, occasionally characteristically with an apical, basal or median thickening, on ave. 41–51 × 4–7 (apex) × 4.5–6 (middle) × 8–13 (base) µm, ratios A/M = 0.9–1.13, A/B = 0.48–0.67, B/M = 1.75–1.97. Epicutis an ixocutis of 30 µm thickness (measured from exsiccata), maximum hyphae width 5–6 µm, sometimes encrusted, shape of trama elements beneath subcutis sausage-shaped and up to 19 µm wide. Caulocystidia similar to cheilocystidia, but less ventricose and very fragile, up to 75 µm long.

Collections examined. S-Greenland: Paamiut, Churchyard, 62°N, 49.67°W, 26 Jul 1985, D. Boertmann (DB 85-21, C-F-119783), 25 m, with *Salix glauca*. **W-Greenland:** Kangerlussuaq, SE of Ravneklippen, 67.00°N, 50.67°W, 29 Aug 2018, T. Borgen (TB18.243, C-F-112530), 200 m, with *Salix* sp. in fen. Sisimiut, Præstefjeld, 66.96°N, 53.74°W, 17 Aug 2016, S.A. Elborne (SAE-2016.072-GR, C-F-106737), 300 m, with *Salix herbacea* and *Bistorta vivipara*. Upernavik, 72.79°N, 56.14°W, 18 Aug 2012, D. Boertmann (DB 12.047, C-F-115623), 0 m, in churchyard. **E-Greenland:** Jameson Land, Nerlerit Inaat/Constable Pynt, around the airport, 70.74°N,

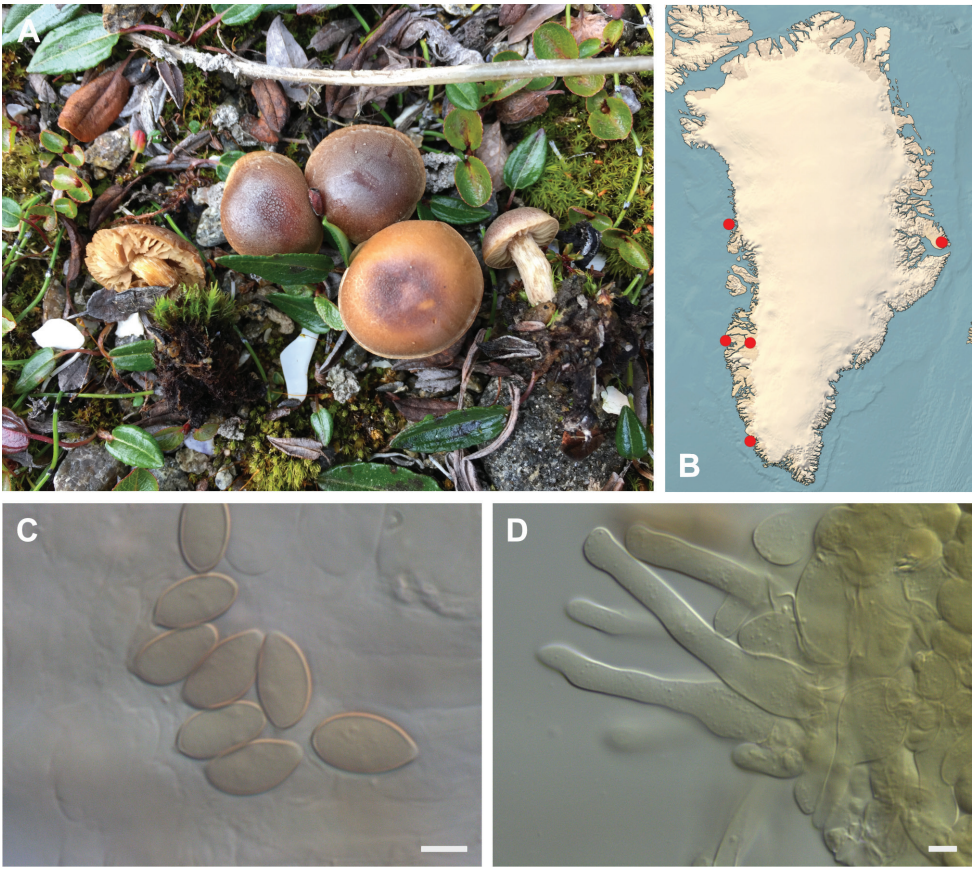

Figure 12. *Hebeloma fuscatum* **A** SAE-2016.072, photograph S.A. Elborne **B** distribution of cited collections **C** spores ×1600 and **D** cheilocystidia ×1000 of SAE-2016.072 in Melzer's reagent. Scale bars: 5 µm; microphotographs H.J. Beker.

22.64°W, 31 Jul 2017, H. Knudsen (HK17.009A, C-F-104897), 50 m. Jameson Land, Nerlerit Inaat/Constable Pynt, delta of Gåseelv valley, 70.77°N, 22.72°W, 11 Aug 2017, S.A. Elborne (SAE-2017.215-GR, C-F-106768), 40 m, with *Salix arctica* along riverside. Jameson Land, Nerlerit Inaat/Constable Pynt, Gåseelv valley, north side, 70.76°N, 22.69°W, 4 Aug 2017, H. Knudsen (HK17.091, C-F-104987), 160 m, with *Salix* sp. in tundra. Jameson Land, Nerlerit Inaat/Constable Pynt, Primulaelv, 70.74°N, 22.67°W, 13 Aug 2017, T. Borgen (TB17C.129, C-F-106783), 180 m, with *Betula* and *Salix* in heathland.

Distribution. Recently described and still only recorded from a few alpine and arctic areas in Europe and arctic Canada (Beker et al. 2016). The Greenland collections are from the Low Arctic zone and High Arctic zone, but the species is rare and scattered. Circumpolar, arctic-alpine.

Habitat and ecology. Eight collections, six with *Salix glauca*, *S. arctica* and *S. herbacea*, two with undetermined *Salix* sp. The presence of *Bistorta* and *Betula* are mentioned, each on one occasion. Soil conditions are variable, but mostly calcareous.

Salix was the only host mentioned by Beker et al. (2016). Some recent records from subalpine woodlands in central Europe suggest it may also associate with conifers (Grilli et al. 2020).

***Hebeloma grandisporum* Beker, U. Eberh. & A. Ronikier; Eberhardt, Ronikier, Schütz & Beker, Mycologia 107(6): 1293, 2015.**
Fig. 13

Macroscopic description. Cap up to 1.0 cm in diameter, convex to umbonate, margin usually smooth, but can be crenulate, becoming upturned with age, tacky when moist, with slight spotting, not hygrophanous, uniformly colored or bicolored, at center clay buff or pale yellowish brown or cinnamon, at margin paler, universal veil absent, partial veil present. Lamellae clay color, emarginate to adnate, maximum depth not recorded, number of lamellae {L}18–28; droplets absent, white fimbriate edge indistinct. Stem 1.0–2.0 × 0.2–0.3 cm, ochre-brown, paler in apex, cylindrical, stem Q 6.0–8.5, fibrillose, pruinose at apex. Context firm, stem interior stuffed, stem flesh not discoloring from base. Smell weakly raphanoid or insignificant. Taste not recorded. Spore deposit not recorded.

Microscopic description. Spores amygdaloid or limoniform, very strongly papillate, on ave. 14–16 × 8.5–9.5 µm, ave. Q = 1.6–1.8, pale brown to yellow brown, weakly guttulate, almost smooth to weakly ornamented (O1 O2), perispore not loosening (P0), distinctly to rather strongly dextrinoid (D2 D3). Basidia 23–44 × 6–10 µm, ave. Q = 3.1–4.3, characteristically 2-spored. Cheilocystidia lageniform or ventricose, occasionally clavate-ventricose, characteristically geniculate and septate, on ave. 40–70 × 5.5–6.5 (apex) × 4.5–5.5 (middle) × 8–10.5 (base) µm, ratios A/M = 1.02–1.44, A/B = 0.53–0.75, B/M = 1.48–2.03. Epicutis an ixocutis, up to 130 µm thick (measured from exsiccata), maximum hyphae width 6 µm, ixocutis hyphae sometimes encrusted, shape of trama elements beneath subcutis isodiametric. Caulocystidia similar to cheilocystidia, up to 120 µm long.

Collections examined. N-Greenland: Zackenberg, Sydkæret, 74.50°N, 20.75°W, 19 Aug 1999, T. Borgen (TB99.376, C-F-104295), 30 m, with *Salix arctica*. **E-Greenland:** Jameson Land, Nerlerit Inaat/Constable Pynt, west side of Nathorst Fjeld, 70.76°N, 22.64°W, 5 Aug 2017, H. Knudsen (HK17.101, C-F-104997), 40 m, with *Salix* sp. in tundra.

Distribution. Recently described from the southern Carpathians in Romania from a single collection. The two Greenland collections are the first recorded since the type has been published. Both are from the High Arctic zone in Greenland at 70° and 74°N, and it is thus in the northernmost group among the 28 Greenland species. The records are the first from North America and the first outside Europe.

Habitat and ecology. Only two records, both most likely with *Salix arctica* and both on calcareous soil. The only previous collection, the type, grew with *S. retusa* L. at 2270 m a.s.l. in the Carpathians (Eberhardt et al. 2015a). Shiryaev et al. (2018) reported from Zmitrovich and Ezhov (2015) the presence of *Hebeloma gigaspermum* Gröger & Zschiesch. from Franz Josefs Land (Russia). According to Beker et al. (2016), *H. gigaspermum* is most likely a synonym of *H. nauseosum* Sacc. Since neither *H. nauseosum* nor

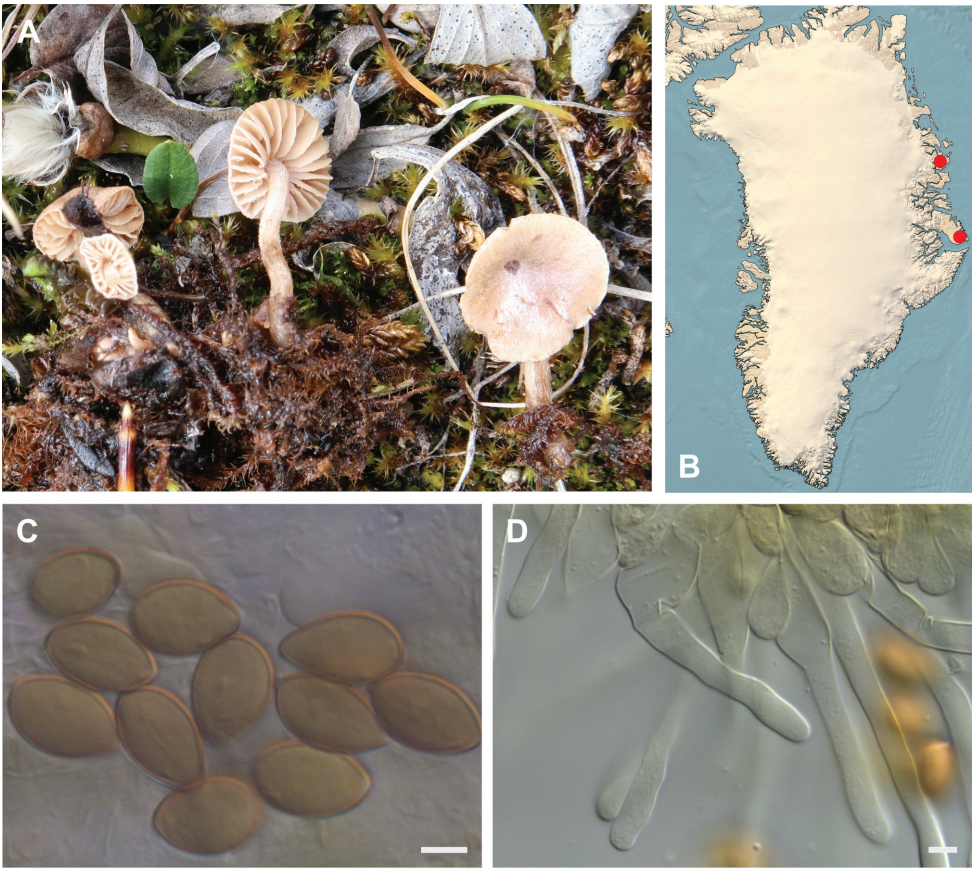

Figure 13. *Hebeloma grandisporum* **A** HK17.101, photograph H. Knudsen **B** distribution of cited collections **C** spores ×1600 and **D** cheilocystidia ×1000 of HK17.101 in Melzer's reagent. Scale bars: 5 µm; microphotographs H.J. Beker.

any other species of *H.* sect. *Sacchariolentia* occurs in arctic areas, it may be that the large spores and the occurrence in the High Arctic zone rather point to *H. grandisporum*.

Notes. *Hebeloma grandisporum* is one of the most easily recognized among the arctic-alpine *Hebeloma* species by the small basidiomes, the large spores, the relatively few, distant lamellae and large, 2-spored basidia. To date, it is the only *Hebeloma*, of which we are aware, that has consistently 2-spored basidia.

Hebeloma hygrophilum **Poumarat & Corriol; Beker, Eberhardt, & Vesterholt, Fungi Europ. (Alassio) 14: 138, 2016.**
Fig. 14

Macroscopic description. Cap 0.6–3.0 cm in diameter, convex, occasionally umbonate, margin smooth, tacky when moist, not hygrophanous, uniformly colored or bicolored, at center red brown, dark brick, at margin clay-buff, sometimes with

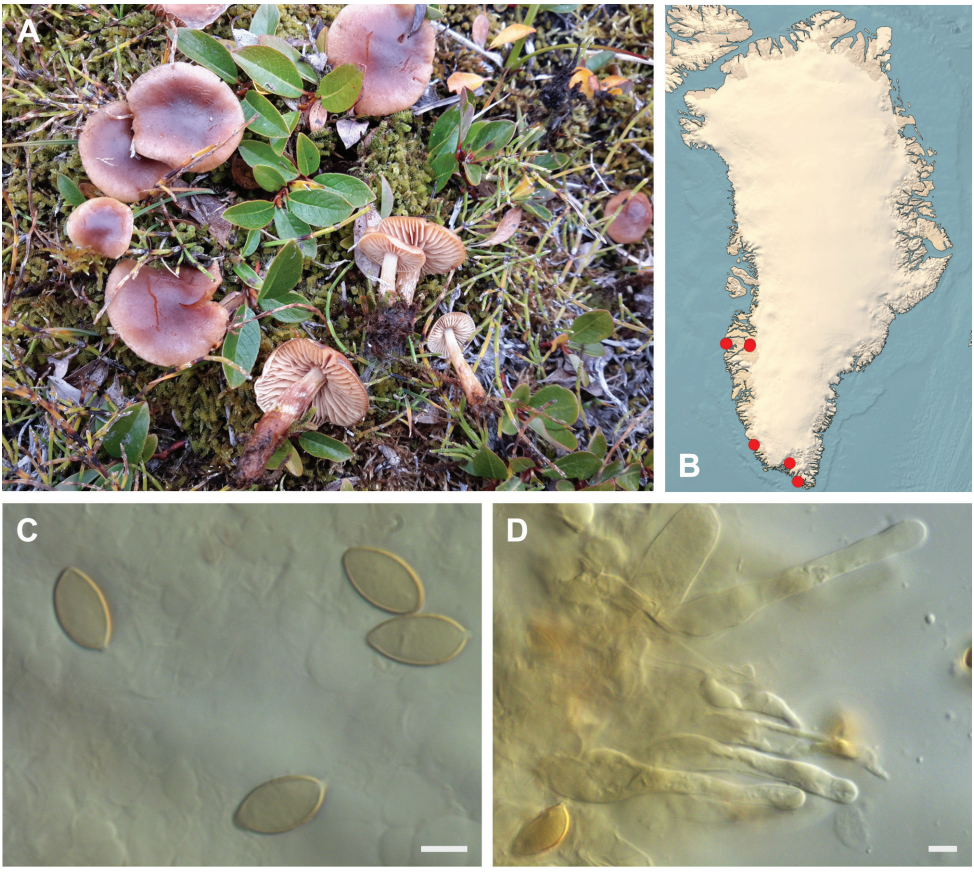

Figure 14. *Hebeloma hygrophilum* **A** HK16.195, photograph H. Knudsen **B** distribution of cited collections **C** spores ×1600 and **D** cheilocystidia ×1000 of HK16.195 in Melzer's reagent. Scale bars: 5 µm; microphotographs H.J. Beker.

whitish fibrils, remains of universal veil variably present, partial veil present. Lamellae at first whitish or pale orange brown, becoming pale cocoa brown, attachment adnate to emarginate, maximum depth not recorded, number of lamellae {L} 23–32; droplets absent, white fimbriate edge usually present, but weak. Stem 2.0–4.3(–5.0) × 0.1–0.45(–0.7) cm, at first whitish, becoming bright orange brown to dirty brown, darker brown towards the base, cylindrical, stem Q (7.1–)10.1–25.8(–35), fibrillose, pruinose to floccose at apex. Context firm, stem interior stuffed, stem flesh discoloring from base. Smell raphanoid, sometimes weakly. Taste mild, raphanoid, later bitter. Spore deposit not recorded.

Microscopic description. Spores shape amygdaloid, fusoid or limoniform, papillate, on ave. 11–13 × 6.0–7.0 µm, ave. Q = 1.7–2.0, brown, guttulate, sometimes weakly, weakly to distinctly ornamented ((O1) O2 (O3)), perispore not or somewhat loosening, (P0 P1), distinctly to rather strongly dextrinoid (D2 D3). Basidia 27–32 × 7–9 µm, ave. Q = 3.2–4.2, mostly four-spored. Cheilocystidia lageniform or ventricose, occasionally cylindrical, occasionally with characteristic apical or median wall

thickening, geniculate or septate (sometimes clamped), 42–64 × 4.5–5.5 (apex) × 4–5 (middle) × 7–11.5 µm, ratios A/M = 0.89–1.24, A/B = 0.36–0.71, B/M = 1.57–2.52. Epicutis an ixocutis, thickness up to 100–130 µm (measured from exsiccata), maximum hyphae width up to 6–7 µm, ixocutis hyphae sometimes encrusted, trama elements beneath subcutis ellipsoid, sausage-shaped, sometimes cylindrical up to 20 µm wide. Caulocystidia cylindrical to ventricose, multi-septate up to 90 µm long.

Collections examined. S-Greenland: E of Tasiusaq, 61.15°N, 45.60°W, 20 Aug 1993, E. Rald (ER 93.519, C-F-105494), 10 m, in meadow. S of Tasiusaq, 61.13°N, 45.62°W, 23 Aug 1993, E. Rald (ER 93.425, C-F-104549), 0 m. Paamiut, Taartoq/Mørke Fiord, 62.01°N, 49.26°W, 29 Aug 1998, T. Borgen (TB98.234, C-F-103511), 5 m, with *Salix glauca* in copse. Narsarsuaq, north of Tasiusaq, 60.199186°N, 44.80696°W, 15 Aug 2019, T. Borgen (TB19.052, C-F-137115), 100 m, with *Salix glauca* in moss on streamside. **W-Greenland:** Kangerlussuaq, east of Ravneklippen, 67.01°N, 50.66°W, 24 Aug 2016, S.A. Elborne (SAE-2016.168-GR, C-F-106746), 120 m, with *Salix glauca* along lakeside copse. Kangerlussuaq, Hassells Fjeld, Kløftsøerne, 67.01°N, 50.71°W, 28 Aug 2018, H. Knudsen (HK18.390A, C-F-111118), 300 m, with *Salix glauca* in bog. Kangerlussuaq, Kløftsøerne, 67°N, 50.71°W, 20 Aug 2016, S.A. Elborne (SAE-2016.105-GR, C-F-106741), 300 m, with *Betula nana* and *Bistorta vivipara* along lakeside. Kangerlussuaq, Kløftsøerne, 67.03°N, 50.68°W, 20 Aug 2016, S.A. Elborne (SAE-2016.116-GR, C-F-106742), 300 m, with *Salix glauca* in copse. Kangerlussuaq, Kløftsøerne, 67.03°N, 50.67°W, 10 Aug 2016, H. Knudsen (HK16.064, C-F-104093), 500 m, in bog. Kangerlussuaq, Kløftsøerne, 67.01°N, 50.71°W, 28 Aug 2018, T. Borgen (TB18.236, C-F-112528), 300 m, with *Salix glauca* in copse. Kangerlussuaq, N slope towards Lake Ferguson, 66.95°N, 50.72°W, 29 Aug 2018, S.A. Elborne (SAE-2018.429-GR, C-F-115622), 548 m, with *Salix arctophila* along lakeside. Sisimiut, camping area north of town, 66.94°N, 53.67°W, 20 Aug 2000, S.A. Elborne (SAE-2000.148-GR, C-F-108600), 0 m, with *Salix arctophila* in bog. Sisimiut, near airport, 66.95°N, 53.67°W, 14 Aug 2016, S.A. Elborne (SAE-2016.005-GR, C-F-106735), 10 m, with *Salix* sp. in bog. Sisimiut, north of Alanngorsuaq, 66.95°N, 53.55°W, 15 Aug 2016, S.A. Elborne (SAE-2016.022-GR, C-F-106736), 30 m, with *Salix* sp. in bog. In valley S of Sisimiut behind the dump, 66.93°N, 53.67°W, 18 Aug 2016, H. Knudsen (HK16.195, C-F-108446), 25 m.

Distribution. Found a number of times in southwestern Greenland. Recently described from subalpine areas in the Pyrenees (France) and known from scattered lowland and montane localities in much of Europe. The northernmost locality is from the Boreal zone in Finland (Rovaniemi) at 66.50°N (Beker et al. 2016), which corresponds well in altitude with Kangerlussuaq and Sisimiut (67°N), but in Greenland these areas are Low Arctic. *Hebeloma hygrophilum* was recently recorded from alpine North America (Rocky Mountains, Cripps et al. 2019). Circumpolar, arctic-alpine, boreal zone.

Habitat and ecology. Fifteen collections, ten with *Salix glauca*, *S. arctophila* or unknown *Salix*. One collection with *Betula nana*. Most collections grew in moist habitats often among *Sphagnum* or the moss *Paludella squarrosa* (Hedw.) Brid. The same type of boggy localities with *Salix planifolia* were reported by Cripps et al. (2019) in the Rocky

Mountains and by Beker et al. (2016) from Europe, where *Salix aurita*, *S. atrocinerea* and possibly more species of *Salix* act as hosts.

***Hebeloma marginatulum* (J. Favre) Bruchet; Bull. mens. Soc. linn. Lyon 39(6(Suppl.)): 43, 1970.**
Fig. 15

Macroscopic description. Cap 1.1–4.7 cm in diameter, convex to umbonate, occasionally papillate, margin smooth, tacky when moist, sometimes hygrophanous, uniformly colored or variably bicolored, at center ochraceous or dark olive buff to brownish olive or umber to sepia to fuscous or dark brick, at margin cream to grayish or pinkish buff to ochraceous or dark olive buff to umber, sometimes very thin; with remains of universal veil, partial veil present. Lamellae initially very pale clay, later clay, emarginate, maximum depth 3–8 mm, number of lamellae {L} 32–45, droplets absent, white fimbriate edge usually weakly present. Stem 1.4–4.5(–6.5) × 0.3–0.7(–0.8) cm, pale sordid ochraceous downwards, cylindrical to slightly clavate, fibrillose, whitish pruinose to floccose at apex. Context watery gray brown in cap, in stem lighter, firm, stem interior stuffed, later hollow, occasionally with superior wick, stem flesh usually discoloring from base. Smell usually raphanoid, but sometimes no smell detected. Taste bitter. Spore deposit clay buff to dark olive buff to grayish brown to brownish olive or umber.

Microscopic description. Spores shape ellipsoid, occasionally amygdaloid or ovoid, on ave. 10.0–13.0 × 5.5–7.5 µm, ave. Q = 1.6–1.9, grayish yellow, rarely guttulate, almost smooth (O1 (O2)), perispore not loosening (P0), not or indistinctly dextrinoid (D0 D1). Basidia (28–)30–34(–37) × 7–9 µm, ave. Q = 4–4.5, mostly four-spored. Cheilocystidia lageniform, ventricose or occasionally cylindrical or clavate, occasionally with characteristic apical thickening, bifurcate, geniculate and septate (sometimes clamped), on ave. 44–69 × 5–7 (apex) × 4.5–5 (middle) × 7.5–10.5 (base) µm, ratios A/M = 1.1–1.4, A/B = 0.53–0.81, B/M = 1.55–2.33. Epicutis an ixocutis, 40–100 µm thick (measured from exsiccata), maximum hyphae width 5–6 µm, variably encrusted, trama elements beneath subcutis ellipsoid, sausage-shaped, occasionally pyriform up to 20 µm wide. Caulocystidia similar to cheilocystidia, but many multi-septate up to 150 µm long.

Collections examined. S-Greenland: Alluitsoq, 60.32°N, 45.27°W, 21 Jul 2003, H.J. Beker (HJB10739), 0 m, with *Betula* sp. and *Salix* sp. in scrubland. Alluitsoq, 60.32°N, 45.27°W, 21 Jul 2003, H.J. Beker (HJB 10742), 0 m, with *Betula* sp. and *Salix* sp. in scrubland. Ivittuut, 61.2°N, 48.17°W, 16 Aug 1991, T. Borgen (TB91.198, C-F-103489), 75 m, with *Salix glauca* in copse. Kangilinnguit, bottom of Laksebund, 61.25°N, 48.08°W, 21 Aug 2018, H. Knudsen (HK18.288, C-F-111113), 100 m, in tundra. Nanortalik municipality, Qinngua valley, 60.14°N, 45°W, 22 Jul 2003, H.J. Beker (HJB 10730), 100 m, with *Betula pubescens* and *Salix glauca* in woodland. Nanortalik municipality, Qinngua valley, 60.14°N, 45°W,

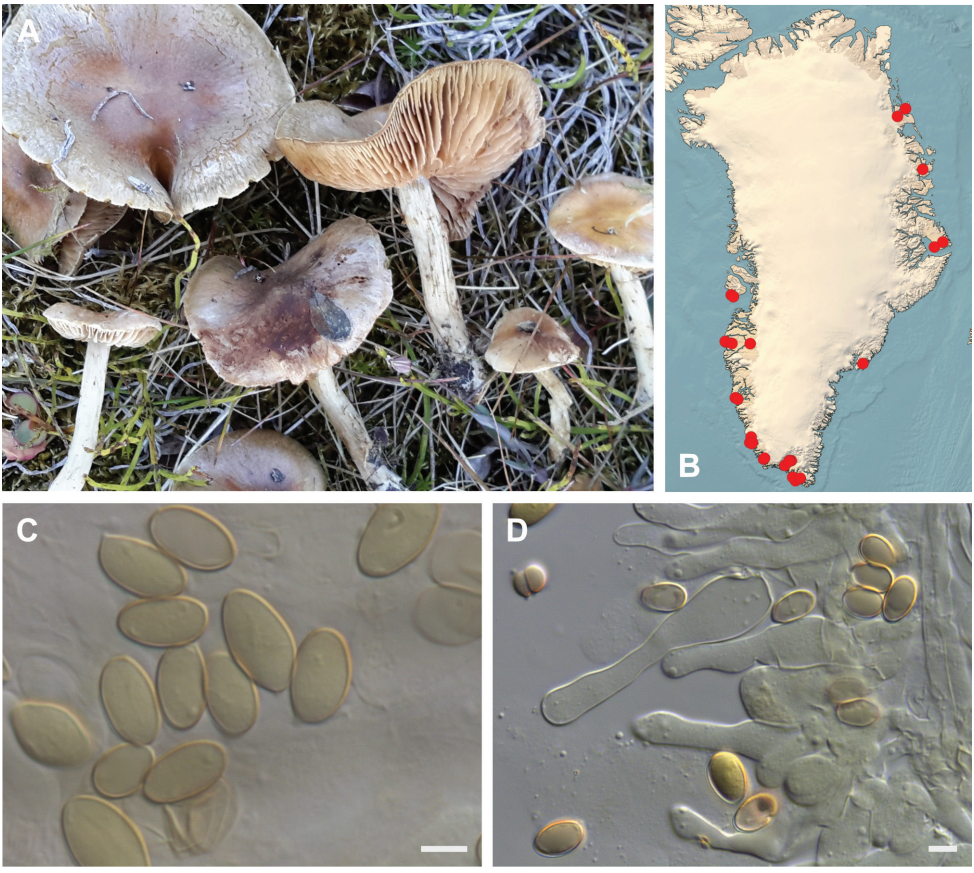

Figure 15. *Hebeloma marginatulum* **A** HK16.082, photograph H. Knudsen **B** distribution of cited collections **C** spores ×1600 and **D** cheilocystidia ×1000 of HK16.082 in Melzer's reagent. Scale bars: 5 µm; microphotographs H.J. Beker.

22 Jul 2003, H.J. Beker (HJB 10732), 100 m, with *Betula pubescens* and *Salix glauca* in woodland. Narsaq, 60.91°N, 46.05°W, 13 Aug 1993, E. Rald (ER 93.320, C-F-104552), 20 m, with *Salix glauca* in heathland. Narsaq, 60.91°N, 46.05°W, 2 Aug 1993, E. Rald (ER 93.111, C-F-104312), 20 m, with *Salix glauca* in heathland. Narsaq, 60.91°N, 46.05°W, 2 Aug 1993, E. Rald (ER 93.112, C-F-106421), 20 m. Narsarsuaq, 61.17°N, 45.42°W, 7 Aug 1985, T. Borgen (TB85.036, C-F-5085), 600 m, with *Salix herbacea* in snowbed. NE of Nunatoq, 60.27°N, 44.54°W, 22 Aug 1993, E. Rald (ER 93.589, C-F-104554), 0 m. N of Tasiusaq, across the fjord from Narsarsuaq, 61.17°N, 45.61°W, 5 Aug 1992, E. Rald (ER 92.109, C-F-104304), 150 m. Paamiut, 62.01°N, 49.4°W, 20 Aug 1993, T. Borgen (TB93.139, C-F-103495), 50 m, with *Salix herbacea* in snowbed. Paamiut, 62.01°N, 49.4°W, 23 Aug 1992, T. Borgen (TB92.027, C-F-103493), 10 m, with *Salix arctophila* and *Salix herbacea* in fens. Paamiut, 62.01°N, 49.4°W, 23 Aug 1992, T. Borgen (TB92.028, C-F-103492), 10 m, with *Salix arctophila* and *Salix herbacea* in tundra.

Paamiut, 62.01°N, 49.4°W, 8 Aug 1981, T. Borgen (TB81.109, C-F-103553), 10 m, with *Salix herbacea*. Paamiut, 61.99°N, 49.66°W, 5 Sep 1986, T. Borgen (TB86.299, C-F-104300), 25 m. Paamiut, 61.99°N, 49.66°W, 4 Aug 1993, E. Rald (ER 93.181, C-F-104314), 25 m, with *Salix glauca* in heathland. Paamiut, 62°N, 49.4°W, 22 Aug 1986, T. Borgen (TB86.247, C-F-103467), 20 m, with *Salix herbacea* and *Bistorta vivipara*. Paamiut Cemetery, 62.01°N, 49.4°W, 19 Aug 1984, T. Borgen (TB84.151, C-F-103538), 10 m, with *Salix arctophila*. Paamiut, Kangerluarsuk S, 62.28°N, 49.58°W, 31 Aug 1995, B. Knudsen (TB95.068, C-F-103505), 150 m. Paamiut, Kangilineq/Kvaneøen, 61.95°N, 49.47°W, 20 Aug 2008, T. Borgen (TB08.146, C-F-106750), 30 m, with *Salix glauca*. Qassiarsuk, Tasiusaq, 61.15°N, 45.52°W, 9 Aug 1992, E. Rald (ER 92.181, C-F-104306), 25 m. Qassiarsuk, Tasiusaq, 61.15°N, 45.52°W, 9 Aug 1992, E. Rald (ER 92.180, C-F-104305), 25 m. Tasiusaq, 61.14°N, 45.63°W, 28 Jul 1993, E. Rald (ER 93.021, C-F-104319), 20 m, with *Salix glauca* in heathland. **W-Greenland:** Disko, Fortune Bay, 69.31°N, 53.88°W, 2 Aug 1986, T. Borgen (TB86.119, C-F-103566), 20 m. Qeqertarsuaq/Disko, Godhavn, 69.24°N, 53.54°W, 28 Jul 1986, T. Borgen (TB86.060, C-F-6922), 0 m. Disko, Qeqertarsuaq, 69.25°N, 53.55°W, 27 Jul 1986, T. Borgen (TB86.072, C-F-5090), 0 m. Kangerluarsunguaq/Kobbefjord, just south of the field station, 64.14°N, 51.39°W, 11 Aug 2009, T. Borgen (TB09K017, C-F-106753), 20 m, with *Salix herbacea* in snowbed. Kangerlussuaq, NE facing slopes along Lake Ferguson, 66.10°N, 50.61°W, 12 Aug 2016, H. Knudsen (HK16.082, C-F-104111), 300 m. Nuuk, airport area, 64.19°N, 51.67°W, 14 Aug 2008, T. Borgen (TB08.126, C-F-106749), 100 m, with *Salix herbacea* in snowbed. Sisimiut, from airport and round the mountain, 66.95°N, 53.72°W, 17 Aug 2016, H. Knudsen (HK16.181, C-F-108419), 30 m. Sisimiut, from airport and round the mountain, 66.95°N, 53.72°W, 17 Aug 2016, H. Knudsen (HK16.180, C-F-108418), 30 m. Sisimiut, into the E valley, 66.90°N, 52.86°W, 15 Aug 2016, H. Knudsen (HK16.134, C-F-104164), 0 m, with *Salix herbacea* and *Salix arctica*. Sisimiut, south of town, 66.93°N, 53.65°W, 18 Aug 2016, S.A. Elborne (SAE-2016.085-GR, C-F-106738), 20 m, with *Salix herbacea* in snowbed. **N-Greenland:** NE of Annekssø, 77.42°N, 21.33°W, 20 Jul 1990, B. Fredskild (BF 90 loc. 5, C-F-5113), 150 m. Stormlandet, N of Depotnæs, 77.6°N, 18.95°W, 20 Aug 1990, B. Fredskild (BF 90 loc. 8, C-F-5147), 20 m. Zackenberg, 74.5°N, 21°W, 14 Aug 2006, T. Borgen (TB06.170, C-F-119778) ,35 m, with *Dryas* sp. and *Salix* sp. in scrubland. Zackenberg, 74.5°N, 21°W, 5 Aug 2006, T. Borgen (TB06.090, C-F-119779), 30 m, with *Dryas* sp. and *Salix arctica* in grassland. Zackenberg, near Teltdammen, 74.5°N, 21°W, 5 Aug 2006, T. Borgen (TB06.090, C-F-119747), 30 m, with *Dryas* sp. and *Salix arctica* in scrubland. Zackenberg, shortly SW of Kamelen, 74.5°N, 21°W, 11 Aug 2006, T. Borgen (TB06.158, C-F-119775), 40 m, with *Salix arctica* and *Bistorta vivipara* in grassland. **E-Greenland:** Jameson Land, Constable Pynt, 70.75°N, 22.67°W, 30 Jul 1988, D. Boertmann (DB GR 88-40, C-F-3453), 2 m, with *Salix arctica*. Jameson Land, Constable Pynt, delta of Jyllandselv, 70.68°N, 24.08°W, 28 Jul 1988, D. Boertmann (DB GR 88-33, C-F-3448), 10 m, with *Salix herbacea*. Jameson Land, Nerlerit Inaat/Constable Pynt, delta of

Gåseelv valley, 70.76°N, 22.65°W, 7 Aug 2017, H. Knudsen (HK17.149, C-F-105051), 40 m. Kuummiut, Torsukattak, 65.87°N, 37.01°W, 2 Aug 2008, T. Borgen (TB08.035, C-F-101622), 35 m.

Distribution. *Hebeloma marginatulum* is widespread and, apparently, one of the most common *Hebeloma* species in Greenland (11.1% of the collections, see Table 3), also common in other parts of North America and present in parts of Europe (Beker et al. 2016; Cripps et al. 2019). It is a truly arctic-alpine species hardly found outside these areas. Arctic-alpine.

Habitat and ecology. Forty-five collections with many hosts. Twenty collections with *Salix* (*S. herbacea* 9, *S. glauca* 6, *S. arctophila* 3 and *S. arctica* 2), two with *Betula pubescens* var. *pumila*, two with *Betula* sp. and three with *Dryas octopetala* and *D. integrifolia* (as always, other potential hosts may have been nearby). In the Rocky Mountains, it is also common, found with *Salix arctica*, *S. reticulata* and *S. planifolia* (Cripps et al. 2019). Beker et al. (2016) have *S. herbacea* and *S. polaris* as the main hosts. *Hebeloma marginatulum* occurs on a variety of soil types seemingly without specific preferences.

Hebeloma mesophaeum (Pers.) Quél.; Mém. Soc. Émul. Montbéliard, Sér. 2, 5: 128, 1872.

Fig. 16

Macroscopic description. Cap 0.7–6.5 cm in diameter, convex when young, usually becoming umbonate, sometimes papillate, margin sometimes involute when young, occasionally crenulate, often eroded, upturned or radially split when older, tacky when moist, not hygrophanous, usually bicolored, rarely unicolored, at center dark pinkish buff to dark olive buff to grayish brown to umber or brownish olive to sepia to clay-buff or cinnamon or yellowish brown to orange brown or dark brick, at margin cream to pinkish buff to grayish buff or clay-buff to dark olive buff to grayish brown or brownish olive to grayish pink, with remains of universal veil, partial veil present. Lamellae when young pale brown, when older ochre brown to fairly dark brown, adnate to emarginate, sometimes with decurrent tooth, rarely decurrent, maximum depth up to 6.5 mm, number of lamellae {L} 30–48, droplets absent, but occasionally visible with × 10 lens or rarely visible with naked eye, white fimbriate edge usually present, sometimes weak. Stem 1.4–8.0(–9.0) × (0.2–)0.3–0.6(–0.8) cm, whitish then pale sordid gray brown, already when young dark sordid brown at base, when young with brownish tomentose velar remnants downwards, cylindrical, rarely tapering or clavate, stem Q (4.3–)4.8–16.3(–18.8), fibrillose, usually pruinose to floccose at apex. Context firm, stem interior stuffed, later hollow, occasionally with superior wick, stem flesh discoloring from base, sometimes very strongly, rarely absent. Smell usually raphanoid, rarely absent. Taste mild to bitter, sometimes raphanoid. Spore deposit dark olive buff to brownish olive to umber.

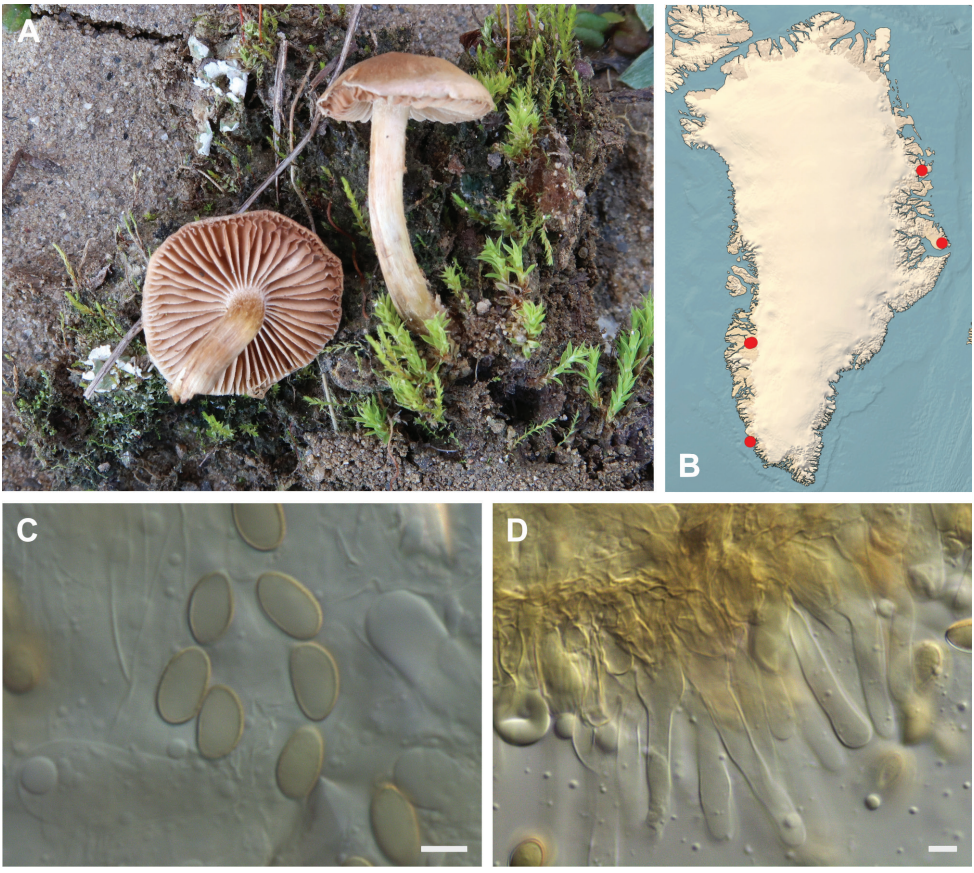

Figure 16. *Hebeloma mesophaeum* **A** HK17.020, photograph H. Knudsen **B** distribution of cited collections **C** spores ×1600 and **D** cheilocystidia ×1000 of HK17.020 in Melzer's reagent. Scale bars: 5 µm; microphotographs H.J. Beker.

Microscopic description. Spores ellipsoid, occasionally ovoid, on ave. 8.0–10.5 × 4.5–6.0 µm, Q = 1.3–1.9, (but see the notes below) yellow through yellow brown to brown, guttulation variable, almost smooth to weakly ornamented (O1 O2), perispore not or somewhat loosening (P0 P1), indistinctly dextrinoid (D0 D1). Basidia 24–31(–32) × 7–9 µm; ave. Q = 3.2–4, mostly four-spored. Cheilocystidia lageniform, ventricose, occasionally cylindrical or rarely clavate, occasionally with characteristic apical or basal wall thickening, sometimes bifurcate, geniculate or septate (sometimes clamped), on ave. 26–62 × 4–6 (apex) × 3.5–6 (middle) × 6–11 (base) µm, ratios A/M = 0.94–1.25, A/B = 0.45–0.98, B/M = 1.36–2.19. Epicutis an ixocutis, 60–350 µm thick (measured from exsiccata), maximum hyphae width 3–10 µm, encrustation variable, trama elements beneath subcutis angular or isodiametric to ellipsoid or cylindrical to sausage-shaped up to 22 µm wide. Caulocystidia similar to cheilocystidia, but less ventricose, up to 130 µm long.

Collections examined. S-Greenland: Paamiut, 62°N, 49.67°W, 6 Sep 1990, T. Borgen (TB90.086, C-F-76757), 20 m, with *Salix glauca*. Paamiut, 62.01°N, 49.67°W, 17 Aug 1990, T. Borgen (TB90.040, C-F-119759), 30 m, with *Bistorta vivipara*. **W-Greenland:** Kangerlussuaq, 67.01°N, 50.72°W, 2 Aug 2016, T. Borgen (TB16.038, C-F-104301), 50 m, with *Salix glauca* in tundra. Kangerlussuaq NE, near a glacier, 67.02°N, 50.66°W, 12 Aug 2000, E. Ohenoja (EO12.8.00.1, OULU F050224), 40 m, in heathland. Kangerlussuaq, Sandflugtsdalen, near the ice cap, 67.0578°N, 50.4571°W, 12 Aug 2000, T. Borgen (TB00.088, C-F-137116), 50 m. Kangerlussuaq, Sandflugtsdalen, 67.06°N, 50.46°W, 12 Aug 2000, T. Borgen (TB00.093, C-F-103521), 50 m, with *Salix glauca* in dunes. Kangerlussuaq, Sandflugtsdalen, 67.06°N, 50.46°W, 12 Aug 2000, T. Borgen (TB00.094, C-F-103522), 200 m, with *Salix glauca* in dunes. Kangerlussuaq, Sandflugtsdalen, 67.06°N, 50.46°W, 12 Aug 2000, A-M. Larsen, T. Borgen (TB00.091, C-F-103520), 50 m, with *Salix glauca* in dunes. Kangerlussuaq, Sandflugtsdalen, c. 15 km E of airport, 67.06°N, 50.46°W, 2 Aug 2016, T. Borgen (TB16.040G, C-F-103578), 50 m, with *Salix glauca* in dunes. **N-Greenland:** Zackenberg, S of the Station, towards Zackenberg River, 74.5°N, 21°W, 10 Aug 1999, T. Borgen (TB99.264, C-F-104297), 50 m, with *Dryas* sp. in scrubland. **E-Greenland:** Jameson Land, Nerlerit Inaat/Constable Pynt, Primulaelv, 70.74°N, 22.67°W, 1 Aug 2017, H. Knudsen (HK17.020, C-F-104908), 180 m.

Distribution. *Hebeloma mesophaeum* is widely distributed, but apparently uncommon in Greenland with only 11 records (2.9%). This is in contrast to the frequency in Europe, where it is very common and widely distributed (Beker et al. 2016). From alpine and arctic Europe, it is known from the Alps, Southern Carpathians, Svalbard and Iceland. Outside Europe and Greenland, there are a few records from the Rocky Mountains (Colorado, Cripps et al. 2019) and arctic Canada (Ohenoja and Ohenoja 2010). It is distributed from the Mediterranean area through the Temperate and Boreal zone to the Arctic and Alpine zones, being less common in the colder areas. Circumpolar, arctic-alpine, temperate, boreal and subarctic.

Habitat and ecology. Eleven collections, six of them with *Salix glauca*, one with *Dryas octopetala* and *D. integrifolia*, one with *Bistorta*, three not reported. One record from the Rocky Mountains was also with *S. glauca*. The soil conditions were variable. *Hebeloma mesophaeum* is widespread and very versatile when it comes to hosts, including many deciduous as well as coniferous hosts (Beker et al. 2016).

Notes. In Beker et al. (2016), it was reported that in arctic and alpine areas there is a chance of confusion with *H. marginatulum*, due to the fact that sometimes *H. mesophaeum*, growing in such habitats, tends to have larger spores. They reported that all the 'large-spored' collections were from Iceland and Svalbard. In Greenland, we have also found collections with larger spores; indeed, nine of the eleven collections discussed here exhibited larger spores in a range from 10.3–11.7 × 6.4–7.1 µm, a similar range to that reported for Svalbard and Iceland. At the time, Beker et al. (2016) did consider creating a variety to address these collections but decided such a course of action was premature and that further study of this variation was required. With regard to the confusion with *H. marginatulum*, the strongly bicolored cap of *H. mesophaeum* should normally aid identification.

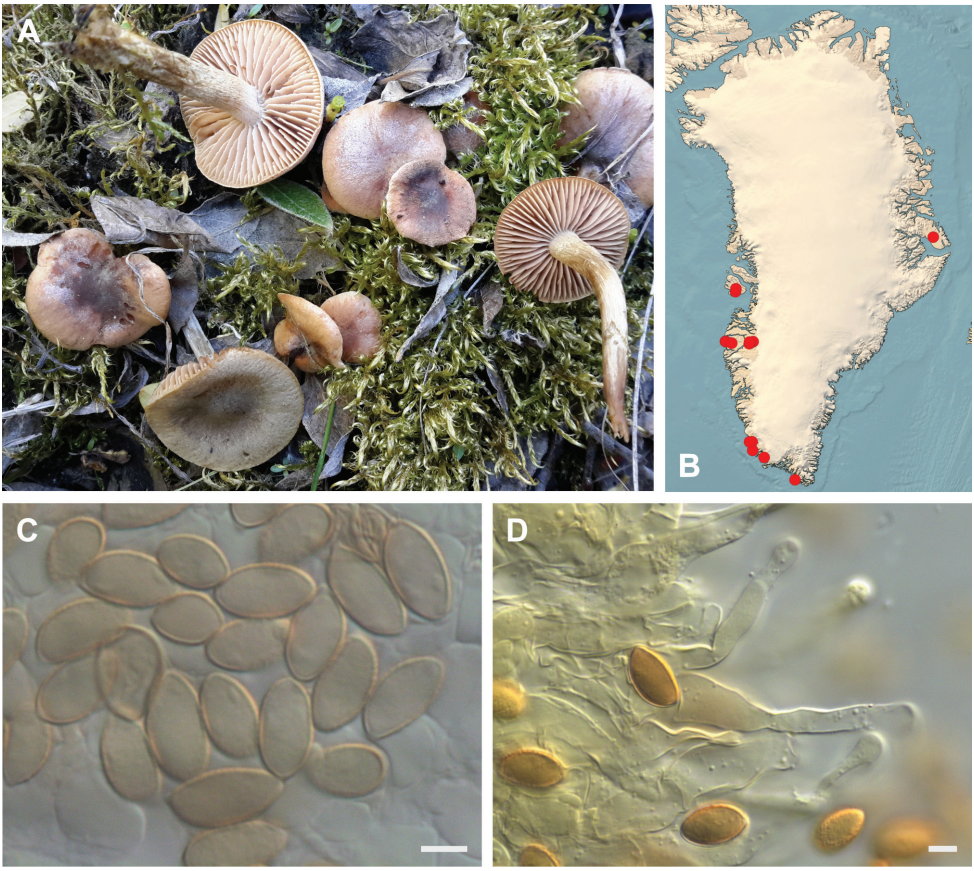

Figure 17. *Hebeloma nigellum* **A** HK16.033, photograph H. Knudsen **B** distribution of cited collections **C** spores ×1600 and **D** cheilocystidia ×1000 of TB85.249 in Melzer's reagent. Scale bars: 5 µm; microphotographs H.J. Beker.

Hebeloma nigellum **Bruchet; Bull. mens. Soc. linn. Lyon 39(6(Suppl.)): 126, 1970.**
Fig. 17

Macroscopic description. Cap 0.7–3.4 cm in diameter, convex to umbonate, occasionally papillate, margin involute, tacky when moist, unicolored or usually bicolored, at center umber to dark brick or snuff brown, at margin cream to pinkish buff, occasionally with remains of universal veil, partial veil present. Lamellae at maturity brownish clay, adnate to emarginate, maximum depth 2.5–6 mm, number of lamellae {L} 22–36, droplets absent, white fimbriate edge present, sometimes weakly. Stem 1.4–5.0 × 0.15–0.4 cm, whitish pruinose at apex, initially whitish lengthily fibrillose, downward, sordid brown, cylindrical, stem Q (6.5–)7.5–12.5(–18.7), fibrillose, pruinose to floccose at apex. Context firm, stem interior stuffed later hollow, flesh discoloring from base, sometimes very strongly. Smell usually raphanoid, sometimes none. Taste bitter, raphanoid. Spore deposit umber.

Microscopic description. Spores mainly amygdaloid, sometimes ellipsoid to ovoid, on ave. 11.0–13.5 × 7.0–7.5 µm, ave. Q = 1.5–1.9, yellow through yellow

brown to brown, guttulation variable, almost smooth to slightly ornamented (O1 O2), perispore not or very slightly loosening (P0 (P1)), rather strongly dextrinoid ((D2) D3). Basidia 25–39(–45) × 7–10(–11) µm, ave. Q = 3.1–3.9, mostly four-spored. Cheilocystidia usually lageniform, ventricose, occasionally cylindrical, occasionally with characteristic apical wall thickening, geniculate or septate (sometimes clamped), 44–65 × 4.5–6.5 (apex) × 4–5.5 (middle) × 6.5–11 (base) µm, ratios A/M = 0.92–1.41, A/B = 0.45–0.89, B/M = 1.45–2.3. Epicutis an ixocutis, 40–75 µm thick (measured from exsiccata), maximum hyphae width 5–6.5 µm, sometimes encrusted, trama elements beneath subcutis ellipsoid, polygonal, sausage-shaped up to 15 µm wide. Caulocystidia rather irregular, similar to cheilocystidia, up to 140 µm long.

Collections examined. S-Greenland: Kangilinnguit, bottom of Laksebund, 61.25°N, 48.08°W, 16 Aug 2018, H. Knudsen (HK18.199, C-F-111110), 100 m, with *Alnus alnobetulae* in scrubland. Nanortalik municipality, Qinngua valley, 60.14°N, 45°W, 6 Aug 1991, T. Borgen (TB91.080, C-F-103490), 250 m, with *Salix glauca* in copse. Paamiut, 62.01°N, 49.4°W, 31 Aug 1986, T. Borgen (TB86.276, C-F-103572), 10 m. Paamiut, 62.01°N, 49.4°W, 14 Aug 1990, T. Borgen (TB90.035, C-F-103479), 10 m. Paamiut, 62.01°N, 49.4°W, 1 Sep 1990, T. Borgen (TB90.073, C-F-103541), 10 m, with *Salix arctophila* along riverside. Paamiut, Kangilineq, Kvaneøen, 61.95°N, 49.47°W, 26 Aug 1984, T. Borgen (TB84.183, C-F-103468), 10 m, with *Salix arctophila*. Paamiut, Kangilineq/Kvaneøen, 61.57°N, 49.28°W, 25 Aug 1985, T. Borgen (TB85.249, C-F-103529), with *Salix*. Paamiut, Kangilineq/Kvaneøen, 61.99°N, 49.66°W, 26 Aug 1990, T. Borgen (TB90.056, C-F-103542), 15 m, with *Salix arctophila* in fenland. **W-Greenland:** Disko, N end of Blæsedalen, 69.5°N, 53.32°W, 25 Jul 1986, T. Borgen (TB86.052, C-F-119739), 300 m, with *Salix herbacea* in snowbed. Kangerlussuaq, Ammaloortup Nunaa W of Lake Ferguson, 66.99°N, 50.61°W, 8 Aug 2016, H. Knudsen (TB16.086G, C-F-103583), 275 m, with *Salix glauca*, *Betula nana* and *Sphagnum* along streamside. Kangerlussuaq, Kløftsøerne, 67.06°N, 50.68°W, 13 Aug 2016, H. Knudsen (HK16.110, C-F-104140), 500 m, with *Salix glauca*. Kangerlussuaq, Lake Ferguson, Tasersuatsiaq, 66.97°N, 50.70°W, 22 Aug 2016, S.A. Elborne (SAE-2016.131-GR, C-F-106743), 100 m, with *Salix glauca* in copse. Kangerlussuaq, NE facing slopes along Lake Ferguson, 66.99°N, 50.61°W, 8 Aug 2016, H. Knudsen (HK16.033, C-F-104063), 300 m, with *Salix glauca* in riverbed. Kangerlussuaq, outlet of Lake Ferguson, 66.99°N, 50.61°W, 6 Aug 2016, T. Borgen (TB16.060G, C-F-103580), 275 m, with *Salix glauca* in scrubland. Kangerlussuaq, W Bridge near Ice cap, 67.09°N, 50.23°W, 2 Aug 2016, T. Borgen (TB16.035G, C-F-103577), 50 m, with *Salix glauca* at lakeside. NW of Nasaassaq, E-valley, E of Sisimiut, 66.93°N, 53.61°W, 18 Aug 2000, E. Horak (ZT9139, ZT9139), 50 m, with *Betula nana*, *Salix glauca* and *Salix herbacea*. Qeqertarsuaq/Disko, Godhavn area, 69.65°N, 53.32°W, 26 Jul 1986, T. Borgen (TB86.065, C-F-119791), 450 m. Sisimiut, 1 km north of the village, 66.94°N, 53.67°W, 19 Aug 2000, E. Ohenoja (EO19.8.00.20, OULU F050653), 0 m, in heathland. Sisimiut, in the E valley, 66.89°N, 52.86°W, 15 Aug 2016, H. Knudsen (HK16.133, C-F-104163), 0 m, with *Salix herbacea*. Sisimiut, Kællingehætten, 66.93°N, 53.59°W, 16 Aug 2016, H. Knudsen (HK16.165A, C-F-

108402), 400 m. **E-Greenland:** Jameson Land, Constable Pynt, Draba Sibirica Elv, 71.15°N, 23.57°W, 28 Jul 1983, D. Boertmann (DB GR 83-80, C-F-119734), 0 m, with *Salix arctica.*

Distribution. *Hebeloma nigellum* is common and widespread in Greenland and present in other parts of North America (Cripps et al. 2019). It is widespread in temperate Europe, but more commonly in arctic-alpine areas (Beker et al. 2016). Circumpolar.

Habitat and ecology. Twenty-one collections, and where the host was specified, 15 were recorded with *Salix* (*S. glauca* 8, *S. arctophila* 3, *S. herbacea* 3, *S. arctica* 1), and one recorded with *Alnus alnobetulae* ssp. *crispa*. The majority are from riversides, lakesides, fens and snowbeds, but also in humid places with *S. arctophila*. Most localities are on neutral ground, but it is found in acid localities as well. In the Rocky Mountains, it was recorded with *Salix planifolia* (Cripps et al. 2019). From lowland Europe Beker et al. 2016 noted *S. aurita* and *S. cinerea* as hosts.

Hebeloma oreophilum **Beker & U. Eberh.; Eberhardt, Ronikier, Schütz & Beker, Mycologia 107(6): 1295, 2016 ("2015").**
Fig. 18

Macroscopic description. Cap 1.0–3.8 cm in diameter, convex to umbonate, sometimes strongly, margin smooth, often involute when young, tacky when moist, usually not hygrophanous, but we have occasionally seen collections that are, unicolored or variably two-colored, at center dark olive buff to brownish olive to umber to cinnamon or sepia to brick to dark brick to fuscous, sometimes cracked, at margin cream to pinkish buff to clay-pink, sometimes margin very thin, usually pruinose to tomentose, usually with remains of universal veil, partial veil present. Lamellae whitish then pale clay brown, emarginate to broadly adnexed, maximum depth 3–8 mm, number of lamellae {L} 40–48, droplets absent or very small (lens), white fimbriate edge sometimes present. Stem 1.5–7.0 × 0.3–0.65 {median} × (0.3–1.0) {base} cm, at first whitish later brown downwards, apically with whitish fibrillose ring zone, sometimes with indistinct belts, downwards with suggestion of a fibrillose ring, pale sordid brown, pale watery brown, downwards dark brown when rubbed, cylindrical, rarely clavate, stem Q (4.2–)5.5–8.7(–15), pruinose at apex. Context firm, stem interior stuffed, later hollow, stem flesh discoloring from base usually. Smell raphanoid. Taste raphanoid, slightly bitter. Spore deposit brownish olive.

Microscopic description. Spores amygdaloid, occasionally ovoid or limoniform, usually weakly papillate, on ave. 11.0–14.0 × 6.5–7.5 µm, ave. Q = 1.6–2.1, yellow brown through brown, guttulation variable, almost smooth to weakly ornamented (O1 O2), perispore not or somewhat loosening (P0 P1), distinctly to rather strongly dextrinoid (D2 D3). Basidia (25–)26–33(–36) × 7–9(–11) µm, ave. Q = 3.3–4.9, mostly four-spored. Cheilocystidia lageniform, ventricose, occasionally cylindrical, occasionally with characteristic apical, median or basal wall thickening, geniculate or septate, 42–57 × 4–6 (apex) × 4–6 (middle) × 8–10 (base) µm, sometimes with yellow-

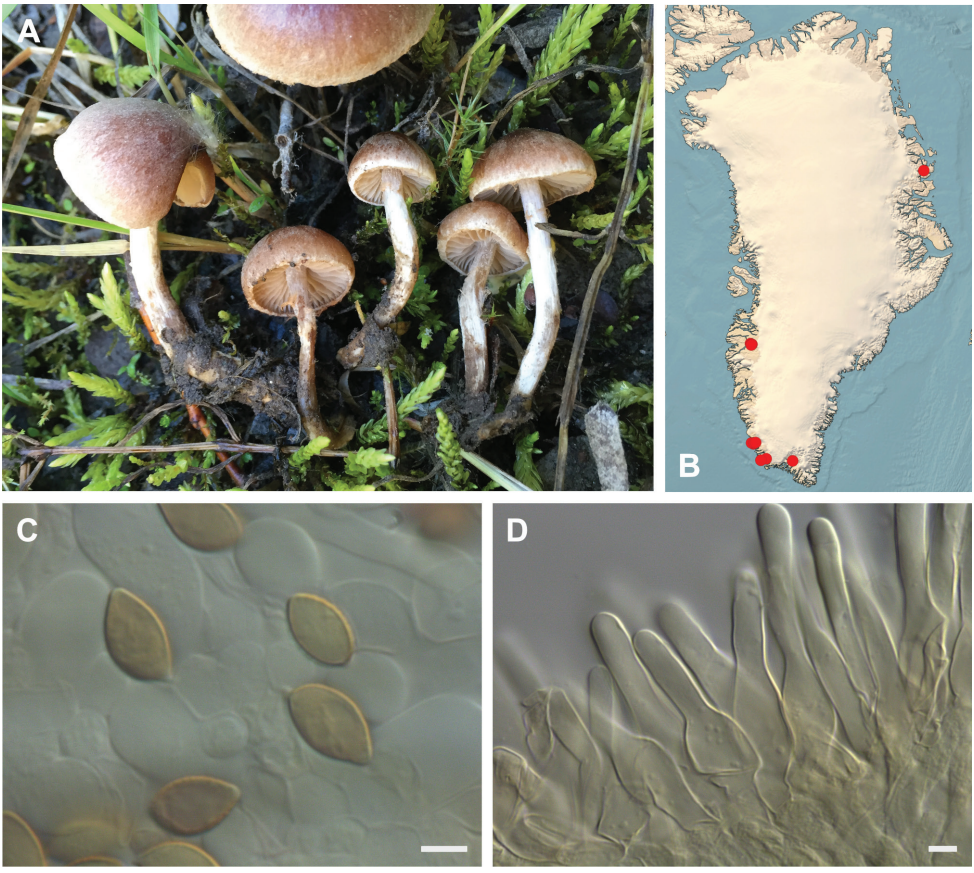

Figure 18. *Hebeloma oreophilum* **A** SAE-2016.134, photograph S.A. Elborne **B** distribution of cited collections **C** spores ×1600 and **D** cheilocystidia ×1000 of HK18.401 in Melzer's reagent. Scale bars: 5 µm; microphotographs H.J. Beker.

ish contents, ratios A/M 1.03–1.24, A/B = 0.44–0.67, B/M = 1.57–2.4. Epicutis an ixocutis, 40–70 µm thick (measured from exsiccata), maximum hyphae width 5–7 µm, without encrustations, trama elements beneath subcutis cylindrical to sausage-shaped up to 18 µm wide. Caulocystidia similar to cheilocystidia but less ventricose more cylindrical, often multi-septate, up to 120 µm long.

Collections examined. S-Greenland: Kangilinnguit, 61.14°N, 48.6°W, 20 Aug 1991, T. Borgen (TB91.233, C-F-103487), 25 m, with *Alnus alnobetulae*. Kangilinnguit at Grønnedal Hut, 61.23°N, 48.08°W, 15 Aug 1985, T. Borgen (TB85.180, C-F-119740), 350 m, with *Salix arctophila* in *Sphagnum*. Narsarsuaq, outer part of Hospital Valley, 61.17°N, 45.43°W, 9 Aug 1985, T. Borgen (TB85.061, C-F-103590), 50 m, with *Betula pubescens* and *Salix glauca*. Paamiut, 62.01°N, 49.4°W, 12 Aug 1990, T. Borgen (TB90.010, C-F-103558), 25 m, with *Salix arctophila* and *Salix herbacea* in snowbed. Paamiut, 62.01°N, 49.4°W, 14 Aug 1990, T. Borgen (TB90.036, C-F-103480), 10 m, with *Salix glauca*. Paamiut, 62.01°N, 49.4°W, 1 Sep 1986, T. Borgen

(TB86.292, C-F-103588), 100 m. Paamiut, 62.01°N, 49.4°W, 5 Aug 1998, T. Borgen (TB98.073, C-F-103509), 35 m, with *Salix herbacea* in fen. Paamiut, "Peters Fjeld", 62.01°N, 49.4°W, 31 Aug 1983, T. Borgen (TB83.035, C-F-103472), 10 m, with *Salix arctophila* in *Sphagnum*. Paamiut, head of Eqaluit, median part, 62.03°N, 49.25°W, 15 Aug 1998, T. Borgen (TB98.120, C-F-103510), 300 m, with *Betula glandulosa* and *Salix glauca* in heathland. Paamiut, Kangilineq /Kvaneøen, 61.95°N, 49.47°W, 6 Sep 1984, T. Borgen (TB84.215, C-F-104298), 20 m, with *Salix herbacea* and *Bistorta vivipara* in snowbed. Paamiut, Kangilineq/Kvaneøen, 61.99°N, 49.66°W, 27 Aug 1984, T. Borgen (TB84.184, C-F-103539), 15 m, with *Salix glauca*. **W-Greenland:** Kangerlussuaq, Kløftsøerne, 67.03°N, 50.80°W, 31 Jul 2016, T. Borgen (TB16.017G, C-F-103576), 300 m, with *Betula nana* and *Salix glauca*, in *Sphagnum* in scrubland. Kangerlussuaq, Lake Ferguson, Tasersuatsiaq, 66.97°N, 50.70°W, 22 Aug 2016, S.A. Elborne (SAE-2016.134-GR, C-F-106744), 100 m, with *Salix glauca* in copse. Kangerlussuaq, NE facing slopes along Lake Ferguson, 66.99°N, 50.61°W, 12 Aug 2016, H. Knudsen (HK16.091, C-F-104120), 300 m, in *Sphagnum* sp. Kangerlussuaq, slopes SW of Lake Ferguson, 66.96°N, 50.69°W, 29 Aug 2018, H. Knudsen (HK18.401, C-F-111120), 380 m, in tundra. **N-Greenland:** Zackenberg, 74.5°N, 21°W, 17 Aug 2006, T. Borgen (TB06.225, C-F-119772), 20 m, with *Salix arctica* in scrubland. Zackenberg, Sydkæret, 74.5°N, 21°W, 19 Aug 1999, T. Borgen (TB99.374, C-F-119758), 30 m, *with Salix arctica* in scrubland. Zackenberg, Sydkæret, 74.5°N, 21°W, 5 Aug 2006, T. Borgen (TB06.098, C-F-119773), 20 m, in fen.

Distribution. Widely distributed and apparently common in Greenland, but never recorded from the East coast (only north east, see habitat). Described recently (Eberhardt et al. 2015a) from an alpine site (1970 m) in Slovakia and still only known from few countries. In Europe, it is recorded from northern Finland, from the Subarctic and Arctic zone and from the High Arctic zone on Svalbard. Outside Europe, it is known from low alpine and alpine sites in the Rocky Mountains and Canada (Beker et al. 2016, Cripps et al. 2019). Circumpolar, arctic-alpine to subarctic.

Habitat and ecology. Eighteen collections, six recorded with *Salix glauca*, four with *S. arctica*, three with *S. arctophila*, two with *S. herbacea* and one recorded under *Alnus alnobetulae* ssp. *crispa*. The absence from the calcareous, well-investigated Jameson Land on the east coast may signal a preference for more acid soil types. In the low alpine Rocky Mountains, Cripps et al. (2019) found it a number of times with *Salix planifolia*, *S. arctica* and *S. glauca*.

***Hebeloma pubescens* Beker & U. Eberh.; Beker, Eberhardt & Vesterholt, Fungi Europ. (Alassio) 14: 173, 2016.**
Fig. 19

Macroscopic description. Cap 1.2–2.4 cm in diameter, convex to umbonate, sometimes papillate, margin smooth, tacky when moist, not hygrophanous, unicolored or variably bicolored, at center grayish brown to yellowish brown or umber, tomentose,

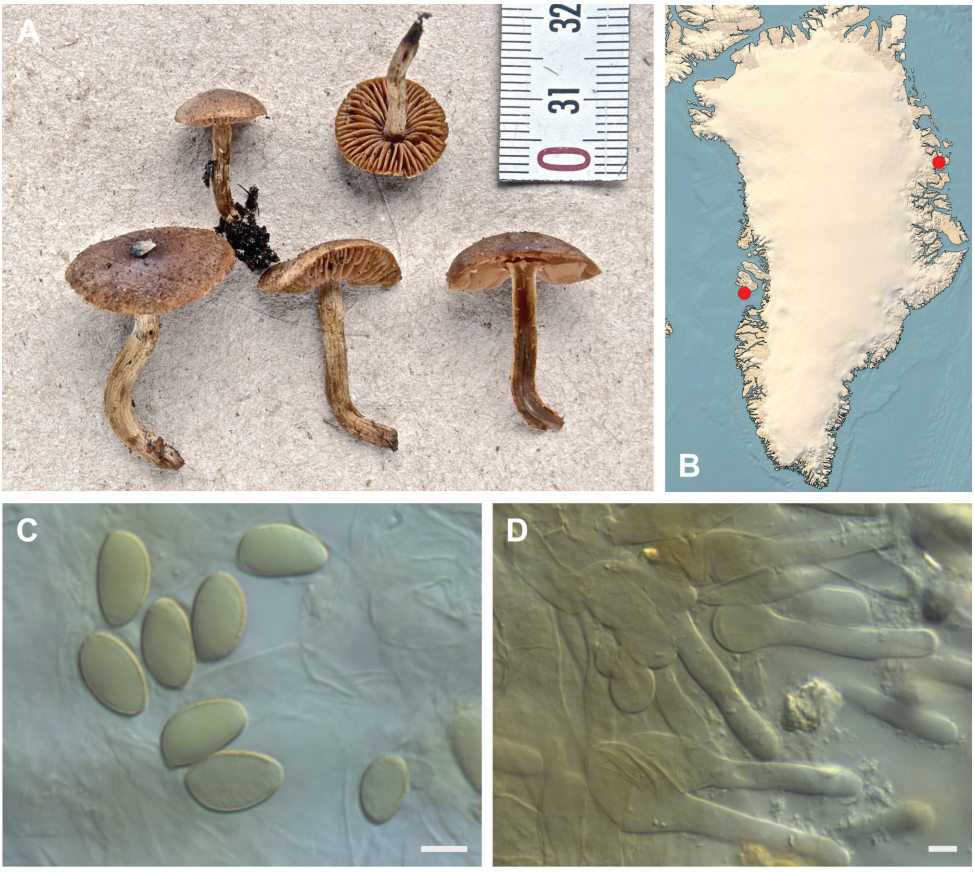

Figure 19. *Hebeloma pubescens* **A** TB99.194, photograph T. Borgen **B** distribution of cited collections; **C** spores ×1600 and **D** cheilocystidia ×1000 of TB99.194 in Melzer's reagent. Scale bars: 5 µm; microphotographs H.J. Beker.

usually covered, particularly at the margin, with soft hairs, at margin dark grayish buff, sometimes with remains of universal veil, partial veil present. Lamellae light brown, later slightly darker, emarginate, maximum depth 2.5–5 mm, number of lamellae {L} 25–32, droplets absent, white fimbriate edge weakly present. Stem 1.1–4.6 × 0.2–0.4 cm, whitish pale floccose in apex, downwards lengthily fibrillose, sordid brown or very pale ochraceous, cylindrical, stem Q (3.7–)4.8–8.3(–9.7), fibrillose. Context firm, stem interior stuffed, later hollow, flesh usually discoloring from base. Smell raphanoid, sometimes strongly. Taste mild. Spore deposit brownish olive.

Microscopic description. Spores ellipsoid, sometimes ovoid, pale yellow to yellow brown, guttulate, sometimes weakly, on ave. 10.0–12.0 × 6.0–6.5 µm, ave. Q = 1.5–1.8, almost smooth or weakly ornamented (O1 O2), perispore not loosening (P0), indextrinoid (D0). Basidia 28–33(-37) × 8–9 µm, ave. Q = 3.1–4.4, mostly four-spored. Cheilocystidia lageniform or ventricose, occasionally with characteristic basal or median wall thickening, septate, on ave. 38–45 × 4.5–6 (apex) × 4.5–6 (middle) × 8–10.5

(base) µm, ratios A/M = 1.02–1.10, A/B = 0.51–0.73, B/M = 1.52–2.10. Epicutis an ixocutis, 90–100 µm thick (measured from exsiccata), maximum hyphae width 6 µm, sometimes encrusted, trama elements beneath subcutis isodiametric up to 15 µm wide. Caulocystidia similar to cheilocystidia but less ventricose, up to 120 µm long.

Collections examined. W-Greenland: Disko, Kangaarsuk, Fortune Bay, 69.25°N, 53.54°W, 3 Aug 1986, T. Borgen (TB86.128, C-F-5089), 0 m, with *Salix* sp. **N-Greenland:** Zackenberg, W of Kærelv, 74.5°N, 21°W, 13 Aug 1999, T. Borgen (TB99.305, C-F-119753), 50 m, with *Dryas* sp. in scrubland. Zackenberg, W of Zackenberg River, 74.5°N, 21°W, 5 Aug 1999, T. Borgen (TB99.194, C-F-119750), 50 m, with *Dryas* sp. and *Salix arctica* in scrubland.

Distribution. Recently described from three records on Svalbard (Beker et al. 2016). The Greenland records are all north of 69° and, together with the type from 78°N, establish this as one of the few agarics, which appear only to occur in the High Arctic zone. The Greenland records are new to North America and the first outside Europe. High Arctic.

Habitat and ecology. Three collections, two with *Dryas* and one with *Salix* sp. The collections from Zackenberg were on rich soil. Beker et al. (2016) described it from Svalbard, where the host was *Salix polaris*.

***Hebeloma spetsbergense* Beker & U. Eberh.; Beker, Eberhardt & Vesterholt, Fungi Europ. (Alassio) 14: 180, 2016.**
Fig. 20

Macroscopic description. Cap 1.0–2.2 cm in diameter, convex to umbonate, sometimes umbilicate, margin smooth, tacky when moist, occasionally hygrophanous, unicolored, sometimes bicolored, at center sepia to fuscous or dark brick, at margin pinkish buff to clay pink to cinnamon, sometimes quite thin margin, without remains of universal veil, partial veil present. Lamellae initially light clay, at maturity slightly more brownish, attachment emarginate, maximum depth 3–5 mm, number of lamellae {L} 18–35, droplets absent, white fimbriate edge sometimes present but weak. Stem (1.5–)1.9–3.1(–3.7) × 0.2–0.3(–0.5) cm, light watery brownish, darker towards base, cylindrical, stem Q (5–)8–12.7(–16.5), fibrillose, usually pruinose at apex. Context firm, stem interior stuffed, later hollow, stem flesh variably discoloring from base. Smell raphanoid sometimes strongly. Taste weakly raphanoid. Spore deposit sepia.

Microscopic description. Spores amygdaloid, occasionally limoniform, guttulation variable, on ave. 12.0–14.5 × 7.5–8.5 µm, ave. Q = 1.5–1.7, yellow brown to brown, almost smooth to weakly ornamented (O1 O2), perispore not loosening (P0), rather strongly dextrinoid (D2 D3). Basidia 27–37(-40) × 9–12 µm, ave. Q = 3.3–3.9, mostly four-spored. Cheilocystidia lageniform, ventricose, occasionally with characteristically median wall thickening, some septate, on ave. 45–60 × 4.5–6 (apex) × 4.5–5 (middle) × 8.5–12 (base) µm, occasionally cystidia with yellow contents, ratios A/M = 0.92–1.25, A/B = 0.43–0.61, B/M = 1.87–2.61. Epicutis an ixocutis, 30–35 µm

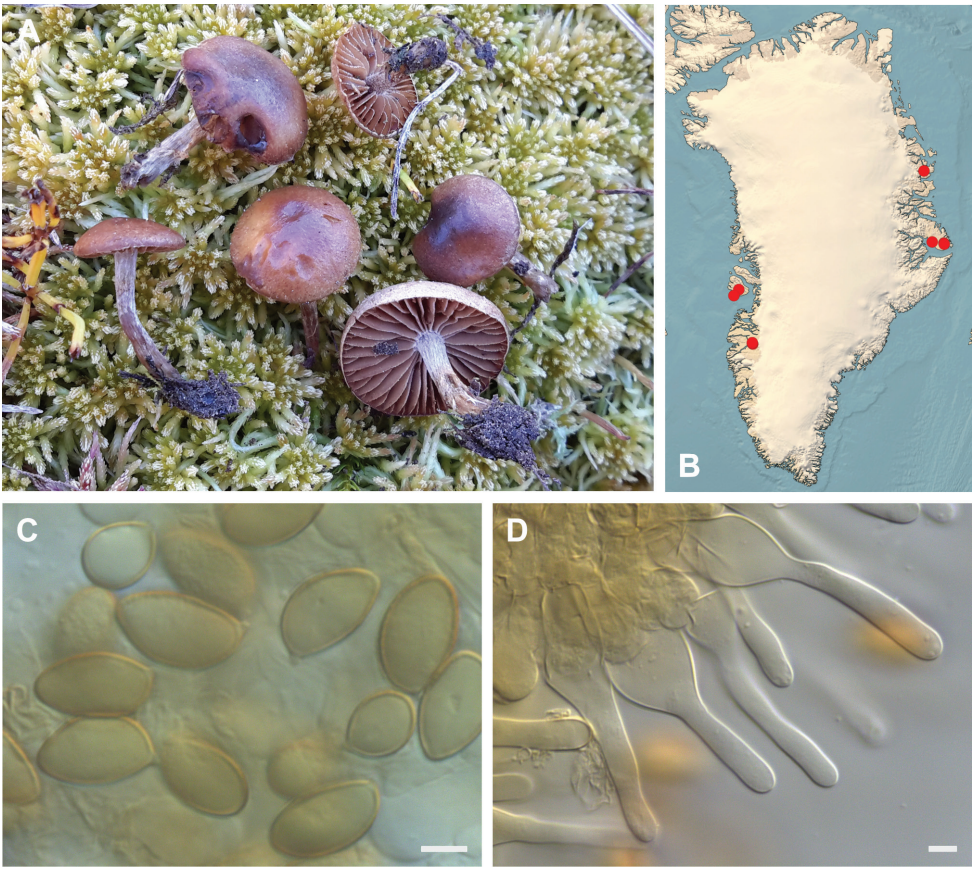

Figure 20. *Hebeloma spetsbergense* **A** HK16.071, photograph H. Knudsen **B** distribution of cited collections **C** spores ×1600 and **D** cheilocystidia ×1000 of HK16.071 in Melzer's reagent. Scale bars: 5 µm; microphotographs H.J. Beker.

thick (measured from exsiccata), maximum hyphae width 5 µm, without encrustations, shape of trama elements beneath subcutis sausage-shaped, up to 18 µm wide. Caulocystidia similar to cheilocystidia but generally larger.

Collections examined. W-Greenland: Disko, Fortune Bay, 69.31°N, 53.88°W, 3 Aug 1986, T. Borgen (TB86.121, C-F-103478), 20 m, with *Salix glauca* in dunes. Qeqertarsuaq/Disko, Godhavn, 69.65°N, 53.32°W, 5 Aug 1986, S.A. Elborne (SAE-86.135-GR, C-F-119733), 0 m, with *Salix glauca* at lakeside. Kangerlussuaq, just west of Lake Ferguson, 66.99°N, 50.61°W, 6 Aug 2016, T. Borgen (TB16.056G, C-F-103579), 50 m, with *Salix glauca* and *Betula nana* in ditch. Kangerlussuaq, Kløftsøerne, 67°N, 50.71°W, 20 Aug 2016, S.A. Elborne (SAE-2016.102-GR, C-F-106740), 270 m, with *Betula nana* and *Bistorta vivipara* along lakeside. Kangerlussuaq, Kløftsøerne, 67.03°N, 50.69°W, 19 Aug 2016, H. Knudsen (HK s.n., C-F-108450), 500 m, with *Salix* sp. and *Betula* sp. Kangerlussuaq, NE facing slopes along Lake Ferguson, 66.99°N, 50.61°W, 12 Aug 2016, H. Knudsen (HK16.071, C-F-104100), 300 m. **N-Greenland:** Zackenberg, just N of Zackenberg Hut, 74.5°N, 21°W, 9 Aug

1999, T. Borgen (TB99.256, C-F-119757), 50 m, with *Salix arctica*, *Bistorta vivipara* and *Sphagnum* in scrubland. **E-Greenland:** Jameson Land, Constable Pynt, Draba Sibirica Elv, 10 km from coast, 71.03°N, 24.23°W, 23 Jul 1983, D. Boertmann (DB GR 83-62, C-F-119801), 50 m, with *Salix arctica* along riverside. Jameson Land, Nerlerit Inaat/Constable Pynt, delta of Gåseelv valley, 70.76°N, 22.65°W, 12 Aug 2017, T. Borgen (TB17C.113, C-F-106781), 40 m, with *Bistorta vivipara* in heathland. Jameson Land, Nerlerit Inaat/Constable Pynt, delta of Gåseelv valley, 70.76°N, 22.65°W, 9 Aug 2017, S.A. Elborne (SAE-2017.174-GR, C-F-106764), 40 m, with *Salix arctica* along riverside. Jameson Land, Nerlerit Inaat/Constable Pynt, Hareelv, 70.7°N, 22.68°W, 2 Aug 2017, S.A. Elborne (SAE-2017.043-GR, C-F-106760), 200 m, with *Salix arctica* in bog. Jameson Land, Nerlerit Inaat/Constable Pynt, near airstrip, 70.74°N, 22.64°W, 6 Aug 2017, T. Borgen (TB17C.050, C-F-106774), 50 m, with *Salix* sp. in fen.

Distribution. Recently described from high arctic Svalbard (Beker et al. 2016). The eleven Greenland records indicate that it is quite common in the High Arctic zone in Greenland north of 67°N. Circumpolar, High Arctic.

Habitat and ecology. Twelve collections, four recorded with *Salix arctica*, four with *S. glauca*, two with *Salix* spp., one with *Betula nana* and one with *Bistorta vivipara*. *Bistorta* is often present near collections of mycorrhizal fungi, but only when it was the only possibility was this host recorded. In the Rocky Mountains, Cripps et al. (2019) reported two collections growing with *S. glauca* and *S. arctica*. In Greenland, *H. spetsbergense* is growing both in acid and calcareous habitats, most often in humid localities like bogs, riversides and ditches. The five collections from Svalbard, including the type, are from localities on base-poor ground with *S. polaris* (Beker et al. 2016).

***Hebeloma* sect. *Denudata* (*Fr.*) Sacc.; Fl. Ital. Crypt. I 15: 691, 1916.**

Veil absent. Cap uni- or bicolored. Lamellae often exuding small hyaline or colored drops. Cheilocystidia long, swollen in the apical part, constricted in the median part, basal part swollen or not. Spores amygdaloid to limoniform, ornamented, sometimes strongly.

***Hebeloma* subsect. *Crustuliniformia Quadr.*; Doc. mycol. 14: 30, 1985 ("1984").**

Cheilocystidia distinctly broadened at apex, base ± cylindrical, wall not thickened. Lamellae edge often with exuded drops.

***Hebeloma alpinum* (J. Favre) Bruchet; Bull. mens. Soc. linn. Lyon 39(6(Suppl.)): 68, 1970.**
Fig. 21

Macroscopic description. Cap 1.7–7.3 cm, convex to umbonate or broadly umbonate; margin smooth, often involute, sometimes crenulate or serrate, tacky when moist, not hygrophanous, almost unicolored, occasionally bicolored, at center cream

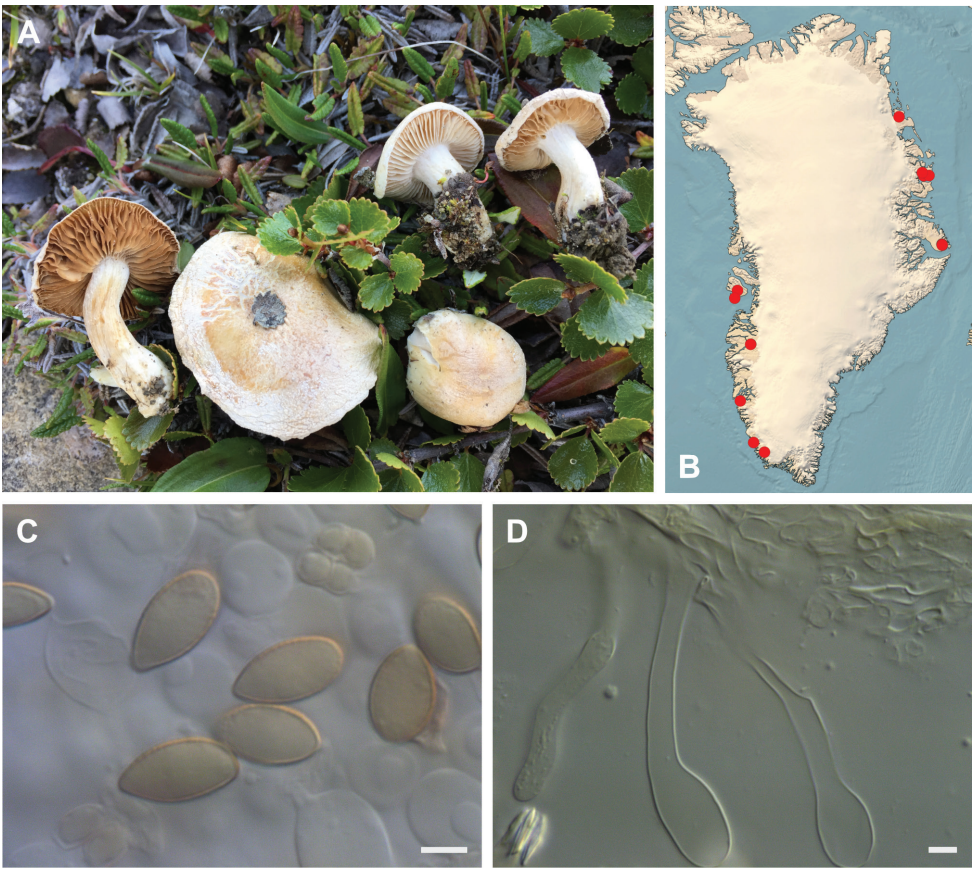

Figure 21. *Hebeloma alpinum* **A** SAE-2017.006, photograph S.A. Elborne **B** distribution of cited collections **C** spores ×1600 and **D** cheilocystidia ×1000 of SAE-2017.006 in Melzer's reagent. Scale bars: 5 µm; microphotographs H.J. Beker.

to pink buff to dark olive buff brown or yellowish brown to brownish olive or umber to sepia, clay buff or cinnamon, margin cream to pink buff or clay buff, sometimes very thin, universal veil absent, partial veil absent. Lamellae whitish, later light gray brown, then sordid brownish, number of lamellae {L} 40–72, emarginate, 0.3–0.9 cm broad, exuded drops usually visible with naked eye, but sometimes absent, with white fimbriate edge. Stem 1.5–5.0 × 0.4–1.2 cm, whitish fimbriate-pruinose in the entire length, later downwards slightly sordid ochraceous, ochre-yellowish or pale brown, base cylindric to clavate, rarely bulbous, occasionally tapering, pruinose to floccose particularly at apex, when fresh with droplets. Trama firm, stem with a stuffed interior, occasionally becoming hollow with age, not discoloring. Smell usually raphanoid, occasionally of cocoa or absent. Taste mild to weakly bitter. Spore deposit dark olive buff, brownish olive to clay buff.

Microscopic description. Spores amygdaloid to limoniform, on ave. 9.5–15 × 5.5–8.5 µm, ave. Q = 1.4–2.2, yellow brown to brown, sometimes guttulate, papillate,

sometimes very strongly, almost smooth to weakly ornamented (O1 O2 (03)), perispore not or somewhat loosening (P0 P1), indextrinoid to weakly dextrinoid (D0 D1 D2). Basidia 28–40(–45) × 8–12 µm, Q = 3–4.3, mostly four-spored. Cheilocystidia mainly clavate-stipitate or spathulate-stipitate, occasionally slenderly clavate or clavate-lageniform, occasional apically thickening, rostrate, septate or sinuate, on ave. 40–71 × 7–10 (apex) × 3.5–5 (middle) × 3.5–6 (base) µm, ratios A/M = 1.6–2.7, A/B = 1.5–2.7, B/M = 0.9–1.2. Pileipellis an ixocutis, 60–160 µm thick (measured from exsiccata), hyphae 5–6 µm broad, some encrusted; trama elements beneath subcutis cylindrical, ellipsoid, thick sausage-shaped, up to 18 µm wide. Caulocystidia similar to cheilocystidia, up to 120 µm long and 11 µm wide.

Collections examined. S-Greenland: Paamiut, 62.01°N, 49.4°W, 18 Aug 1984, T. Borgen (TB84.148, C-F-103537), 25 m, with *Salix herbacea* and *Salix glauca*. Sermiliarsuk, Sioralik, Aasivii, 65.53°N, 48.33°W, 30 Aug 1997, T. Borgen (TB97.153a, C-F-103507), 50 m, with *Betula pubescens* and *Salix glauca* in copse. Sermiliarsuk, Sioralik, Aasivii, 65.53°N, 48.33°W, 30 Aug 1997, T. Borgen (TB97.152, C-F-103506), 50 m, with *Dryas integrifolia* in heathland. **W-Greenland:** Disko, Qeqertarsuaq, 69.24°N, 53.54°W, 5 Aug 1986, T. Borgen (TB86.141, C-F-103565), 0 m. Disko, Skarvefjeld at Qeqertarsuaq, 69.65°N, 53.32°W, 2 Aug 1986, T. Borgen (TB86.115, C-F-103458), 400 m, with *Dryas integrifolia*. Kangerlussuaq, airport area, 67.02°N, 50.69°W, 1 Aug 1995, T. Borgen (TB95.004, C-F-103503), 50 m, with *Salix glauca* and *Betula nana* in copse. Kangerlussuaq, Hassells Fjeld, Kløftsøerne, 67.01°N, 50.71°W, 28 Aug 2018, H. Knudsen (HK18.390D, C-F-111119), 50 m, with *Salix glauca* in tundra. Kangerlussuaq, near hotel, 67.02°N, 50.7°W, 7 Aug 1986, T. Borgen (TB86.153, C-F-101230), 50 m, with *Salix glauca* and *Betula nana* in tundra. Kobbefjord, NuukBasic, 64.08°N, 51.23°W, 24 Aug 2018, H. Knudsen (HK18.308, C-F-111115), 5 m, in tundra. **N-Greenland:** Daneborg, 0.5 km E of Airstrip, 74.2°N, 20.1°W, 29 Jul 2006, T. Borgen (TB06.034, C-F-119763), 20 m, with *Dryas* sp. in heathland. V. Clausen Fjord, 77.52°N, 20.66°W, 13 Aug 1990, B. Fredskild (BF 90 loc. 6, C-F-5180), 0 m. Zackenberg, Aucellabjerg, 74.47°N, 21°W, 9 Aug 2006, T. Borgen (TB06.137, C-F-119766), 160 m, with *Dryas* sp. and *Salix arctica* in heathland. Zackenberg, Aucellabjerg, 74.47°N, 21°W, 11 Aug 1999, T. Borgen (TB99.283, C-F-119808), 100 m, with *Dryas* sp. in heathland. Zackenberg, few 100 m west of Zackenberg River, 74.47°N, 21°W, 3 Aug 1999, T. Borgen (TB99.199, C-F-104294), 50 m, with *Dryas* sp. in scrubland. Zackenberg, just S of Kamelen, 74.47°N, 21°W, 27 Jul 1999, T. Borgen (TB99.115, C-F-119806), 50 m, with *Dryas* sp. and *Salix arctica* at riverside. Zackenberg, just S of Teltdammen, 74.47°N, 21°W, 20 Jul 1999, T. Borgen (TB99.027, C-F-119742), 40 m, with *Dryas* sp. in scrubland. Zackenberg, just S of Teltdammen, 74.3°N, 21°W, 20 Jul 1999, T. Borgen (TB99.023, C-F-119744), 40 m, with *Dryas* sp. and *Salix* sp. in scrubland. Zackenberg, just W of Kærelv, 74.47°N, 21°W, 30 Jul 1999, T. Borgen (TB99.159, C-F-119807), 30 m, with *Salix arctica* and *Bistorta vivipara* on solifluction lobe. **E-Greenland:** Jameson Land, Nerlerit Inaat/Constable Pynt, 70.74°N, 22.65°W, 31 Jul 2017, S.A. Elborne (SAE-2017.008-GR, C-F-106758), 10 m, with *Dryas* sp. and *Salix* sp. in tundra. Jameson Land, Nerlerit Inaat/Constable Pynt, 70.74°N, 22.67°W,

31 Jul 2017, S.A. Elborne (SAE-2017.006-GR, C-F-106757), 60 m, with *Betula nana* and *Dryas* sp. in tundra. Jameson Land, Nerlerit Inaat/Constable Pynt, around the airport, 70.74°N, 22.64°W, 31 Jul 2017, H. Knudsen (HK17.001, C-F-104889), 50 m. Jameson Land, Nerlerit Inaat/Constable Pynt, around the airport, 70.74°N, 22.64°W, 31 Jul 2017, H. Knudsen (HK17.005, C-F-104893), 50 m. Jameson Land, Nerlerit Inaat/Constable Pynt, around the airport, 70.74°N, 22.64°W, 31 Jul 2017, H. Knudsen (HK17.006, C-F-104894), 50 m. Jameson Land, Nerlerit Inaat/Constable Pynt, around the airport, 70.74°N, 22.64°W, 31 Jul 2017, H. Knudsen (HK17.007, C-F-104895), 50 m. Jameson Land, Nerlerit Inaat/Constable Pynt, delta of Gåseelv valley, 70.76°N, 22.65°W, 8 Aug 2017, T. Borgen (TB17C.089, C-F-106779) ,40 m, with *Bistorta vivipara* in fenland. Jameson Land, Nerlerit Inaat/Constable Pynt, delta of Gåseelv valley, 70.76°N, 22.65°W, 6 Aug 2017, H. Knudsen (HK17.123, C-F-105024), 40 m. Jameson Land, Nerlerit Inaat/Constable Pynt, delta of Gåseelv valley, 70.76°N, 22.65°W, 7 Aug 2017, H. Knudsen (HK17.148, C-F-105050), 40 m. Jameson Land, Nerlerit Inaat/Constable Pynt, Gåseelv, Harris Fjeld, 70.75°N, 22.68°W, 3 Aug 2017, H. Knudsen (HK17.062, C-F-104951), 95 m. Jameson Land, Nerlerit Inaat/Constable Pynt, Hareelv, 70.7°N, 22.68°W, 2 Aug 2017, H. Knudsen (HK17.049, C-F-104938), 200 m. Jameson Land, Nerlerit Inaat/Constable Pynt, Hareelv, 70.7°N, 22.68°W, 2 Aug 2017, H. Knudsen (HK17.054, C-F-104943), 200 m. Jameson Land, Nerlerit Inaat/Constable Pynt, Hareelv, 70.7°N, 22.68°W, 10 Aug 2017, S.A. Elborne (SAE-2017.188-GR, C-F-106766), 100 m, with *Salix arctica* in bog. Jameson Land, Nerlerit Inaat/Constable Pynt, Mt. Harris, 70.75°N, 22.68°W, 6 Aug 2017, T. Borgen (TB17C.053, C-F-106775), 100 m, with *Dryas* sp. and *Bistorta vivipara* in heathland. Jameson Land, Nerlerit Inaat/Constable Pynt, north of Primulaelv, 70.75°N, 22.66°W, 1 Aug 2017, S.A. Elborne (SAE-2017.014-GR, C-F-106759), 10 m, with *Dryas* sp. Jameson Land, Nerlerit Inaat/Constable Pynt, Primulaelv, 70.74°N, 22.67°W, 13 Aug 2017, T. Borgen (TB17C.134, C-F-106784), 180 m, with *Bistorta vivipara*. Jameson Land, Nerlerit Inaat/Constable Pynt, Primulaelv, 70.74°N, 22.67°W, 13 Aug 2017, H. Knudsen (HK17.278, C-F-105185), 180 m. Jameson Land, Nerlerit Inaat/Constable Pynt, Primulaelv, 70.74°N, 22.67°W, 1 Aug 2017, H. Knudsen (HK17.023, C-F-104912), 180 m, in tundra.

Distribution. *Hebeloma alpinum* is one of the five most often recorded *Hebeloma* species in Greenland, with 36 records (almost 10%) of those considered here. This is in good accordance with Beker et al. (2016), who pointed out that this is "the most common *Hebeloma* species we have collected in arctic/alpine areas". It occurs all over Greenland, from Sermiliarsuk in the south (61.6°N) to Zackenberg (74.5°N) and V. Clausen Fjord (77.5°N) in the north. In Constable Pynt in East Greenland in 2017 it was the most common of all mushrooms. In Europe, it is known from the major mountain ranges (the Alps, the Pyrenees, the Tatras, the Carpathians, Black Mountains in Montenegro), from supraboreal Iceland (Beker et al. 2016). It has been reported in North America from the Rocky Mountains (Montana, Cripps et al. 2019). Arctic-alpine, boreal and subarctic.

Habitat and ecology. The 36 collections are all from calcareous localities. The preferred host is *Dryas integrifolia* but possibly also *D. octopetala*. When these two

occur together as in NE Greenland, they often hybridize, and can be difficult to identify. Only a few collections are reported with other hosts like *Salix arctica*, *S. herbacea*, *Betula pubescens*, *B. nana* and even *Bistorta vivipara*. The only record from Rocky Mountains was associated with *S. arctica* and *S. glauca*. Beker et al. 2016 also have records with *S. polaris*, *S. retusa* and *S. reticulata*.

Notes. The shape of the cheilocystidia clearly points to subsect. *Crustuliniformia*. Within this subsection, it is recognized among the other species by its habitat in arctic-alpine localities, the number of lamellae being usually between 40 and 60 and the size of the spores, on average > 11 µm long and > 6 µm wide. The squat and robust stature is a good character in the field.

Hebeloma bellotianum Berk. is a closely related or synonymous species from Bellot Island in the Canadian Arctic (Eberhardt et al. 2015b). Unfortunately, attempts to sequence the type have been unsuccessful. It has spores on ave. 14.7 × 7.1 µm whereas the largest average measurements of 72 collections of *H. alpinum* is 13.7 × 7.7 µm.

***Hebeloma arcticum* Beker & U. Eberh. sp. nov.**
MycoBank No: 838874
Figs 22, 23

Type. Greenland. Sisimiut: at the bridge on the road to the airport (approx. 66.944317N, 53.670444W, alt. approx. 0 m a.s.l.), 14 Aug. 2016, H. Knudsen (HK16.119) (***Holotype*:** C-F-104149; Database Record: HJB17673; Genbank: ITS = MW445587, *Tef1*a = MW452584 and *RPB2* = MW452593).

Diagnosis. Favoring arctic type habitats with many cheilocystidia clavate-stipitate and rather strongly dextrinoid but indistinctly ornamented spores.

Etymology. *arcticus* (adj. Latin), meaning the arctic, to emphasize the habitat within which this mushroom has been discovered.

Macroscopic description. Cap (1.7–) 2.4–2.9 (–3.8) cm, plano-convex, with or without suggestion of obtuse umbo, with decurved margin then applanate, only weakly viscid even after heavy rainfall, dull, almost glabrous, marginal zone whitish pale due to a fine adpressed tomentum, often eroded, usually bicolored, center ochre, paler towards the margin becoming very pale brownish, hardly hygrophanous but a few hygrophanous dots. Lamellae emarginate with tooth, ventricose, number of lamellae {L} 36–44, up to 4 mm wide, initially pale, darker (clay buff) at maturity with whitish fimbriate edge and usually some watery droplets or droplets visible with a x10 lens. Stem (2.8–) 4.1–4.4 (–6.0) × 0.5–0.7 (–0.9) cm, to 0.6–0.9 cm at base, whitish fibrillose to pruinose, cylindrical, narrowly fistulose, downwards pale yellowish to pale brownish when rubbed. Context firm, thick particularly in center, whitish pale, watery when moist, in age slightly brownish downwards in stipe. Smell weakly herbaceous-raphanoid. Taste mild. Spore print at most clay buff (Munsell 10YR6/4; in TB 90.071).

Microscopic description. Spores amygdaloid, ellipsoid or ovoid, on ave. (across eight collections) 10.8–12.0 × 6.4–6.9 µm, ave. Q = 1.65–1.83, (for the holotype, measuring 102 spores, 5% to 95% percentile range 10.4–13.2 × 5.9–7.2 µm with

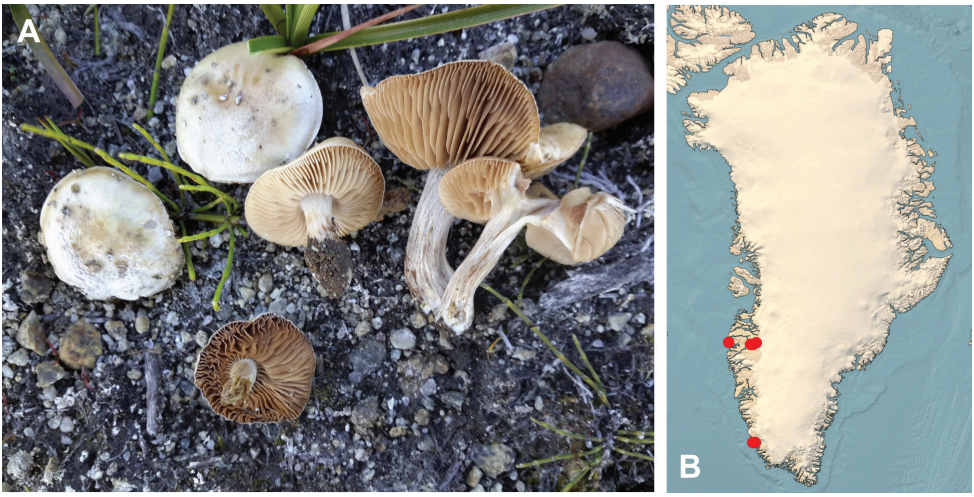

Figure 22. *Hebeloma arcticum* **A** HK16.119 (holotype), photograph H. Knudsen **B** distribution of cited collections.

median 11.9 × 6.5 µm and ave. 11.9 × 6.5 µm and S.D. for length 0.84 µm and for width 0.39 µm, and Q value 5% to 95% percentile range 1.57–2.04, with median 1.83 and ave. 1.83 with S. D. 0.14), yellow brown, guttulate, not papillate, almost smooth (O1), perispore not loosening (P0), distinctly to strongly dextrinoid (D2 D3). Basidia (20) 22–37 × 6–10 µm; ave. Q 3.0–3.7, (for the holotype 25–37 × 7–9, ave. Q 3.6), mostly four-spored. Cheilocystidia mainly clavate-stipitate, sometimes clavate-ventricose, more rarely capitate-stipitate, occasional apical or median wall thickening, sometimes septate (occasionally clamped), on ave. 36–57 × 6–9 (apex) × 4–5 (middle) × 4–6.5 (base) µm, ratios A/M = 1.5–2.3, A/B = 1.2–2.0, B/M = 1.0–1.4, (for the holotype, width near apex, 5% to 95% percentile range 6.5–8.3 µm, with median 7.4 µm and ave. 7.4 µm with S.D. 0.63 µm and over all 45 × 7.4 (apex) × 5 (middle) × 6.5 (base) µm). Pileipellis an ixocutis, up to 90 µm thick (measured from exsiccata), hyphae up to 6 µm broad, none encrusted; trama elements beneath subcutis isodiametric to ellipsoid or thick sausage-shaped, up to 17.5 µm wide. Caulocystidia similar to cheilocystidia, up to 90 µm long.

Other collections examined. S-Greenland: Paamiut, 62.01°N, 49.4°W, 31 Aug 1986, T. Borgen (TB86.277A, C-F-103571), 10 m, with *S. arctophila*, 62.01°N, 49.4°W, 4 Sep 1990, T. Borgen (TB90.083, C-F-103555), 10 m, with *Salix glauca* and *Bistorta vivipara* in fenland. Paamiut, 62.01°N, 49.4°W, 1 Sep 1990, T. Borgen (TB90.071, C-F-103483), 10 m, with *Salix glauca* and *Bistorta vivipara*. Paamiut, near cemetery, 61.9941°N, 49.6666°W, 21 Aug 2008, T. Borgen (TB08.153, C-F-106751), 15 m, with *Salix glauca*. **W-Greenland:** Kangerlussuaq, Ringsødalen, Ringsøen, 66.9853°N, 50.9464°W, 9 Aug 2016, T. Borgen (TB16.095, C-F-103584), 180 m, with *Salix glauca*. Kangerlussuaq, Ringsødalen, Ringsøen, 66.9853°N, 50.9464°W, 9 Aug 2016, H. Knudsen (HK16.044, C-F-104080), 180 m, with *Salix glauca*. Kangerlussuaq, Russels Glacier, 67.0977°N, 50.2318°W, 12 Aug 2000, S.A. Elborne (SAE-2000.021-GR, C-F-108472), 220 m, with *Salix glauca*.

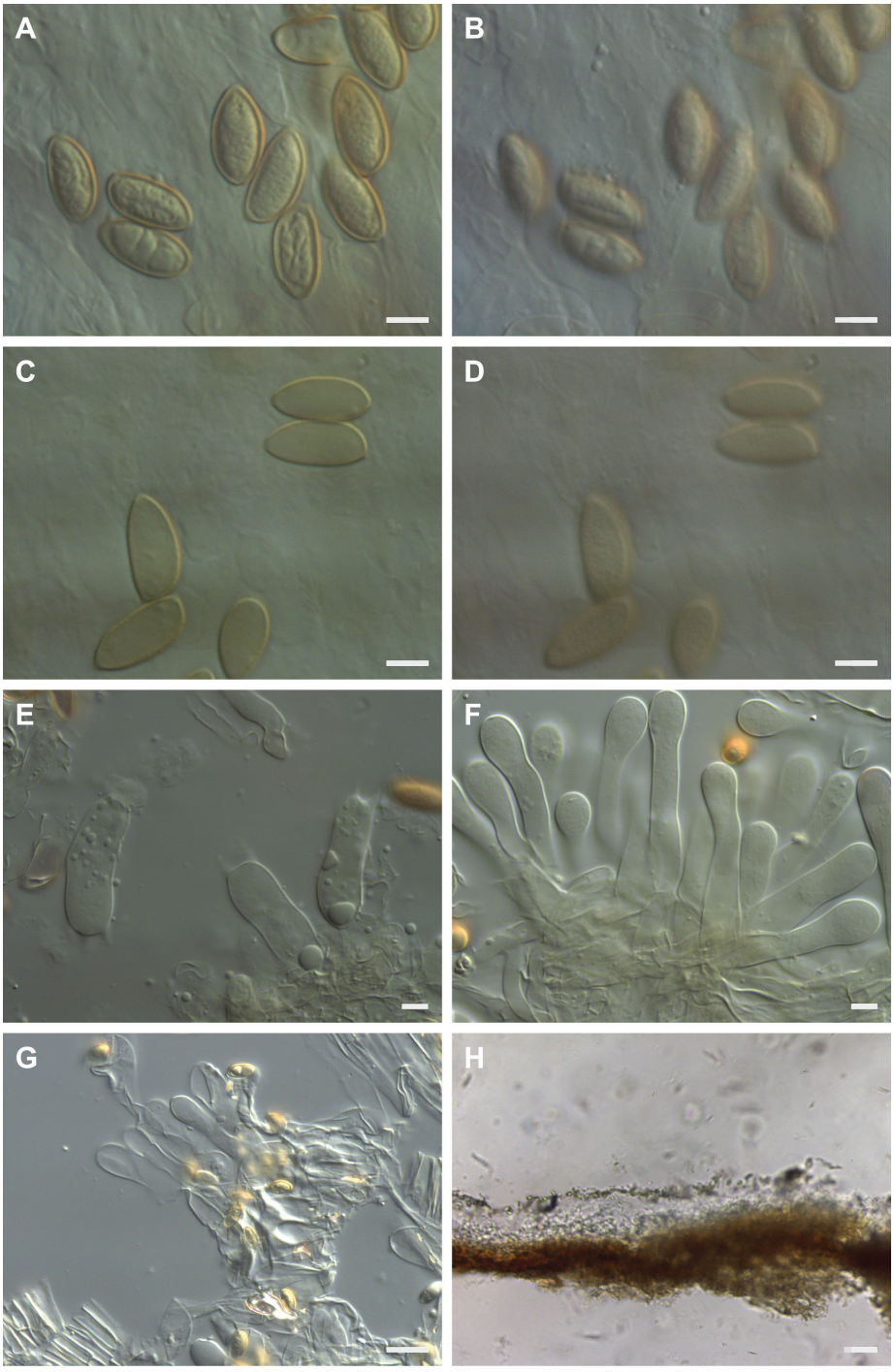

Figure 23. *Hebeloma arcticum* HK16.119 (holotype) **A** spores ×1600 and **B** spore ornamentation ×1600 in Melzer's reagent **C** spores and **D** spore ornamentation ×1600 in KOH **E** basidia cheilocystidia and **F** cheilocystidia ×1000 in Melzer's reagent **G** caulocystidia ×500 in KOH **H** cutis ×125 in KOH. Scale bars: 5 µm (**A–F**); 10 µm (**G**); 50 µm (**H**); microphotographs H.J. Beker.

Distribution. This is a new species known from a number of records in the Low Arctic zone in southern and western Greenland. The fact that it was collected several times independently may indicate that it is quite common in these areas.

Habitat and ecology. Eight collections, seven with *Salix glauca* one with *S. arctophila*. Most collections are from mineral-poor ground.

Notes. The mainly clavate-stipitate cheilocystidia indicate that this species belongs in *H.* sect. *Denudata* and there in *H.* subsect. *Crustuliniformia.* Few species of the subsection have almost smooth spores or spores that are rather strongly dextrinoid. The combination of almost smooth and rather strongly dextrinoid spores is unique in this subsection. Molecular results support its placement within this subsection. Within *H.* sect. *Denudata*, based on the spore characters, *H. arcticum* is readily identifiable. To be noted is also the unusual shape of the spores; while many spores are amygdaloid, many others appear more ellipsoid or cylindrical, again uncommon for this section of *Hebeloma.* As Figs 5A-B show, *H. arcticum* is well distinct from related taxa and is in a supported clade (Fig. 5B) with other members of *H.* subsect. *Crustuliniformia*, but is not a member of the *H. alpinum*-complex. The clade of the species is supported by 100% bootstrap in the analysis of three loci (Fig. 5B), but based on current knowledge, ITS alone is sufficient to recognize the taxon; in the ITS tree (not shown) calculated prior to concatenation of the data, *H. arcticum* received 84% bootstrap support.

***Hebeloma aurantioumbrinum* Beker, Vesterh. & U. Eberh.; Eberhardt, Beker & Vesterholt, Persoonia 35: 116, 2015.**

Fig. 24

Macroscopic description. Cap 0.8–3.6 cm in diameter, umbonate or campanulate, sometimes slightly tomentose or adpressed subtomentose, at high magnification, margin smooth, tacky when moist, not generally hygrophanous, but often with hygrophanous spots, uniformly colored or variably bicolored, at center yellow brown to cinnamon to umber, but with orange elements, at margin pinkish buff to clay buff, usually very thin, without traces of any veil. Lamellae initially whitish then becoming darker and brown with maturity, emarginate, maximum depth 2 mm, number of lamellae {L} 26–42, droplets present and visible, white fimbriate edge present. Stem 1.0–4.0 × 0.15–0.5 cm, whitish lengthily fibrillose on whitish-pale ground, then sordid buff or yellowish, cylindrical, occasionally clavate, stem Q (4.7–)5.5–7, pruinose, particularly at apex. Context firm, stem interior stuffed, flesh not discoloring from base. Smell raphanoid, sometimes weakly. Taste mild or slightly bitter. Spore deposit clay buff.

Microscopic description. Spores amygdaloid, not or weakly papillate, on ave. 10.0–12.0 × 6.0–7.0 µm, ave. Q = 1.6–1.9, pale brown to yellow-brown to brown, guttulate, almost smooth to weakly ornamented (O1 O2 (O3)), perispore not or somewhat loosening (P0 P1), indistinctly to weakly dextrinoid (D1 D2). Basidia 28–38(-43) × 7–9(–11) µm, ave. Q = 3.2–4.4, mostly four-spored. Cheilocystidia clavate-stipitate, occasionally spathulate-stipitate or clavate-lageniform, occasionally

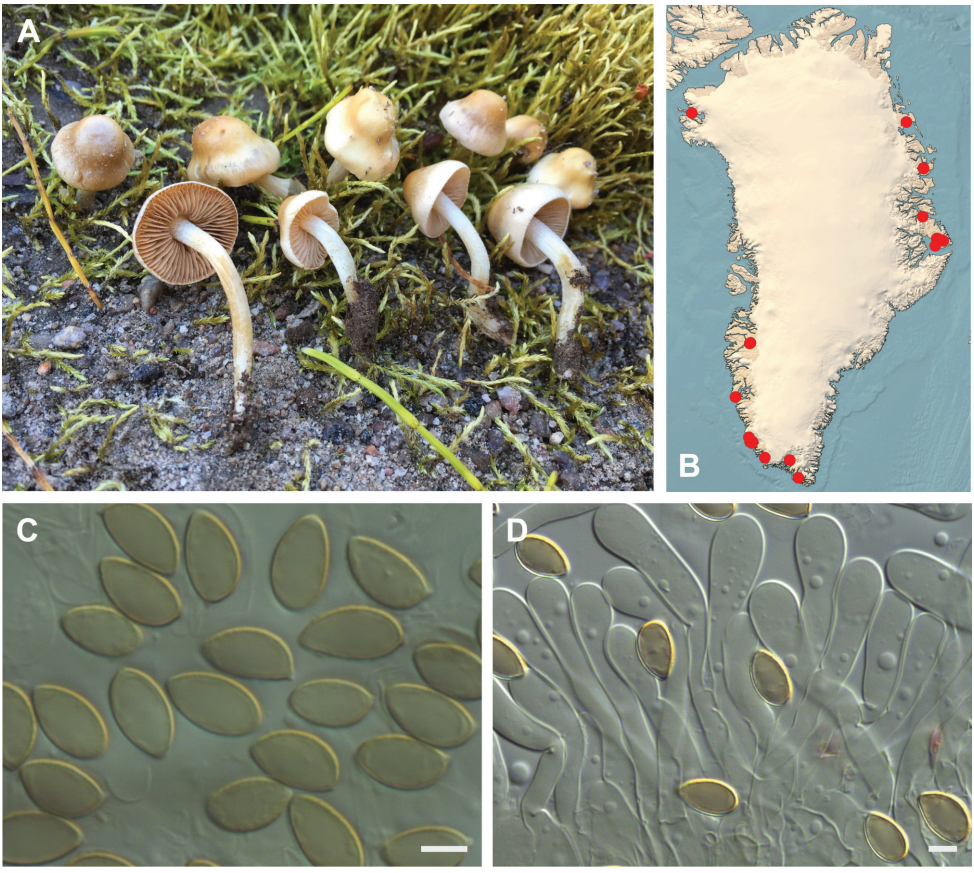

Figure 24. *Hebeloma aurantioumbrinum* **A** SAE-2016.146, photograph S.A. Elborne **B** distribution of cited collections **C** spores ×1600 and **D** cheilocystidia ×1000 of SAE-2016.146 in Melzer's reagent. Scale bars: 5 µm; microphotographs H.J. Beker.

characteristically with a median wall thickening, geniculate or septate, on ave. 45–61 × 7–8.5 (apex) × 4–5 (middle) × 4.5–5.5 (base) µm, with yellow contents, ratios A/M = 1.61–1.95, A/B = 1.62–1.98, B/M = 0.97–1.18. Epicutis an ixocutis, up to 70 µm thick (measured from exsiccata), maximum hyphae width 6 µm, sometimes encrusted, trama elements beneath subcutis ellipsoid up to 6 µm wide. Caulocystidia similar to cheilocystidia, up to 75 µm long.

Collections examined. S-Greenland: Kangilineq/Kvaneøen, 61.95°N, 49.47°W, 25 Aug 1990, T. Borgen (TB90.057, C-F-103482), 40 m. Kangilinnguit, bottom of Laksebund, 61.25°N, 48.08°W, 21 Aug 2018, H. Knudsen (HK18.296, C-F-111114), 100 m, in tundra. North of Tasiusaq, across the fjord from Narsarsuaq, 61.17°N, 45.61°W, 31 Jul 1993, E. Rald (ER 93.091, C-F-104321), 150 m, in *Sphagnum* at the lakeside. Nugarssuk, 60.26°N, 44.76°W, 9 Aug 1993, E. Rald (ER 93.262, C-F-104315), 0 m. Paamiut, 62.01°N, 49.4°W, 23 Aug 1985, T. Borgen (TB85.239, C-F-103459), 90 m, with *Salix herbacea* and *Salix arctophila* in bog. Paamiut, 62.01°N,

49.4°W, 5 Aug 1993, T. Borgen (TB93.070, C-F-103502), 10 m. Paamiut, 62.01°N, 49.4°W, 1 Sep 1990, T. Borgen (TB90.072, C-F-103484), 10 m, with *Salix glauca* and *Bistorta vivipara*. Paamiut, 62.01°N, 49.4°W, 17 Aug 1990, T. Borgen (TB90.041, C-F-103481), 10 m, with *Salix glauca*. Paamiut, 62.01°N, 49.4°W, 19 Aug 1985, T. Borgen (TB85.217, C-F-103526), 10 m, with *Salix herbacea* in snowbed. Paamiut, 62.01°N, 49.4°W, 31 Aug 1986, T. Borgen (TB86.277B, C-F-137117), 10 m, with *Salix* sp. Paamiut, 62.01°N, 49.4°W, 19 Aug 1984, T. Borgen (TB84.150, C-F-119792), 15 m, with *Salix arctophila* and *Bistorta vivipara* in fenland. Paamiut, 62.01°N, 49.4°W, 15 Aug 1984, T. Borgen (TB84.132, C-F-103461), 15 m, with *Salix herbacea* in snowbed. Paamiut, 62.01°N, 49.67°W, 12 Aug 1984, T. Borgen (TB84.112, C-F-119737), 20 m, with *Salix* sp. Paamiut, 62.01°N, 49.4°W, 16 Aug 1984, T. Borgen (TB84.135, C-F-103462), 10 m, with *Salix arctophila*, *Bistorta vivipara* in fenland. Paamiut, 62°N, 49.67°W, 26 Jul 1985, D. Boertmann (DB 85-17, C-F-119784), 25 m, with *Salix* sp. in bog. Paamiut, 62°N, 49.67°W, 26 Jul 1985, D. Boertmann (DB 85-28, C-F-119785), 25 m, with *Salix* sp. in bog. Paamiut, Avigaat, 62.23°N, 49.83°W, 22 Sep 1990, T. Borgen (TB90.133, C-F-103485), 60 m, with *Salix herbacea* and *Bistorta vivipara*. Paamiut, Navigation School area, 62.01°N, 49.4°W, 17 Aug 1990, T. Borgen (TB90.039, C-F-103546), 10 m, with *Salix herbacea* and *Bistorta vivipara*. Paamiut, Navigation School area, 62.01°N, 49.4°W, 13 Aug 1990, T. Borgen (TB90.029, C-F-103545), 10 m, with *Salix herbacea*. Paamiut, Navigation School area, 62.01°N, 49.4°W, 12 Aug 1990, T. Borgen (TB90.012, C-F-103547), 10 m, with *Salix herbacea*. Paamiut, Navigation School area, 62.01°N, 49.4°W, 12 Aug 1990, T. Borgen (TB90.011, C-F-103548), 10 m, with *Salix herbacea*. Paamiut, Telesletten, 62.01°N, 49.4°W, 23 Aug 1986, T. Borgen (TB86.251, C-F-103570), 10 m. **W-Greenland:** Kangerlussuaq, Lake Ferguson, Tasersuatsiaq, 66.96°N, 50.70°W, 22 Aug 2016, S.A. Elborne (SAE-2016.146-GR, C-F-106745), 350 m, with *Salix glauca* in streambed. Kangerlussuaq, NE facing slopes along Lake Ferguson, 66.99°N, 50.61°W, 12 Aug 2016, H. Knudsen (HK16.089, C-F-104118), 300 m. Nuuk, 64.19°N, 51.67°W, 14 Aug 1987, S.A. Elborne (SAE-1987.113-GR, C-F-119789), 300 m, with *Salix herbacea* in snowbed. Nuuk, airport area, 64.19°N, 51.67°W, 5 Aug 1987, H. Knudsen (HK87.004, C-F-119790), 100 m. Nuuk, Lille Malene, 64.19°N, 51.67°W, 17 Aug 1987, H. Knudsen (HK87.218, C-F-119788), 100 m. **N-Greenland:** Qaanaaq, 77.47°N, 69.18°W, 8 Aug 1988, S.A. Elborne (SAE-1988.149-GR, C-F-1461), 50 m. Danmarkshavn, Mørkefjord Station, 76.93°N, 20.32°W, 7 Aug 1984, B. Lauritsen (BL s.n., C-F-3637), 10 m. Danmarkshavn, Mørkefjord Station, 76.93°N, 20.32°W, 26 Jul 1982, B. Lauritsen (BL s. n., C-F-119797), 10 m. Zackenberg, Gadekæret, 74.5°N, 21°W, 21 Jul 1999, T. Borgen (TB99.044, C-F-119751), 40 m, with *Salix arctica* and *Bistorta vivipara* in scrubland. Zackenberg, Teltdammen, 74.5°N, 21°W, 5 Aug 2006, T. Borgen (TB06.091, C-F-119741), 30 m, with *Salix arctica* in scrubland. Zackenberg, Teltdammen, 74.5°N, 21°W, 5 Aug 2006, T. Borgen (TB06.091, C-F-119781), 30 m, with *Salix arctica* in scrubland. Zackenberg, Ulvehøj, 74.47°N, 21°W, 11 Aug 2006, T. Borgen (TB06.150, C-F-119768), 40 m, with *Salix arctica* in snowbed. Zackenberg, Østkæret, 74.47°N, 21°W, 22 Aug 2006, T. Borgen (TB06.259, C-F-119771),

40 m, with *Salix arctica* in fenland. **E-Greenland:** Jameson Land, Constable Pynt, beginning of Lollandselv, 70.92°N, 23.18°W, 31 Jul 1989, S.A. Elborne (SAE-89.430, C-F-2424), 500 m, with *Salix arctica* on riverside. Jameson Land, Constable Pynt, camp at 'Vindelv', river wnw of pt.330, 71°N, 23.47°W, 30 Jul 1989, H. Knudsen (HK89.366, C-F-2309), 230 m, with *Salix arctica*. Jameson Land, Constable Pynt, delta of Jyllandselv, 70.68°N, 24.06°W, 28 Jul 1988, D. Boertmann (DB GR 88-22, C-F-119787), 0 m. Jameson Land, Constable Pynt, Gåseelv, 70.77°N, 22.7°W, 18 Jul 1989, S.A. Elborne (SAE-89.121, C-F-2327), 80 m, with *Salix arctica* on lakeside. Lower east Skeldal, Kong Oscars Fjord, 72.27°N, 24.28°W, 17 Aug 1962, T.T. Elkington (s.n., C-F-6992), 150 m, with *Cassiope* in tundra and heathland. Lower east Skeldal, Kong Oscars Fjord, 72.27°N, 24.28°W, 17 Aug 1962, T.T. Elkington (s.n., C-F-6993), 150 m, with *Cassiope*, tundra and heathland.

Distribution. *Hebeloma aurantioumbrinum* is one of the five most commonly recorded *Hebeloma* in Greenland with 10.5% of the records considered here. It is common and widely distributed in arctic areas in Europe (Beker et al. 2016). From alpine areas, it is known from North America (Cripps et al. 2019), but not from the well-investigated alpine mountains in Europe (Beker et al. 2016). Circumpolar, arctic-alpine.

Habitat and ecology. Forty collections with a number of hosts recorded, including: *Salix herbacea* (11), *S. arctica* (5), *S. glauca* (5), *S. arctophila* (3), *Salix* sp. (5), *Bistorta vivipara* (8, but never as the only possible associate). The localities are also scattered between wet and dry places, but favoring wet areas with *S. herbacea*, without having a preference for specific soil conditions. Beker et al. (2016) also found a preference for *Salix*, including *S. polaris*.

***Hebeloma geminatum* Beker, Vesterh. & U. Eberh.; Eberhardt, Beker & Vesterholt, Persoonia 35: 122, 2015.**
Fig. 25

Macroscopic description. Cap 2.0–12.0 cm in diameter, usually convex, sometimes broadly umbonate or applanate, margin usually smooth, occasionally involute, crenulate or upturned with age, tacky when moist, not hygrophanous usually uniformly colored, rarely bicolored, at center usually cream or whitish, sometimes a little yellowish, at margin paler, cream to whitish, without any traces of veil. Lamellae initially very pale brown, later clay-brown, adnate to emarginate, maximum depth 4–8 mm, number of lamellae {L} 62–100, with visible droplets and white fimbriate edge. Stem 1.5–11.0 × 0.7–1.5 {median} × 0.7–1.6 {base} cm, initially whitish, later pale brownish, initially pruinose, apex with watery droplets, cylindrical to clavate, stem Q (2.1–)2.5–9.2(–10.6), floccose. Context firm, stem interior stuffed, becoming hollow with age, flesh usually not discoloring from base. Smell raphanoid. Taste mild, raphanoid. Spore deposit brownish olive to grayish brown.

Microscopic description. Spores amygdaloid, on ave. 10.0–11.0 × 5.5–6.5 µm, ave. Q = 1.7–1.9, grayish yellow to yellow-brown to brown, guttulate, weakly to

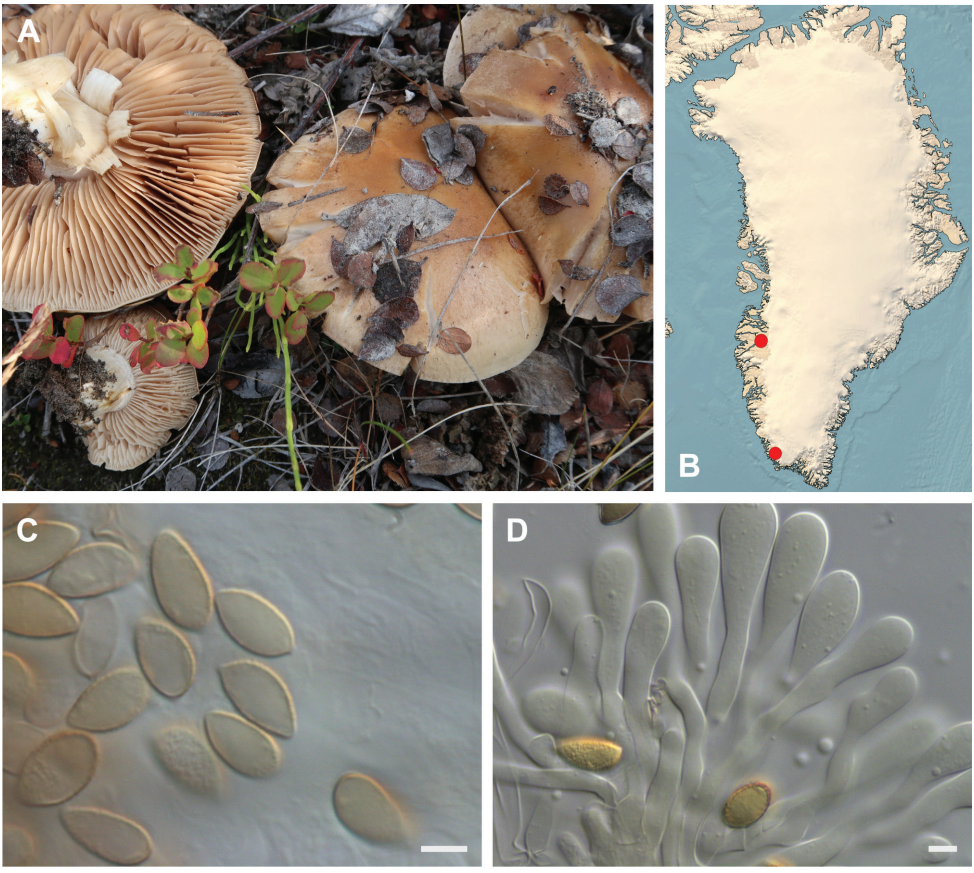

Figure 25. *Hebeloma geminatum* **A** HK18.379B, photograph H. Knudsen **B** distribution of cited collections **C** spores ×1600 and **D** cheilocystidia ×1000 of HK18.379B in Melzer's reagent. Scale bars: 5 µm; microphotographs H.J. Beker.

distinctly ornamented (O2 O3), perispore somewhat loosening ((P0) P1 (P2)), indextrinoid or indistinctly dextrinoid (D0 D1). Basidia 25–35 × 7–9 µm, ave. Q = 3.3–4.3, mostly four-spored. Cheilocystidia clavate-stipitate or spathulate-stipitate and occasionally capitate-stipitate or clavate-lageniform, occasionally characteristically bifurcate, with a median wall thickening, septate or sinuate, on ave. 50–72 × 8–10.5 (apex) × 4–4.5 (middle) × 3.5–5 (base) µm, ratios A/M = 1.76–2.57, A/B = 1.68–2.85, B/M = 0.81–1.19. Epicutis an ixocutis, 110–200 µm thick (measured from exsiccata), maximum hyphae width 5–8 µm, variably encrusted, trama elements beneath subcutis cylindrical, ellipsoid, sausage-shaped up to 16 µm wide. Caulocystidia similar to cheilocystidia, up to 70 µm long and 12 µm wide.

Collections examined. S-Greenland: Sermiliarsuk, Sioralik, Aasivii, 65.53°N, 48.33°W, 30 Aug 1997, T. Borgen (TB97.154a, C-F-103508), with *Betula pubescens*, 50 m. **W-Greenland:** Kangerlussuaq, c. 2 km W of the Airport, Mt. Hassel, 67.06°N, 50.68°W, 10 Aug 2000, A-M. Larsen, T. Borgen (TB00.065, C-F-103514),

50 m, with *Salix glauca* in copse. Kangerlussuaq, Hassells Fjeld, Kløftsøerne, 67.01°N, 50.71°W, 27 Aug 2018, H. Knudsen (HK18.379B, C-F-111117), 300 m, with *Salix glauca*, *Betula nana* in heathland.

Distribution. Only known from two localities in southwestern Greenland. Generally distributed over much of Europe, but lacking in the Mediterranean region. Northernmost European localities are from Norway at just above 70°N. This species has already been recorded in North America (https://mycoportal.org/portal/collections/list.php, accessed 2 Dec 2020) but how common it is, is not yet known. Temperate and boreal, with a few records from the Low Arctic zone.

Habitat and ecology. Only three collections with *Salix glauca*, *Betula nana* and *B. pubescens*, but when recorded on 27 Aug. 2018, on the south-exposed side of Mt. Hassell, it was numerous and, remarkably, the only agaric present. From Europe, there are a number of hosts recorded, including many deciduous and coniferous trees (Beker et al. 2016).

***Hebeloma helodes* J. Favre; Beitr. Kryptfl. Schweiz 10(3): 214, 1948.**
Fig. 26

Macroscopic description. Cap 1.3–3.8 cm in diameter, convex or sometimes weakly umbonate becoming umbilicate with age, margin usually involute at least when young, tacky when moist, not hygrophanous, mostly uniformly colored or variably bicolored, at center light ochraceous to yellowish to yellowish-brown or pale reddish brown and at margin whitish to pale cream, sometimes with remains of universal veil. Lamellae initially whitish later persistently cream, attachment emarginate, occasionally adnate, maximum depth 3–4.5 mm, number of lamellae {L} 33–54, droplets present and visible at least with × 10 lens, white fimbriate edge present. Stem 1.5–6.5 × 2.0–7.0 {median} × (2–)2.9–6.5(–7) {base} cm, whitish tomentose flocculose in the entire length, cylindrical to clavate, stem Q (3.3–)4.7–20, floccose. Context firm, stem interior stuffed, later becoming hollow, stem flesh not discoloring from base but with some weak discoloration with age. Smell raphanoid. Taste mild, raphanoid. Spore deposit dark olive buff to brownish olive.

Microscopic description. Spores amygdaloid, on ave. 9.0–11.0 × 5.0–6.0 µm, ave. Q = 1.6–2.0, yellow to pale brown, usually guttulate, weakly to distinctly ornamented (O2 O3), perispore somewhat to distinctly loosening ((P0) P1 P2), indextrinoid to indistinctly dextrinoid, rarely distinctly dextrinoid (D0 D1 (D2)). Basidia 22–27(–30) × 7–9 µm, ave. Q = 2.8–4.2, mostly four-spored. Cheilocystidia clavate-stipitate to capitate stipitate, occasionally more clavate-lageniform, often with characteristic apical or less frequently median wall thickening, occasionally septate, on ave. 44–63 × 8.5–11.5 (apex) × 4–5 (middle) × 3.5–5.5 (base) µm, ratios A/M = 1.90–2.86, A/B = 2.02–3.38, B/M = 0.77–1.17. Epicutis an ixocutis, 100–135 µm thick (measured from exsiccata), maximum hyphae width 5–6 µm, sometimes encrusted, trama elements beneath subcutis sausage-shaped up to 15 µm wide. Caulocystidia similar to cheilocystidia, but short, up to 11 µm wide at apex.

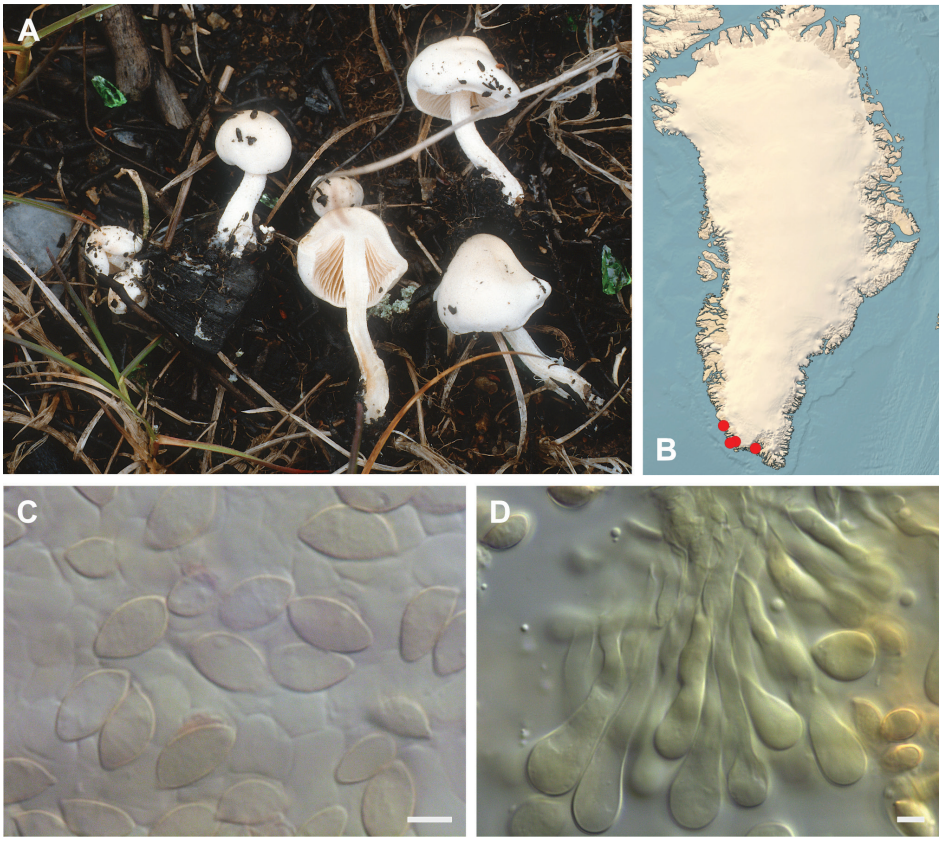

Figure 26. *Hebeloma helodes* **A** TB88.114, photograph T. Borgen **B** distribution of cited collections **C** spores ×1600 and **D** cheilocystidia ×1000 of TB88.114 in Melzer's reagent. Scale bars: 5 µm; microphotographs H.J. Beker.

Collections examined. S-Greenland: Kangilinnguit, 61.14°N, 48.6°W, 10 Aug 1985, T. Borgen (TB85.072, C-F-103460), 25 m, with *Alnus alnobetulae* in copse. Kangilinnguit, 61.14°N, 48.6°W, 11 Aug 1985, T. Borgen (TB85.090, C-F-103476), 25 m, with *Alnus alnobetulae* in copse. Kangilinnguit, 61.23°N, 48.10°W, 10 Aug 1985, T. Borgen (TB85.065, C-F-103525), 25 m, with *Salix glauca* in heathland. Narsaq, 60.91°N, 46.05°W, 3 Aug 1993, E. Rald (ER 93.153, C-F-104317), 20 m, with *Salix glauca* in scrubland. Paamiut, 62.01°N, 49.4°W, 29 Aug 1988, T. Borgen (TB88.114, C-F-4003), 50 m, in scrubland.

Distribution. Only found in a few localities in southern Greenland. Generally distributed in warm and cold temperate Europe with a few records from subarctic Norway and Finland and missing in southern Europe. The Greenland records fit well with the European records, the records from southern Greenland (Paamiut, 62.01) being the northernmost hitherto found.

Habitat and ecology. Five collections from heath- and scrubland recorded with *Salix glauca* and *Alnus alnobetulae*. Beker et al. (2016) suspect association with various deciduous tree families.

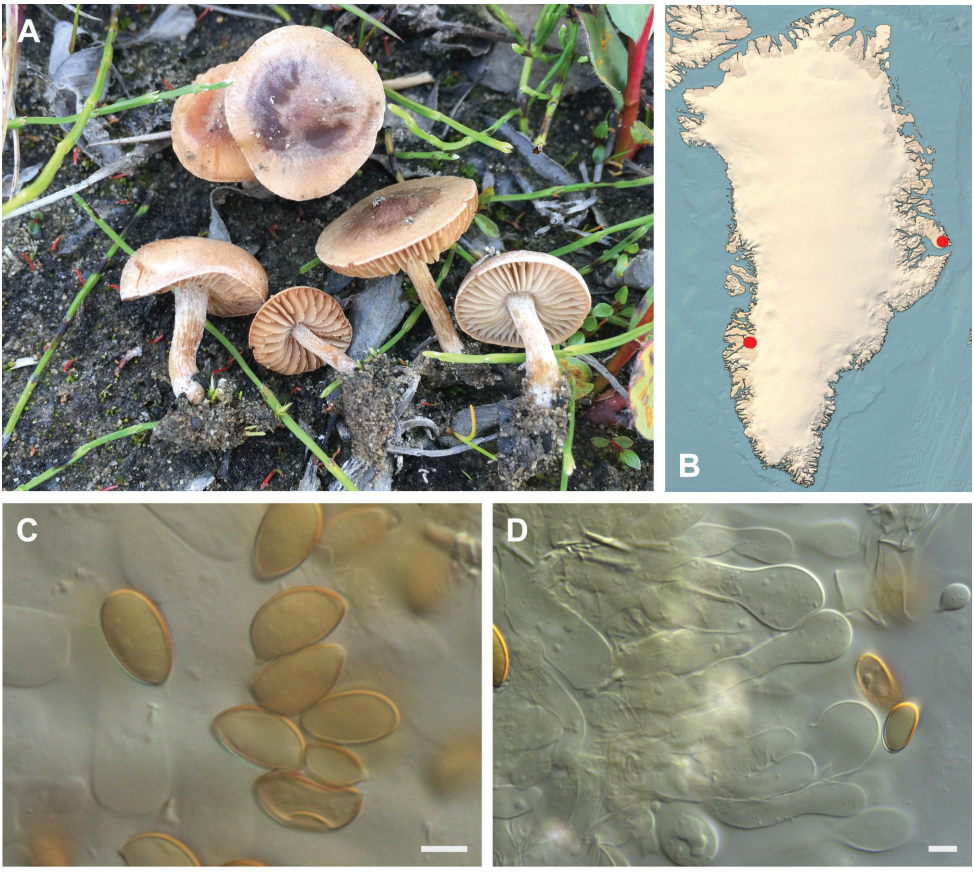

Figure 27. *Hebeloma louiseae* **A** SAE-2017.125, photograph S.A. Elborne **B** distribution of cited collections **C** spores ×1600 and **D** cheilocystidia ×1000 of HK17.128A.146 in Melzer's reagent. Scale bars: 5 µm; microphotographs H.J. Beker.

Hebeloma louiseae **Beker, Vesterh. & U. Eberh.; Eberhardt, Beker & Vesterholt, Persoonia 35: 127, 2015.**
Fig. 27

Macroscopic description. Cap 0.7–2.2 cm in diameter, convex to broadly umbonate, margin smooth to crenulate, tacky when moist, not hygrophanous, uniformly colored or indistinctly bicolored, at center clay-buff to dark olive buff, margin very thin, grayish pink or central color extending to margin, with no traces of veil. Lamellae initially pale, later sordid clay-brown, emarginate, maximum depth 2 mm, number of lamellae {L} 28–40, droplets often absent but occasionally visible even with the naked eye, white fimbriate edge present. Stem 0.8–2.5 × 0.2–0.3 {median} × 0.1–0.3 {base} cm, initially pale, later sordid brownish, cylindrical to clavate, occasionally tapering, stem Q (4–)4.6–7.6(–9.2), pruinose to slightly fibrillose. Context firm, interior stuffed, flesh discoloring weakly from base. Smell absent or raphanoid. Taste not recorded. Spore deposit grayish brown.

Microscopic description. Spores amygdaloid, limoniform, weakly to strongly papillate, on ave. 12.0–13.0 × 7.0–7.5 µm, ave. Q = 1.6–1.8, yellow brown to brown, guttulate, almost smooth to weakly ornamented (O1 O2), perispore not loosening (P0), indextrinoid to indistinctly dextrinoid (D0 D1 (D2)). Basidia 24–56 × 6–12 µm, ave. Q = 3.2–4.6, mostly four-spored. Cheilocystidia clavate-stipitate, occasionally spathulate-stipitate or capitate-stipitate or clavate-lageniform, occasionally with characteristic apical wall thickening, occasionally bifurcate, septate or sinuate, on ave. 42–59 × 6–11 (apex) × 4.0–5.5 (middle) × 3.5–6.0 (base) µm, ratios A/M = 1.48–2.51, A/B = 1.99–2.92, B/M = 0.81–1.24. Epicutis an ixocutis, up to 100 µm thick (measured from exsiccata), maximum hyphae width 6 µm, sometimes encrusted, trama elements beneath subcutis cylindrical, sausage-shaped. Caulocystidia similar to cheilocystidia, up to 75 µm long.

Collections examined. W-Greenland: Kangerlussuaq, c. 2 km W of the Airport, 67.06°N, 50.68°W, 10 Aug 2000, A-M. Larsen, T. Borgen (TB00.061, C-F-103518), 50 m, with *Salix glauca* in ditch. Kangerlussuaq, Sandflugtsdalen, 67.06°N, 50.42°W, 25 Aug 2016, S.A. Elborne (SAE-2016.197-GR, C-F-106747), 110 m, with *Salix glauca* in dune slack. **E-Greenland:** Jameson Land, Nerlerit Inaat/Constable Pynt, delta of Gåseelv valley, 70.76°N, 22.65°W, 6 Aug 2017, H. Knudsen (HK17.128, C-F-105029), 40 m. Jameson Land, Nerlerit Inaat/Constable Pynt, delta of Gåseelv valley, 70.76°N, 22.65°W, 6 Aug 2017, S.A. Elborne (SAE-2017.125A-GR, C-F-106763), 40 m, with *Salix arctica* at riverside. Jameson Land, Nerlerit Inaat/Constable Pynt, delta of Gåseelv valley, 70.77°N, 22.69°W, 6 Aug 2017, S.A. Elborne (SAE-2017.125B-GR, C-F-106763), 15 m, with *Salix arctica* at riverside.

Distribution. Recently described from Svalbard (Beker et al. 2016). The five Greenland collections all occurred north of 67°N and thus provide evidence that *H. louiseae* is a species of the High Arctic zone. It has not yet been recorded in alpine regions. The Greenland collections are the first from North America and the first outside Europe.

Habitat and ecology. Five collections, with *Salix glauca* and *S. arctica* in calcareous soil and seemingly moist localities. From Svalbard it was recorded with *S. polaris* (Beker et al. 2016).

Notes. *Hebeloma louiseae* is easily recognized among the arctic *Hebeloma* species by the small basidiomes, the relatively few lamellae and the large basidia, although not present in every collection.

***Hebeloma minus* Bruchet; Bull. mens. Soc. linn. Lyon 39(6(Suppl.)): 126, 1970.**
Fig. 28

Macroscopic description. Cap 0.9–3.1 cm in diameter, convex to umbonate, margin smooth, sometimes involute, tacky when moist, sometimes hygrophanous especially when frosted, almost uniformly colored, occasionally more bicolored, at center dark pinkish buff to dark olive buff or clay-buff to brownish olive, grayish brown or umber, at margin pinkish to grayish buff or clay-buff, occasionally pruinose (givré), without

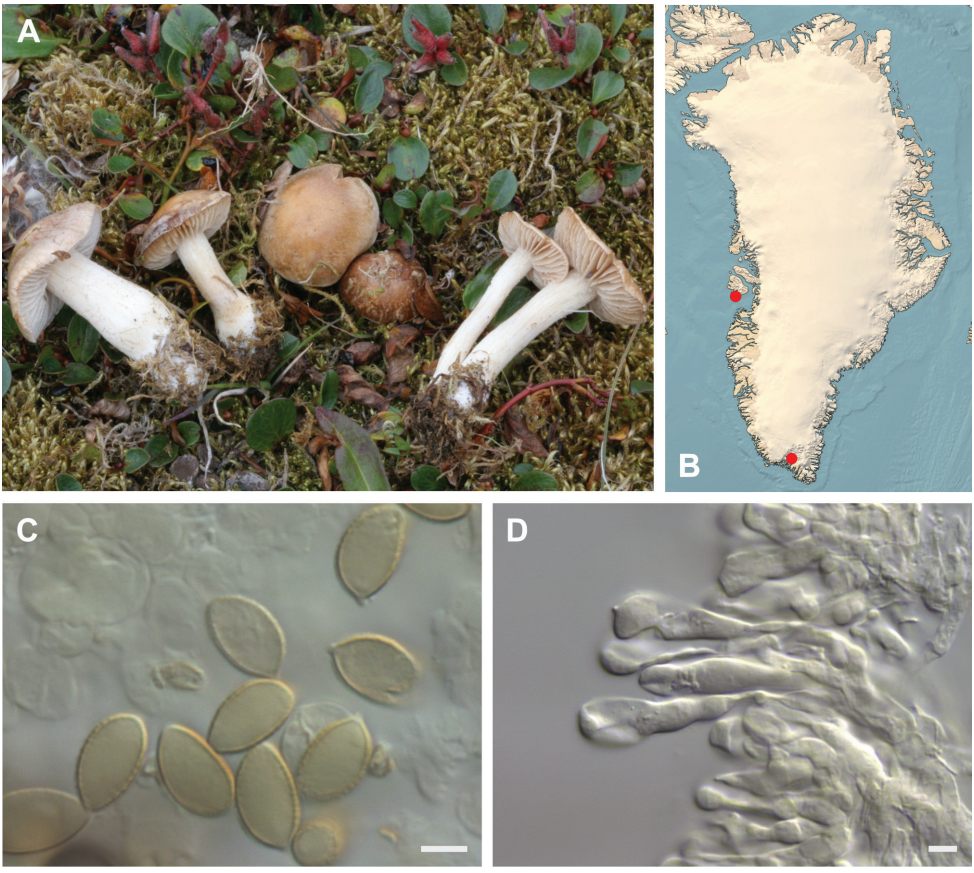

Figure 28. *Hebeloma minus* **A** HJB11945 (from Svalbard), photo H.J. Beker, reproduced by kind permission from Beker et al. (2016) **B** distribution of cited collections **C** spores ×1600 and **D** cheilocystidia ×1000 of TB86.085 in Melzer's reagent. Scale bars: 5 µm; microphotographs H.J. Beker.

any traces of veil. Lamellae clay buff, emarginate to adnate, maximum depth 3.5–5 mm, number of lamellae {L} 30–34, droplets often visible, occasionally absent or visible with × 10 lens, white fimbriate edge present. Stem 1.0–4.0 × 0.1–0.8 {median} × 0.1–1.0 {base} cm, stem Q (4–)4.8–14(–20), fairly strongly whitish fibrillose-flocculose, cylindrical to clavate, rarely bulbous, fibrillose, pruinose, floccose, particularly noticeable at apex. Context firm, stem interior stuffed, hollow with age, flesh discoloring from base at most very weakly. Smell raphanoid. Taste mild, occasionally weakly bitter or raphanoid. Spore deposit brownish olive.

Microscopic description. Spores amygdaloid, occasionally limoniform, papillate, on ave. 11.0–13.0 × 6–7.5 µm, ave. Q = 1.6–1.9, yellow to brown, usually guttulate, weakly to distinctly ornamented (O2 O3), perispore not or somewhat loosening (P0 P1 (P2)), indistinctly to weakly dextrinoid (D1 D2). Basidia 27–40 × 7–11 µm, ave. Q = 2.8–4.1, mostly four-spored. Cheilocystidia capitate-stipitate, clavate-stipitate or occasionally clavate-lageniform, occasionally with characteristic apical or median wall

thickening, sometimes geniculate or septate, on ave. 40–60 × 8–11.0 (apex) × 3.5–5 (middle) × 3–6 (base) µm, ratios A/M = 1.87–2.67, A/B = 1.81–3.02, B/M = 0.84–1.24. Epicutis an ixocutis, 40–100 µm thick (measured from exsiccata), maximum hyphae width 6–6.5 µm, some encrusted, trama elements beneath subcutis cylindrical, sausage-shaped, up to 30 µm wide. Caulocystidia similar to cheilocystidia but larger, up to 100 µm long.

Collections examined. S-Greenland: Qassiarsuk, Tasiusaq, 61.15°N, 45.52°W, 21 Jul 1984, T. Læssøe (TL 84.041, C-F-119793), 25 m. **W-Greenland:** Qeqertarsuaq/Disko, Godhavn, Østerlien, 69.25°N, 53.54°W, 30 Jul 1986, T. Borgen (TB86.085, C-F-104302), 40 m, with *Salix glauca* in copse.

Distribution. Only two collections, from southwestern Greenland. Although described 50 years ago, *H. minus* is still only known from a few collections in Iceland and Svalbard, and from the French, Italian and Swiss Alps at 2200–2700 m. The Icelandic localities are from the upper boreal zone, but close to the oroboreal zone, which is equivalent to the alpine zone (Rivas-Martinez et al. 2004). The Svalbard localities are in the High Arctic, whereas the two Greenland collections are both from the Low Arctic zone. This is a truly arctic-alpine species. It is new to North America and these are the first records outside Europe.

Habitat and ecology. Two collections, one recorded with *Salix glauca*. Beker et al. (2016) list *S. herbacea*, *S. reticulata*, *S. retusa* and *Dryas octopetala* as hosts from arctic and alpine sites in Europe.

Hebeloma subsect. *Clepsydroida* Beker & U. Eberh.; Fungal Biol. 120: 82, 2015 ("2016").

Cheilocystidia distinctly broadened at apex, base ± swollen, wall often thickened at the middle. Lamellae edge often with exuded drops, but sometimes dried away.

Hebeloma ingratum Bruchet; Bull. mens. Soc. linn. Lyon 39: 125, 1970.

Fig. 29

Macroscopic description. Cap 1.8–7.5 cm in diameter, convex to umbonate, margin often involute when young, sometimes serrate or crenulate, tacky when moist, occasionally hygrophanous, usually bicolored but sometimes unicolored, at center usually brown tones from ochraceous to cinnamon, at margin cream, occasionally 3–4 mm from margin a circle of water spots can be visible, without any traces of veil. Lamellae pale clay brown, adnate to emarginate, maximum depth 3–5 mm, number of lamellae {L} 50–80, droplets absent or visible with × 10 lens, occasionally with naked eye, white fimbriate edge usually present, sometimes very strongly. Stem 1.5–6.8 × 0.4–1.2 {median} × 0.5–1.3 {base} cm, stem Q (2.5–)4.4–11.1(–11.5), white lengthily fibrillose and white flocculose, most distinct in the upper half, cylindrical to clavate, occasionally subbulbous to bulbous. Context firm, interior stuffed, later hollow, rarely with

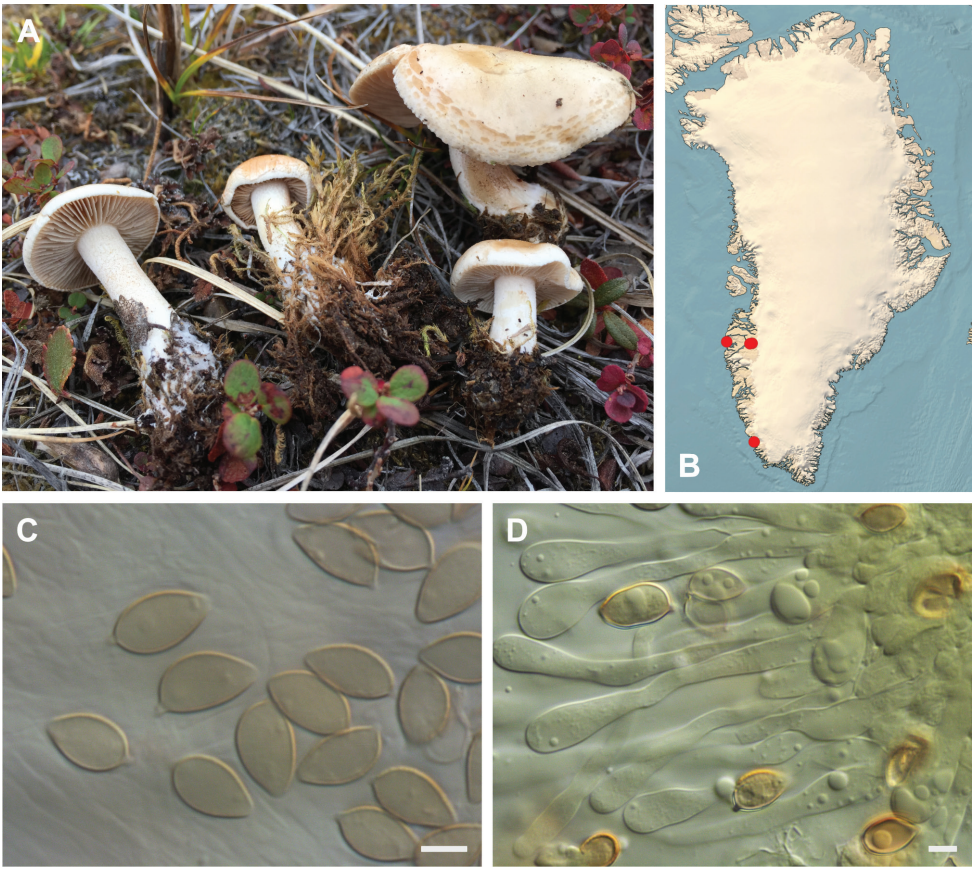

Figure 29. *Hebeloma ingratum* **A** SAE-2016.208, photograph S.A. Elborne **B** distribution of cited collections **C** spores ×1600 and **D** cheilocystidia ×1000 of SAE-2016.208 in Melzer's reagent. Scale bars: 5 µm; microphotographs H.J. Beker.

superior wick, flesh not discoloring from base or sometimes weakly. Smell raphanoid. Taste raphanoid, usually mild, but sometimes bitter. Spore deposit dark olive buff to brownish olive to yellowish brown or umber.

Microscopic description. Spores amygdaloid, sometimes limoniform, variably papillate from absent to very strongly, on ave. 10.0–11.0 × 5.5–6.5 µm, ave. Q = 1.7–1.9, yellow to yellow brown, usually guttulate, weakly to distinctly ornamented (O2 O3), perispore somewhat to distinctly loosening ((P0) P1 P2), indistinctly to weakly dextrinoid (D1 D2). Basidia (20–)24–30(–33) × 6–10 µm, ave. Q = 3.2–3.9, mostly four-spored. Cheilocystidia clavate-lageniform, occasionally clavate-stipitate or ventricose, occasionally with characteristic apical or median wall thickening, sometimes geniculate or septate, on ave. 42–55 × 5–7 (apex) × 3.5–4.5 (middle) × 5–6.5 (base) µm, ratios A/M = 1.4–1.74, A/B = 0.9–1.28, B/M = 1.4–1.64. Epicutis and ixocutis, 75–300 µm thick (measured from exsiccata), maximum hyphae width 5–6.5 µm, sometimes encrusted, trama elements beneath subcutis oblong to sausage-shaped up

to 15 µm wide. Caulocystidia up to 150 µm long, often cylindrical or slenderly clavate at the apex.

Collections examined. S-Greenland: Paamiut, Taartoq/Mørke Fiord, 62.01°N, 49.26°W, 4 Sep 1993, T. Borgen (TB93.205, C-F-103501), 20 m, with *Betula glandulosa* and *Salix glauca* in heathland. **W-Greenland:** Kangerlussuaq, fjord shore south of town, 66.98°N, 50.69°W, 26 Aug 2016, S.A. Elborne (SAE-2016.208-GR, C-F-106748), 20 m, with *Salix glauca* and *Betula nana* along streamside. Kangerlussuaq, Sandflugtsdalen, 67.02°N, 50.42°W, 21 Aug 1987, H. Knudsen (HK87.262, C-F-119732), 200 m, with *Betula nana* and *Salix glauca*. Sisimiut, 4 km E of the village, 66.94°N, 53.59°W, 18 Aug 2000, E. Ohenoja (EO18.8.00.36, OULU F050503), 70 m, in heathland.

Distribution. Only known from two well-studied areas in low arctic southern and western Greenland, north to 67°. The general European distribution is in the Temperate zone, missing in southern Europe and with one record in the Hemiboreal zone in Finland. The Greenland records are the northernmost known and the first from North America and the first outside Europe.

Habitat and ecology. Four collections from heath- and scrubland. Hosts are uncertain, both *Betula nana* and *B. glandulosa* as well as *Salix glauca* were present. No preference for a specific ecology. Beker et al. (2016) also list *Betula* and *Salix*, but also *Fagus*, *Quercus* and *Populus* as possible hosts.

***Hebeloma vaccinum* Romagn.; Bull. trimest. Soc. mycol. Fr. 81: 333, 1965.**
Fig. 30

Macroscopic description. Cap 0.9–6.1 cm in diameter, convex, later umbonate, margin usually involute when young, sometimes crenulate or scalloped, tacky when moist, not hygrophanous, usually bicolored, but sometimes almost unicolored, at center from clay-buff to yellowish brown and dark olive buff to dark brick or rust brown, at margin cream to gray-buff to clay-buff, pale and very thin, without any traces of veil. Lamellae light, then sordid gray-brown, adnexed to emarginate, maximum depth 2–6 mm, number of lamellae {L} 32–60, droplets visible with naked eye or sometimes with × 10 lens, white fimbriate edge present. Stem 0.9–5.5 × 0.3–1.3 {median} × 0.3–1.3 {base} cm, stem Q (2.2–)2.7–9(–13.3), white flocculose on pale brown ground, downwards watery gray-brown, later watery ochre-brown, not darker at base, base cylindrical to clavate or bulbous, sometimes with encrusted sand, pruinose to floccose, particularly at apex. Context firm, stem interior stuffed, later hollow, sometimes with superior wick, flesh not discoloring from base. Smell raphanoid, sometimes of cocoa. Taste sometimes raphanoid, sometimes bitter. Spore color brownish olive to sepia.

Microscopic description. Spores mainly amygdaloid, sometimes fusoid or limoniform, papillate, on ave. 12.0–14.5 × 6.5–8.0 µm, ave. Q = 1.6–2.0, yellow-brown to brown, sometimes guttulate, distinctly to fairly strongly ornamented ((O2) O3 O4), perispore somewhat to distinctly loosening ((P0) P1 P2), weakly to rather strongly

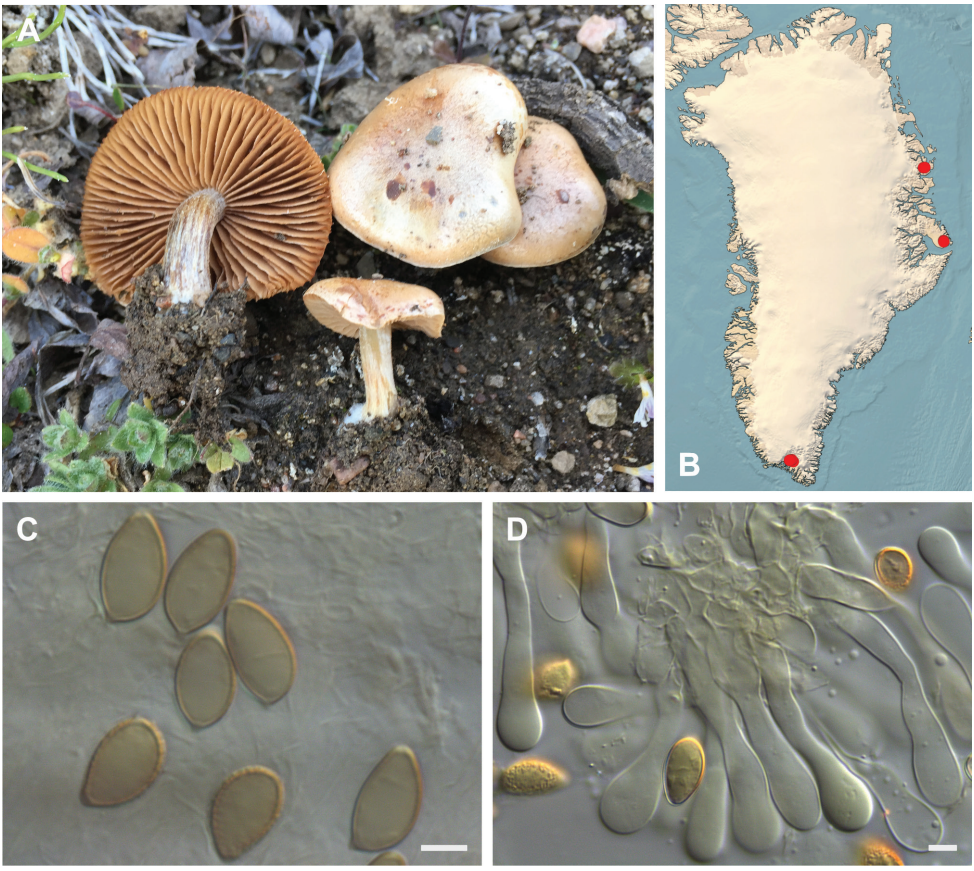

Figure 30. *Hebeloma vaccinum* **A** SAE-2017.194, photograph S.A. Elborne **B** distribution of cited collections **C** spores ×1600 and **D** cheilocystidia ×1000 of SAE-2017.194 in Melzer's reagent. Scale bars: 5 µm; microphotographs H.J. Beker.

dextrinoid (D2 D3). Basidia 27–39 (–42) × 7–12 µm, ave. Q = 3–4.5, mostly four-spored. Cheilocystidia clavate-lageniform, capitate-lageniform, sometimes clavate-stipitate or capitate-stipitate or ventricose, occasionally characteristically with apical or median wall thickening, sometimes geniculate, septate or sinuate, on ave. 41–64 × 6–8 (apex) × 3–5 (middle) × 4.5–8 (base) µm, ratios A/M = 1.43–2.31, A/B = 0.84–1.53, B/M = 1.28–1.92. Epicutis and ixocutis, 40–125 µm thick (measured from exsiccata), maximum hyphae width 5–6.5 µm, sometimes encrusted, trama elements beneath subcutis sausage-shaped, occasionally spherical up to 16 µm wide. Caulocystidia similar to cheilocystidia, up to 90 µm long, often with many septa.

Collections examined. S-Greenland: Narsarsuaq, 61.08°N, 45.26°W, 7 Aug 1985, T. Borgen (TB85.045, C-F-103477), 150 m, with *Dryas integrifolia* in heathland. Narsarsuaq, Hospitalsdalen, 61.17°N, 45.41°W, 1 Aug 1992, E. Rald (ER 92.038, C-F-104308), 60 m, with *Salix glauca* and *Betula glandulosa*. Narsarsuaq, 61.17°N, 45.41°W, 17 Aug 2015, H. Knudsen (HK15.069, C-F-8222), 60 m, with

Salix glauca and *Betula pubescens* at pathside. Qassiarsuk, Tasiusaq, 61.15°N, 45.52°W, 19 Aug 1992, E. Rald (ER 92.323, C-F-104311), 25 m. Tasiusaq, 61.14°N, 45.63°W, 28 Jul 1993, E. Rald (ER 93.022, C-F-104320), 20 m, with *Salix glauca* in fenland. **N-Greenland:** Zackenberg, Aucellabjerg, 74.5°N, 21°W, 20. Aug. 2006, T. Borgen (TB06.246, C-F-119780), 300 m, with *Salix arctica* and *Bistorta vivipara* in scrubland. Zackenberg, just E of the station, 74.5°N, 21°W, 26 Jul 1999, T. Borgen (TB99.109, C-F-119755), 40 m, with *Dryas* sp. and *Salix* sp. in scrubland. Zackenberg, just S of the Field Station, 74.48°N, 20.76°W, 19 Jul 1999, T. Borgen (TB99.008, C-F-119804), 30 m, with *Dryas* sp. and *Bistorta vivipara*. **E-Greenland:** Jameson Land, Nerlerit Inaat/Constable Pynt, delta of Gåseelv valley, 70.76°N, 22.65°W, 8 Aug 2017, T. Borgen (TB17C.073, C-F-106778), 40 m, in heathland. Jameson Land, Nerlerit Inaat/Constable Pynt, Hareelv, 70.71°N, 22.69°W, 10 Aug 2017, S.A. Elborne (SAE-2017.194-GR, C-F-106767), 100 m, with *Salix arctica* in tundra. Jameson Land, Nerlerit Inaat/Constable Pynt, Primulaelv, 70.74°N, 22.67°W, 1 Aug 2017, H. Knudsen (HK17.022B, C-F-104911), 180 m. Jameson Land, Nerlerit Inaat/Constable Pynt, Primulaelv, 70.74°N, 22.67°W, 1 Aug 2017, H. Knudsen (HK17.021, C-F-104909), 180 m. Jameson Land, Nerlerit Inaat/Constable Pynt, Primulaelv, 70.74°N, 22.67°W, 1 Aug 2017, H. Knudsen (HK17.022A, C-F-104910), 180 m.

Distribution. Widely distributed in Greenland and apparently common in the localities where it was found; missing in western Greenland. It is widely distributed in the Temperate zone in Europe (Beker et al. 2016) with a few records in subarctic areas in Sweden (Härjedalen) and the Oroboreal zone in Iceland (Egilsstadir, 65°N). The Greenland collections from Zackenberg (74.5°N) are the northernmost recorded, to date. *Hebeloma vaccinum* was recently recorded from the alpine Rocky Mountains (Cripps et al. 2019), but these Greenland records are the first from arctic North America.

Habitat and ecology. Thirteen collections, all from calcareous or mineral rich areas. Hosts are *Dryas*, *Salix glauca* and *S. arctica*. Beker et al. (2016) concluded that the Salicaceae (*Salix* and *Populus*) are the host family for this species, with *S. repens* L. as the most often recorded host in Europe, but also *S. lanata* L.

***Hebeloma* subsect. *Hiemalia Quadr.*; Doc. mycol. 14: 30, 1985 ("1984").**

Cheilocystidia distinctly broadened at apex, base ± swollen, wall often thickened at the middle. Spores with a majority that are weakly ornamented (O2) and the perispore which is not consistently or distinctly loosening (rarely P2 and never P3) and the pileus color which always has brown or buff tones at least in the center.

***Hebeloma hiemale* Bres.; Fung. trident. 2(11–13): 52, 1892.**
Fig. 31

Macroscopic description. Cap 1.1–8.0 cm in diameter, convex to umbonate, often broadly, margin smooth, sometimes involute, undulate in older specimens, tacky when moist, occasionally spotted, rarely hygrophanous, almost uniformly

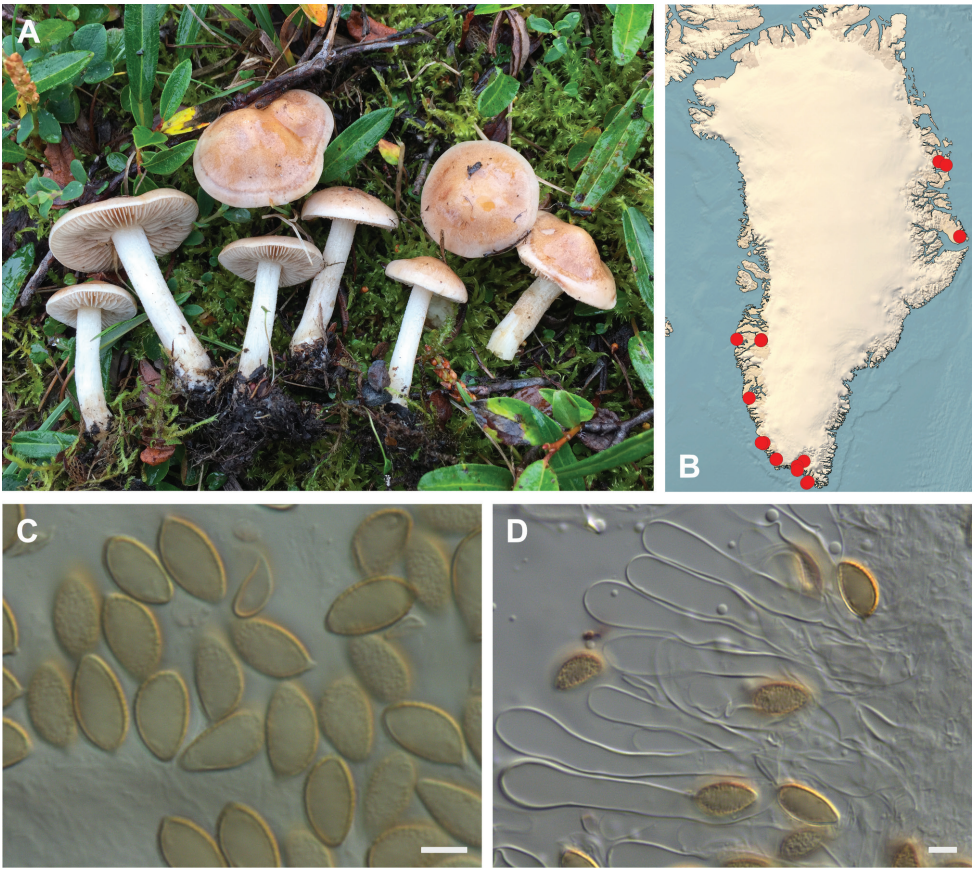

Figure 31. *Hebeloma hiemale* **A** SAE-2018.225, photograph S.A. Elborne **B** distribution of cited collections **C** spores ×1600 and **D** cheilocystidia ×1000 of SAE-2018.225 in Melzer's reagent. Scale bars: 5 µm; microphotographs H.J. Beker.

colored or variably bicolored, at center warm buff to grayish buff or dark pinkish buff through honey or ochraceous and dark olive buff to umber and clay pink or orange brown, at margin pale cream to cream to honey or pale pinkish buff, without any traces of veil. Lamellae when young very pale but becoming darker with maturity, emarginate to adnate, maximum depth 3–7 mm, number of lamellae {L} 35–71, droplets usually visible with naked eye or × 10 lens, occasionally absent, white fimbriate edge present. Stem (1.3–)1.5–10.75(–12) × (0.3–)0.35–1.2 {median} × (0.3–)0.55–1.4(–1.5) {base} cm, stem Q 2.5–17.2(–17.4), whitish to pale brownish at middle, hardly discoloring, gradually sordid brown in the mid portion, cylindrical to clavate, rarely subbulbous, usually pruinose particularly at apex, rarely with mycelial chords. Context firm, stem interior stuffed, becoming hollow with age and often with a superior wick, flesh often discoloring from base, particularly after handling. Smell raphanoid, sometimes with hints of cocoa, rarely absent. Taste mild to weakly bitter. Spore color dark olive buff or grayish brown through brownish olive to umber.

Microscopic description. Spores amygdaloid, limoniform, variably papillate, on ave. 10.0–12.5 × 5.0–7.5 µm, ave. Q = 1.6–2.1, yellow to yellow brown, usually guttulate, weakly, occasionally distinctly ornamented ((O1) O2 (O3)), perispore not or somewhat loosening (P0 P1 (P2)), indistinctly to weakly dextrinoid ((D0) D1 D2). Basidia 23–39(-43) × 7–10 µm, ave. Q = 3.2–4.3, mostly four-spored, often stipitate. Cheilocystidia usually clavate-lageniform, but occasionally slenderly clavate, clavate-stipitate, cylindrical or ventricose, rarely spathulate-lageniform or tapering, occasionally characteristically with apical or median wall thickening, sometimes geniculate or septate, rarely sinuate or rostrate, on ave. 40–65 × 5.5–9 (apex) × 3.5–5 (middle) × 4.5–7.5 (base) µm, ratios A/M = 1.46–2.48, A/B = 0.97–1.8, B/M = 1.26–1.77. Epicutis an ixocutis, 60–200 µm thick (measured from exsiccata), maximum hyphae width 4–6 µm, sometimes encrusted, trama elements beneath subcutis cylindrical, ellipsoidal, sausage-shaped up to 17 µm wide. Caulocystidia similar to cheilocystidia, up to 75 µm long, often septate, septa sometimes clamped, many cylindrical.

Collections examined. S-Greenland, Kangilinnguit, 61.21°N, 48.12°W, 20 Aug 2018, H. Knudsen (HK18.269, C-F-111112), 125 m, in tundra. Kangilinnguit, Arsuk Fjord, 61.23°N, 48.07°W, 19 Aug 2018, S.A. Elborne (SAE-2018.225-GR, C-F-112771), 100 m, with *Salix glauca* and *Bistorta vivipara* in heathland. Kangilinnguit, at Grønnedal Hut, 61.23°N, 48.08°W, 15 Aug 1985, T. Borgen (TB85.182, C-F-103466), 400 m, with *Salix herbacea* and *Harrimanella hypnoides* in snowbed. Nanortalik, 60.08°N, 45.14°W, 12 Aug 1991, T. Borgen (TB91.136, C-F-103465), 50 m, with *Salix* sp. Nanortalik municipality, Qinngua valley, 60.14°N, 45°W, 9 Aug 1991, T. Borgen (TB91.112, C-F-119782), 230 m, with *Salix glauca* in scrubland. Narsaq, 60.91°N, 46.05°W, 13 Aug 1993, E. Rald (ER 93.330, C-F-104550), 20 m, with *Salix glauca* and *Betula glandulosa* in heathland. Narsaq, 60.91°N, 46.05°W, 3 Aug 1993, E. Rald (ER 93.152, C-F-104318), 20 m. Narsarsuaq, Hospitalsdalen, 61.1715°N, 45.41°W, 10 Aug 1984, T. Læssøe (TL 84.608, C-F-119794), 60 m. Paamiut, 62.01°N, 49.4°W, 8 Aug 1981, T. Borgen (TB81.112, C-F-103552), 10 m, with *Salix glauca*. Paamiut, 62.01°N, 49.4°W, 27 Aug 1993, T. Borgen (TB93.159, C-F-103496), 20 m, with *Salix herbacea*. Paamiut, 62.01°N, 49.4°W, 31 Aug 1995, T. Borgen (TB95.114, C-F-103504), 30 m, with *Salix glauca*, *Betula glandulosa* in heathland. Paamiut, 62.01°N, 49.4°W, 6 Sep 1990, T. Borgen (TB90.087, C-F-103540), 10 m, with *Salix glauca*. Paamiut, 62.01°N, 49.4°W, 6 Sep 1990, T. Borgen (TB90.084a, C-F-103549), 10 m, with *Salix glauca*. Paamiut, 62.01°N, 49.4°W, 8 Sep 1990, T. Borgen (TB90.104a, C-F-103550), 10 m, with *Salix glauca* and *Salix herbacea*. Paamiut, 61.99°N, 49.66°W, 22 Aug 2008, T. Borgen (TB08.157, C-F-106752), 15 m, with *Salix glauca* and *Bistorta vivipara*. Paamiut, 62.01°N, 49.4°W, 31 Aug 1993, T. Borgen (TB93.183, C-F-103497), 50 m, with *Salix glauca* in heathland. Paamiut, 62.01°N, 49.4°W, 8 Sep 1993, T. Borgen (TB93.210, C-F-103499), 10 m. Paamiut, 62.01°N, 49.4°W, 1 Sep 1993, T. Borgen (TB93.187, C-F-103498), 10 m, with *Salix herbacea*. Paamiut, 62.01°N, 49.4°W, 28 Aug 1993, T. Borgen (TB93.155, C-F-103500), 10 m, with *Salix herbacea* in snowbed. Paamiut, Kangilineq /Kvaneøen, 61.95°N, 49.47°W, 25 Aug 1985, T. Borgen (TB85.250, C-F-119786), 20 m, with *Salix arctophila* in

fenland. Paamiut, Navigation School area, 62.01°N, 49.4°W, 13 Aug 1990, T. Borgen (TB90.032, C-F-103543), 10 m, with *Salix herbacea* in snowbed. Paamiut, Navigation School area, 62.01°N, 49.4°W, 13 Aug 1990, T. Borgen (TB90.019, C-F-103544), 10 m, with *Salix herbacea* and *Bistorta vivipara*. Paamiut, Taartoq/Mørke Fiord, 61.99°N, 49.66°W, 29 Aug 1998, T. Borgen (TB98.201, C-F-104292), 25 m, with *Salix glauca*. Qaqortoq, 60.72°N, 46.04°W, 13 Aug 1993, E. Rald (ER 93.302, C-F-104551), 30 m, with *Salix glauca*. **W-Greenland:** Kangerlussuaq, 67.01°N, 50.72°W, 11 Aug 1986, T. Borgen (TB86.203, C-F-103568), 50 m. Kangerlussuaq, near a glacier, 67.03°N, 50.64°W, 12 Aug 2000, E. Ohenoja (EO12.8.00.1, OULU F050224), 229 m. Kangerlussuaq, c. 2 km W of the Airport, Mt. Hassel, 67.012°N, 50.856°W, 10 Aug 2000, A-M. Larsen, T. Borgen (TB00.069, C-F-103515), 50 m, with *Salix glauca* in copse. Kangerluarsunnguaq, Kobbefjord, end of fiord, 64.14°N, 51.35°W, 26 Aug 2018, S.A. Elborne (SAE-2018.357-GR, C-F-112904), 100 m, with *Salix glauca* in copse. NW below Nasaasaaq, E-valley, E of Sisimiut, 66.93°N, 53.61°W, 18 Aug 2000, E. Horak (ZT8901, ZT8901), 50 m, with *Salix glauca*. **N-Greenland:** Daneborg, 0.5 km E of Airstrip, 74.2°N, 20.1°W, 29 Jul 2006, T. Borgen (TB06.033, C-F-119770), 20 m, with *Dryas* in heathland. Daneborg, slope NW of The Weather Station, 74.2°N, 20.1°W, 31 Jul 2006, T. Borgen (TB06.061, C-F-119769), 20 m, with *Dryas* sp. in heathland. Zackenberg, 74.5°N, 21°W, 3 Aug 2006, T. Borgen (TB06.081, C-F-119777), 50 m, with *Dryas integrifolia* and *Dryas octopetala* in scrubland. Zackenberg, 74.5°N, 21°W, 7 Aug 2006, T. Borgen (TB06.120, C-F-119765), 50 m, with *Dryas* in heathland. Zackenberg, 74.5°N, 21°W, 2 Aug 2006, T. Borgen (TB06.067, C-F-119743), 50 m, with *Dryas* sp. and *Salix arctica* in scrubland. Zackenberg, Aucellabjerg, 74.5°N, 21°W, 27 Jul 1999, T. Borgen (TB99.118, C-F-119756), 150 m, with *Dryas* sp. and *Salix arctica* in scrubland. Zackenberg, Aucellabjerg, 74.5°N, 21°W, 20 Aug 2006, T. Borgen (TB06.250, C-F-119764), 400 m, with *Dryas* sp., *Bistorta vivipara* and grassland. Zackenberg, Aucellabjerg, 74.5°N, 21°W, 9 Aug 2006, T. Borgen (TB06.128, C-F-119767), 300 m, with *Dryas* sp. in heathland. Zackenberg, Aucellabjerg, 74.5°N, 21°W, 11 Aug 1999, T. Borgen (TB99.280, C-F-119802), 150 m, tundra. Zackenberg, between West River and Solkæret, 74.5°N, 21°W, 9 Aug 1999, T. Borgen (TB99.258, C-F-119745), 30 m, with *Dryas* sp. and *Salix arctica* in scrubland. Zackenberg, just W of Kærelv, 74.5°N, 21°W, 30 Jul 1999, T. Borgen (TB99.160, C-F-119809), 30 m, with *Salix arctica* and *Bistorta vivipara* in solifluction lobe in snowbed. Zackenberg, shortly E of Kærelv, 74.5°N, 21°W, 13 Aug 1999, T. Borgen (TB99.304, C-F-119803), 50 m, with *Dryas* sp. in heathland. Zackenberg, Ulvehøj, 74.5°N, 21°W, 29 Jul 1999, T. Borgen (TB99.146, C-F-104296), 40 m, with *Salix arctica* in scrubland. **E-Greenland:** Jameson Land, Nerlerit Inaat/Constable Pynt, delta of Gåseelv valley, 70.76°N, 22.65°W, 8 Aug 2017, T. Borgen (TB17C.078, C-F-106777), 40 m, with *Salix glauca* in copse. Jameson Land, Nerlerit Inaat/Constable Pynt, Primulaelv, 70.74°N, 22.67°W, 7 Aug 2017, T. Borgen (TB17C.072, C-F-106776), 180 m, with *Bistorta vivipara* in heathland.

Distribution. One of the five most commonly recorded *Hebeloma* species in Greenland, with 11.6% of the records. Common and widespread in Europe; also

recorded from other parts of North America (https://mycoportal.org/portal/collections/list.php, accessed 2 Dec 2020). To our knowledge not recorded from alpine sites in Europe (Beker et al. 2016).

Habitat and ecology. Forty-four collections, mainly with *Salix glauca* (15), *Dryas* (10) and *S. herbacea* (6). Minor hosts are *S. arctophila* and *S. arctica*, and two collections were difficult to separate from the roots of *Bistorta vivipara*. Found in all types of habitats from scrubland, grassland and heathland to snowbeds. In the Rocky Mountains, the hosts are *S. arctica*, *S. glauca*, *S. planifolia*, *S. reticulata*, *Betula nana* and *Dryas* (Cripps et al. 2019). For lowland Europe, there is a long list of deciduous trees as probable hosts (Beker et al. 2016).

Hebeloma sect. *Velutipes* Vesterh.; Ann. Micol. A. G. M. T. 1: 60, 2004.

Stem velute, usually pruinose at least at apex, bulbous. Cheilocystidia gently clavate towards the apex, occasionally ventricose, spores rather strongly to very strongly dextrinoid.

Hebeloma leucosarx P.D. Orton; Trans. Br. mycol. Soc. 43(2): 244, 1960.

Fig. 32

Macroscopic description. Cap 1.8–9.0 cm in diameter, convex, later umbonate, sometimes turned upwards with age, margin often involute when young, later smooth or eroded or wavy, tacky when moist, rarely spotted, sometimes hygrophanous, usually bicolored, often with thin margin but may be unicolored when young, at center dark pinkish buff to ochraceous or dark olive buff or yellowish brown to clay buff or cinnamon to umber or brick, at margin cream to honey or pinkish buff to ochraceous or dark olive buff or clay-pink, without any remains of veil. Lamellae light gray brown to vinaceous buff, adnate to emarginate, maximum depth 2.5–9 mm, number of lamellae {L} 50–70, droplets usually visible but sometimes absent, white fimbriate edge present. Stem (3.0–)3.7–11.0 × 0.3–1.4 {median} × 0.8–2.0 {base} cm, stem Q (6–)6.8–14(–17.5), whitish, often clavate to bulbous, sometimes cylindrical, pruinose to floccose, particularly at apex, sometimes more velutinate, sometimes with mycelial chords. Context firm, stem interior hollow, sometimes with superior wick, flesh discoloring from base. Smell raphanoid, sometimes with hint of cacao. Taste raphanoid, sometimes weakly bitter. Spore deposit brownish olive to umber.

Microscopic description. Spores amygdaloid, occasionally limoniform, not or weakly papillate, on ave. 9.5–12.0 × 5.5–7.0 µm, ave. Q = 1.6–2.0 yellow brown to brown, guttulate, almost smooth to weakly ornamented but occasionally distinctly ornamented (O1 O2 O3), perispore not or somewhat loosening (P0 P1), weakly to strongly dextrinoid, reaction often very slow (D2 D3 (D4)). Basidia 24–33(–35) × 7–8(–10) µm, ave. Q = 3–4.1, mostly four-spored. Cheilocystidia slenderly clavate, occasionally clavate-stipitate or ventricose, occasionally with characteristic apical wall thickening, occasionally bifurcate, geniculate or septate, on ave. 41–67 × 6.5–8.5

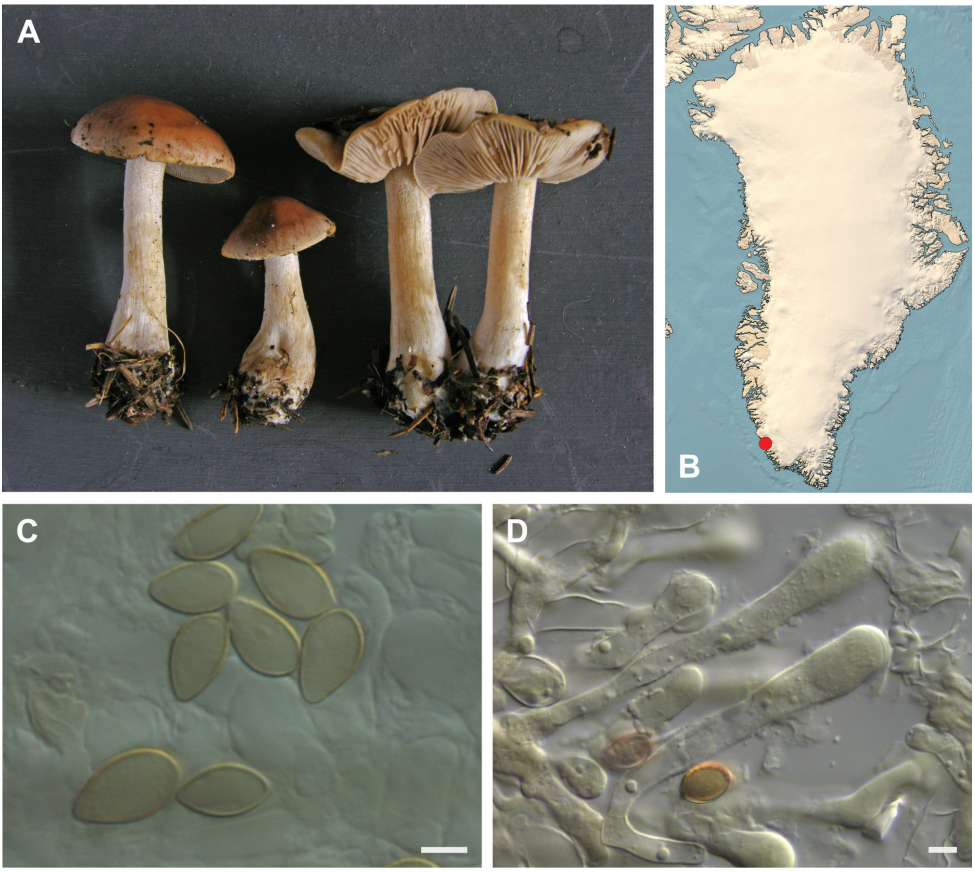

Figure 32. *Hebeloma leucosarx* **A** JV06-757 (from Denmark), photo J. Vesterholt, reproduced by kind permission from Beker et al. (2016) **B** distribution of cited collections **C** spores ×1600 and **D** cheilocystidia ×1000 of TB81.211 in Melzer's reagent. Scale bars: 5 µm; microphotographs H.J. Beker.

(apex) × 4–5.5 (middle) × 4.5–6.5 (base) µm, ratios A/M = 1.42–1.72, A/B = 1.15–1.68, B/M = 0 .94–1.33. Epicutis an ixocutis, 80–200 thick (measured from exsiccata), maximum hyphae width 5 µm, sometimes encrusted, trama elements beneath subcutis ellipsoid to sausage-shaped, occasionally polygonal up to 20 µm wide. Caulocystidia similar to cheilocystidia, up to 200 µm long, often septate and markedly lageniform.

Collections examined. S-Greenland: Paamiut, head of Eqaluit, median part, 62.03°N, 49.25°W, 15 Aug 1998, T. Borgen (TB98.119, C-F-103513), 300 m, with *Betula glandulosa* and *Salix glauca* in heathland. Paamiut, Taartoq/Mørke Fiord, 62.01°N, 49.26°W, 29 Aug 1981, T. Borgen (TB81.211, C-F-103551), ca. 100 m, with *Betula glandulosa* in heathland.

Distribution. Only two records, both from the same area. The general distribution of the species is temperate, to the middle boreal zone. The Greenland records are both from low arctic areas. *Hebeloma leucosarx* is missing from lowland regions of southern Europe (Beker et al. 2016; Grilli et al. 2020).

Habitat and ecology. Among the 28 species of *Hebeloma* found in Greenland, *H. leucosarx* is the only species that may primarily be associating with *Betula* rather than *Salix*, based on the observations of Beker et al. (2016) from Europe. According to their monograph, in Europe, the main hosts are conifers and *Betula* (Beker et al. 2016); for the above records, the host is most likely *B. glandulosa*, although in one record *S. glauca* is mentioned as present.

***Hebeloma subconcolor* Bruchet; Bull. mens. Soc. linn. Lyon 39 (6 (Suppl.)): 127, 1970.**

Fig. 33

Macroscopic description. Cap 0.8–2.1 cm, convex to umbonate, sometimes broadly, margin smooth, sometimes involute, tacky when moist, usually almost unicolored, at center clay buff to gray brown to dark olive buff to sepia, sometimes pruinose particularly when young, margin sometimes paler, even cream, veil absent. Lamellae when young whitish, later distinctly gray, adnate to emarginate, 3–4 mm broad, number of lamellae {L} 20–32, droplets usually visible with naked eye, but occasionally only with × 10 lens or absent, edge white fimbriate. Stem 1.5–4.5 × 0.3–0.6 cm, {median} × 0.35–0.75 {base} mm, velute, usually pruinose at apex, cylindrical, base clavate or sometimes bulbous. Context firm, in stem stuffed, later hollow, discoloring brownish from base. Smell raphanoid, sometimes strongly. Taste bitter, raphanoid. Spore deposit clay buff.

Microscopic description. Spores amygdaloid, limoniform, sometimes weakly papillate, on ave. 10.5–12.5 × 6.5–7.0 µm, ave. Q 1.6–1.85, usually guttulate, pale, yellow brown to brown, almost smooth to very weakly ornamented (O1 O2), perispore not or somewhat loosening (P0 P1), weakly to rather strongly dextrinoid (D2 D3). Basidia 26–33(–36) × 8–9 µm, Q = 3.4–3.9, mostly four-spored. Cheilocystidia slenderly clavate, sometimes cylindrical, clavate-lageniform or ventricose, occasionally with a characteristic apical wall thickening, occasionally bifurcate, geniculate or septate, on ave. 47–69 × 6.5–9 (apex) × 5–6.5 (middle) × 5–7.5 (base) µm, ratios A/M = 1.36–1.71, A/B = 1.22–1.86, B/M = 0 .92–1.26. Epicutis an ixocutis, 60–75 µm (measured from dried specimens), maximum hyphae width 5.5–6 µm, sometimes encrusted, shape of trama elements beneath subcutis ellipsoid, isodiametric, sausage-shaped up to 20 µm wide. Caulocystidia similar to cheilocystidia, up to 120 µm long and 11 µm wide, multi-septate.

Collections examined. S-Greenland: Kangilinnguit-Ivittuut, 61.21°N, 48.12°W, 18 Aug 2018, H. Knudsen (HK18.232, C-F-111111), 125 m, in tundra. Narsarsuaq, 61.17°N, 45.40°W, 17 Aug 2015, H. Knudsen (HK15.089, C-F-8242), 60 m, with *Salix glauca*. Nuuk, Qooqqut, 64.26°N, 50.92°W, 15 Aug 1987, T. Borgen (TB87.117, C-F-4002), ca. 30 m, with *Salix glauca* in ditch. Paamiut, 61.99°N, 49.66°W, 4 Aug 1993, E. Rald (ER 93.168, C-F-104313), 25 m. Paamiut, 62.01°N, 49.4°W, 14 Aug 1990, T. Borgen (TB90.033, C-F-104299), 25 m. Paamiut, N of the Navigation School area, 62.02°N,

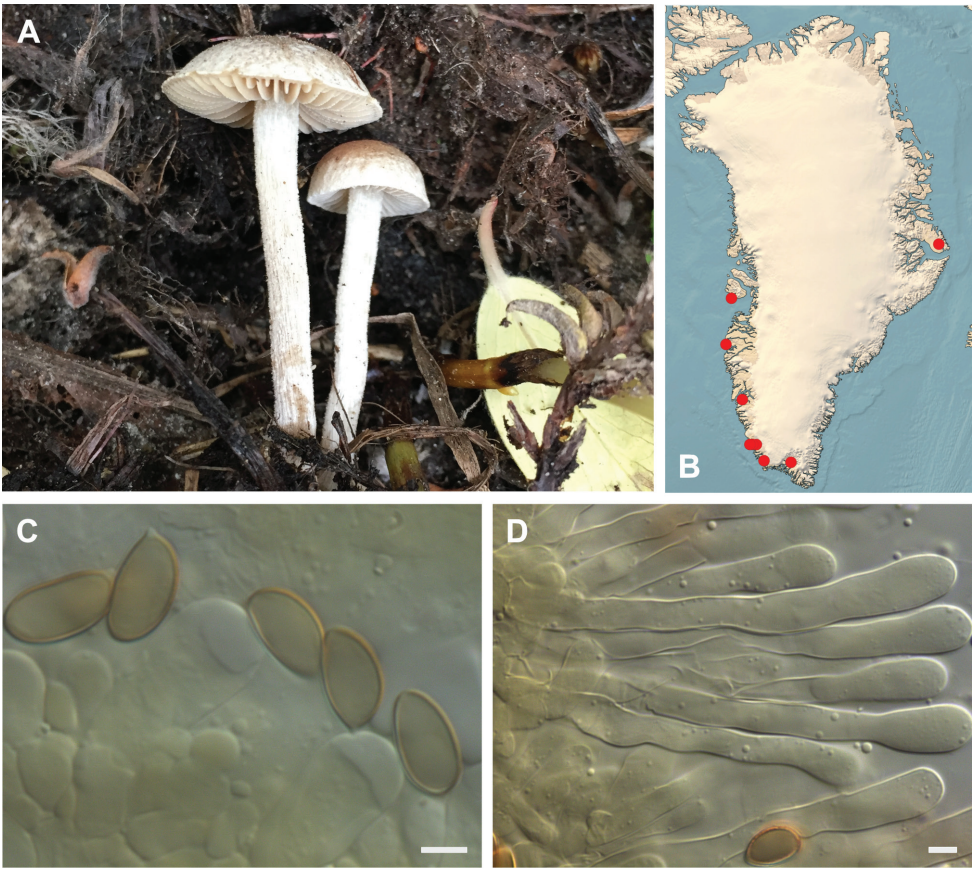

Figure 33. *Hebeloma subconcolor* **A** SAE-2016.090, photograph S.A. Elborne **B** distribution of cited collections **C** spores ×1600 and **D** cheilocystidia ×1000 of SAE-2016.090 in Melzer's reagent. Scale bars: 5 µm; microphotographs H.J. Beker.

49°W, 3 Aug 1990, T. Borgen (TB90.018, C-F-119761), ca. 40 m, with *Bistorta vivipara* and *Salix herbacea*. **W-Greenland:** Disko, Fortune Bay, 69.31°N, 53.88°W, 3 Aug 1986, T. Borgen (TB86.122, C-F-103587), 20 m. Sisimiut, south of town, 66.95°N, 53.66°W, 18 Aug 2016, S.A. Elborne (SAE-2016.090-GR, C-F-106739), 20 m, with *Salix glauca* in copse. **E-Greenland:** Jameson Land, Constable Pynt, Ugleelv, 70.88°N, 22.85°W, 24 Jul 1989, H. Knudsen (HK89.302, C-F-2195), 100 m.

Distribution. *Hebeloma subconcolor* is a truly arctic-alpine species with nine records from low and high arctic areas in Greenland. It was recently reported from two collections from alpine North America (Colorado, Cripps et al. 2019), but the records here are the first from arctic North America. Described from the European Alps by Bruchet 50 years ago, it is still only known from few other locations and it must be considered a rather rare species.

Habitat and ecology. Nine collections of *H. subconcolor* are verified, but only sparse info is given on hosts and ecology. *Salix glauca*, *S. herbacea* and *Bistorta vivipara*

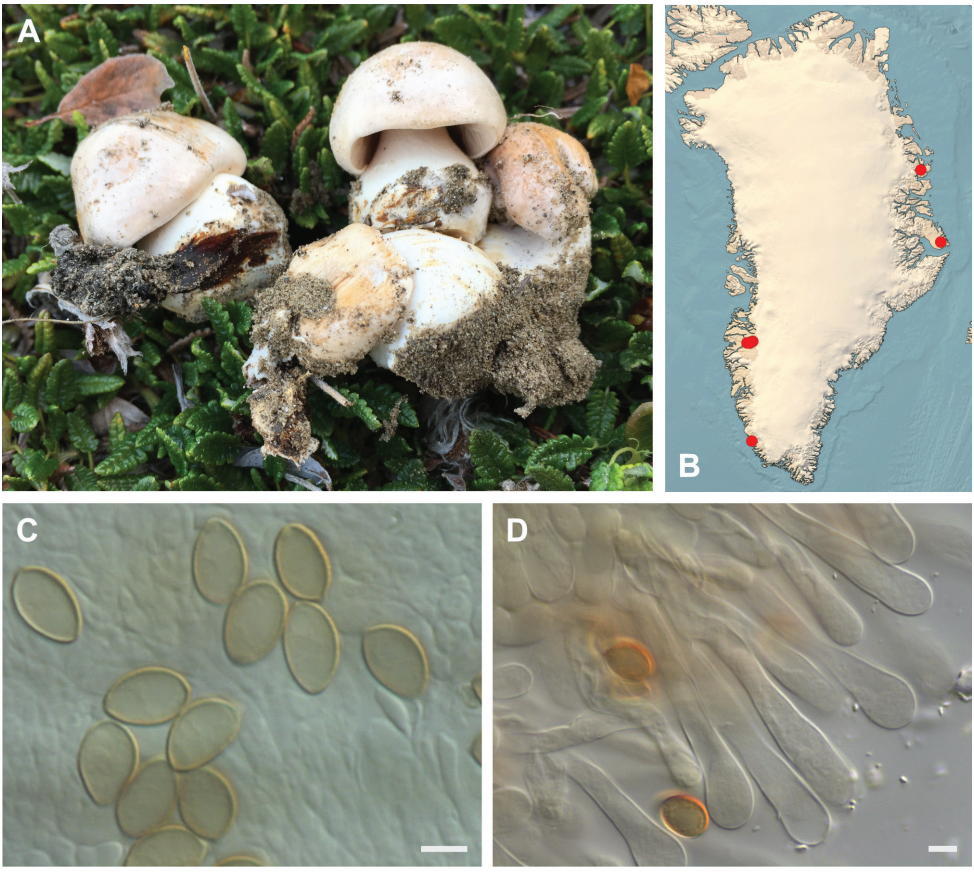

Figure 34. *Hebeloma velutipes* **A** SAE-2017.110, photograph S.A. Elborne **B** distribution of cited collections **C** spores ×1600 and **D** cheilocystidia ×1000 of SAE-2017.110 in Melzer's reagent. Scale bars: 5 µm; microphotographs H.J. Beker.

are mentioned as possible hosts. Most localities are on acid soil in agreement with the conclusion of Beker et al. (2016), who, in Europe, had *S. herbacea* listed as possible host for each cited collection of the species.

Hebeloma velutipes **Bruchet; Bull. Mens. Soc. Linn. Lyon 39(6(Suppl.)): 127, 1970.**
Fig. 34

Macroscopic description. Cap 1.6–8.2 cm in diameter, convex to umbonate, margin often involute when young, sometimes crenulate, occasionally upturned and wavy with age, tacky when moist, occasionally spotted, not hygrophanous, unicolored or variably bicolored, at center whitish to cream or buff to ochraceous or more rarely dark olive buff or yellowish brown or brownish olive, at margin white to cream or buff, without remains of veil. Lamellae clay brown, adnate to emarginate, occasionally with decurrent

tooth, maximum depth 2–9 mm, number of lamellae {L} 50–78, droplets visible, occasionally only visible with × 10 lens, rarely absent, white fimbriate edge present, sometimes very distinct. Stem 0.5–10.4 × 0.3–1.6 {median} × 0.4–2.7 {base} cm, stem Q (0.6–)2.5–12.1(–14.4), whitish, base usually clavate to bulbous, sometimes cylindrical, usually velutinate, often pruinose or floccose at least on the upper half. Context firm, stem interior stuffed, later hollow, often with superior wick, occasionally with basal wick, flesh generally not discoloring from base. Smell usually raphanoid, sometimes earthy. Taste usually bitter and raphanoid. Spore deposit brownish olive to umber.

Microscopic description. Spores amygdaloid, occasionally limoniform, variably papillate, but usually at most weakly, on ave. 9–13 × 5.5–7.5 µm, Q = 1.5–1.9, yellow through yellow brown to brown, usually guttulate, almost smooth to very weakly ornamented (O1 O2 (O3)), perispore not or somewhat loosening (P0 P1), rather strongly dextrinoid ((D2) D3 (D4)). Basidia 24–38(–43) × 6–10 µm, ave. Q = (3–)3.5–4.9, mostly four-spored. Cheilocystidia slenderly clavate, some clavate-lageniform, cylindrical or ventricose, more rarely clavate-stipitate, occasionally characteristically bifurcate, geniculate or septate (sometimes clamped), on ave. 43–73 × 6.5–9 (apex) × 4–6 (middle) × 4–7 (base) µm, ratios A/M = 1.31–1.73, A/B = 1.07–1.73, B/M = 0.86–1.34. Epicutis an ixocutis, 80–200 µm thick (measured from exsiccata), maximum hyphae width 4–8 µm, sometimes encrusted, trama elements beneath subcutis cylindrical, ellipsoid, isodiametric, sausage-shaped up to 12 µm wide. Caulocystidia similar to cheilocystidia, but more irregular, up to 200 µm long.

Collections examined. S-Greenland: Paamiut, 62.01°N, 49.4°W, 19 Aug 1998, T. Borgen (TB98.158, C-F-103512), 75 m, with *Salix glauca* in tundra. **W-Greenland:** Kangerlussuaq near the Ice cap, 67.10°N, 50.23°W, 12 Aug 2000, A-M. Larsen, T. Borgen (TB00.073, C-F-103519), 220 m, with *Salix glauca* in copse. Kangerlussuaq, airport area, 67.04°N, 50.41°W, 10 Aug 1986, T. Borgen (TB86.179, C-F-103557), 30 m, with *Salix glauca* and *Betula nana*. Kangerlussuaq, Ringsødalen, Kellyville, 66.99°N, 50.95°W, 14 Aug 2000, S.A. Elborne (SAE-2000.041-GR, C-F-108492), 180 m, at lakeside. Kangerlussuaq, Sandflugtsdalen, c. 15 km E of of the airport, 67.07°N, 50.46°W, 8 Aug 2016, T. Borgen (TB16.087, C-F-103582), 200 m, with *Salix glauca* and *Sphagnum* in scrubland. Kangerlussuaq, Store Saltsø, 66.99°N, 50.59°W, 15 Aug 2000, S.A. Elborne (SAE-2000.051-GR, C-F-108502), 260 m, with *Betula nana* in heathland. **N-Greenland:** Zackenberg, Aucellabjerg, at Kærelv, 74.5°N, 21°W, 14 Aug 1999, T. Borgen (TB99.336, C-F-119749), 100 m, with *Dryas* sp. and *Salix arctica* in scrubland. Zackenberg, W of Kærelv, 74.5°N, 21°W, 13 Aug 1999, T. Borgen (TB99.309, C-F-119754), 40 m, with *Dryas* sp. in scrubland. **E-Greenland:** Jameson Land, Nerlerit Inaat/Constable Pynt, delta of Gåseelv valley, 70.76°N, 22.65°W, 9 Aug 2017, H. Knudsen (HK17.186, C-F-105090), 40 m. Jameson Land, Nerlerit Inaat/Constable Pynt, delta of Gåseelv valley, 70.76°N, 22.66°W, 6 Aug 2017, S.A. Elborne (SAE-2017.110-GR, C-F-106762), 65 m, with *Dryas* sp.

Distribution. *Hebeloma velutipes* is one of the most common *Hebeloma* species in Europe and widely distributed all over Europe (Beker et al. 2016). In Greenland, it is also widespread, but relatively uncommon. From alpine Europe it is known from the

Pyrenees, the Alps and Lower Tatra, and from arctic Europe from Svalbard and Iceland (Beker et al. 2016). Outside Europe and Greenland, it is known from alpine sites in the Rocky Mountains (Colorado, Montana, Cripps et al. 2019).

Habitat and ecology. Ten collections, all but one (Paamiut) from calcareous localities. *Salix glauca* and *Dryas* are main hosts, one record is with *Betula nana*. In the Rocky Mountains, *H. velutipes* is also recorded with *Dryas octopetala*, *Salix glauca* and *S. reticulata* (Cripps et al. 2019). In Europe numerous hosts are recorded, see Beker et al. (2016).

Hebeloma sect. *Naviculospora*

Hebeloma islandicum Beker & U. Eberh.; Beker, Eberhardt & Vesterholt, Fungi Europ. (Alassio) 14: 414, 2016.

Fig. 35

Macroscopic description. Cap 2.0–4.0 cm in diameter, convex to umbonate, margin involute when young, smooth, tacky when moist, not hygrophanous, uniformly colored or bicolored, at center dark olive buff to yellowish brown, at margin cream, innately fibrillose, sometimes with remnants of universal veil. Lamellae initially pale clay, in age often brownish, emarginate, maximum depth 5 mm, number of lamellae {L} 40–50, droplets visible with naked eye, with white fimbriate edge. Stem 1.7–2.5 × 0.4–0.6 {median} × 0.5–0.7 {base} cm, stem Q 3.4–5.5, whitish pale, finely flocculose-tomentose in the entire length with clavate base. Context firm, stem interior stuffed, later hollow, flesh usually discoloring from base. Smell raphanoid. Taste mild or slightly bitter. Spore deposit not recorded.

Microscopic description. Spores amygdaloid, often limoniform, papillate, on ave. 11.0–12.5 × 6.5–7.0 µm, ave. Q = 1.7–1.8, yellow to yellow brown, guttulate, at most weakly ornamented ((O1) O2), perispore not or somewhat loosening (P0 P1), weakly to rather strongly dextrinoid (D2 D3). Basidia 28–40 × 6–9 µm, ave. Q = 3.7–4.9, mostly four-spored. Cheilocystidia irregular, a mixture of clavate-stipitate, clavate-lageniform, ventricose and slenderly clavate, with occasional characters, geniculate, septate (sometimes clamped) or rostrate, on ave. 44–55 × 6.5–8.5 (apex) × 4–5 (middle) × 4–8 (base) µm, ratios A/M = 1.63–1.98, A/B = 1.04–1.85, B/M = 1.05–1.73. Epicutis an ixocutis, up to 120 µm thick (measured from exsiccata), maximum hyphae width 6 µm, some encrusted, trama elements beneath subcutis ellipsoid, cylindrical, thick sausage-shaped up to 20 µm wide. Caulocystidia irregular like cheilocystidia up to 140 µm long.

Collections examined. S-Greenland: Paamiut, N of town, 62.01°N, 49.4°W, 5 Sep 1986, T. Borgen (TB86.291, C-F-103573), 10 m, with *Salix herbacea* in snowbed.

Distribution. Only one record, from southern Greenland. Until recently only known from the type from the north-western, arctic part of Iceland. As discussed above, two more collections have been discovered from herbarium exsiccata at O; both, collected in Norway at above 60°N at altitudes of more than 1000 m

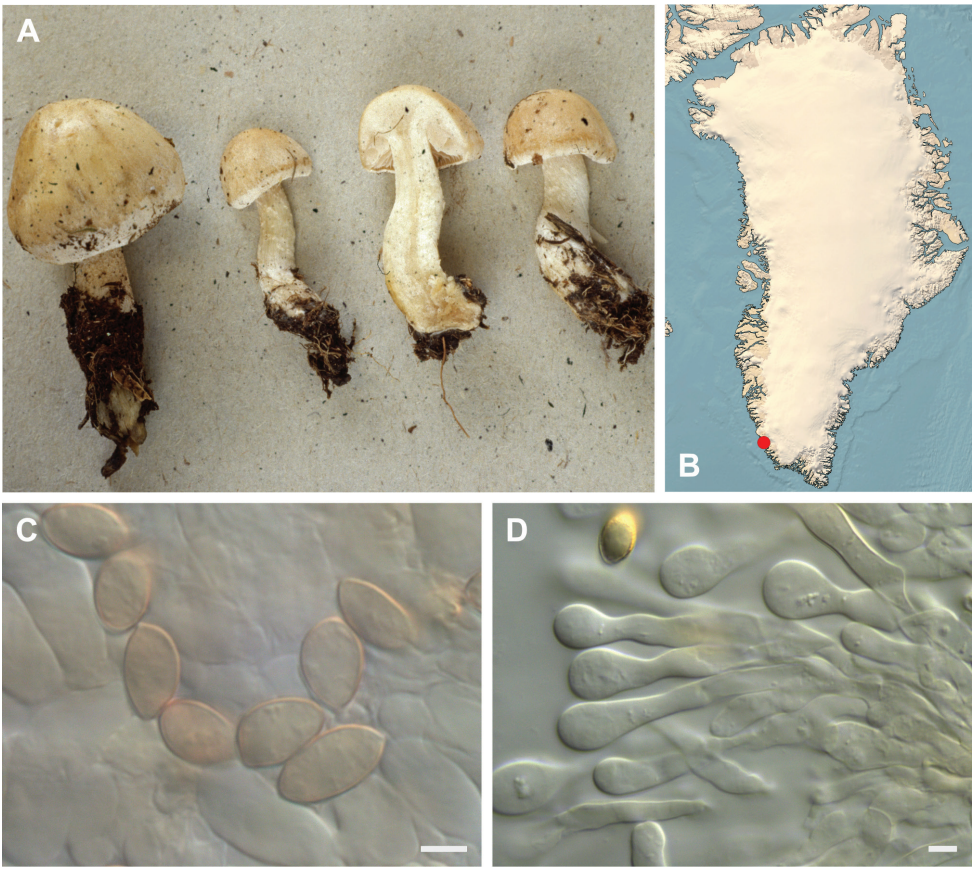

Figure 35. *Hebeloma islandicum* **A** TB19.81, photograph T. Borgen **B** distribution of cited collections; **C** spores ×1600 and **D** cheilocystidia ×1000 of TB86.291 in Melzer's reagent. Scale bars: 5 µm; microphotographs H.J. Beker.

(Eberhardt et al. in press). The above record from Greenland is from an arctic area and extends the distribution to North America. It is seemingly a very rare species. Although T.B. investigated the area around Paamiut regularly for 20 years, he only collected it once.

Habitat and ecology. All four known collections appear to have been associated with *Salix herbacea* in a wet snowbed.

Notes. *Hebeloma islandicum* was the only species recorded during the course of this study, which was not belonging to *H.* sects *Denudata*, *Hebeloma* or *Velutipes*. This species was described in Beker et al. (2016) on the basis of a single, but distinctive, collection from Iceland. The authors placed it within *H.* sect. *Naviculospora*. However, the authors acknowledged that it did not sit comfortably within any of their accepted sections. Within this section, this is the only species known to associate with *Salix*. Since its publication, two further collections have been discovered in Norway (Eberhardt et al. in press).

Molecularly, this species is unambiguous. The ITS of the collection presented here is almost identical with the ITS of the type (693/694 pos. identical, all positions are matching (one G/T in the type sequence matched by a clean G). Most similar, but always less than 98% similar, are *H. naviculosporum* and *H. nanum* (both *H.* sect. *Naviculospora*).

Discussion

This is the first monograph of *Hebeloma* in Greenland. With 381 analyzed collections (378 with ITS sequences) and 28 species, this is also the study encompassing the largest number of collections of this genus in Greenland. The sample includes one species new to science, *H. arcticum*, and collections of two species, *H. islandicum* and *H. louiseae*, that have previously been reported only from Iceland and Norway or Svalbard, respectively. Because of the inconsistencies in the application of names and interpretation of species that prevailed for a long time, we here ignore earlier works.

Much of Greenland is not easily accessible and the attention that different collection sites received is directly linked to their geographic setting, the available infrastructure and, last but not least, the biography of the main collectors. Thus, even the main collecting sites are not directly comparable: Paamiut, where T.B. lived for 20 years and Narsarsuaq, the airport which was the main access to Greenland for all collectors, were more heavily and frequently forayed than Zackenberg where T.B. collected for two seasons, and Jameson Land that was only visited in 1989 and 2017. It appears likely that this is the reason why Paamiut has the highest number of species and may be why three species (*H. clavulipes*, *H. islandicum* and *H. leucosarx*) were collected only there. While it cannot be claimed that this sample of collections is a truly random set, it is the case that the collectors did try to collect samples of every *Hebeloma* they noticed, and they did visit a number of different sites across Greenland, over some 40 years. So, it is likely to be a fairly representative sample of the sites visited at the time they were visited.

This paper follows earlier publications (Eberhardt et al. 2015a, b, 2016; Beker et al. 2016; Grilli et al. 2016; Cripps et al. 2019) in the delimitation of species. Thus, morphology (sometimes in combination with ecology) takes the lead in the delimitation of species in the absence of a clear molecular signal. This is done under the assumption that, if the species are truly distinct, then more in-depth molecular studies will reveal differences in future. If this were not the outcome, it would be much easier lumping species later than revisiting material later in order to separate taxa.

Greenland is rich in species that are difficult to delimit from one another and particularly rich with regard to members of *H.* sect. *Hebeloma*: we have not yet found a locus (or set of loci) that unambiguously separates between all species. Here, as in the species complexes around *H. alpinum* and *H. velutipes*, we do not expect the evolution to be treelike, thus network analyses are a viable option. The sequence data we have is from dikarya (earlier attempts to 'phase' dikarya failed in many cases), and intragenomic variation occurs regularly in many species. Intragenomic variation is difficult to process in networks and sequence "variants" represented by a single circle may in

fact differ by ambiguous positions or through the presences of indels. The numbers of collections roughly doubled from the datasets used by Cripps et al. (2019) that were used as starting point for these analyses. Largely, the results obtained here support the results of Cripps and co-workers and, in most cases, the intraspecific variation or the lack of interspecific variation within Greenland matches that of the sequences from other parts of the northern hemisphere.

Notable exceptions are *H. alpinicola*, which, with Greenland samples included, and the number of collections increased, appears less clearly distinct from *H. dunense* than it did in the earlier study. *Hebeloma helodes* and *H. aurantioumbrinum* are also less distinct in their ITS in Greenland than they appeared in Cripps et al. (2019).

New additions such as *H. arcticum*, *H. ingratum* and *H. louiseae* are all clearly distinct from other species. For *H. arcticum* and *H. louiseae* this is also confirmed in the tree analysis. *Hebeloma ingratum* has close relatives (*H. fragilipes* and *H. pseudofragilipes*) that are not considered here. Apparent geographical structure in some of the networks, i.e. *H. marginatulum*, *H. hiemale* or *H. velutipes*, may include information with regard to the recolonization of Greenland after the last glaciation, but numbers are too low to draw any conclusions.

Beker et al. (2016) reported 25 species of *Hebeloma* that occur in arctic-alpine habitats of Europe, including Svalbard, out of 84 species for the whole of Europe. Five of the 25 species (*H. aanenii*, *H. laterinum*, *H. pallidolabiatum*, *H. perexiguum* and *H. salicicola*) have not yet been recorded in Greenland. With regard to *H. pallidolabiatum* and *H. perexiguum*, these species are, to date, only known from Svalbard and appear to be very rare. They may be endemic to Svalbard or simply not yet discovered in other areas of the Polar Regions. Three species, *H. arcticum*, *H. colvinii*, *H. excedens*, are currently only recorded from North America, including Greenland. *Hebeloma alpinicola* is described from North America, but was recently also found in Europe (Grilli et al. 2020). Also, a further four species, included here within the arctic funga of Greenland, are known from Europe but have never yet been recorded in arctic or alpine habitats. These are: *H. clavulipes*, *H. helodes*, *H. hygrophilum* and *H. leucosarx*. This means, that we now have 33 species of *Hebeloma* that have been recorded in arctic or alpine habitats.

Species of *Hebeloma* present in arctic and alpine habitats were classified by Beker et al. (2016) as "specialists" and "opportunists". Specialists were defined as species that are widespread in such habitats, whereas opportunists are species that are more common in boreal habitats but are occasionally found in arctic and alpine habitats. Table 3 shows the classification into these two categories for the species confirmed for Greenland.

It is often impossible to remove ambiguous host information from collection metadata. Only in a few cases is a single host recorded as present. Further, if the collector is not aware of a potential host association, the person is likely not to record the presence of such hosts. A number of potential host genera and species have been named in different parts of this paper. While *Salix* appears to be the most common ectomycorrhizal host, there are cases, as noted above, when *Dryas*, rather than *Salix*, may be the symbiont; this appears to be the case, particularly in dry and calcareous localities and appears especially true for *H. alpinum* and *H. hiemale*, for which we have found *Dryas* to be the only or

the closest possible symbiont on several occasions. Less frequently, we found *Dryas* as the likely symbiont for *H. dunense*, *H. marginatulum*, *H. mesophaeum*, *H. pubescens*, *H. vaccinum*, and *H. velutipes*. A few collections were made under *Alnus alnobetulae* ssp. *crispa*, but, in every case, other possible associates were almost certainly present. Also, a number of collections were made where *Bistorta* was the most likely symbiont.

We have no reason to assume that host associations of *Hebeloma* species are fundamentally different in Greenland from other arctic or alpine areas of the world. Sequences from root samples of *B. vivipara* from Svalbard suggested an association with members of *H.* sects *Denudata* and *Hebeloma* (Brevik et al. 2010, Beker et al. 2018). While all 25 arctic or alpine species discussed in Beker et al. (2016) appeared able to associate with *Salix*, that is not clearly true for the additional species recorded from Greenland. In particular, according to Beker et al., *H. leucosarx* appears to associate most commonly with *Betula* or conifers. However, this may be an exception, and, for the most part, sections of *Hebeloma* that do not include species associating with *Salix*, are lacking from Greenland. Thus, compared to Europe, the Greenland funga does not include any species of H. sects *Duracinus*, *Myxocybe*, *Naviculospora* (other than *H. islandicum*, which does not sit comfortably within that section), *Porphyrospora*, *Pseudoamarescens*, *Scabripora*, *Sinapizantia*, *Syrjense* or *Theobromina*. The only section that includes species associating with *Salix* (Beker et al. 2016) that has not been collected in Greenland, or other arctic areas, as far as we are aware, is *H.* sect. *Sacchariolentia*.

Hebeloma species associate with all important host groups in Greenland (*Bistorta*, *Dryas* and *Salix*) and MOTUs (molecular operational taxonomic units) assigned to the genus have been retrieved consistently in metagenomics studies of arctic or alpine habitats including these hosts, often among the more often retrieved ectomycorrhizal fungi (e.g. Bjorbækmo et al. 2010; Timling et al. 2012; Mundra et al. 2015; Morgado et al. 2016 and many others). It is often not possible to assign such MOTUs to species with any degree of certainty (Eberhardt et al. 2018), but it does appear that *Hebeloma* is one of the important players in the ectomycorrhizal communities of arctic habitats.

Acknowledgements

Borgen, Elborne and Knudsen received funding from Aage V. Jensen Foundation for expeditions to Greenland in 2016, 2017 and 2018 with the purpose of taking photos of arctic basidiomycetes for a forthcoming arctic-alpine funga, for which we are very grateful. A number of Danish and foreign colleagues placed their material at our disposal for which we are also grateful (see Material and Methods). Jan Vesterholt inspired and helped us with identifications at an early state of the research. Christian Lange at the Fungarium at The Natural History Museum of Denmark helped in various matters with the handling of the material. We also thank the numerous local helpers in Constable Pynt, in the Arsuk community and at Kangilinnguit, at the Zackenberg Research Station, at Daneborg and the Greenland Institute of Natural Resources in Nuuk and their field station in Kobbefjord. All this local help and kindness is necessary and greatly appreciated when working in these areas, which are difficult to access. We

are very much obliged to A. Bogaerts and P. Ballings of the Botanic Garden Meise (BR) for help with handling various loans from a variety of herbaria. We are grateful to the reviewers and the editor for their efforts.

References

Ayling SC, Brown TA (2008) Novel methodology for construction and pruning of quasi-median networks. BMC Bioinformatics 9: e115. https://doi.org/10.1186/1471-2105-9-115

Beker HJ, Eberhardt U, Schütz N, Gulden G (2018) A review of the genus *Hebeloma* in Svalbard. Mycoscience 59: 303–309. https://doi.org/10.1016/j.myc.2017.12.001

Beker HJ, Eberhardt U, Vesterholt J (2010) *Hebeloma* hiemale Bres. in arctic/alpine habitats. North American Fungi 5: 51–65.

Beker HJ, Eberhardt U, Vesterholt J (2016) *Hebeloma* (Fr.) P. Kumm. Fungi Europaei Edizioni Tecnografica, Lomazzo, 1232 pp.

Beker HJ, Eberhardt U, Vesterholt J, Hawksworth DL (2013) Proposal to conserve the name *Hebeloma* (*Basidiomycetes*: *Agaricales*: *Strophariaceae*) with a conserved type. Taxon 62: 1058–1059. https://doi.org/10.12705/625.26

Bjorbækmo MFM, Carlsen T, Brysting A, Vrålstad T, Høiland K, Ugland KI, Geml J, Schumacher T, Kauserud H (2010) High diversity of root associated fungi in both alpine and arctic *Dryas octopetala*. BMC Plant Biology 10: e244. https://doi.org/10.1186/1471-2229-10-244

Borgen T, Elborne SA, Knudsen H (2006) A checklist of the Greenland basidiomycetes. In: Boertmann D, Knudsen H (Eds) Arctic and Alpine Mycology 6. Proceedings of the Sixth International Symposium on Arcto-Alpine Mycology (ISAM 6), Greenland, 11–21 August 2000, 37–59.

Brevik A, Moreno-Garcia J, Wenelczyk J, Blaalid R, Bronken Eidesen P, Carlsen T (2010) Diversity of fungi associated with *Bistorta vivipara* (L.) Delarbre root systems along a local chronosequence on Svalbard. Agarica 29: 15–26.

Cripps C, Eberhardt U, Schütz N, Beker HJ, Evenson VS, Horak E (2019) The genus *Hebeloma* in the Rocky Mountain alpine zone. MycoKeys 46: 1–54. https://doi.org/10.3897/mycokeys.46.32823

Eberhardt U, Beker HJ, Vila J, Vesterholt J, Llimona X, Gadjieva R (2009) *Hebeloma* species associated with *Cistus*. Mycological Research 113: 153–162. https://doi.org/10.1016/j.mycres.2008.09.007

Eberhardt U, Ronikier A, Schütz N, Beker HJ (2015a) The genus *Hebeloma* in the alpine belt of the Carpathians including two new species. Mycologia 107: 1285–1303. https://doi.org/10.3852/15-097

Eberhardt U, Beker HJ, Vesterholt J (2015b) Decrypting the *Hebeloma crustuliniforme* complex: European species of *Hebeloma* section *Denudata* subsection *Denudata*. Persoonia 35: 101–147. https://doi.org/10.3767/003158515X687704

Eberhardt U, Beker HJ, Vesterholt J, Schütz N (2016) The taxonomy of the European species of *Hebeloma* section *Denudata* subsections *Hiemalia*, *Echinospora* subsect. nov. and *Clepsydroida* subsect. nov. and five new species. Fungal Biology 120: 72–103. https://doi.org/10.1016/j.funbio.2015.09.014

Eberhardt U, Schütz N, Krause C, Beker HJ (2018) *Hebelomina* (Agaricales) revisited and abandoned. Plant Ecology and Evolution 151: 96–109. https://doi.org/10.5091/plecevo.2018.1361

Eberhardt U, Weholt Ø, Pettersen M, Schütz N, Beker HJ (in press) *Hebeloma* of Norway. Agarica.

Edler D, Klein J, Antonelli A, Silvestro D (2020 [early view]) raxmlGUI 2.0: A graphical interface and toolkit for phylogenetic analyses using RAxML. Methods in Ecology and Evolution: 1–5. https://doi.org/10.1111/2041-210X.13512

Elborne SA, Knudsen H (1990) Larger fungi associated with *Betula pubescens* in Greenland. Meddelelser om Grønland Bioscience 33: 77–88.

Feilberg J (1984) A phytogeographical study of South Greenland. vascular plants. Medelelser om Grønland 238. Bioscience 15: 1–72.

Fredskild B (1996) A phytogeographical study of the vascular plants of West Greenland. Bioscience 45: 1–157.

Gardes M, Bruns TD (1993) ITS primers with enhanced specificity for basidiomycetes – application to the identification of mycorrhizae and rusts. Molecular Ecology 2: 113–118. https://doi.org/10.1111/j.1365-294X.1993.tb00005.x

Gorbunova IA (2019) New data on agaricoid basidiomycetes of the Republic of Altai (West Siberia). Novosti Sistematiki Nizshikh Rastenii 53: 67–77. https://doi.org/10.31111/nsnr/2019.53.1.67

Grilli E, Beker HJ, Eberhardt U, Schütz N (2020) *Hebeloma* (Fr.) P. Kumm. – Supplement based on collections from Italy. Fungi Europaei 14A. Candusso Editrice, Origgio, 470 pp.

Grilli E, Beker HJ, Eberhardt U, Schütz N, Leonardi M, Vizzini A (2016) Unexpected species diversity and contrasting evolutionary hypotheses in *Hebeloma* sections *Sinapizantia* and *Velutipes* in Europe. Mycological Progress 15: 1–46. https://doi.org/10.1007/s11557-015-1148-6

Gulden G, Lange M (1971) Studies in the macromycete flora of Jotunheimen, the central mountain massif of south Norway. Norwegian Journal of Botany 18: 1–46.

Huson DH, Bryant D (2006) Application of phylogenetic networks in evolutionary studies. Molecular Biology and Evolution 23: 254–267. https://doi.org/10.1093/molbev/msj030

Karatygin IV, Nezdoiminogo EL, Novozhilov YK, Zhurbenko MP (1999) Russian Arctic Fungi. Checklist. St.-Petersburg, Russian Academy of Sciences, V.L. Komarov Botanical Institute, 212 pp.

Katoh K, Rozewicki J, Yamada KD (2019) MAFFT online service: multiple sequence alignment, interactive sequence choice and visualization. Briefings in Bioinformatics 20: 1160–1166. https://doi.org/10.1093/bib/bbx108

Kauff F, Lutzoni F (2002) Phylogeny of the Gyalectales and Ostropales (Ascomycota, Fungi): among and within order relationships based on nuclear ribosomal RNA small and large subunits. Molecular Phylogenetics and Evolution 25: 138–156. https://doi.org/10.1016/S1055-7903(02)00214-2

Kauffman CH (1918) The Agaricaceae of Michigan. Wynkoop Hallenbeck Crawford Co., Lansing, 924 pp. https://doi.org/10.5962/bhl.title.58545

Lamoure D, Lange M, Petersen PM (1982) Agaricales found in the Godhavn area, West Greenland. Nordic Journal of Botany 2: 85–90. https://doi.org/10.1111/j.1756-1051.1982.tb01438.x

Lange M (1957) Macromycetes. Part 3. 1. Greenland Agaricales (pars). Macromycetes Caeteri. 2. Ecological and plant geographical studies. Meddelelser om Grønland 148: 1–125.

Liu YL, Whelen S, Hall BD (1999) Phylogenetic relationships among ascomycetes: evidence from an RNA polymerase II subunit. Molecular Biology and Evolution 16: 1799–1808. https://doi.org/10.1093/oxfordjournals.molbev.a026092

Matheny PB (2005) Improving phylogenetic inference of mushrooms with RPB1 and RPB2 nucleotide sequences (*Inocybe*; Agaricales). Molecular Phylogenetics and Evolution 35: 1–20. https://doi.org/10.1016/j.ympev.2004.11.014

Miller OK (1998) *Hebeloma* in the arctic and alpine tundra in Alaska. In: Mukhin VA, Knudsen H (Eds) Proceedings of the Fifth International Symposion on Arcto-Alpine Mycology (Labytnangi, Russia, August 15–27, 1996). Yekaterinburg Publishers, Yekaterinburg, 86–97.

Morgado LN, Semenova TA, Welker JM, Walker MD, Smets E, Geml J (2016) Long term increase in snow depth leads to compositional changes in arctic ectomycorrhizal fungal communities. Global Change Biology 22: 3080–3096. https://doi.org/10.1111/gcb.13294

Mundra S, Bahram M, Tedersoo L, Kauserud H, Halvorsen R, Bronken Eidesen P (2015) Temporal variation of *Bistorta vivipara*-associated ectomycorrhizal fungal communities in the High Arctic. Molecular Ecology 24(24): 6289–6302. https://doi.org/10.1111/mec.13458

Nezdoiminogo EL (1994) Dark-spored agarics in Russian Arctic. Mikologiya i fitopatologiya 28: 8–15.

Ohenoja E, Ohenoja M (2010) Larger fungi of the Canadian Arctic. North American Fungi 5: 85–96.

Peck CH (1875) Report of the Botanist (1874) Annual Report on the New York State Museum of Natural History 28: 31–88.

Petersen PM (1977) Investigations on the ecology and phenology of the Macromycetes in the Arctic. Meddelelser om Grønland 199: 1–72.

Ritchie D (1946) *Hebeloma colvini*, a rare mushroom from a sandy beach. Castanea 11: 125–127. https://doi.org/10.1080/00131724609339958

Rivas-Martinez S, Penas A, Diaz TE (2004) Biogeographic maps of Europe. Cartographic Service University of León, León. [ISBN 84-9773-276-6 / Depósito Legal LE-1110/06]

Schoch CL, Seifert KA, Huhndorf S, Robert V, Spouge JL, Levesque CA, Chen W, Fungal Barcoding Consortium (2012) Nuclear ribosomal internal transcribed spacer (ITS) region as a universal DNA barcode marker for Fungi. Proceedings of the National Academy of Sciences 109: 6241–6246. https://doi.org/10.1073/pnas.1117018109

Shiryaev AG, Zmitrovich IV, Ezhov ON (2018) Taxonomic and ecological structure of basidial macromycetes biota in polar deserts of the northern hemisphere. Contemporary Problems of Ecology 11: 458–471. https://doi.org/10.1134/S1995425518050086

Smith AH, Evenson VS, Mitchel DH (1983) The Veiled Species of *Hebeloma* in the Western United States. University of Michigan Press, Ann Arbor, 219 pp. https://doi.org/10.3998/mpub.12590

Stamatakis A (2014) RAxML Version 8: a tool for phylogenetic analysis and post-analysis of large phylogenies. Bioinformatics 30: 1312–1313. https://doi.org/10.1093/bioinformatics/btu033

Stielow JB, Lévesque CA, Seifert KA, Meyer W, Irinyi L, Smits D, Renfurm R, Verkley GJM, Groenewald M, Chaduli D, Lomascolo A, Welti S, Lesage-Meessen L, Favel A, Al-Hatmi ASM, Damm U, Yilmaz N, Houbraken J, Lombard L, Quaedvlieg W, Binder M, Vaas LAI, Vu D, Yurkov A, Begerow D, Roehl O, Guerreiro M, Fonseca A, Samerpitak K, van Diepingen AD, Dolatabi S, Moreno LF, Sasaregola S, Mallet S, Jacques N, Roscini L, Egidi E, Bizet C, Garcia-Hermoso D, Martîn MP, Deng S, Groenewald JZ, Boekhout T, de Beer ZW, Barnes I, Duong TA, Wingfield MJ, de Hoog GS, Crous PW, Lewis CT, Hambleton S, Moussa TAA, Al-Zahrani OA, Louis-Seize G, Assabgui R, McCormick W, Omer G, Dukik K, Cardinali G, Eberhardt U, de Vries M, Robert V (2015) One fungus, which genes? Development and assessment of universal primers for potential secondary fungal DNA barcodes. Persoonia 35: 242–263. https://doi.org/10.3767/003158515X689135

Timling I, Taylor DL (2012) Peeking through a frosty window: molecular insights into the ecology of arctic soil fungi. Fungal Ecology 5: 419–429. https://doi.org/10.1016/j.funeco.2012.01.009

Vesterholt J (2005) The Genus *Hebeloma*. Fungi of Northern Europe 3. Svampetryk, Tilst, Denmark, 146 pp.

Vesterholt J (1989) A revision of *Hebeloma* sect. *Indusiata* in the nordic countries. Nordic Journal of Botany 9: 289–319. https://doi.org/10.1111/j.1756-1051.1989.tb01004.x

Watling R (1983) Larger cold-climate fungi. Sydowia, Annales Mycologici Serie II 36: 308–325.

Watling R (1977) Larger fungi from Greenland. Astarte 10: 61–71. https://doi.org/10.1007/BF00468015

White TJ, Bruns T, Lee S, Taylor J (1990) Amplification and direct sequencing of fungal ribosomal RNA genes for phylogenetics. In: Innis MA, Gelfand H, Sninsky JS, White TJ (Eds) A Guide to Methods and Applications. Academic Press, San Diego, 315–322. https://doi.org/10.1016/B978-0-12-372180-8.50042-1

Zmitrovich IV, Ezhov ON (2015) Agaricoid fungi (Basidiomycota, Agaricomycetes). In: Matveeva NV (Ed.) Rasteniya i griby polyarnykh pustyn' severnogo polushariya (The Plants and Fungi of Polar Deserts of Northern Hemisphere). Marafon, St. Petersburg, 211–225.

MycoKeys 79: 119–128 (2021)
doi: 10.3897/mycokeys.79.63700
https://mycokeys.pensoft.net

RESEARCH ARTICLE

A peer-reviewed open-access journal
MycoKeys
Launched to accelerate biodiversity research

First record of the rare genus *Typhrasa* (Psathyrellaceae, Agaricales) from China with description of two new species

Sheng-Nan Wang[1*], Ya-Ping Hu[2*], Jun-Liang Chen[3], Liang-Liang Qi[4], Hui Zeng[5], Hui Ding[2], Guang-Hua Huo[1], Lin-Ping Zhang[1], Fu-Sheng Chen[1], Jun-Qing Yan[1]

1 *Jiangxi Key Laboratory for Conservation and Utilization of Fungal Resource; Key Laboratory of State Forestry Administration on Forest Ecosystem Protection and Restoration of Poyang Lake Watershed, Jiangxi Agricultural University, Nanchang, Jiangxi 330045, China* **2** *Institute of Environmental Sciences, Ministry of Ecology and Environment/ State Environmental Protection Scient-ific Observation and Research Station for Ecological Environment of Wuyi Mountains 8 Jiangwangmiao Street, Nanjing 210042, China* **3** *Science and Technology Research Center of Edible Fungi, Qingyuan, Zhejiang, 323800, China* **4** *Microbiology Research Institute, Guangxi Academy of Agriculture Sciences, Nanning, 530007, China* **5** *Institute of Edible Fungi, Fujian Academy of Agricultural Sciences; National and Local Joint Engineering Research Center for Breeding & Cultivation of Features Edible Fungi, Fuzhou 350014, China*

Corresponding authors: Fu-Sheng Chen (chenfush@hotmail.com); Jun-Qing Yan (yanjunqing1990@126.com)

Academic editor: R. Henrik Nilsson | Received 28 January 2021 | Accepted 6 April 2021 | Published 23 April 2021

Citation: Wang S-N, Hu Y-P, Chen J-L, Qi L-L, Zeng H, Ding H, Huo G-H, Zhang L-P, Chen F-S, Yan J-Q (2021) First record of the rare genus *Typhrasa* (Psathyrellaceae, Agaricales) from China with description of two new species. MycoKeys 79: 119–128. https://doi.org/10.3897/mycokeys.79.63700

Abstract

Typhrasa is a rare genus that comprises two species and that has previously been reported only from Europe and North America. The present study expands the geographical scope of the genus by describing two new species – *T. polycystis* and *T. rugocephala* – from subtropical China. The new species are supported by morphological characteristics and phylogenetic analyses (ITS, LSU and *tef-1a*). The new species have very similar morphological characteristics and are 98% similar in their ITS region. However, *T. rugocephala* has two types of long gills at the same time, rarely fusiform pleurocystidia with rostrum. Detailed descriptions, colour photos, illustrations and a key to related species are presented in this paper.

Keywords

Basidiomycota, macromycetes, morphology, phylogenetic analysis, taxonomy

* These authors contributed equally to this work.

Introduction

The genus *Typhrasa* Örstadius & E. Larss. was established in 2015. It is characterised by a hygrophanous cap, crowded gills with white edge, small-to-medium-sized spores, large hymenial cystidia with intracellular oily drops or globules and a hymeniderm or paraderm pileipellis (Örstadius et al. 2015). The genus includes two species, *T. gossypina* (Bull.) Örstadius & E. Larss. and *T. nanispora* Örstadius, Hauskn. & E. Larss., the former being previously reported occasionally from some countries in Europe, North America and Asia within the genus *Psathyrella* (Fr.) Quél (Smith 1972; Kits van Waveren 1985; Knudsen and Vesterholt 2012; Örstadius et al. 2015). In addition, *Psathyrella delineata* (Peck) A.H. Sm., *P. canadensis* A.H. Sm. and *P. subtenacipes* A.H. Sm. are also reported to have oily drops in their cystidia (Smith 1972; Kits van Waveren 1985) and seems to be a candidate for *Typhrasa*. However, *P. delineata* and *P. canadensis* were combined into *T. gossypina*, based on the morphology (Örstadius et al. 2015). During investigations in subtropical China during 2018–2020, *Typhrasa* was recorded for the first time in China with two unrecorded species, which were frequently collected. Based on morphological characters and phylogenetic analyses, they are described as new species in this paper.

Materials and methods

Morphological studies

Macromorphological characters and habitat details were noted from fresh, young to mature basidiomata (over five basidiomata for each species) in the field. The location of the collection point is marked on the map (Suppl. material 1: Fig. S1). Colour codes are from the Methuen Handbook of Colour (Kornerup and Wanscher 1978). Micromorphological characters were observed with a light microscope (Olympus BX53). Sections from dry specimens were observed in water, 5% aqueous potassium hydroxide (KOH) solution, 10% aqueous ammonia ($NH_3 \cdot H_2O$) solution and Melzer's Reagent, separately. More than fifty basidiospores, cystidia and basidia in 5% aqueous KOH solution were measured under the microscope. Basidiospore measurements were recorded in front and profile view. The measurements and Q values are given as (a)b–c(d), in which "a" is the lowest value, "b–c" covers a minimum of 90% of the values and "d" is the highest value. "Q" represents the ratio of length to width of a spore (Bas 1969; Ge et al. 2017; Na and Bau 2019). Specimens are deposited in the Herbarium of Fungi, Jiangxi Agricultural University (**HFJAU**) and Herbarium of Mycology, Jilin Agricultural University (**HMJAU**).

DNA extraction and sequencing

DNA was extracted from dried specimens with the NuClean Plant Genomic DNA kit (CWBIO, China). Three regions (ITS, LSU and *Tef-1a*) were generated for the

Table 1. Sequences used in this study. Newly generated sequences are given in bold. Type material is indicated in the column Voucher.

Taxa	Voucher	Locality	ITS	LSU	*tef-1α*
Cystoagaricus hirtosquamulosus	Ramsholm800927	Finland	KC992945	KC992945	–
C. olivaceogriseus	WK 8/15/63-5 (MICH) Type	USA	KC992948	KC992948	–
C. sylvestris	LÖ191-92	Sweden	KC992949	KC992949	–
C. squarrosiceps	Laessoe44835	Ecuador	KC992950	–	–
C. strobilomyces	E. Nagasawa 9740		AY176347	AY176348	–
Kauffmania larga	LAS97-054	Sweden	DQ389695	DQ389695	–
K. larga	LÖ223-90	Sweden	DQ389694	DQ389694	KJ732824
Psathyrella delineata	CCB171	USA	KY744151		
P. delineata	TMW02	USA	MF686534		
P. delineata	MGW1406	USA	KY777378		
Typhrasa gossypina	180524-H08	Korea	MN082538	–	–
T. gossypina	BRNM:705622	Austria	AM712293	–	–
T. gossypina	BRNM:705609	Czech	AM712292	–	–
T. gossypina	WU:25069	Austria	AM712294	–	–
T. gossypina	Schumacher024	Germany	KC992946	KC992946	KJ732825
T. nanispora	Barta980706 Type	Austria	KC992947	KC992947	–
T. polycystis	HFJAU1454 Type	China:Jiangxi	**MW466538**	**MW466544**	**MW475280**
T. polycystis	HFJAU1520	China:Fujian	**MW466539**	**MW466545**	**MW475281**
T. polycystis	HFJAU1349	China:Jiangxi	**MW466540**	–	–
T. rugocephala	HFJAU1467 Type	China:Zhejiang	**MW466541**	**MW466546**	**MW475282**
T. rugocephala	HFJAU1455	China:Zhejiang	**MW466542**	**MW466547**	**MW475283**
T. rugocephala	HFJAU1476	China:Zhejiang	**MW466543**	**MW466548**	–
Outgroup					
Psathyrella oboensis	DED 8234 Type	SãoTomé	NR148107	–	–
P. pertinax	LO259-91 Neotype	Sweden	DQ389701	DQ389701	KJ732809

study, which were amplified with primers ITS1/ITS4 (White et al. 1990), LR0R/LR7 (Hopple and Vilgalys 1999) and EF983F/EF2218R (Örstadius et al. 2015), respectively. PCR was performed using a touchdown programme: 5 min at 95 °C; 1 min at 95 °C; 30 s at 65 °C (add -1 °C per cycle); 1 min at 72 °C; 15 cycles; 1 min at 95 °C; 30 s at 50 °C; 1 min at 72 °C; 20 cycles; and 10 min at 72 °C (Yan and Bau 2018). The DNA sequencing was done by Qing Ke Biotechnology Co. Ltd. (Wuhan City, China).

Data analyses

The ITS, LSU and *Tef-1a* datasets were assembled following Örstadius et al. (2015) and BLAST in GenBank. Sequences from a total of 24 taxa were analysed using five data partitions (ITS, LSU, Tef 1st, Tef 2nd and Tef 3rd). The details are presented in Table 1. Sequences were aligned separately in MAFFT v.7 (Katoh and Standley 2013). The best-fit models of nucleotide evolution for ITS, LSU, Tef 1st, Tef 2nd and Tef 3rd datasets (GTR+G, GTR+I, SYM, SYM and GTR+G, respectively) were obtained in MrModeltest v.2.3 (Nylander et al. 2008). Phylogenetic analysis was conducted using Bayesian Inference (BI) in MrBayes v.3.2.6 (Ronquist et al. 2012). Gaps were treated as missing data following Örstadius et al. (2015). Four Monte Carlo Markov

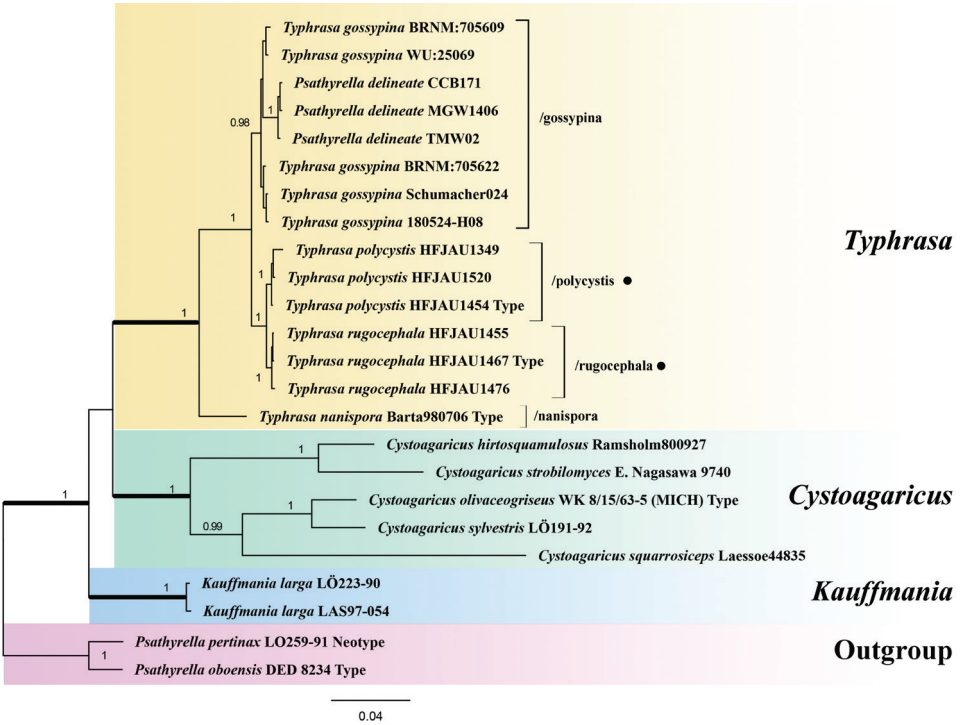

Figure 1. Phylogram generated by Bayesian Inference (BI) analysis, based on sequences of a concatenated dataset from three nuclear markers (ITS, LSU and *tef-1α*) rooted with *Psathyrella* spp. Bayesian posterior probabilities ≥ 0.95 are shown. ● indicates the newly-described species.

Chains (MCMC) were run for five million generations, sampling every 100th generation. The first 25% of trees were discarded as burn-in (Ronquist et al. 2012). The sequence alignment is deposited in TreeBASE (http://purl.org/phylo/treebase/phylows/study/TB2:S27860).

Results

Based on the BLAST results of the full length of the ITS region, two new species were found sharing less than 98.0% similarity with the known species of *Typhrasa*, respectively: 97% with *T. gossypina* and 92% with *T. nanispora*. The Bayesian analysis (Figure 1) comprised material from three major genera, all of which are identified as monophyletic with very strong support (BPP = 1), viz. *Typhrasa*, *Cystoagaricus* Singer and *Kauffmania* Örstadius & E. Larss., in agreement with the study published by Örstadius et al. (2015). Our collections of the two new *Typhrasa* species formed a joint, strongly supported clade (BPP = 1) and both new species received strong support as monophyletic (BPP ≥ 0.97). The collections of *T. gossypina* (Bull.) Örstadius & E. Larss. clustered together and appeared as a sister to the group consisting of the two new species.

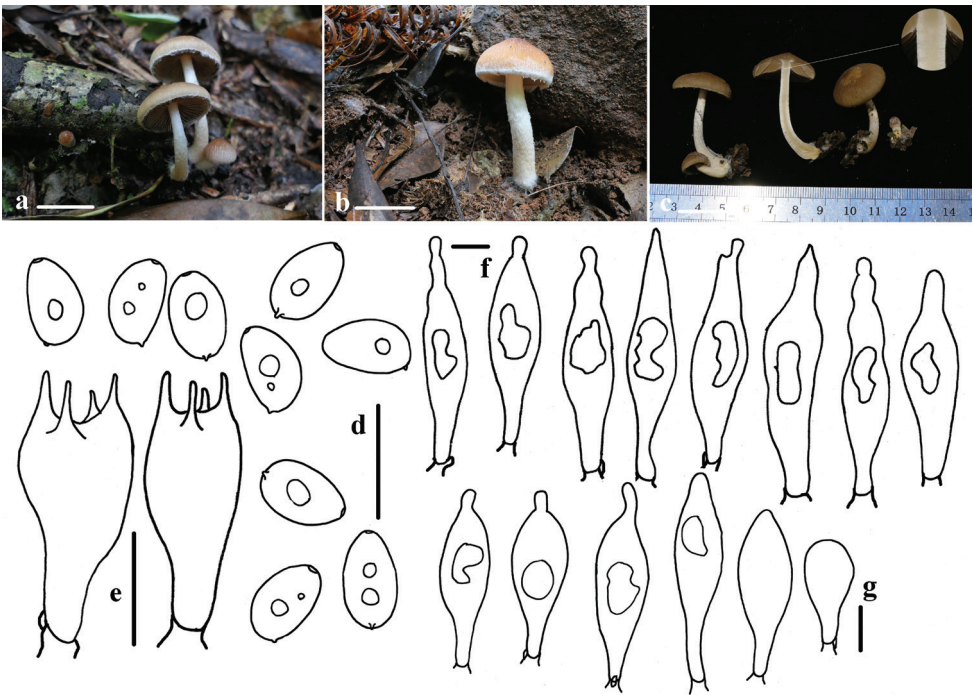

Figure 2. Basidiomata and microscopic features of *Typhrasa polycystis* **a–c** basidiomata **d** basidiospores **e** basidia **f** pleurocystidia **g** cheilocystidia. Scale bars: 20 mm (**a–c**); 10 μm (**d–g**).

Taxonomy

Typhrasa polycystis **J.Q Yan & S.N. Wang sp. nov.**
MycoBank No: 838482
Fig. 2

Diagnosis. Differs from *Typhrasa gossypina* by its smaller spores (7.1–8.2 × 4.3–5.1 μm).

Holotype. China. Jiulianshan National Nature Reserve, Jiangxi Province, 25 June 2020, Jun-Qing Yan, HFJAU1454.

Etymology. Referring to the characteristics of the pleurocystidia.

Description. Pileus 20–35 mm, extending hemispherically to expanded, plane with or without umbo, surface with slightly ridge-like folds or smooth, hygrophanous, brown (7D6–7C6), pale brown (6B6–6C6) at the margin. Veil distinct, fibrous or fluffy, white (7C1), markedly appendiculate at margin, falling off easily. Context thin and fragile, hygrophanous at pileus, about 3.0 mm at the centre. Gills 4.0–5.0 mm broad, moderately close, pale cinnamon (6C6–6D5) with a white (6C1) edge, adnexed. Stipe 30–45 mm long, 5.0–8.0 mm thick, white (6C1), hollow, pulverulent at apex, with fibrils and fluffy from pellicular veil remnants below, falling off easily.

Spores (6.9)7.1–8.2 × (4.2)4.3–5.1(5.2) µm, Q = (1.4)1.5–1.8(1.9), ellipsoid to oblong-ellipsoid, profile flattened on one side, 4.1–5.0(5.2) µm broad, smooth, reddish-brown (8C5–8C6) in water, yellow-brown (7D6–7D7) in 5% KOH or 10% $NH_3 \cdot H_2O$, becoming darker (7E4–7F4) in 5% KOH, germ pore small and indistinct, 1–2 guttulate, inamyloid. Basidia 21–24 × 7.5–8.5 µm, 4-spored, clavate, hyaline. Pleurocystidia 55–81(87) × 11–17(18) µm, variously shaped, often fusiform and lageniform, with rostrum; rarely fusiform with subacute to acute apex or cystiform with rostrum, with one or two large internal oily drops, oily drops colourless and distinct or indistinct in 5% KOH, glassy-yellow (5B6–5B7) and very distinct in Melzer's Reagent. Cheilocystidia (24)30–54(58) × (9)10–15(16) µm, similar to pleurocystidia, abundant, rarely mixed with pyriform or clavate cells. Trama of gills consisting of parallel hyphae. Pileipellis a 2–3 cells deep layer of subglobose or pyriform cells which are 24–36 µm wide. Veil composed of hyphae 6.5–14.5 µm-broad, thin-walled and fawn (5A2-A3) hyphae in 5% KOH. Clamps present in trama of gills, hyphae of stipe and at the base of the basidia and cystidia.

Ecology and distribution. Saprotrophic, solitary to slightly caespitose on rotten hard wood or humus in mixed forests.

Other specimens examined. China. Jiulianshan National Nature Reserve, Jiangxi Province, 28 May 2018, Guang-Hua Huo, Lin-Ping Zhang, HFJAU1349. Wuyishan National Nature Reserve, Fujian Province, 27.748888°N, 117.7625°E, 761 alt., 12 June 2020, Liangliang Qi, Yupeng Ge, HFJAU1520, HMJAU58461.

Typhrasa rugocephala **J.Q Yan & S.N. Wang sp. nov.**
MycoBank No: 838483
Fig. 3

Diagnosis. Differs from *Typhrasa polycystis* by having two types of long gills and rarely rostrum can be found in fusiform pleurocystidia.

Holotype. China. Baishanzu National Nature Reserve, Zhejiang Province, 27.734233°N, 119.186943°E, 1184 m alt. 28 June 2020, Sheng-Nan Wang, HFJAU1467.

Etymology. Referring to the surface of the pileus.

Description. Pileus 35–55 mm, spreading hemispherically to oblate with a slight umbo, surface with distinct ridge-like folds, hygrophanous, reddish-brown (8E5–8F6), pale brown (6D7–6C7) at the margin, drying tawny (7D6–7E6), striate, sometimes faintly, at margin. Veil distinct, fibrous or fluffy, white (7C1), markedly appendiculate at margin, falling off easily. Context thin and fragile, hygrophanous, about 2.5 mm at the centre. Gills 5.0–7.0 mm broad, moderately close; when young, dirty white (7B1), becoming cinnamon (7C6–7D5) with a white edge (7C1); two types of long gills arranged at intervals: A: adnate to slightly decurrent, B: emarginate- adnexed. Stipe 40–60 mm long, 5.0–10 mm thick, white (7C1), hollow, pulverulent at apex, with fibrils and fluffy from pellicular veil remnants below, falling off easily.

Spores (6.5)6.8–7.9(8.3) × 4.5–5.2(5.4) µm, Q = (1.3)1.4–1.7, ellipsoid to oblong-ellipsoid, profile flattened on one side, 4.1–5.0(5.2) µm broad, smooth, red-

Figure 3. Basidiomata and microscopic features of *Typhrasa rugocephala* **a–d** basidiomata **e** basidiospores **f** basidia **g** pleurocystidia **h** cheilocystidia. Scale bars: 20 mm (**a–d**); 10 μm (**e–h**).

dish-brown (8C6–8C7) in water, yellow-brown (7D6–7D7) in 5% KOH or 10% $NH_3 \cdot H_2O$, becoming darker (7E4–7E5) in 5% KOH, germ pore small and indistinct, 1–2 guttulate, inamyloid. Basidia 18–23 × 7.0–8.0 μm, 4-spored, clavate, hyaline. Pleurocystidia 42–68 × 13–17 μm, thin-walled, fusiform, apex obtuse to subacute, rarely cystiform with a short rostrum, with one or two large internal oily drops, oily drops colourless and distinct or indistinct in 5% KOH, glassy-yellow (5B6–5B7) and very distinct in Melzer's Reagent. Cheilocystidia scanty, 33–48 × 10–15 μm, similar to pleurocystidia, few and scattered, mix with pyriform or clavate, 21–39 × 11–13 μm-sized cells. Trama of gills consisting of parallel hyphae. Pileipellis a 2–3 cells deep layer of subglobose or pyriform cells which are 18–32 μm wide. Veil composed of 5.4–8.4 μm-broad hyphae, thin-walled and fawn (5A2-A3) hyphae in 5% KOH. Clamps rare, but observed in trama of gills, hyphae of stipe and at the base of the basidia and cystidia.

Ecology and distribution. Saprotrophic, solitary or gregarious on soil or humus in broad-leaved forests.

Other specimens examined. China. Baishanzu National Nature Reserve, Zhejiang Province, 24 June 2020, Ya-Ping Hu, HFJAU1476; 28 June 2020, Sheng-Nan Wang, HFJAU1455, HMJAU58462.

Discussion

Typhrasa was established by Örstadius et al. (2015), based on the main characters of having rostrate, hymenial cystidia with oily drops. Only *T. gossypina* and *T. nanispora* Örstadius, Hauskn. & E. Larss. were reported in that study. *T. gossypina*, as the type species of the genus, was, therefore, separated from *Psathyrella* (Fr.) Quél. This species can be separated from the two new species through its longer spores up to 9.0 μm long, 5.0–6.0 μm broad in front view and pleurocystidia often with a long rostrum (Kits van Waveren 1985; Örstadius et al. 2015). *T. nanispora* has smaller spores, 5.0–6.0 × 3.0–4.0 μm and can be thereby easily be distinguished (Örstadius et al. 2015). *T. rugocephala* is very easily confused with *T. polycystis*, but the former has two types of long gills arranged at intervals, scanty cheilocystidia and rarely rostrum can be found in fusiform pleurocystidia. In addition, *P. subtenacipes* are also reported to have oily drops in their cystidia (Smith 1972) and seems to be a candidate for *Typhrasa*, but study of type material is needed to settle this question. Morphologically, the spores of *P. subtenacipes* are up to 7.8–9.5 × 5.0–5.6 μm, significantly larger than the two new species (Smith et al. 1950; Smith 1972). A key to these related species is presented below:

Key to related species

1 Spores up to 9.5 μm long, 5.0–5.6 μm broad..... ***P. subtenacipes***
– Not as above **2**
2 Spores less than 6.0 μm long..... ***T. nanispora***
– Spores over 6.0 μm long **3**
3 Spores 7.0–9.0 μm long, 5.0–6.0 μm broad in front view..... ***T. gossypina***
– Spores smaller, less than 8.0 μm long and 5.0 μm broad in front view **4**
4 Long gills have two types concurrently: adnate to slightly decurrent and emarginate-adnexed, fusiform, apex obtuse to subacute, rarely cystiform with a short rostrum, cheilocystidia scanty..... ***T. rugocephala***
– Gills adnexed, pleurocystidia variously-shaped, often fusiform and lageniform with rostrum ..... ***T. polycystis***

Acknowledgements

This work is supported by the National Natural Science Foundation of China (31960008), Jiangxi Provincial Natural Science Foundation (20202BABL213041). The project was supported by the biodiversity investigation, observation and assessment programme (2019–2023) of the Ministry of Ecology and Environment of China (2110404); Central Public-Interest Scientific Institution Basal Research Fund (GYZX200203). Sincere thanks to the anonymous reviewers of the manuscript.

References

Bas C (1969) Morphology and subdivision of *Amanita* and a monograph of its section *Lepidella*. Persoonia 5(1): 96–97.

Ge Y, Yang S, Bau T (2017) *Crepidotus lutescens* sp. nov. (Inocybaceae, Agaricales), an ochraceous salmon colored species from northeast of China. Phytotaxa 297(2): 189. https://doi.org/10.11646/phytotaxa.297.2.6

Hopple JJ, Vilgalys R (1999) Phylogenetic relationships in the mushroom genus *Coprinus* and dark-spored allies based on sequence data from the nuclear gene coding for the large ribosomal subunit RNA: divergent domains, outgroups, and monophyly. Molecular Phylogenetics & Evolution 13(1): 1–19. https://doi.org/10.1006/mpev.1999.0634

Katoh K, Standley DM (2013) MAFFT multiple sequence alignment software version 7: improvements in performance and usability. Molecular Biology & Evolution 30(4): 772–780. https://doi.org/10.1093/molbev/mst010

Kits van Waveren E (1985) The Dutch, French and British species of *Psathyrella*. Persoonia 2: 1–284.

Knudsen H, Vesterholt J (2012) Funga Nordica. Agaricoid, boletoid, cyphelloid and gasteroid genera. Nordsvamp, Copenhagen.

Kornerup A, Wanscher JHK (1978) The Methuen Handbook of Colour 3rd edn. Eyre Methuen Ltd. Reprint., London.

Na Q, Bau T (2019) *Mycena* section Sacchariferae: three new species with basal discs from China. Mycological Progress 18(3): 483–493. https://doi.org/10.1007/s11557-018-1456-8

Nylander J (2004) MrModeltest 2.3. Computer program and documentation distributed by the author. Evolutionary Biology Centre, Uppsala University, Uppsala.

Örstadius L, Ryberg M, Larsson E (2015) Molecular phylogenetics and taxonomy in Psathyrellaceae (Agaricales) with focus on psathyrelloid species: introduction of three new genera and 18 new species. Mycological Progress 14(5): 1–42. https://doi.org/10.1007/s11557-015-1047-x

Ronquist F, Teslenko M, Van Der Mark P, Ayres DL, Darling A, Höhna S, Larget B, Liu L, Suchard MA, Huelsenbeck JP (2012) MrBayes 3.2: efficient Bayesian phylogenetic inference and model choice across a large model space. Systematic Biology 61(3): 539–542. https://doi.org/10.1093/sysbio/sys029

Smith A, Stuntz D (1950) New or Noteworthy Fungi from Mt. Rainier National Park. Mycologia 42(1): 80–134. https://doi.org/10.2307/3755245

Smith AH (1972) The North American species of *Psathyrella*. The New York Botanical Garden 24: 1–633.

White TJ, Bruns TD, Lee SB, Taylor JW, Innis MA, Gelfand DH, Sninsky JJ (1990) Amplification and direct sequencing of Fungal Ribosomal RNA Genes for phylogenetics. In: Innis MA, Gelfand DH, Sninsky JJ, White TJ (Eds) PCR Protocols: a guide to methods and applications. Academic Press, San Diego, 315–322. https://doi.org/10.1016/B978-0-12-372180-8.50042-1

Yan JQ, Bau T (2018) *Psathyrella alpina* sp. nov. (Psathyrellaceae, Agaricales), a new species from China. Phytotaxa 349(1): 85–91. https://doi.org/10.11646/phytotaxa.349.1.11

Supplementary material 1

Figure S1. Collection site of *Typhrasa rugocephala* and *T. polycystis*

Authors: Sheng-Nan Wang, Ya-Ping Hu, Jun-Liang Chen, Liang-Liang Qi, Hui Zeng, Hui Ding, Guang-Hua Huo, Lin-Ping Zhang, Fu-Sheng Chen, Jun-Qing Yan

Data type: image

Link: https://doi.org/10.3897/mycokeys.79.63700.suppl1

MycoKeys 79: 129–148 (2021)
doi: 10.3897/mycokeys.79.66302
https://mycokeys.pensoft.net

RESEARCH ARTICLE

A peer-reviewed open-access journal
MycoKeys
Launched to accelerate biodiversity research

A new clitocyboid genus *Spodocybe* and a new subfamily Cuphophylloideae in the family Hygrophoraceae (Agaricales)

Zheng-Mi He[1,2], Zhu L. Yang[1,2]

1 *CAS Key Laboratory for Plant Diversity and Biogeography of East Asia, Kunming Institute of Botany, Chinese Academy of Sciences, Kunming, 650201, China* **2** *Yunnan Key Laboratory for Fungal Diversity and Green Development, Kunming Institute of Botany, Chinese Academy of Sciences, Kunming, 650201, China*

Corresponding author: Zhu L. Yang (fungi@mail.kib.ac.cn)

Academic editor: M.P. Martín | Received 22 March 2021 | Accepted 19 April 2021 | Published 26 April 2021

Citation: He Z-M, Yang ZL (2021) A new clitocyboid genus *Spodocybe* and a new subfamily Cuphophylloideae in the family Hygrophoraceae (Agaricales). MycoKeys 79: 129–148. https://doi.org/10.3897/mycokeys.79.66302

Abstract

Phylogenetically, the genera *Cuphophyllus*, *Ampulloclitocybe* and *Cantharocybe* are treated as basal in the family Hygrophoraceae, despite weak support. However, the exact phylogenetic positions of the three genera have remained unresolved, and taxa related to these genera are poorly known. In this study, a new clitocyboid genus *Spodocybe* was proposed based on multigenic phylogenetic inference datasets and morphological evidence. The analyses of ITS as well as two combined datasets ITS-nrLSU-*rpb2* and ITS-nrLSU-*rpb1-rpb2-tef1-α-atp6* supported that (1) *Spodocybe* formed a well-supported monophyletic clade; and (2) sisters *Spodocybe* and *Ampulloclitocybe*, along with *Cantharocybe* and *Cuphophyllus* also formed a monophyletic lineage, as sister to the rest of the Hygrophoraceae. Meanwhile, two new species, namely *S. rugosiceps* and *S. bispora*, from southwestern China, were documented and illustrated. These results support the new proposed genus *Spodocybe*, and that *Spodocybe*, *Ampulloclitocybe*, *Cantharocybe* and *Cuphophyllus* should be retained in the Hygrophoraceae as a new subfamily Cuphophylloideae.

Keywords

Ampulloclitocybe, *Cantharocybe*, *Cuphophyllus*, morphological characters, phylogenetic analysis, taxonomy

Introduction

The widespread genus *Clitocybe* (Fr.) Staude currently encompasses large numbers of species with clitocyboid habit, sharing the features of saprophytic nutrition, funnel-shaped pileus, decurrent lamellae, a usually white, cream or pale colored spore-deposit and smooth and inamyloid spores (Singer 1986; Breitenbach and Kraenzlin 1991; Læssøe and Petersen 2019). As a consequence of the poor, broad and unrepresentative morphological characteristics, the genus appeared heterogeneous and was subsequently proven to be polyphyletic based on the phylogenetic analysis (Moncalvo et al. 2002; Harmaja 2003).

Based on phylogenetic analyses over the past 20 years, (i) many new genera within the Tricholomatoid clade were proposed to accommodate previous *Clitocybe* species deviating from the core Clitocybeae clade (Matheny et al. 2006), such as *Cleistocybe* Ammirati, A.D. Parker & Matheny (Ammirati et al. 2007), *Trichocybe* Vizzini (Vizzini et al. 2010), *Atractosporocybe* P. Alvarado, G. Moreno & Vizzini, *Leucocybe* Vizzini, P. Alvarado, G. Moreno & Consiglio and *Rhizocybe* Vizzini, G. Moreno, P. Alvarado & Consiglio (Alvarado et al. 2015); (ii) Several clitocyboid groups were reconfirmed as independent genera, for instance, *Singerocybe* Harmaja (Qin et al. 2014) and *Infundibulicybe* Harmaja (Binder et al. 2010); and (iii) some others were even transferred to the Hygrophoroid clade (Binder et al. 2010), such as *Ampulloclitocybe* Redhead, Lutzoni, Moncalvo & Vilgalys (Redhead et al. 2002) and *Cantharocybe* H.E. Bigelow & A.H. Sm. (Hosen et al. 2016). However, many clitocyboid taxa remain to be reclassified.

The molecular phylogenetic relationships among members of the Hygrophoraceae Lotsy were well studied by Lodge et al. (2014). In their work, the family was divided into subfamily Hygrophoroideae E. Larss., Lodge, Vizzini, Norvell & S.A. Redhead, Hygrocyboideae Padamsee & Lodge, Lichenomphalioideae Lücking & Redhead and Cuphophylloid grade. Meanwhile, the Cuphophylloid grade was retained in the Hygrophoraceae as the base comprising the genera *Cuphophyllus* (Donk) Bon, *Ampulloclitocybe* and *Cantharocybe*, despite weak phylogenetic support (Matheny et al. 2006; Binder et al. 2010; Lodge et al. 2014). Consequently, the taxonomic problem of the three genera on whether to be included or excluded in the Hygrophoraceae has remained unresolved.

Recently, some collections were shown to be closely related to *Clitocybe trulliformis* (Fr.) P. Karst. based on ITS-BLAST searches while at the same time they were surprisingly related to taxa of the genus *Cuphophyllus* based on nrLSU-BLAST searches. As far as we know, *C. trulliformis* and allied species were lacking taxonomic revision, especially regarding their molecular phylogenetic status. Furthermore, the phylogenetic delimitation of the Hygrophoraceae was ambiguous due to the uncertain positions of *Cuphophyllus*, *Ampulloclitocybe* and *Cantharocybe*. Hence, the aims of this study were (a) to propose and describe a new genus of the Hygrophoraceae for species related to *C. trulliformis* based on morphological and molecular analyses and (b) to reconstruct the phylogeny of the Hygrophoraceae for determining the exact phylogenetic placements of *Cuphophyllus*, *Ampulloclitocybe* and *Cantharocybe* with multi-gene data.

Materials and methods

Specimens

Twenty-three specimens of species similar to *C. trulliformis* and related species were collected from southwestern and northeastern China and western Germany, during 2007 to 2020. The fresh fruitbodies were dried using heat or silica gel. Voucher specimens were deposited in the Herbarium of Kunming Institute of Botany, Chinese Academy of Sciences (KUN-HKAS). Detail information of these specimens is given in Table 1.

Morphological observation

Macroscopic characters of species were described based on the raw field record data and photographs. Colors used in description referred to Kornerup and Wanscher (1978). For the microscopic structure observation, tissue sections of dried specimens were mounted in 5% KOH solution or distilled water and structures of lamellar trama, pileipellis and stipitipellis, basidia and basidiospores were observed with a light microscopy. For the description of lamellar trama structure, seven types, including regular, subregular, divergent, pachypodial, bidirectional, tri-directional and interwoven, were used following Lodge et al. (2014). Besides, Melzer's reagent was applied to test the amyloidity of the basidiospores. In the description of basidiospores, the abbreviation [n/m/p] represent that the measurements were made on n basidiospores from m basidiomes of p collections. The range notation (a)b–c(d) stands for the dimensions of basidiospores in which b–c contains a minimum of 90% of the measured values while a and d in the brackets stand for the extreme values. In addition, a Q value show the length/width ratio of basidiospores and a Qm value for average Q ± standard deviation. All microstructures were illustrated by hand drawing.

DNA extraction, PCR and sequencing

Total genomic DNA was extracted using the Ezup Column Fungi Genomic DNA Purificaton Kit (Sangon Biotech, Shanghai, China) according to the manual. For the PCR amplification, (1) Primers ITS5 and ITS4 (White et al. 1990) were used for the internal transcribed spacer (ITS); (2) LROR and LR5 (Vilgalys and Hester 1990) for the nuclear ribosomal large subunit (nrLSU); (3) EF1-983F and EF1-1953R (Matheny et al. 2007), designed primers SPO-TEF1-F (5'-ATTGCYGGYGGTACYGGTGA-3') and SPO-TEF1-R (5'-TCVAGDGATTTACCTGTHCGRC-3') or another pair of designed primers HYG-TEF1-F (5'-CTTGCCTTYACTCTYGGYGTCC-3') and HYG-TEF1-R (5'-GCGAACTTGCASGCAATGTG-3') for the translation elongation factor 1-α (*tef1-a*); (4) RPB1-Af and RPB1-Cr (Matheny et al. 2002) or designed primers SPO-RPB1-F (5'-ACGAGGTTGYGTGGTGAAAT-3') and SPO-RPB1-R (5'-GGAGGNGGDACHGGCATNA-3') for the DNA-directed RNA polymerase II second largest subunit 1 (*rpb1*); (5) RPB2-6F and RPB2-7.1R (Matheny 2005) for the

Table 1. Specimens used in phylogenetic analysis and their GenBank accession numbers. The newly generated sequences are shown in bold.

Species	Voucher	Locality	GenBank accession number					
			ITS	nrLSU	*rpb2*	*rpb1*	*tef1-α*	*atp6*
Acantholichen pannarioides	MDF352	Costa Rica	KT429795	KT429807	KT429817			
Acantholichen campestris	DIC595b	Brazil	KT429798	KT429810	KT429818			
Acantholichen galapagoensis	MDF058	Ecuador	KT429785	KT429800	KT429812			
Ampulloclitocybe clavipes	KUN-HKAS 54426	China: Jilin	**MW616462**	**MW600481**	**MW656471**	**MW656467**	**MW656461**	**MW656478**
	AFTOL-ID 542		AY789080	AY639881	AY780937	AY788848	AY881022	
	DJL06TN40	USA	FJ596912	KF381542	KF407938			
Arrhenia auriscalpium	TUB 011588			DQ071732				
Arrhenia acerosa	Lueck2	Germany	KP965766	KP965784				
Cantharellula umbonata	CBS 398.79	France	MH861222	MH872990				
Cantharocybe gruberi	AFTOL-ID 1017	USA	DQ200927	DQ234540	DQ385879	DQ435808	DQ059045	
	AH24539	Spain	JN006422	JN006420				
Cantharocybe brunneovelutina	DJL-BZ-1883	Belize	NR160458	NG068731				
Cantharocybe virosa	TENN63483	India	KX452405	JX101471				
	Iqbal-568	Bangladesh	KX452403	KF303143				
Chromosera cyanophylla	AFTOL-ID 1684	USA	DQ486688	DQ457655	KF381509			
Chromosera ambigua	GE18008-1	France	MK645573	MK645587	MK645593			
Chromosera lilacina	GE18035	Canada	MK645577	MK645591	MK645597			
Chromosera xanthochroa	GE18033	Canada	MK645576	MK645590	MK645596			
Chrysomphalina chrysophylla	AFTOL-ID 1523	USA	DQ192180	DQ457656				
Chrysomphalina grossula	OSC 113683		EU644704	EU652373				
Clitocybe aff. *costata*	DJL06TN80	USA	FJ596913					
Clitocybe herbarum	G0171	Hungary		MK277719				
Clitocybe trulliformis	14562	Italy	JF907809					
	4804	Russia	MH930178					
Clitocybe cf. *trulliformis*	G0460	Hungary		MK277728				
Clitocybe sp.	NAMA 2015-206	USA	MH910535					
Clitocybe sp.	NAMA 2015-318	USA	MH910563					
Clitocybe sp.	Mushroom Observer 302917	USA	MK607556					
Cora pavonia	DIC215	Ecuador	KF443238	KF443261	KF443275			
Cora aspera	DIC110	Bolivia	KF443230	KF443257	KF443267			
Cora reticulifera	DIC119	Ecuador	KF443239	KF443262	KF443269			
Cora squamiformis	DIC146	Bolivia	KF443240	KF443263	KF443273			
Corella brasiliensis	MDF017	Bolivia	KF443229	KF443255	KF443276			
Corella aff. *Melvinii*	MDF200	Brazil	KJ780569	KY861725				
Cuphophyllus pratensis	Lueck7	Germany	KP965771	KP965789				
	DJL-Scot-8	UK	KF291057	KF291058				
Cuphophyllus aurantius	CFMR PR-6601	Puerto Rico	KF291099	KF291100	KF291102			
Cuphophyllus aff. *pratensis*	AFTOL-ID 1682	USA	DQ486683	DQ457650		DQ435804		
Cuphophyllus sp.	KUN-HKAS 105671	China: Tibet	**MW762875**	**MW763000**	**MW789179**	**MW789163**		
Cyphellostereum galapagoense	CDS 41163	Ecuador	NR158415	NG068806				
Cyphellostereum imperfectum	DIC115	Guatemala	KF443218	KF443243	KF443277			
Dictyonema interruptum	Ertz 10475	Portugal		EU825967	KF443282			
Dictyonema schenckianum	DIC113	Brazil	KF443225	KF443251	KF443285			
Eonema pyriforme	G1063	Poland		MK278075				
Gliophorus psittacinus	CFMR DEN-25	Denmark	KF291075	KF291076	KF291078			
Gliophorus graminicolor	TJB-10048 (CORT)	Australia	KF381520	KF381545	KF407936			
Gliophorus aff. *laetus*	CFMR PR-5408	Puerto Rico	KF291069	KF291070				
Glioxanthomyces nitidus	GDGM41710	China: Jilin	MG712283	MG712282	MG711911			

Species	Voucher	Locality	GenBank accession number					
			ITS	nrLSU	*rpb2*	*rpb1*	*tef1-α*	*atp6*
Haasiella splendidissima	Herb. Roux n. 4044	France	JN944400	JN944401				
	Herb. Roux n. 3666	Moldova	JN944398	JN944399				
Haasiella venustissima	A. Gminder 971488	Italy	KF291092	KF291093				
	E. C. 08191	Italy	JN944393	JN944394				
Humidicutis marginata	JM96/33			AF042580				
Humidicutis auratocephalus	AFTOL-ID 1727	USA	DQ490624	DQ457672	DQ472720	DQ447906		
Humidicutis dictiocephala	QCAM6000	Ecuador	KY689661	KY780120				
Humidicutis sp.	CFMR BZ-3923	Belize	KF291110	KF291111				
Hygroaster nodulisporus	AFTOL-ID 2020	USA		EF561625				
Hygroaster albellus	AFTOL-ID 1997	Puerto Rico	KF381521	EF551314				
Hygrocybe conica	FO 46714			DQ071739				
Hygrocybe cf. *acutoconica*	CFMR NC-256	USA	KF291117	KF291118	KF291120			
Hygrocybe coccinea	AFTOL-ID 1715	USA	DQ490629	DQ457676	DQ472723	DQ447910	GU187705	
Hygrocybe aff. *conica*	AFTOL-ID 729		AY854074	AY684167	AY803747			
Hygrophorus eburneus	US97/138	Germany		AF430279				
	GDGM70059	USA	MT093608					
Hygrophorus chrysodon	KUN-HKAS 82501	China: Tibet	**MW616463**	**MW600482**	**MW656472**		**MW656462**	**MW656479**
	KUN-HKAS 112569	China: Tibet	**MW762876**	**MW763001**	**MW789180**	**MW789164**	**MW773440**	**MW789195**
Hygrophorus flavodiscus	KUN-HKAS 68013	China: Yunnan	**MW616464**	**MW600483**	**MW656473**	**MW656468**	**MW656463**	**MW656480**
	KUN-HKAS 55043	China: Yunnan	**MW616465**	**MW600484**	**MW656474**	**MW656469**	**MW656464**	**MW656481**
Hygrophorus gliocyclus	KUN-HKAS 79929	China: Tibet	**MW616466**	**MW600485**	**MW656475**		**MW656465**	**MW656482**
Hygrophorus hypothejus	KUN-HKAS 56550	Germany	**MW616467**	**MW600486**	**MW656476**	**MW656470**		**MW656483**
Hygrophorus pudorinus	AFTOL-ID 1723	USA	DQ490631	DQ457678	DQ472725	DQ447912	GU187710	
Hygrophorus sp. 1	KUN-HKAS 112566	China: Yunnan	**MW762877**	**MW763002**	**MW789181**	**MW789165**	**MW773441**	**MW789196**
Hygrophorus sp. 2	KUN-HKAS 87261	China: Jilin	**MW616468**	**MW600487**	**MW656477**		**MW656466**	**MW656484**
Hygrophorus sp. 3	KUN-HKAS 112567	China: Tibet	**MW762878**	**MW763003**	**MW789182**	**MW789166**	**MW773442**	**MW789197**
Hygrophorus sp. 4	KUN-HKAS 112568	China: Tibet	**MW762879**	**MW763004**	**MW789183**	**MW789167**	**MW773443**	**MW789198**
Lichenomphalia hudsoniana	GAL18249	USA	JQ065873	JQ065875				
Lichenomphalia meridionalis	S-270-FB1	Japan	LC428308	LC428307				
Neohygrocybe ovina	GWG H. ovina Rhosisaf (ABS)	UK	KF291233	KF291234	KF291236			
Neohygrocybe griseonigra	GDGM 44492	China	MG779451	MG786565				
Neohygrocybe ingrata	DJL05TN62 (TENN)	USA	KF381525	KF381558	KF381516			
Neohygrocybe subovina	GRSM 77065	USA	KF291140	KF291141				
Spodocybe bispora	KUN-HKAS 73310	China: Yunnan	**MW762880**	**MW763005**	**MW789184**	**MW789168**	**MW773444**	**MW789199**
	KUN-HKAS 73332	China: Yunnan	**MW762881**	**MW763006**	**MW789185**	**MW789169**	**MW773445**	**MW789200**
	KUN-HKAS 112564	China: Yunnan	**MW762882**	**MW763007**	**MW789186**	**MW789170**	**MW773446**	**MW789201**
Spodocybe rugosiceps	KUN-HKAS 112561	China: Yunnan	**MW762883**	**MW763008**	**MW789187**	**MW789171**	**MW773447**	**MW789202**
	KUN-HKAS 81981	China: Yunnan	**MW762884**	**MW763009**	**MW789188**	**MW789172**		**MW789203**
	KUN-HKAS 69830	China: Yunnan	**MW762885**	**MW763010**	**MW789189**	**MW789173**	**MW773448**	**MW789204**

Species	Voucher	Locality	GenBank accession number					
			ITS	nrLSU	*rpb2*	*rpb1*	*tef1-α*	*atp6*
Spodocybe rugosiceps	KUN-HKAS 71071	China: Yunnan	**MW762886**	**MW763011**	**MW789190**	**MW789174**	**MW773449**	**MW789205**
	KUN-HKAS 112562	China: Yunnan	**MW762887**	**MW763012**	**MW789191**	**MW789175**	**MW789159**	**MW789206**
	KUN-HKAS 112563	China: Yunnan	**MW762888**	**MW763013**	**MW789192**	**MW789176**	**MW789160**	**MW789207**
Spodocybe sp. 1	KUN-HKAS 112560	China: Jilin	**MW762889**	**MW763014**	**MW789193**	**MW789177**	**MW789161**	**MW789208**
Spodocybe sp. 2	KUN-HKAS 112565	China: Yunnan	**MW762890**	**MW763015**	**MW789194**	**MW789178**	**MW789162**	**MW789209**
Porpolomopsis calyptriformis	CFMR ENG-3	UK	KF291242	KF291243	KF291245			
Porpolomopsis aff. *calyptriformis*	DJL05TN80 (TENN)	USA	KF291246	KF291247	KF291249			
Porpolomopsis lewelliniae	TJB-10034 (CORT)	Thailand	KF291238	KF291239	KF291241			
Pseudoarmillariella ectypoides	AFTOL-ID 1557	USA	DQ192175	DQ154111	DQ474127	DQ516076	GU187733	
Pseudoarmillariella bacillaris	KUN-HKAS 76377	China	KC222315	KC222316				
Sinohygrocybe tomentosipes	GDGM 50075	China: Hunan	MG685873	MG696902	MG696906			
	GDGM 43351	China: Sichuan	MG685872	MG696901	MG696905			
Amylocorticium cebennense	CFMR HHB-2808	USA	GU187505	GU187561	GU187770	GU187439	GU187675	
Aphroditeola olida	DAOM 226047	Canada	KF381518	KF381541				
Macrotyphula fistulosa	IO. 14. 214	Spain	MT232352	KY224088		MT242317	MT242354	
Macrotyphula juncea	IO. 14. 177	Sweden	MT232353	MT232306	MT242337		MT242355	
Macrotyphula phacorrhiza	IO. 14. 167	Sweden	MT232364	MT232315	MT242348	MT242326	MT242367	
	IO.14. 200	France	MT232363	MT232314	MT242347		MT242366	
Phyllotopsis nidulans	IO. 14. 196	Spain	MT232308		MT242338	MT242319	MT242357	
Phyllotopsis sp.	AFTOL-ID 773		DQ404382	AY684161	AY786061	DQ447933	DQ059047	
Pleurocybella porrigens	UPS F-611822	Sweden	MT232355	MT232309	MT242339			
Plicaturopsis crispa	AFTOL-ID 1924	USA	DQ494686	DQ470820	GU187816			
Pterulicium echo	ZRL20151311		LT716065	KY418881	KY419026	KY418979	KY419076	
Pterulicium gracilis	IO. 14. 142	Sweden	MT232356	MT232310			MT242358	
Sarcomyxa serotina	AFTOL-ID 536	USA	DQ494695	AY691887	DQ859892	DQ447938	GU187754	
Serpulomyces borealis	CFMR L-8014	USA	GU187512	GU187570	GU187782		GU187686	
Tricholomopsis decora	AFTOL-ID 537		DQ404384	AY691888	DQ408112	DQ447943	DQ029195	
Tricholomopsis osiliensis	ZRL20151760		LT716068	KY418884	KY419029		KY419079	
Typhula capitata	IO. 15. 122	Spain	MT232357	MT232312	MT242341	MT242321	MT242360	
Typhula incarnata	IO. 14. 92	Sweden	MT232362	MT232313	MT242346	MT242325		
Typhula micans	IO. 14. 165	Sweden	MT232361	KY224102	MT242345	MT242324	MT242364	

DNA-directed RNA polymerase II second largest subunit 2 (*rpb2*); and (6) ATP6-3 and ATP-6 (Kretzer and Bruns 1999) for ATP synthase subunit 6 (*atp6*).

The PCR mixtures contained 1× PCR buffer, 1.5mM $MgCl_2$, 0.2mM dNTPs, each primer at 0.4 μM, 1.25U of *Taq* polymerase (Sangon Biotech, Shanghai, China), and 1 μL of DNA template in a total volume of 25 μL. Reactions were performed with the following program: initial denaturation at 94 °C for 5 min, 35 cycles at 94 °C for 30 s, 50 °C (*atp6*), 52 °C (nrLSU, *tef1-a*, *rpb1* and *rpb2*) or 54 °C (ITS) for 30 s, and 72 °C for 30 s (ITS and *atp6*), 50 s (nrLSU and *rpb2*) or 75 s (*tef1-a* and *rpb1*), and for terminal elongation, the reaction batches were incubated at 72 °C for 10 min. All PCR products were detected by 2% agarose gel electrophoresis and then sent to the Kunming branch of Tsingke Biological Technology Co., Ltd. (Beijing, China) for sequencing.

Phylogenetic tree construction

Sequences used for phylogenetic analysis (presented in Table 1) were aligned by using MAFFT v7.471 (Katoh and Standley 2016) and then manually adjusted by using BIOEDIT v7.2.5 (Hall 1999). The intron regions of *tef1-a*, *rpb2* and *rpb1* were excluded except the conserved rpb1-intron2. Three datasets of ITS-nrLSU-*rpb2*, ITS-nrLSU-*rpb1-rpb2-tef1-a-atp6* and ITS (Suppl. materials 1, 2 and 3) were used to construct phylogenetic trees. The two multi-gene matrixes were generated by SEQUENCEMATRIX 1.7.8 (Vaidya et al. 2011). GTR + I + G was inferred as the best-fit model for the three matrixes selected according to the AIC in MRMODELTEST v2.4 (Nylander 2004). Maximum likelihood (ML) trees with 1000 bootstrap replicates and Bayesian inferences were generated with RAXML v8.0.20 (Stamatakis 2006) and MRBAYES v3.2.7 (Ronquist and Huelsenbeck 2003), respectively.

Results

Molecular phylogenetic analysis

As shown in Table 1, a total of 393 sequences (109 ITS, 110 nrLSU, 40 *tef1-a*, 38 *rpb1*, 74 *rpb2* and 22 *atp6*) from 118 samples were used in the phylogenetic analyses, 131 (23 ITS, 23 nrLSU, 20 *tef1-a*, 20 *rpb1*, 23 *rpb2* and 22 *atp6*) of which were newly generated in the present study.

The combined dataset ITS-nrLSU-*rpb2* comprised 221 sequences from 88 samples with a total of 3135 positions. In the three-gene tree (Fig. 1), 11 specimens from four novel *Spodocybe* species collected in this study, *C.* cf. *trulliformis* and *C. herbarum* formed a strongly supported monophyletic clade (BP = 100%, PP = 1.0), as sister to *Ampulloclitocybe* (BP = 63%, PP = 0.98). The phylogenetic analysis showed that the new proposed genus *Spodocybe* should be placed within the Hygrophoraceae, although intergeneric branched orders among *Spodocybe*, *Ampulloclitocybe*, *Cantharocybe* and *Cuphophyllus* were unstable with low support values.

In order to accurately determine the position of *Spodocybe* in the family Hygrophoraceae and better clarify the phylogenetic relationships of *Spodocybe*, *Ampulloclitocybe*, *Cantharocybe* and *Cuphophyllus*, a further six-gene matrix ITS-nrLSU-*rpb1-rpb2-tef1-a-atp6* composed of 179 sequences from 54 samples with 5405 positions was used to rebuild the Hygrophoraceae tree. As revealed by the six-gene phylogenetic analysis (Fig. 2), the branch support level of the six-gene tree was obviously improved, compared with that of the previous three-gene tree. The monophyly of *Spodocybe* clade was strongly supported (BP = 100%, PP = 1.00), including *Spodocybe rugosiceps* (BP = 100%, PP = 1.00), *S. bispora* (BP = 100%, PP = 1.00) and two unnamed *Spodocybe* species. *Spodocybe* and *Ampulloclitocybe* were sister clades (BP = 78%, PP = 0.99), then further clustered with *Cantharocybe* (BP = 59%, PP = 0.97) and finally together with *Cuphophyllus* formed an independ-

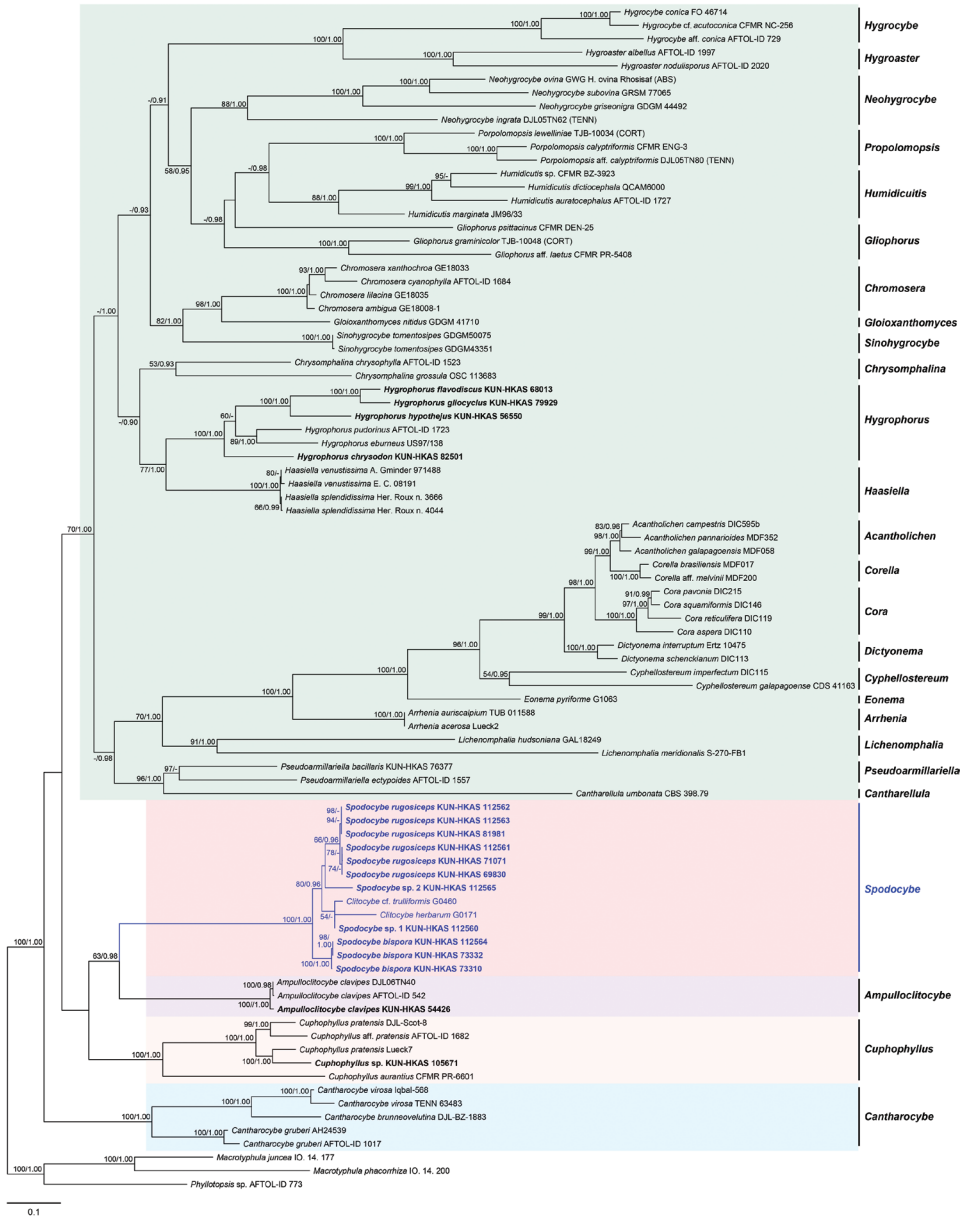

Figure 1. ML analysis of Hygrophoraceae combined ITS, nrLSU and *rpb2* sequence data, with *Macrotyphula juncea*, *Macrotyphula phacorrhiza* and *Phyllotopsis* sp. as outgroups. Bootstrap values (BP) ≥ 50% from ML analysis and Bayesian posterior probabilities (PP) ≥ 0.90 are shown at nodes. The newly generated sequences are shown in bold.

ent lineage (BP = 85%, PP = 1.00). Meanwhile, this lineage (Cuphophylloideae) comprising the four genera was well-supported (BP = 83%, PP = 1.00) as sister to the rest of the Hygrophoraceae.

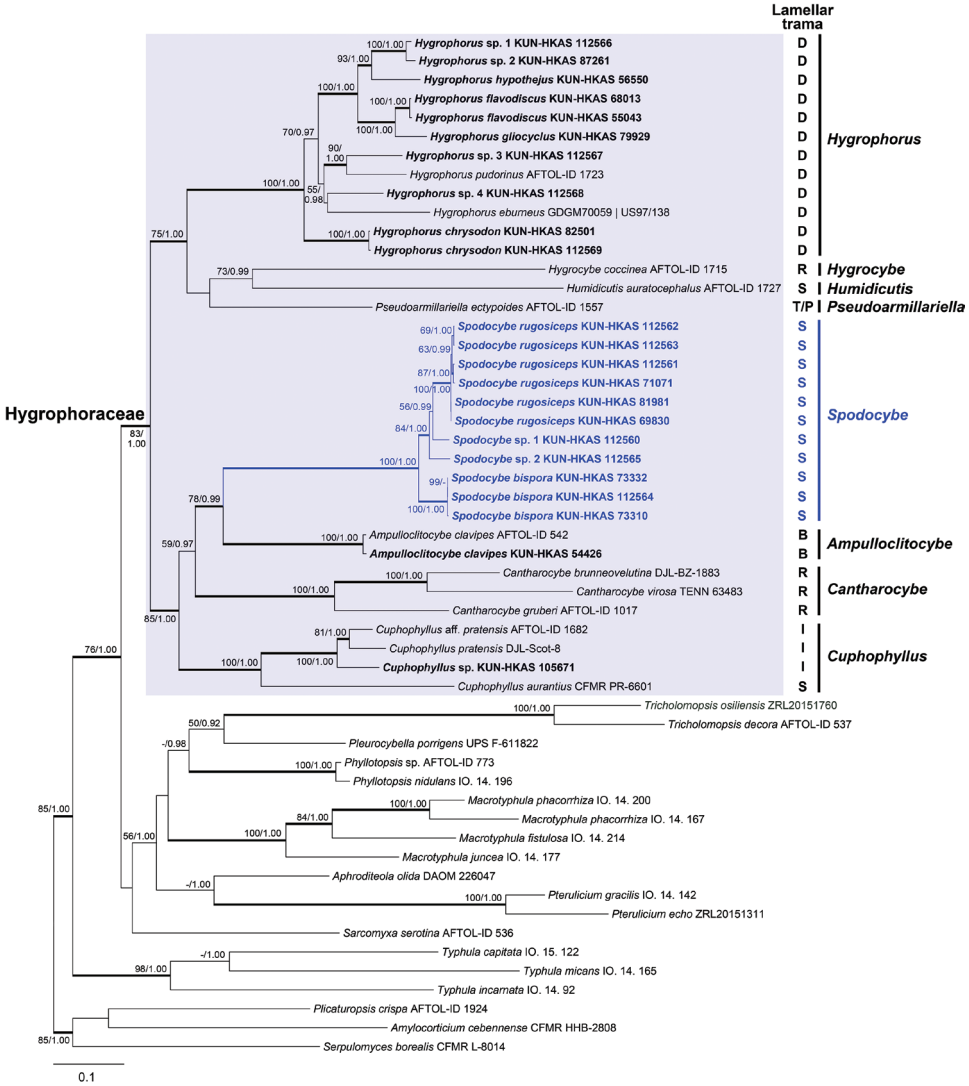

Figure 2. ML analysis of Hygrophoraceae combined ITS, nrLSU, *rpb1*, *rpb2*, *tef1-a* and *atp6* sequence data, with representatives of Amylocorticiaceae, Pterulaceae and the Hygrophoroid clade (*Aphroditeola*, *Macrotyphula*, *Phyllotopsis*, *Pleurocybella*, *Sarcomyxa*, *Tricholomopsis* and *Typhula*) as outgroups. Bootstrap values (BP) ≥ 50% from ML analysis and Bayesian posterior probabilities (PP) ≥ 0.90 are shown at nodes. Branches with BP ≥ 75% and PP ≥ 0.95 are bolded. The newly generated sequences are shown in bold. Lamellar trama type B for bidirectional, D for divergent, I for interwoven, P for pachypodial, R for regular, S for subregular, T for tri-directional. Lamellar trama types of specimens collected in this study were identified by ourselves and others referred to Lodge et al. (2014) and Hosen et al. (2016).

In addition, an ITS dataset (23 sequences, 1053 positions) was applied to phylogenetic analysis for displaying the relationships among *Spodocybe* species from this study and species of *Clitocybe* treated from GenBank. In the ITS tree (Fig. 3), *Spodocybe*

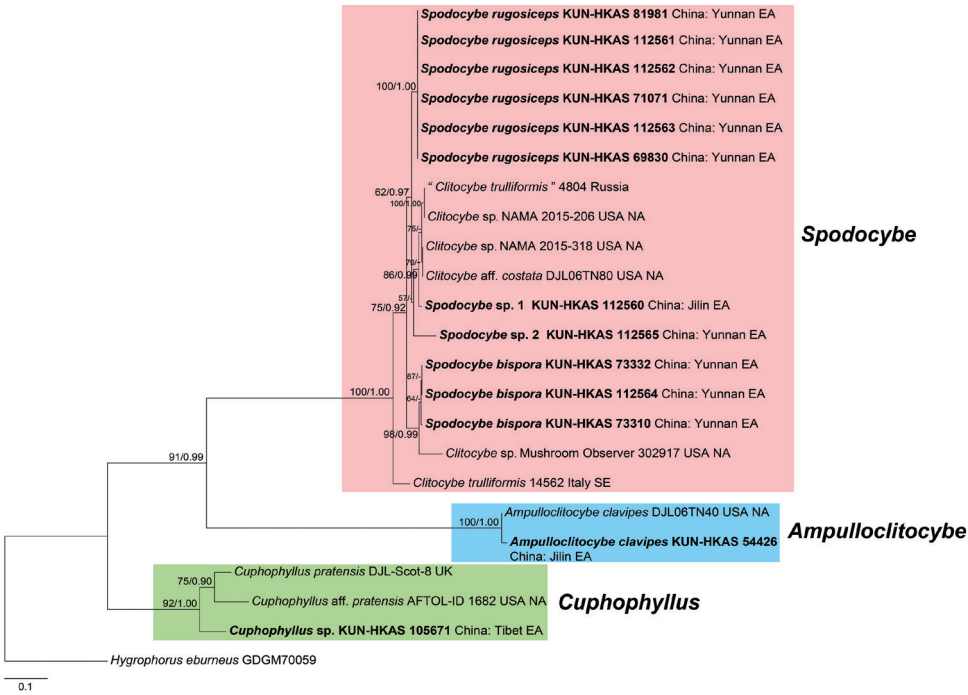

Figure 3. Phylogram showing the phylogenetic relationships among *Spodocybe* species and species of *Clitocybe* treated from Genbank based on ITS sequence data, with representatives of *Ampulloclitocybe*, *Cuphophyllus* and *Hygrophorus* as outgroups (rooted with *Hygrophorus eburneus*). Bootstrap values (BP) ≥ 50% from ML analysis and Bayesian posterior probabilities (PP) ≥ 0.90 are shown at nodes. The newly generated sequences are shown in bold. EA, NA and SE refer to East Asia, North America and South Europe, respectively.

species formed a highly supported monophyletic clade with *C. trulliformis* and related species (BP = 100%, PP = 1.00), which was also a sister clade to *Ampulloclitocybe* with strong support (BP = 91%, PP = 0.99).

Taxonomy

Cuphophylloideae Z. M. He & Zhu L. Yang, subf. nov.
MycoBank No: 839377

Diagnosis. Characterized generally by clitocyboid basidiomes, convex to funnel-shaped pileus, decurrent lamellae, absence of veils, inamyloid basidiospores and presence of clamps.

Etymology. From the type genus *Cuphophyllus*.

Type genus. *Cuphophyllus* (Donk) Bon.

Description. Basidiomes small, medium-sized to large, mostly clitocyboid, rarely omphalinoid or mycenoid; veils absent. Pileus convex, applanate to funnel-shaped; surface usually dry, smooth, lubricous or rarely viscid. Lamellae decurrent to deeply

decurrent. Basidiospores ellipsoid, oblong or subglobose, thin-walled and inamyloid. Pileipellis usually a cutis, sometimes ixocutis or trichoderm. Lamellar trama regular, subregular, interwoven or bidirectional. Clamp connections present.

Habitat, ecology and distribution. Usually gregarious or caespitose on ground, rarely on wood; widespread in temperate and tropical regions.

The genera *Ampulloclitocybe*, *Cantharocybe*, *Cuphophyllus* and *Spodocybe* are included in the subfamily Cuphophylloideae, which is in correspondence with Cuphophylloid grade of Lodge et al. (2014) plus *Spodocybe*.

***Spodocybe* Z. M. He & Zhu L. Yang, gen. nov.**
MycoBank No: 839050

Diagnosis. Differs from *Ampulloclitocybe* by its small basidiomes and subregular lamellar trama rather than medium-sized basidiomes and bidirectional lamellar trama. Differs from *Cuphophyllus* in the ratio of basidia to basidiospore length less than 5, and lamellar trama subregular rather than interwoven. Differs from *Cantharocybe* in its absence of cheilo- and caulocystidia, having small basidiomes rather than large ones and having subregular lamellar trama rather than regular one.

Etymology. *Spodo-* refers to grey; *-cybe* refers to head; that is a *Clitocybe*-like genus with gray pileus.

Type species. *Spodocybe rugosiceps* Z. M. He & Zhu L. Yang.

Description. Basidiomes small, clitocyboid. Pileus convex, applanate to infundibuliform; surface dry, greyish (2B1), grey-brown (5C4) to dark grey-brown (5E4); center depressed with age. Lamellae decurrent to deeply decurrent, white (1A1) to cream (1A2), thin, moderately crowded, sometimes furcate and interveined. Stipe central, subcylindrical, concolorous with pileus. Basidiospores ellipsoid, oblong to cylindrical, colourless, hyaline, smooth, thin-walled, inamyloid; ratio of basidia to basidiospore length less than 5. Pileipellis and stipitipellis a cutis. Lamellar trama subregular. Clamp connections abundant, present in all parts of basidiome.

Habitat, ecology and distribution. Saprophytic, usually gregarious or caespitose on the ground of coniferous or coniferous and broad-leaved mixed forest; distributed in the temperate and subtropical zones from June to November.

***Spodocybe rugosiceps* Z. M. He & Zhu L. Yang, sp. nov.**
MycoBank No: 839052
Figs 4A, B, 5

Diagnosis. Differs from *S. bispora* in having a rugose pileus, smaller basidiospores and 4-spored rather than 2-spored basidia. Differs from *C. trulliformis* in having smaller basidiospores and a rugose rather than felty-squamulose pileus.

Etymology. *rugosiceps* refers to the rugose pileus.

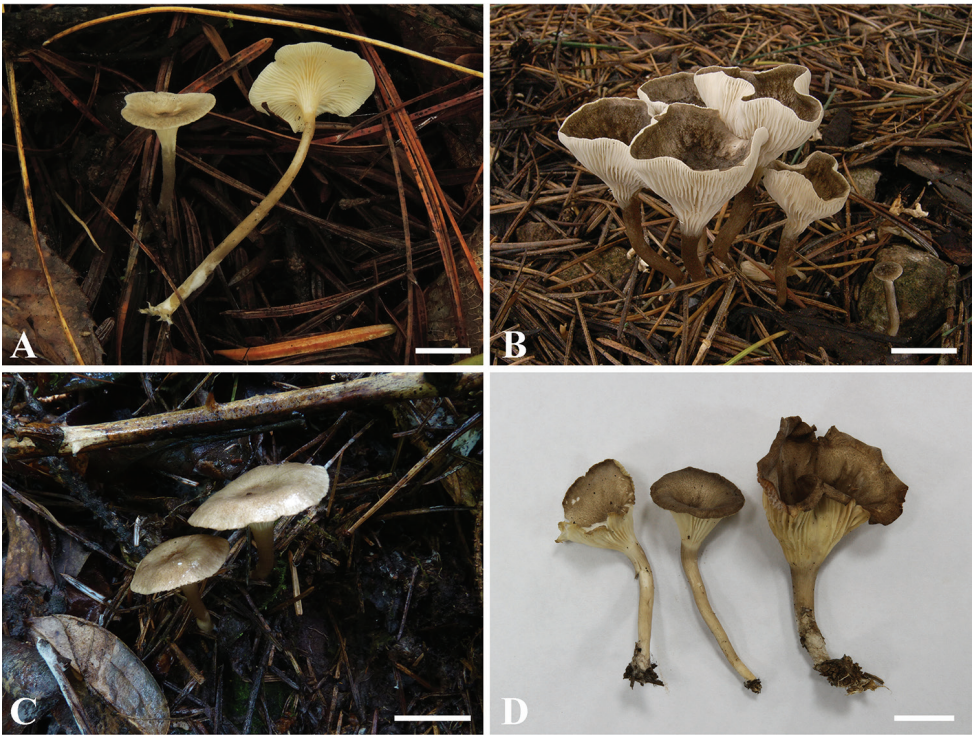

Figure 4. Basidiomes of described *Spodocybe* species. **A, B** *Spodocybe rugosiceps* (KUN-HKAS 112563, KUN-HKAS 112562, respectively) **C, D** *Spodocybe bispora* (KUN-HKAS 73332, KUN-HKAS 112562, respectively). Scale bars: 1 cm.

Type. China. Yunnan Province: Kunming City, near Yeya Lake, at 25.136658°N, 102.873027°E, alt. 2000 m, 11 Aug 2020, Z. M. He 72 (KUN-HKAS 112563, holotype).

Description. Basidiomes small, clitocyboid. Pileus 0.5–2 cm in diam, at first nearly applanate, then concave; surface dry and rugose, gray-brown (5E2-4) to gray-black (4F2-4) in the center and gray-brown (5C2-4) or gray (5B1-2) towards margin; center often slightly umbonate; margin straight and undulating; context thin and white (1A1) to cream (1A2). Lamellae deeply decurrent, white (1A1) to cream (1A2), thin (up to 2 mm high), crowded, sometimes forked and intervenose. Stipe 2.5–6 × 0.2–0.4 cm, central, narrowly cylindrical to subcylindrical, sometimes flexuous, hollow; surface dry and nearly smooth, concolorous with pileus; context white (1A1).

Basidiospores [60/3/3] 5–6 (6.5) × (2.5)3–3.5(4) μm, Q = (1.38)1.55–1.95(2), Qm = 1.73 ± 0.14, elongate, colorless, hyaline, smooth, thin-walled, inamyloid. Basidia 20–24 × 5–6 μm, clavate, 4-spored, colorless, hyaline, thin-walled; sterigmata up to 4 μm long; ratio of basidia to basidiospore length values about 3–5. Cystidia absent. Lamellar trama subregular; hyphae colorless, hyaline, cylindrical, thin-walled, 3–10 μm wide. Pileipellis a cutis, but in places upright or trichodermial in appearance, made up with thin-walled cylindrical hyphae 3–9 μm wide. Stipitipellis a cutis, composed of

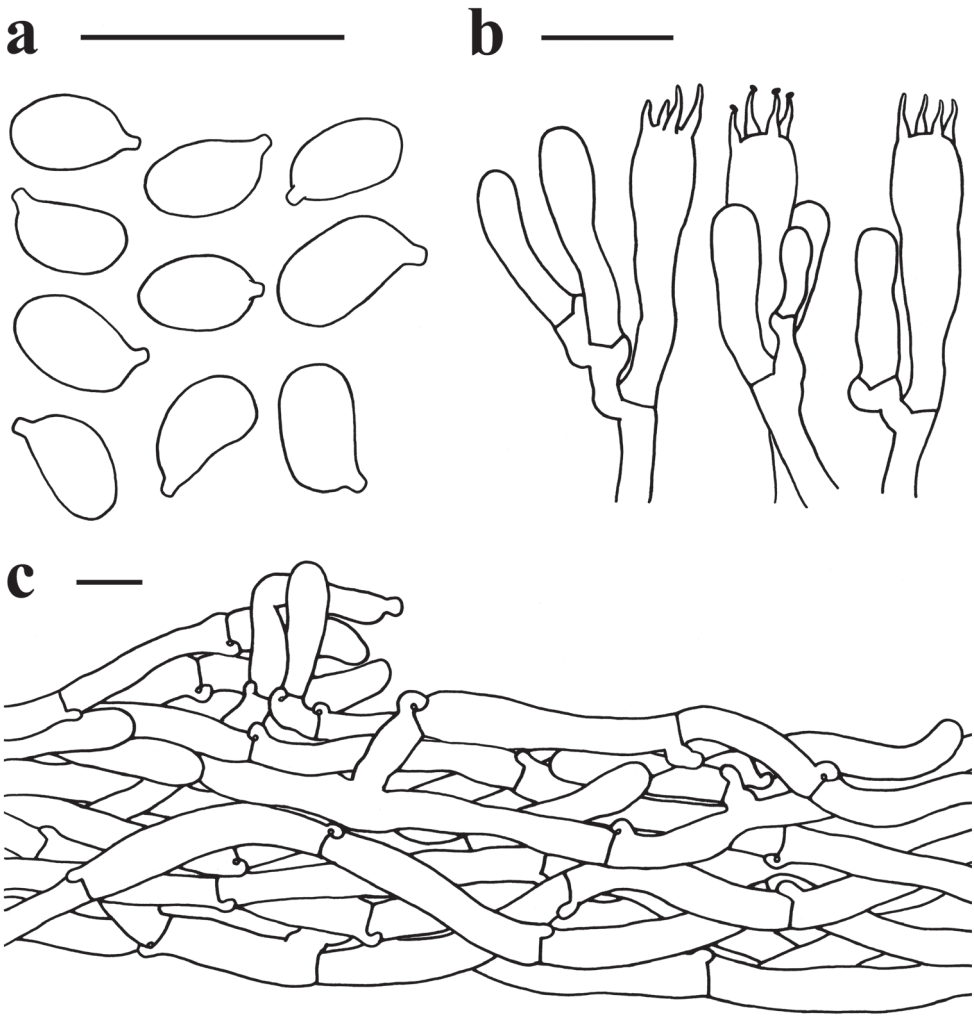

Figure 5. Microscopic features of *Spodocybe rugosiceps* (KUN-HKAS 112563, holotype) **a** basidiospores **b** basidia **c** pileipellis. Scale bars: 10 μm.

thin-walled cylindrical hyphae 3–10 μm wide. Clamp connections present in all parts of basidiome.

Habitat, ecology and distribution. Gregarious or caespitose, growing saprotrophically in forest litter, often under conifers, on the ground, known from subtropical zone of Yunnan, China; from July to October.

Additional specimens examined. China. Yunnan Province: Dali Bai Autonomous Prefecture, Yunlong Country, Tianchi National Nature Reserve, at 25.850365°N, 99.274236°E, alt. 2509 m, 28 Sep 2019, X. H. Wang 7471 (KUN-HKAS 112561); Kunming City, Fangwang Tree Farm, at 25.063737°N, 102.870690°E, alt. 2262 m, 22 Sep 2011, Z. L. Yang 5586 (KUN-HKAS 71071); Kunming City, Kunming Institute

of Botany, at 25.147081°N, 102.748855°E, alt. 1990 m, 24 Aug 2020, Z. L. Yang 6391 (KUN-HKAS 112562); Kunming City, Qiongzhu Temple, at 25.071304°N, 102.630934°E, alt. 1900 m, 28 Jul 2013, T. Guo 779 (KUN-HKAS 81981); Yulong Country, Lashi Village, at 26.883902°N, 100.234594°E, alt. 2655 m, 31 Jul 2011, L. P. Tang 1369 (KUN-HKAS 69830).

***Spodocybe bispora* Z. M. He & Zhu L. Yang, sp. nov.**
MycoBank No: 839054
Figs 4C, D, 6

Diagnosis. Differs from *S. rugosiceps* in having a nearly smooth pileus, larger basidiospores and 2-spored rather than 4-spored basidia. Differs from *C. trulliformis* in having a nearly smooth rather than felty-squamulose pileus.

Etymology. *Bispora* refers to 2-spored.

Type. China. Yunnan Province: Baoshan City, Longyang District, Shuizhai Village, at 25.273967°N, 99.306216°E, alt. 2400 m, 12 Aug 2011, J. Qin 324 (KUN-HKAS 73310, holotype).

Description. Basidiomes small, clitocyboid. Pileus 1.5–3 cm in diam, plano-convex to funnel-shaped; surface dry and nearly smooth, greyish-brown (4B2-3) to grey-brown (4E3-5); center depressed, usually with a low umbo, somewhat darker; margin generally straight and undulating, incurved when old; context thin and white (1A1). Lamellae deeply decurrent, white (1A1) to cream (1A2), thin, 1–2 mm high, relatively crowded, sometimes forked and intervenose. Stipe 1–3 × 0.2–0.4 cm, central, subcylindrical, hollow; surface dry and nearly smooth, concolorous with pileus; context white (1A1).

Basidiospores [60/3/3] (7)7.5–10.5(11.5) × 3–4 μm, Q = (2.05)2.11–3(3.33), Qm = 2.56 ± 0.3, cylindrical, colorless, hyaline, smooth, thin-walled, inamyloid. Basidia 20–30 × 4–5.5 μm, clavate, 2-spored, colorless, hyaline, thin-walled; sterigmata up to 10 μm long; ratio of basidia to basidiospore length less than 5 (about 2–4). Cystidia absent. Lamellar trama subregular, colorless, hyaline, made up of thin-walled cylindrical hyphae with 3–10 μm wide. Pileipellis a cutis, composed of thin-walled cylindrical hyphae 3–11 μm wide. Stipitipellis a cutis, composed of thin-walled cylindrical hyphae 3–10 μm wide. Clamp connections in all parts of basidiomes.

Habitat, ecology and distribution. Saprophytic, usually gregarious on the ground of coniferous or coniferous and broad-leaved mixed forest, known from Yunnan, China; July to September.

Additional specimens examined. China. Yunnan Province: Kunming City, Qipan Mountain, at 26.060020°N, 102.576823°E, alt. 1900 m, 25 Jul 2020, Z. M. He 35 (KUN-HKAS 112564); Nujiang City, Lanping Country, No. 311 Provincial Highway, at 26.636613°N, 99.557809°E, alt. 2660 m, 14 Aug 2011, J. Qin 346 (KUN-HKAS 73332).

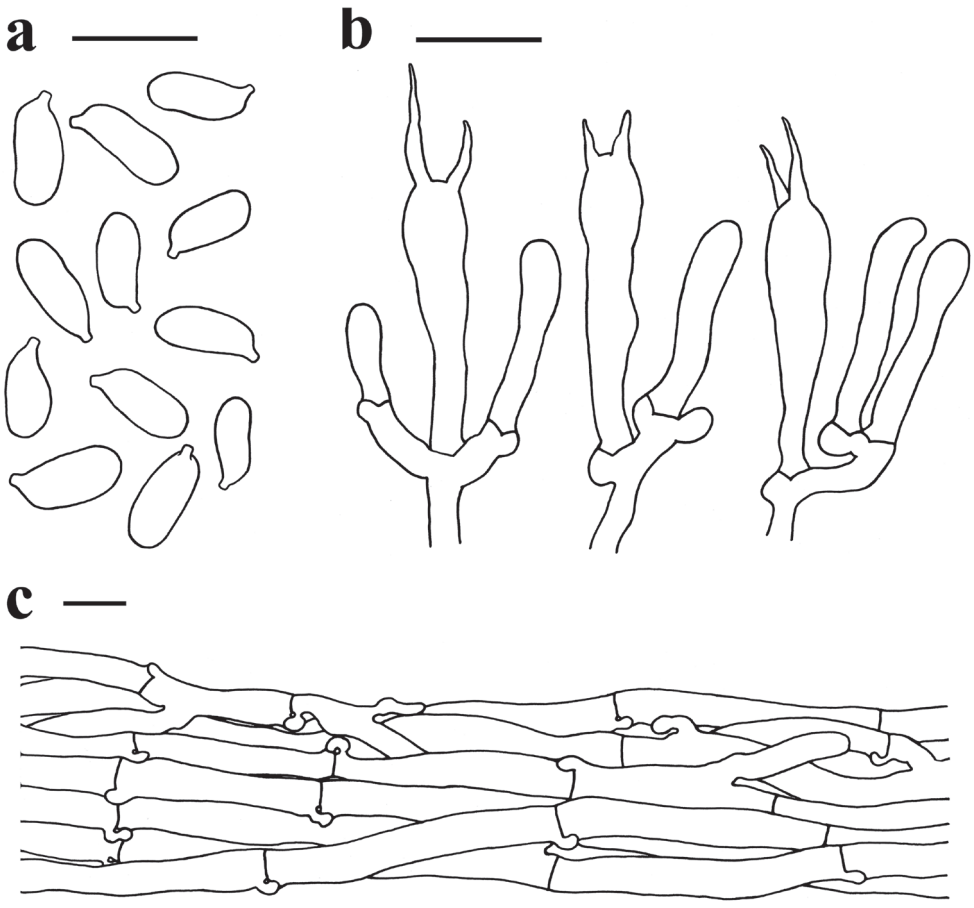

Figure 6. Microscopic features of *Spodocybe bispora* (KUN-HKAS 73310, holotype) **a** basidiospores **b** basidia **c** pileipellis. Scale bars: 10 μm.

Discussion

The new genus *Spodocybe*

In our current study, the new clitocyboid species were clustered into a monophyletic lineage (BP = 100%, PP = 1.00) in the Hygrophoraceae according to the multi-gene phylogenetic analysis (Figs 1, 2). As a result, the new generic name *Spodocybe* is proposed here to accommodate the new lineage, which is irrelevant to Clitocybeae of the Tricholomatoid clade (Matheny et al. 2006; Alvarado et al. 2015). The three-gene tree of the Hygrophoraceae (Fig. 1) in this study presented basically consistent topological structure with Lodge et al. (2014), and showed that *Spodocybe* was a sister to *Ampulloclitocybe* located within the family Hygrophoraceae and further confirmed by a six-gene tree (Fig. 2).

Besides the molecular analyses, morphological data also support its separation from the relative genera. *Spodocybe* shares clitocyboid basidiomes, decurrent lamellae, inamyloid basidiospores and the presence of clamps with the other genera *Ampulloclitocybe*, *Cuphophyllus* and *Cantharocybe*. However, the genus *Ampulloclitocybe*, typified by *A. clavipes*, differs from *Spodocybe* in having medium-sized basidiomes and bidirectional lamellar trama (Harmaja 2002; Lodge et al. 2014). Afterwards, *Cuphophyllus* differs from *Spodocybe* in having long basidia, typically 7–8 (rarely 5–6) times the length of the basidiospores, highly interwoven lamellar trama, rarely subregular (Voitk et al. 2020). Finally, *Cantharocybe* differs from *Spodocybe* in having large basidiomes, broad lamellae, cheilo- and caulocystidia, clamps but not on all hyphal septa or at the base of every basidium and more regular lamellar trama (Ovrebo 2011; Hosen et al. 2016). In view of the four genera above with different structures in lamellar trama (Fig. 2), the type of lamellar trama can become a good distinguishing microscopic character for them.

For a long time, *C. trulliformis* has been placed in the genus *Clitocybe* based on the clitocyboid feature and habit since 1879 (Karsten 1879). However, *C. trulliformis* shares many morphological characteristics with *Spodocybe*, such as the small basidioma with applanate to infundibuliform pileus, grey-brown pileus and stipe, decurrent and whitish lamellae, and smooth and inamyloid basidiospores (Bas et al. 1995). Besides, the ITS phylogenetic analysis in our study (Fig. 3) showed that *C. trulliformis* and related *Clitocybe* species were involved in the *Spodocybe* clade as well, indicating that *C. trulliformis* and related species should be placed with *Spodocybe*. In consequence, it is foreseeable that *C. trulliformis* and other related clitocyboid species will eventually be moved to *Spodocybe*. Accordingly, more taxonomic work is needed in future.

The placements of *Spodocybe*, *Cuphophyllus*, *Ampulloclitocybe* and *Cantharocybe*

In previous studies, *Cuphophyllus*, *Ampulloclitocybe* and *Cantharocybe* were treated as basal in Hygrophoraceae (Lodge et al. 2014), but their phylogenetic placements were not resolved. In a six-gene phylogenetic analysis by Binder et al. (2010) and a three-gene analysis by Wang et al. (2018), *Ampulloclitocybe* and *Cantharocybe* were located between *Cuphophyllus* and the rest of the Hygrophoraceae, but without support. While two four-gene analyses by Lodge et al. (2014) showed that *Ampulloclitocybe* and *Cantharocybe* were sister clades as basal to *Cuphophyllus* along with the rest of the Hygrophoraceae with weak support. However, in our six-gene analysis (Fig. 2), the new proposed genus *Spodocybe* and *Ampulloclitocybe* were sisters (BP = 78%, PP = 0.99) and they clustered with *Cantharocybe* followed by *Cuphophyllus*, forming a supported monophyletic sister clade to the rest of the Hygrophoraceae (BP = 83%, PP = 1.00). Hence, *Spodocybe*, *Ampulloclitocybe*, *Cantharocybe* and *Cuphophyllus* should be retained in Hygrophoraceae, and a new subfamily, Cuphophylloideae, is proposed to accommodate the lineage.

Acknowledgements

The authors are very grateful to their colleagues at Kunming Institute of Botany, Chinese Academy of Sciences, including Drs. Xiang-Hua Wang, Jiao Qin, Bang Feng, Qi Zhao and Master students Hua Qu and Si-Peng Jian for collecting and providing specimens; and Drs. Gang Wu, Yang-Yang Cui, Qing Cai for providing help on morphological observation and phylogenetic analysis. This study was financed by Yunnan Ten-Thousand-Talents Plan – Yunling Scholar Project and Postdoctoral Directional Training Foundation of Yunnan Province.

References

Alvarado P, Moreno G, Vizzini A, Consiglio G, Manjón JL, Setti L (2015) *Atractosporocybe*, *Leucocybe* and *Rhizocybe*: three new clitocyboid genera in the Tricholomatoid clade (Agaricales) with notes on *Clitocybe* and *Lepista*. Mycologia 107(1): 123–136. https://doi.org/10.3852/13-369

Ammirati JF, Parker AD, Matheny PB (2007) *Cleistocybe*, a new genus of Agaricales. Mycoscience 48(5): 282–289. https://doi.org/10.1007/S10267-007-0365-5

Bas C, Kuyper TW, Noordeloos ME, Vellinga EC (1995) Flora agaricina neerlandica 3: critical monographs on families of agarics and boleti occurring in the Netherlands. A. A. Balkema, Rotterdam, 183 pp.

Binder M, Larsson KH, Matheny PB, Hibbett DS (2010) Amylocorticiales ord. nov. and Jaapiales ord. nov.: early diverging clades of Agaricomycetidae dominated by corticioid forms. Mycologia 102(4): 865–880. https://doi.org/10.3852/09-288

Breitenbach J, Kraenzlin F (1991) Fungi of Switzerland 3: Boletales and Agaricales. Mykologia, Luzern, 361 pp.

Hall TA (1999) BioEdit: a user-friendly biological sequence alignment editor and analysis program for windows 95/98/NT. Nucleic Acids Symposium Series 41: 95–98.

Harmaja H (2002) *Amylolepiota*, *Clavicybe* and *Cystodermella*, new genera of the Agaricales. Karstenia 42(2): 39–48. https://doi.org/10.29203/ka.2002.386

Harmaja H (2003) Notes on *Clitocybe* s. lato (Agaricales). Annales Botanici Fennici 40(3): 213–218.

Hosen MI, Li TH, Lodge DJ, Rockefeller A (2016) The first ITS phylogeny of the genus *Cantharocybe* (Agaricales, Hygrophoraceae) with a new record of *C. virosa* from Bangladesh. Mycokeys 14: 37–50. https://doi.org/10.3897/mycokeys.14.9859

Karsten PA (1879) Rysslands, Finlands och den Skandinaviska halföns Hattsvampar. Förra Delen: Skifsvampar. Bidrag till Kännedom av Finlands Natur och Folk 32: 1–571.

Katoh K, Standley DM (2016) A simple method to control over-alignment in the MAFFT multiple sequence alignment program. Bioinformatics 32(13): 1933–1942. https://doi.org/10.1093/bioinformatics/btw108

Kornerup A, Wanscher JH (1978) Methuen handbook of colour (3rd edn). Eyre Methuen, London, 252 pp.

Kretzer AM, Bruns TD (1999) Use of *atp6* in fungal phylogenetics: an example from the Boletales. Molecular Phylogenetics and Evolution 13(3): 483–492. https://doi.org/10.1006/mpev.1999.0680

Læssøe T, Petersen JH (2019) Fungi of temperate Europe. Princeton University Press, Princeton, 1708 pp.

Lodge DJ, Padamsee M, Matheny PB, Aime MC, Cantrell SA, Boertmann D, Kovalenko A, Vizzini A, Dentinger BTM, Kirk PM, Ainsworth AM, Moncalvo JM, Vilgalys R, Larsson E, Lücking R, Griffith GW, Smith ME, Norvell LL, Desjardin DE, Redhead SA, Ovrebo CL, Lickey EB, Ercole E, Hughes KW, Courtecuisse R, Young A, Binder M, Minnis AM, Lindner DL, Ortiz-Santana B, Haight J, Læssøe T, Baroni TJ, Geml J, Hattori T (2014) Molecular phylogeny, morphology, pigment chemistry and ecology in Hygrophoraceae (Agaricales). Fungal Diversity 64: 1–99. https://doi.org/10.1007/s13225-013-0259-0

Matheny PB (2005) Improving phylogenetic inference of mushrooms with RPB1 and RPB2 nucleotide sequences (*Inocybe*; Agaricales). Molecular Phylogenetics and Evolution 35(1): 1–20. https://doi.org/10.1016/j.ympev.2004.11.014

Matheny PB, Liu YJ, Ammirati JF, Hall BD (2002) Using RPB1 sequences to improve phylogenetic inference among mushrooms (*Inocybe*, Agaricales). American Journal of Botany 89(4): 688–698. https://doi.org/10.3732/ajb.89.4.688

Matheny PB, Hofstetter V, Aime MC, Moncalvo JM, Ge ZM, Yang ZL, Slot JC, Ammirati JF, Baroni TJ, Bougher NL, Hughes NW, Lodge DJ, Kerrigan R, Seidl MT, Aanen DK, DeNitis M, Daniele GM, Desjardin DE, Kropp BR, Norvell LL, Parker A, Vellinga EC, Vilgalys R, Hibbett DS (2006) Major clades of Agaricales: a multilocus phylogenetic overview. Mycologia 98(6): 982–995. https://doi.org/10.1080/15572536.2006.11832627

Matheny PB, Wang Z, Binder M, Curtis JM, Lim YW, Nilsson H, Hughes KW, Hofstetter V, Ammirati JF, Schoch CL, Langer E, Langer G, McLaughlin DJ, Wilson AW, Frøslev T, Ge ZW, Kerrigan RW, Slot JC, Yang ZL, Baroni TJ, Fischer M, Hosaka K, Matsuura K, Seidl MT, Vauras J, Hibbett DS (2007) Contributions of *rpb2* and *tef1* to the phylogeny of mushrooms and allies (Basidiomycota, Fungi). Molecular Phylogenetics and Evolution 43(2): 430–451. https://doi.org/10.1016/j.ympev.2006.08.024

Moncalvo JM, Vilgalys R, Redhead SA, Johnson JE, James TY, Aime MC, Hofstetter V, Verduin SJW, Larsson E, Baroni TJ, Thorn RG, Jacobsson S, Clémençon H, Miller Jr OK (2002) One hundred and seventeen clades of euagarics. Molecular Phylogenetics and Evolution 23(3): 357–400. https://doi.org/10.1016/S1055-7903(02)00027-1

Nylander JAA (2004) MrModeltest v2. Program distributed by the author. Evolutionary Biology Centre, Uppsala University.

Ovrebo CL (2011) A new *Cantharocybe* from Belize with notes on the type of *Cantharocybe gruberi*. Mycologia 103(5): 1102–1109. https://doi.org/10.3852/10-360

Qin J, Feng B, Yang ZL, Li YC, Ratkowsky D, Gates G, Takahashi H, Rexer KH, Kost GW, Karunarathna SC (2014) The taxonomic foundation, species circumscription and continental endemisms of *Singerocybe*: evidence from morphological and molecular data. Mycologia 106(5): 1015–1026. https://doi.org/10.3852/13-338

Redhead SA, Lutzoni F, Moncalvo JM, Vilgalys R (2002) Phylogeny of agarics: partial systematics solutions for core omphalinoid genera in the Agaricales (euagarics). Mycotaxon 83: 19–57.

Ronquist F, Huelsenbeck JP (2003) MrBayes 3: Bayesian phylogenetic inference under mixed models. Bioinformatics 19(12): 1572–1574. https://doi.org/10.1093/bioinformatics/btg180

Singer R (1986) The Agaricales in Modern Taxonomy (4th edn). Koeltz Scientific Books, Koenigstein, 981 pp.

Stamatakis A (2006) RAxML-VI-HPC: maximum likelihood-based phylogenetic analyses with thousands of taxa and mixed models. Bioinformatics 22(21): 2688–2690. https://doi.org/10.1093/bioinformatics/btl446

Vaidya G, Lohman DJ, Meier R (2011) Sequencematrix: concatenation software for the fast assembly of multi-gene datasets with character set and codon information. Cladistics 27(2): 171–180. https://doi.org/10.1111/j.1096-0031.2010.00329.x

Vilgalys R, Hester M (1990) Rapid genetic identification and mapping of enzymatically amplified ribosomal DNA from several *Cryptococcus* species. Journal of Bacteriology 172(8): 4238–4246. https://doi.org/10.1128/JB.172.8.4238-4246.1990

Vizzini A, Musumeci E, Murat C (2010) *Trichocybe*, a new genus for *Clitocybe puberula* (Agaricomycetes, Agaricales). Fungal Diversity 42: 97–105. https://doi.org/10.1007/s13225-010-0030-8

Voitk A, Saar I, Lodge DJ, Boertmann D, Berch SM, Larsson E (2020) New species and reports of *Cuphophyllus* from northern North America compared with related Eurasian species. Mycologia 112(2): 438–452. https://doi.org/10.1080/00275514.2019.1703476

Wang CQ, Zhang M, Li TH, Liang XS, Shen YH (2018) Additions to tribe Chromosereae (Basidiomycota, Hygrophoraceae) from China, including *Sinohygrocybe* gen. nov. and a first report of *Gloioxanthomyces nitidus*. Mycokeys 38: 59–76. https://doi.org/10.3897/mycokeys.38.25427

White TJ, Bruns T, Lee S, Taylor J (1990) Amplification and direct sequencing of fungal ribosomal RNA genes for phylogenetics. In: Innis MA, Gelfand DH, Sninsky JJ, White TJ (Eds) PCR protocols: a guide to methods and applications. Academic Press, San Diego, 315–322. https://doi.org/10.1016/B978-0-12-372180-8.50042-1

Supplementary material 1

Alignment of ITS-LSU-RPB2 dataset used in the three-gene phylogenetic analysis

Authors: Zheng-Mi He, Zhu L. Yang

Data type: fasta file

Explanation note: ITS: 1-1380, LSU: 1381–2356, RPB2: 2357–3135.

Link: https://doi.org/10.3897/mycokeys.79.66302.suppl1

Supplementary material 2

Alignment of ITS-LSU-RPB1-RPB2-TEF1-ATP6 dataset used in the six-gene phylogenetic analysis

Authors: Zheng-Mi He, Zhu L. Yang

Data type: fasta file

Explanation note: ITS: 1–1217, LSU: 1218–2158, RPB1: 2159–3358, RPB2: 3359–4089, TEF1: 4090–4967, ATP6: 4968–5405

Link: https://doi.org/10.3897/mycokeys.79.66302.suppl2

Supplementary material 3

Alignment of ITS dataset used in the single-gene phylogenetic analysis

Authors: Zheng-Mi He, Zhu L. Yang

Data type: fasta file

Link: https://doi.org/10.3897/mycokeys.79.66302.suppl3

MycoKeys 79: 149–172 (2021)
doi: 10.3897/mycokeys.79.63908
https://mycokeys.pensoft.net

RESEARCH ARTICLE

A peer-reviewed open-access journal
MycoKeys
Launched to accelerate biodiversity research

Phylogeny and diversity of *Bjerkandera* (Polyporales, Basidiomycota), including four new species from South America and Asia

Chao-Ge Wang[1], Josef Vlasák[2], Yu-Cheng Dai[1]

1 *School of Ecology and Nature Conservation, Beijing Forestry University, Beijing 100083, China* **2** *Biology Centre, Czech Academy of Sciences, Institute of Plant Mol. Biol., Branišovská 31, CZ-370 05 České Budějovice, Czech Republic*

Corresponding author: Yu-Cheng Dai (yuchengd@yahoo.com)

Academic editor: R. H. Nilsson | Received 3 February 2021 | Accepted 13 April 2021 | Published 26 April 2021

Citation: Wang C-G, Vlasák J, Dai Y-C (2021) Phylogeny and diversity of *Bjerkandera* (Polyporales, Basidiomycota), including four new species from South America and Asia. MycoKeys 79: 149–172. https://doi.org/10.3897/mycokeys.79.63908

Abstract

Four new species of *Bjerkandera*, viz. *B. ecuadorensis*, *B. fulgida*, *B. minispora*, and *B. resupinata* **spp. nov.**, are described from tropical America and Asia. *B. ecuadorensis* is characterised by dark grey to black pore surface, a monomitic hyphal system, hyaline to yellowish-brown generative hyphae, and ellipsoid basidiospores measuring 3.9–4.5 × 2.7–3 µm. *B. fulgida* is distinguished from the other species in the genus by clay buff to pale brown and shiny pore surface. *B. minispora* is characterised by white tomentose pore mouth and small basidiospores measuring 3.1–4.2 × 2–2.8 µm. *B. resupinata* is characterised by resupinate basidiomata, pinkish buff to pale brownish pore surface, and ellipsoid to broadly ellipsoid basidiospores measuring 4.5–6 × 3.2–4.1 µm. All these new species grow on angiosperm trunks or rotten wood, and cause a white rot. The closely related taxa to four new species are discussed. An identification key to the ten accepted species of *Bjerkandera* is provided, and a phylogeny comprising all known *Bjerkandera* species is provided.

Keywords

Phylogeny, polypore, taxonomy, wood-decaying fungi

Introduction

The genus *Bjerkandera* P. Karst. (Polyporales, Basidiomycota), typified by *B. adusta* (Willd.) P. Karst., was established by Karsten (1879). It is traditionally characterised by annual, effused-reflexed to pileate basidiomata, the presence of a dark resinous layer between context and tubes, grey to black pore surface, which contrasts with the pale cream context, a monomitic hyphal system with abundant clamps on generative hyphae, oblong ellipsoid to ellipsoid, hyaline, thin-walled basidiospores, and a white-rotting ecology (Murrill 1907; Ryvarden and Gilbertson 1993; Núñez and Ryvarden 2001; Westphalen et al. 2015; Cui et al. 2019). Based on the above morphological studies, *Bjerkandera* and *Gloeoporus* Mont. share some important characteristics, and both genera are confused about definition (Pilát 1937; Corner 1989; Motato-Vásquez et al. 2020). Also, *Tyromyces* P. Karst. is defined by white, annual, resupinate to pileate basidiomata, a mono-dimitic hyphal system with clamped generative hyphae, and a white-rotting ecology, so *Tyromyces* and *Bjerkandera* overlap in many characteristics (Ryvarden 1991; Pouzar 1966; Núñez and Ryvarden 2001). Due to these similarities, Pouzar (1966) considered *Bjerkandera* as subgenus of *Tyromyces* (Kotlaba and Pouzar 1964). Nevertheless, recent phylogenetic analyses have showed that *Bjerkandera*, *Gloeoporus*, and *Tyromyces* belong to different clades in the families Phanerochaetaceae Jülich (Syn. Bjerkanderaceae Jülich 1981), Irpicaceae Spirin & Zmitr., and Incrustoporiaceae Jülich, respectively (Binder et al. 2013; Floudas and Hibbett 2015; Justo et al. 2017; Jung et al. 2018; Viktor and Bálint 2018; Cui et al. 2019; Motato-Vásquez et al. 2020). Morphologically, *Tyromyces* differs in pale tubes not darkening upon drying, and *Gloeoporus* usually has a continuum hymenium (covering the dissepiments) and gelatinous tubes (Ryvarden and Gilbertson 1993), while species of *Bjerkandera* have distinct sterile dissepiments, and corky to hard corky tubes.

Bjerkandera is a common polypore genus that grows mostly on dead angiosperm wood and has a wide distribution around the world. Two species, *Bjerkandera adusta* (Willd.) P. Karst. and *B. fumosa* (Pers.) P. Karst., are well recognised in the northern hemisphere (Gilbertson and Ryvarden 1986; Jung et al. 2014; Ryvarden and Melo 2017; Cui et al. 2019). *Tyromyces atroalbus* (Rick) Rajchenb. was combined into *Bjerkandera* based on morphology and molecular phylogenetic analysis (Westphalen et al. 2015). Recently, two new species, *Bjerkandera albocinerea* Motato-Vásq., Robledo & Gugliotta and *B. centroamericana* Kout, Westphalen & Tomšovský, were described from the neotropics based on morphological characters and molecular data (Westphalen et al. 2015; Motato-Vásquez et al. 2020). Additionally, *B. mikrofumosa* Ryvarden was described from Venezuela without molecular data (Ryvarden 2016), but DNA sequences from this species were generated by Motato-Vásquez et al. (2020).

During a study on polypores collected from China, Ecuador, and Thailand, four unknown species of *Bjerkandera* were distinguished by both morphological and molecular data. They are described and illustrated in this study. In this study, nuclear ribosomal RNA genes were used to determine the phylogenetic position of the new species. Furthermore, an identification key to all the accepted species in the genus is provided.

Materials and methods

Morphological studies

The studied specimens are deposited in the herbaria of the Institute of Microbiology, Beijing Forestry University (**BJFC**), and the private herbarium of Josef Vlasák (**JV**), which will later be deposited at the National Museum Prague of Czech Republic (**PRM**). Morphological descriptions are based on field notes and herbarium specimens. Microscopic analyses follow Miettinen et al. (2018). In the description: **KOH** = 5% potassium hydroxide, **IKI** = Melzer's reagent, **IKI–** = neither amyloid nor dextrinoid, **CB** = Cotton Blue, **CB+** = cyanophilous in Cotton Blue, **CB–** = acyanophilous in Cotton Blue, **L** = arithmetic average of all spore length, **W** = arithmetic average of all spore width, **Q** = L/W ratios, and **n** = number of spores/measured from given number of specimens. Colour terms are cited from Anonymous (1969) and Petersen (1996).

Molecular studies and phylogenetic analysis

A CTAB rapid plant genome extraction kit-DN14 (Aidlab Biotechnologies Co., Ltd, Beijing) was used to obtain DNA from dried specimens, and to perform the polymerase chain reaction (PCR) according to the manufacturer's instructions with some modifications (Shen et al. 2019; Sun et al. 2020). Two DNA gene fragments – internal transcribed spacer (ITS) and large subunit nuclear ribosomal RNA gene (nLSU) – were amplified using the primer pairs ITS5/ITS4 and LR0R/LR7 (White et al. 1990; Hopple and Vilgalys 1999) (http://www.biology.duke.edu/fungi/mycolab/primers.htm). The PCR procedures for ITS and nLSU followed Zhao et al. (2013) in the phylogenetic analyses. DNA sequencing was performed at Beijing Genomics Institute and the newly-generated sequences were deposited in GenBank (Sayers et al. 2021). Sequences generated for this study were aligned with additional sequences downloaded from GenBank using BioEdit (Hall 1999) and ClustalX (Thompson et al. 1997). The final ITS and nLSU datasets were subsequently aligned using MAFFT v.7 under the E-INS-i strategy with no cost for opening gaps and equal cost for transformations (command line: mafft –genafpair –maxiterate 1000) (Katoh and Standley 2013) and visualised in BioEdit (Hall 1999).

In this study, nuclear ribosomal RNA genes were used to determine the phylogenetic position of the new species. The sequence alignment was deposited at TreeBase (submission ID 27872). Sequences of *Tyromyces chioneus* (Fr.) P. Karst, obtained from GenBank, was used as outgroup (Westphalen et al. 2015).

The phylogenetic analyses followed the approach of Han et al. (2016) and Zhu et al. (2019). Maximum parsimony (MP), maximum likelihood (ML), and Bayesian inference (BI) analyses were conducted for the datasets of ITS and nLSU sequences. The best-fit evolutionary model was selected by hierarchical likelihood ratio tests (hLRT) and Akaike Information Criterion (AIC) in MrModeltest 2.2 (Nylander 2004) after scoring 24 models of evolution in PAUP* version 4.0b10 (Swofford 2002).

The MP topology and bootstrap values (MP-BS) obtained from 1000 replicates were computed in PAUP* version 4.0b10 (Swofford 2002). All characters were equally weighted, and gaps were treated as missing. Trees were inferred using the heuristic search option with TBR branch swapping and 1000 random sequence additions. Max-trees were set to 5,000 branches of zero length were collapsed, and all parsimonious trees were saved. Descriptive tree statistics tree length (TL), composite consistency index (CI), retention index (RI), rescaled consistency index (RC), and homoplasy index (HI) were calculated for each maximum parsimonious tree (MPT) generated. Sequences were also analysed using Maximum Likelihood (ML) with RAxML-HPC2 through the CIPRES Science Gateway (www.phylo.org; Miller et al. 2009). Branch support (BT) for ML analysis was determined by 1000 bootstrap replicates.

Bayesian phylogenetic inference and Bayesian posterior probabilities (BPP) were computed with MrBayes 3.1.2 (Ronquist and Huelsenbeck 2003). Four Markov chains were run for 3,500,000 generations until the split deviation frequency value was less than 0.01 and trees were sampled every 100 generations. The first 25% of the sampled trees were discarded as burn-in and the remaining ones were used to reconstruct a majority rule consensus and calculate Bayesian posterior probabilities (BPP) of the clades.

Branches that received bootstrap support for maximum parsimony (≥ 75% MP-BT), maximum likelihood (≥75% (ML-BS)), and Bayesian posterior probabilities (≥ 0.95BPP) were considered as significantly supported.

Results

Phylogeny

The combined ITS and nLSU dataset contained sequences from 75 specimens, comprising a total of 40 species (Table 1). The dataset had an aligned length of 2158 characters, of which 1410 (65%) characters are constant, 208 (0.1%) are variable and parsimony-uninformative and 540 (25%) are parsimony informative. Maximum parsimony analysis yielded eleven equally-parsimonious tree (TL = 2701, CI = 0.439, RI = 0.751, RC = 0.330, HI = 0.561), and a strict consensus tree of these trees is shown in Fig. 1. The best model-fit applied in the Bayesian analysis was GTR+I+G, lset nst = 6, rates = invgamma, and prset statefreqpr = dirichlet (1, 1, 1, 1). Bayesian analysis resulted in the nearly congruent topology with an average standard deviation of split frequencies = 0.006804 to MP and ML analysis, and thus only the MP tree was provided.

In our phylogeny (Fig. 1), the genus *Bjerkandera* was supported as a monophyletic clade, which was consistent with previous studies on monophyly nature of *Bjerkandera* (Westphalen et al. 2015; Motato-Vásquez et al. 2020). *Bjerkandera ecuadorensis*, *B. fulgida*, *B. minispora*, and *B. resupinata* were nested within the *Bjerkandera* forming four distinct lineages (95/98/1.00, 90/87/1.00, 100/100/1.00, and 60/85/0.90 respectively).

Table 1. Information on the sequences used in this study. New sequences are shown in bold.

Species	Specimen number	Countries	GenBank accession numbers	
			ITS	LSU
Aurantiporus croceus	Miettinen-16483	Malaysia	KY948745	KY948901
Bjerkandera adusta	**Dai 14516**	**China**	**MW507097**	**MW520204**
B. adusta	**Dai 15665**	**China**	**MW507098**	**MW520205**
B. adusta	**Dai 15495**	**China**	**MW507099**	–
B. adusta	SFC20120409-08	Rep. Korea	KJ704814	KJ704829
B. adusta	SFC20111029-15	Rep. Korea	KJ704813	KJ704828
B. adusta	**Dai 13201**	**France**	**MW507100**	**MW520206**
B. adusta	**Dai 12640**	**Finland**	**MW507101**	–
B. albocinerea	MV 346	Brazil	MH025421	MH025421
B. albocinerea	RP 317	Brazil	MH025420	–
B. albocinerea	**Dai 16411**	**USA**	**MW507102**	**MW520207**
B. atroalba	MW 425	Brazil	KT305930	KT305930
B. atroalba	MV 158	Brazil	KT305932	KT305932
B. atroalba	**Dai 17457**	**Brazil**	**MW507103**	**MW520208**
B. centroamericana	JK0610/A13	Mexico	KT305934	KT305934
B. centroamericana	JK0610/A7	Mexico	KT305933	KT305933
B. centroamericana	**JV1704/97**	**Costa Rica**	**MW507104**	–
B. ecuadorensis	**JV1906/C16-J**	**Ecuador**	**MW507105**	–
B. fulgida	**Dai 16107**	**China**	**MW507106**	**MW520209**
B. fulgida	**Dai 12284**	**China**	**MW507107**	–
B. fulgida	**Dai 13597**	**China**	**MW507108**	**MW520210**
B. fumosa	SFC20121009-04	Rep. Korea	KJ704824	KJ704839
B. fumosa	**Dai 21100**	**China**	**MW507109**	**MW520211**
B. fumosa	**Dai 21087**	**China**	**MW507110**	–
B. fumosa	**Cui 10747**	**China**	**MW507111**	**MW520212**
B. fumosa	**Dai 12674B**	**Finland**	**MW507112**	**MW520213**
B. fumosa	N37	Latvia	FJ903376	–
B. fumosa	Homble 1900	Norway	KF698740	KF698751
B. mikrofumosa	MV 353	Brazil	MH025416	MH025416
B. mikrofumosa	MV 363	Brazil	MH023526	MH023526
B. mikrofumosa	**JV1707/10J-1**	**Costa Rica**	**MW507113**	–
B. mikrofumosa	**JV1707/10J-2**	**Costa Rica**	**MW507114**	–
B. minispora	**Dai 15234**	**China**	**MW507115**	**MW520214**
B. minispora	**Cui 5376**	**China**	**MW507116**	**MW520215**
B. resupinata	**Dai 16642**	**Thailand**	**MW507117**	**MW520216**
B. resupinata	**Cui 8017**	**China**	**KU509526**	–
Byssomerulius corium	KHL 8593	–	AY463389	AY586640
Ceriporia viridans	KHL 8765	–	AF347109	AF347109
Ceriporiopsis alboaurantia	Cui 4136	China	KF845955	KF845948
C. alboaurantia	Cui 2877	China	KF845954	KF845947
C. aneirina	TAA 181186	Estonia	FJ496683	FJ496704
C. aneirina	H 6002107	Finland	FJ496682	FJ496705
C. carnegieae	RLG-7277-T	USA	KY948792	KY948854
C. carnegieae	JV1209/45	USA	KX081134	–
C. carnegieae	**JV0407/27-J**	**USA**	**MW507122**	–
C. fimbriata	Dai 11672	China	KJ698633	KJ698637
C. fimbriata	Cui 1671	China	KJ698634	KJ698638
C. gilvescens	BRNM 710166	Czech	FJ496684	FJ496720
C. gilvescens	BRNM 709970	Czech	EU546104	FJ496721
C. pseudogilvescens	BRNM 686416	Slovakia	FJ496679	FJ496703
C. pseudogilvescens	TAA 168233	Estonia	FJ496673	FJ496702
***Ceriporiopsis* sp.**	**JV1512/13-J**	**Costa Rica**	**MW507118**	–
Gloeoporus taxicola	SK 0075	Sweden	JX109847	JX109847
G. pannocinctus	FP 135015	USA	MG572755	MG572739
G. thelephoroides	BZ 2896	Belize	MG572757	MG572741
Hapalopilus nidulans	FD-512	USA	KP135419	–
Hydnophlebia chrysorhiza	FD-282	USA	KP135338	KP135217

Species	Specimen number	Countries	GenBank accession numbers	
			ITS	LSU
Hyphodermella corrugata	KHL 3663	Norway	EU118630	EU118630
Irpex lacteus	DO 421951208	Sweden	JX109852	JX109852
Merulius tremellosus	FD-323	USA	–	KP135231
Mycoacia fuscoatra	KHL 13275	Estonia	JN649352	JN649352
M. nothofagi	KHL 13750	France	GU480000	GU480000
Phanerochaete chrysosporium	BKM-F-1767	–	HQ188436	GQ470643
P. sordida	KHL 12054	Norway	EU118653	EU118653
Phlebia nitidula	GB 020830	Sweden	EU118655	EU118655
P. radiata	AFTOL 484	–	AY854087	AF287885
Phlebiopsis gigantea	FP-70857-Sp	USA	KP135390	KP135272
Porostereum spadiceum	KUC 2013051	Rep. Korea	KJ668473	KJ668325
Terana caerulea	FP 10473	USA	KP134980	KP135276
Trametopsis cervina	TJV 93216 T	USA	JN165020	JN164796
Tyromyces chioneus	Miettinen 7487	Finland	HQ659244	HQ659244
T. fissilis	**Dai 18182**	**China**	**MW507119**	**MW520217**
T. fissilis	**Dai 19583**	**China**	**MW507120**	**MW520218**
T. fissilis	BRNM 699803	Czech	HQ728292	HQ729002
T. fissilis	**Dai 19589**	**China**	**MW507121**	–

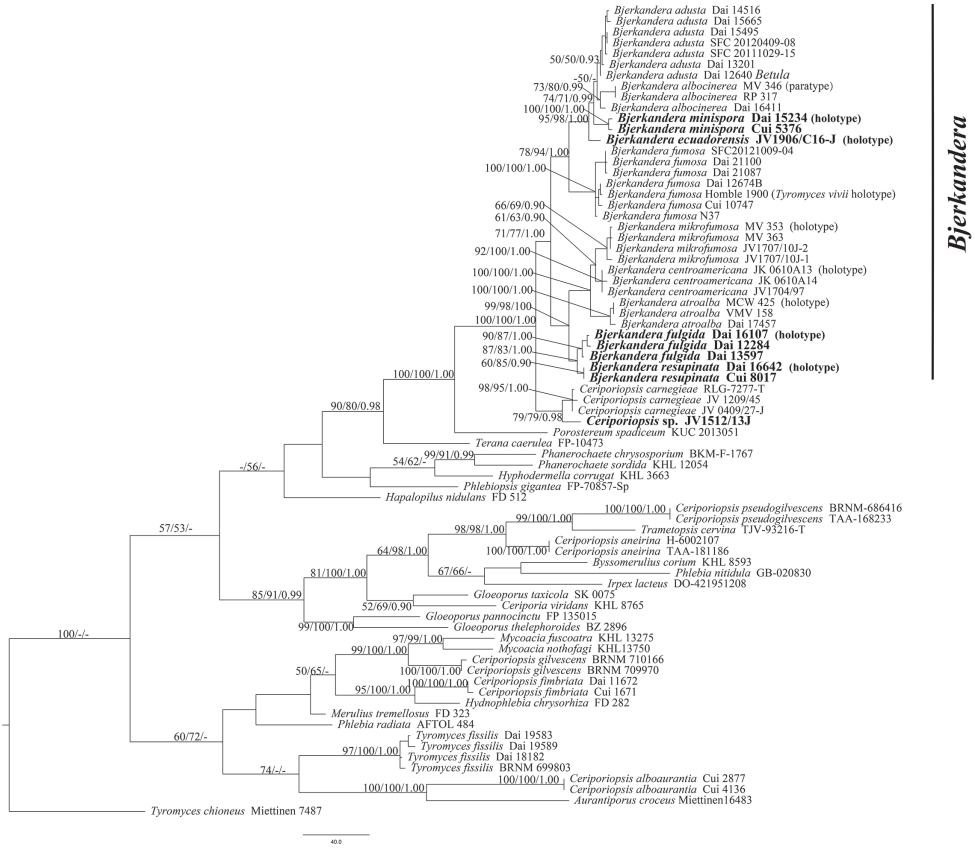

Figure 1. Phylogeny of *Bjerkandera* and related species generated by maximum parsimony analysis, based on combined ITS and nLSU sequences. Bootstrap support for maximum parsimony (MP), maximum likelihood (ML), and Bayesian posterior probabilities: (BPP) ≥ 50% (MP-BT), 50% (ML-BS) and 0.90 (BPP) are given in relation to the branches.

Taxonomy

***Bjerkandera ecuadorensis* Y.C. Dai, Chao G. Wang & Vlasák, sp. nov.**
MycoBank No: 538578
Figs 2, 3

Diagnosis. *Bjerkandera ecuadorensis* is characterised by grey to dark-brown pore surface, tiny pores (7–9 per mm), and ellipsoid basidiospores measuring 3.9–4.5 × 2.7–3 µm.

Type. Ecuador, Pichincha Province, volcan Pasochoa, 3300 m, VI. 2019, J. Vlasák Jr. JV 1906/C16-J (holotype in PRM, isotypes in JV and BJFC032992).

Etymology. *Ecuadorensis* (Lat.): referring to the species being found in Ecuador.

Basidiomata. Annual, pileate, soft corky, without odor or taste when fresh, becoming corky when dry, projecting up to 4 cm, 5 cm wide and 1.3 mm thick at base. Pileal surface pinkish-buff to buff, glabrous, faintly zonate, margin blunt. Pore surface grey to dark-brown, becoming almost black when touched or bruised; sterile margin distinct, up to 2 mm wide; pores round to angular, 7–9 per mm; dissepiments thin, entire. Context buff-yellow, slightly fibrous to corky, up to 1 mm thick. Tubes concolorous with the pore surface and darker than context, corky, up to 0.3 mm long, and with a distinct dark line between tubes and context.

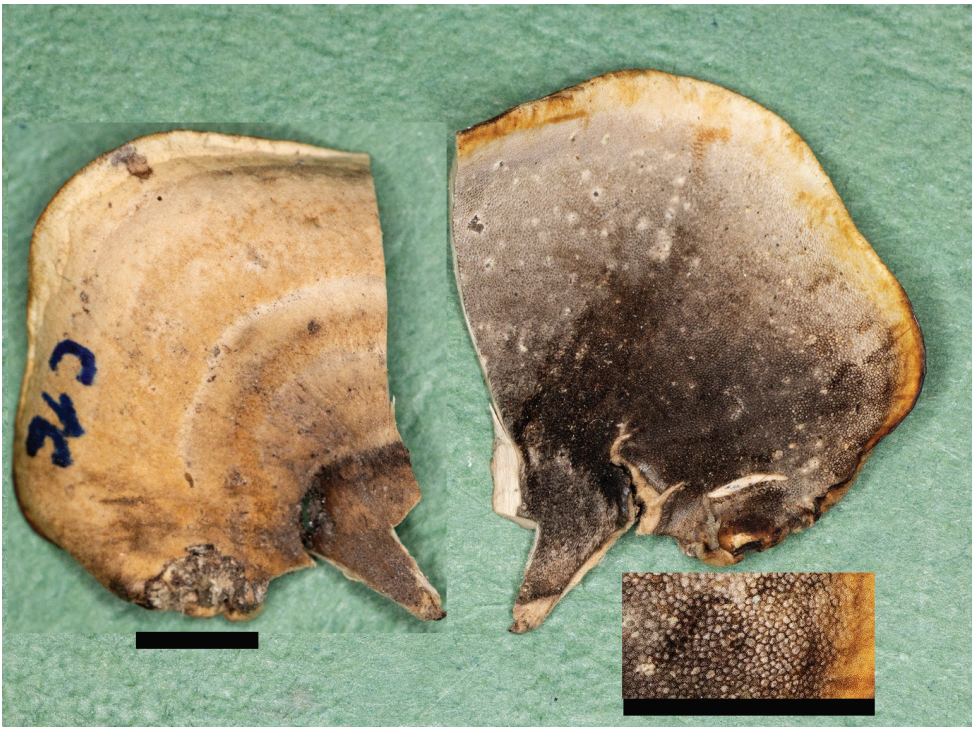

Figure 2. Pileal surface and pore surface of *Bjerkandera ecuadorensis* (holotype, JV 1906/C16-J). Scale bars: 4 mm.

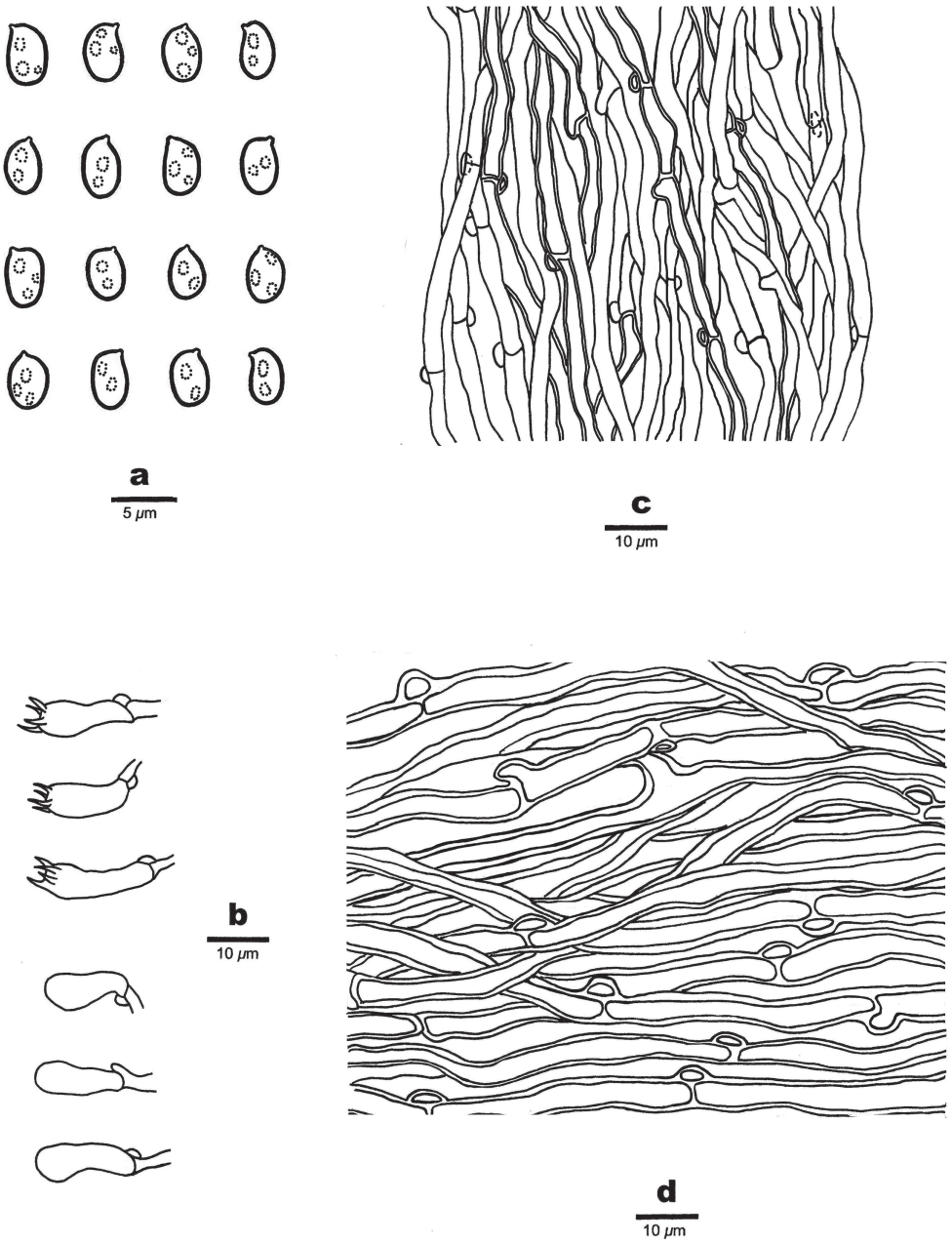

Figure 3. Microscopic structures of *Bjerkandera ecuadorensis* (holotype, JV 1906/C16-J) **a** basidiospores **b** basidia and basidioles **c** hyphae from trama **d** hyphae from context.

Hyphal structure. Hyphal system monomitic; generative hyphae with clamp connections, smooth, hyaline to yellowish-brown, CB+, IKI–; tissues becoming dark in KOH.

Context. Generative hyphae thick-walled with a wide lumen, occasionally branched, densely compacted, and more or less regularly arranged to loosely interwoven, up to 3.8–6 µm in diam.

Tubes. Generative hyphae thin- to slightly thick-walled, rarely branched, subparallel along the tubes to loosely interwoven, 2.5–3.8 µm in diam. Cystidia and cystidioles absent. Basidia clavate to barrel-shaped, with four sterigmata and a basal clamp connection, 13–14.5 × 4.5–5.5 µm; basidioles of similar shape to basidia, but smaller.

Basidiospores. Ellipsoid, hyaline, thin-walled, smooth, often with one or more guttules, CB–, IKI–, (3.8–)3.9–4.5 × 2.7–3 µm, L = 4.09 µm, W = 2.86 µm, Q = 1.43 (n = 30/1).

Remarks. *Bjerkandera ecuadorensis* is characterised by grey to dark-brown pore surface, small pores (7–9 per mm), hyaline to yellowish-brown generative hyphae, and ellipsoid basidiospores measuring 3.9–4.5 × 2.7–3 µm. Morphologically, *Bjerkandera ecuadorensis* is similar to *B. minispora* in having pinkish-buff to buff pileal surface and round to angular pores (6–9 per mm), but the latter has buff-yellow pore surface and smaller basidiospores (3.1–4.2 × 2–2.8 µm). *Bjerkandera adusta* resembles *B. ecuadorensis* by having grey to dark-brown pore surface, distinct sterile margin, but the former has short-cylindric to subellipsoid and bigger basidiospores (4.5–6 × 2.5–3.5 µm, Ryvarden and Melo 2017).

***Bjerkandera fulgida* Y.C. Dai & Chao G. Wang, sp. nov.**
MycoBank No: 838579
Figs 4, 5

Diagnosis. *Bjerkandera fulgida* is characterised by the clay buff to pale brown and shiny pore surface, and ellipsoid to broadly ellipsoid basidiospores measuring 3.9–4.5 × 2.8–3.3 µm.

Type. China. Hainan Province, Lingshui County, Diaoluoshan Forest Park, 18°42'N, 109°49'E, rotten angiosperm wood, 13.XI.2015, Y.C. Dai 16107 (holotype BJFC020200).

Etymology. *Fulgida* (Lat.): referring to the species having the shiny pore surface.

Basidiomata. Annual, effused-reflexed, soft corky, without odor or taste when fresh, becoming corky upon drying, resupinating up to 5.5 cm long, 3 cm wide and 1.3 mm thick, with a pileal projection up to 0.6 cm, 2.3 cm wide and 1.3 mm thick at base. Pileal surface pinkish buff to clay-buff, glabrous and faintly zonate when dry; margin acute. Pore surface clay-buff to pale brown, bruised part becoming dark brown to black when dry, shiny; sterile margin up to 2 mm wide; pores round or sometimes angular, 6–8 per mm; dissepiments thin, entire. Context pale cream, slightly fibrous to corky, up to 0.5 mm thick. Tubes concolorous with the pore surface, darker than context, corky, up to 0.8 mm long, with a distinct dark line between tubes and context.

Hyphal structure. Hyphal system monomitic; generative hyphae with clamp connections, smooth, hyaline to yellowish, CB+, IKI–; tissues becoming dark in KOH.

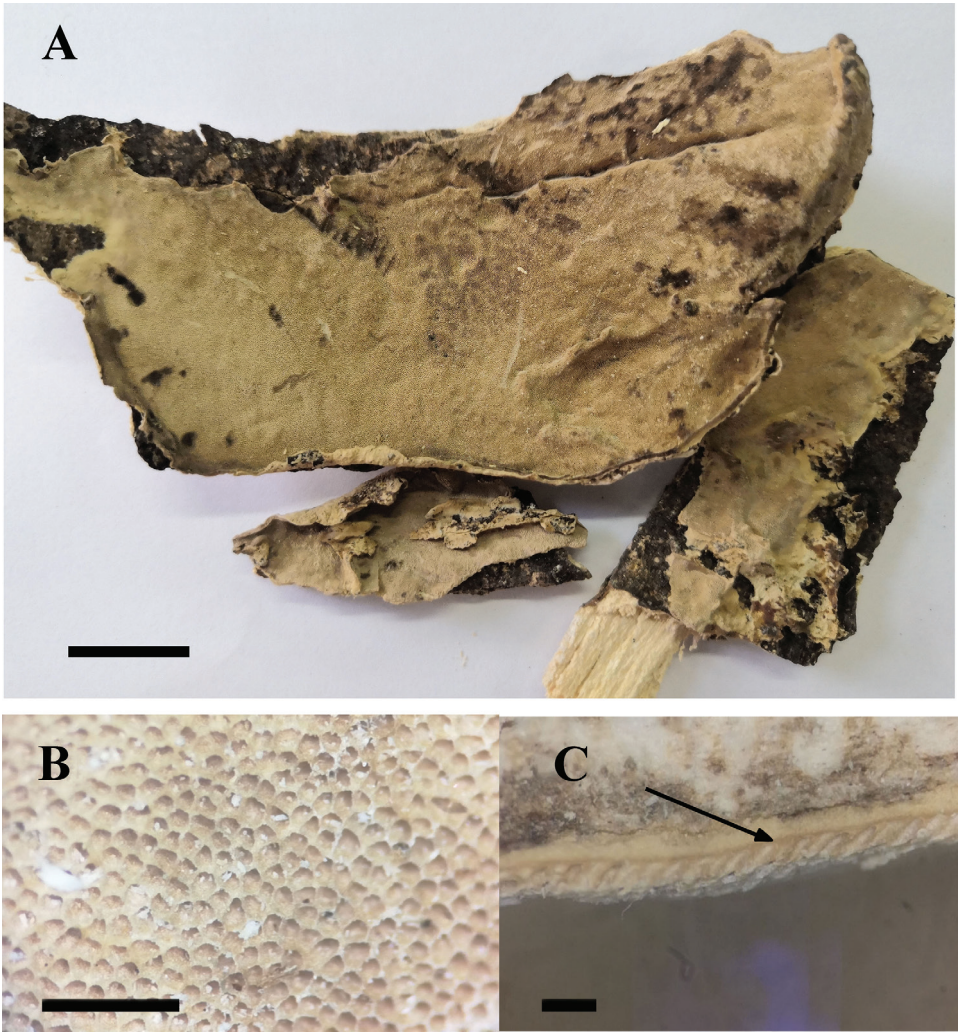

Figure 4. *Bjerkandera fulgida* (holotype, Y.C. Dai 16107) **A** basidiomata **B** poroid surface detail **C** a dark line between tubes and context. Scale bars: 1 cm (**A**); 1 mm (**B, C**).

Context. Hyphae thick-walled with a wide lumen, occasionally branched, loosely interwoven, 3–5 µm in diam.

Tubes. Hyphae thin- to slightly thick-walled, frequently branched, agglutinated and loosely interwoven, 2.5–3.5 µm in diam. Cystidia and cystidioles absent. Basidia clavate to more or less pyriform, with four sterigmata and a basal clamp connection, 10–12 × 4–5.5 µm; basidioles of similar shape to basidia, but smaller. Crystals present among hymenium.

Basidiospores. Ellipsoid to broadly ellipsoid, hyaline, thin-walled, smooth, CB–, IKI–, (3.8–)3.9–4.5 × (2.6–)2.8–3.3(–3.4) µm, L = 4.21 µm, W = 3.02 µm, Q = 1.37–1.43 (n = 90/3).

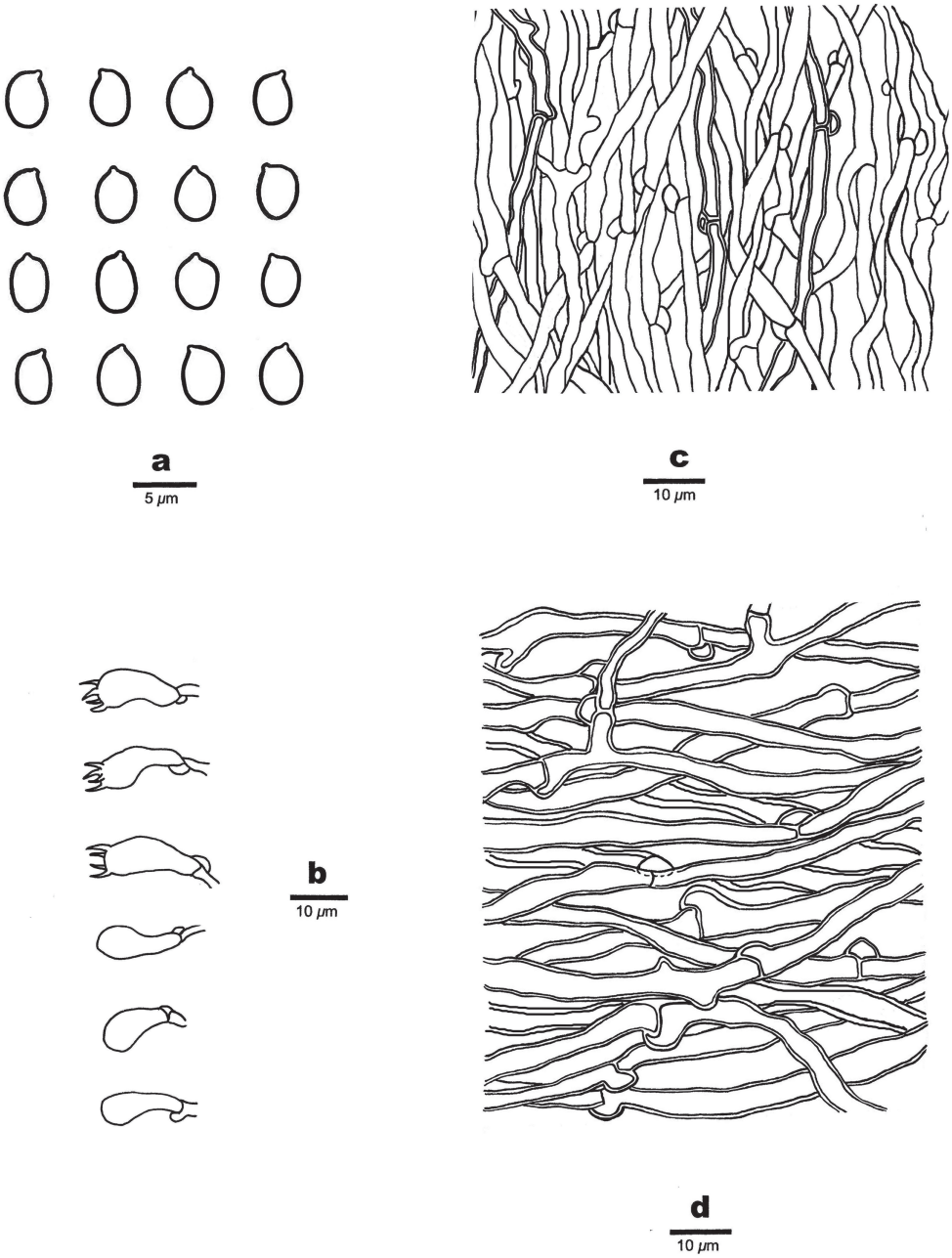

Figure 5. Microscopic structures of *Bjerkandera fulgida* (holotype, Y.C. Dai 16107) **a** basidiospores **b** basidia and basidioles **c** hyphae from trama **d** hyphae from context.

Additional specimens (paratypes) examined. China. Yunnan Province, Jinghong, Sanchahe Nature Reserve, 22°09'N, 100°51'E, fallen angiosperm trunk, 24. VI. 2011, Y.C. Dai 12284 (BJFC010566); Xishuangbanna Tropical Botanical

Garden, fallen angiosperm trunk, 21°55'N, 101°15'E, 21.X.2013, Y.C. Dai 13597 (BJFC015059).

Remarks. *Bjerkandera fulgida* is characterised by the resupinate to effused-reflexed basidiomata, clay buff to pale brown and shiny pore surface, and ellipsoid to broadly ellipsoid basidiospores measuring 3.9–4.5 × 2.8–3.3 µm. Phylogenetically, *Bjerkandera resupinata* nests in a sister clade to *B. fulgida* (Fig. 1), also having morphological similarities, as the pore surface coloration and presence of branched hyphae in the tubes. However, *B. resupinata* differs in having resupinate basidiomata, larger pores (4–6 per mm), and basidiospores measuring 4.5–6 × 3.2–4.1 µm.

Bjerkandera minispora **Y.C. Dai & Chao G. Wang, sp. nov.**
MycoBank No: 838580
Figs 6, 7

Diagnosis. The tiny pores (6–9 per mm), and ellipsoid small basidiospores measuring 3.1–4.2 × 2–2.8 µm set this species apart from others in *Bjerkandera*.

Type. China. Hainan Province, Wuzhishan County, Wuzhishan Nature Reserve, 18°54'N, 109°42'E, fallen angiosperm trunk, 31. V. 2015, Y.C. Dai 15234 (holotype BJFC019345).

Etymology. *Minispora* (Lat.): referring to the species having small basidiospores.

Basidiomata. Annual, pileate, solitary or imbricate, soft corky, without odor or taste when fresh, becoming corky when dry. Pilei flabelliform, projecting up to 4 cm, 5 cm wide and 3 mm thick at base. Pileal surface pinkish-buff to buff, becoming dark when touched, velutinate to glabrous, azonate; margin a bit acute. Pore surface buff-yellow, ash-grey to pale brown when dry, touched or bruised parts becoming almost black; sterile margin distinct, up to 1.5 mm wide; pores tiny, round to angular, 6–9 per mm; pores mouth sometimes with white tomentum; dissepiments thin, entire to lacerate. Context cream to pinkish-buff, corky, up to 2 mm thick. Tubes concolorous with the pore surface, darker than context, corky, up to 1 mm long, with a distinct dark line between tubes and context.

Hyphal structure. Hyphal system monomitic; generative hyphae with clamp connections, smooth, hyaline to pale yellow, CB+, IKI–; tissues becoming dark in KOH.

Context. Generative hyphae thick-walled with a wide lumen, moderately branched, loosely interwoven, 3.5–6 µm in diam.

Tubes. Generative hyphae thin-walled, frequently branched, agglutinated and loosely interwoven, 2.5–3.5 µm in diam. Cystidia and cystidioles absent. Basidia clavate, sometimes with an intermediate constriction, with four sterigmata and a basal clamp connection, 9.5–11.5 × 4–5 µm; basidioles of similar shape to basidia, but smaller.

Basidiospores. Oblong-ellipsoid to ellipsoid, hyaline, thin-walled, smooth, often with one or more guttules, CB–, IKI–, (3–)3.1–4.2(–4.8) × 2–2.8(–3) µm, L = 3.64 µm, W = 2.4 µm, Q = 1.49–1.54 (n = 60/2).

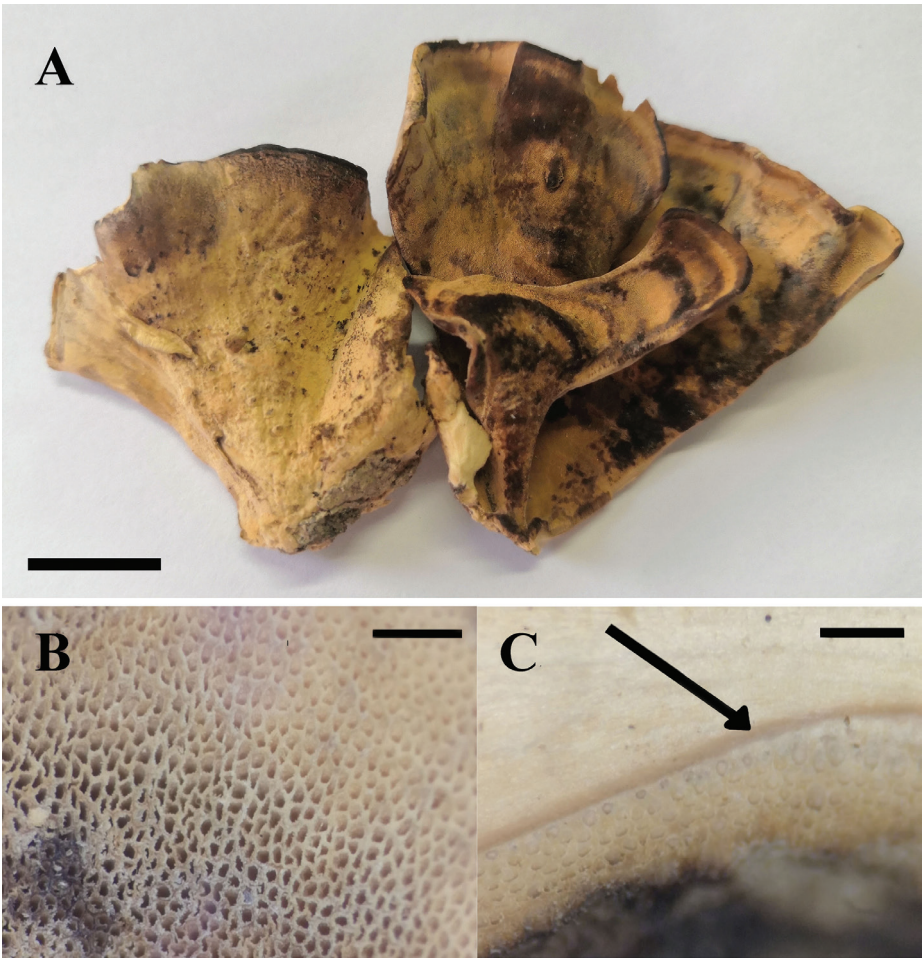

Figure 6. *Bjerkandera minispora* (holotype, Y.C. Dai 15234) **A** basidiomata **B** poroid surface detail **C** a dark line between tubes and context. Scale bars: 1 cm (**A**); 1 mm (**B, C**).

Additional specimen (paratype) examined. China. Hainan Province, Wuzhishan County, Wuzhishan Nature Reserve, 18°54'N, 109°42'E, fallen angiosperm trunk, 24. XI. 2007, B.K. Cui 5376 (BJFC003417).

Remarks. The buff-yellow pore surface, darkening when touched or bruised, the small pores (6–9 per mm) sometimes with white tomentum, and the ellipsoid small basidiospores (3.1–4.2 × 2–2.8 μm) set this species apart from others in *Bjerkandera*. *Bjerkandera albocinerea* resembles *B. minispora* by oblong-ellipsoid to ellipsoid basidiospores, but the former has sordid white fresh pileal surface, and dark brownish grey pore surface (Motato-Vásquez et al. 2020). *Bjerkandera ecuadorensis* is similar to *B. minispora* in having pinkish-buff to buff pileal surface and round to angular pores (6–9 per mm), but the former has grey to dark-brown pore surface and bigger basidiospores measuring 3.9–4.5 × 2.7–3 μm.

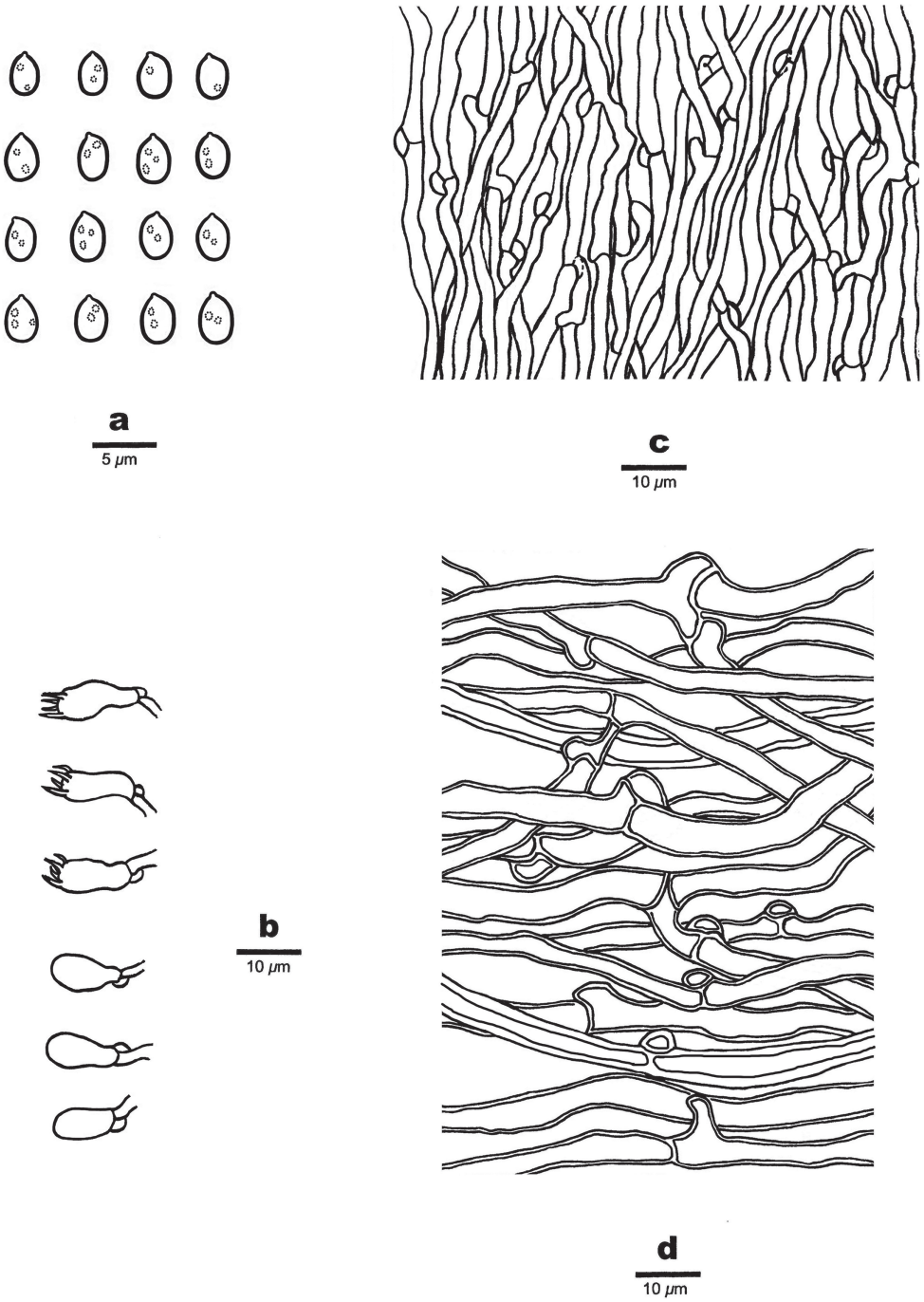

Figure 7. Microscopic structures of *Bjerkandera minispora* (holotype, Y.C. Dai 15234) **a** basidiospores **b** basidia and basidioles **c** hyphae from trama **d** hyphae from context.

Bjerkandera resupinata **Y.C. Dai & Chao G. Wang, sp. nov.**
MycoBank No: 838581
Figs 8, 9

Diagnosis. Differs from other species of *Bjerkandera* by resupinate basidiomata.

Type. Thailand. Chiang Rai, Doi Mae Salong, rotten angiosperm trunk, 22. VII. 2016, Y.C. Dai 16642 (holotype BJFC022752).

Etymology. *Resupinata* (Lat.): referring to the species having resupinate basidiomata.

Basidiomata. Annual, resupinate, adnate, soft corky, without odor or taste when fresh, becoming corky when dry, up to 6 cm long, 2 cm wide, 0.5 mm thick at base. Pore surface pinkish buff to pale brownish when dry, becoming dark grey in bruised parts; sterile margin distinct, thinning out, somewhat incised, up to 3 mm wide; pores round to angular, 4–6 per mm; dissepiments thin, entire to lacerated. Subiculum pale cream, slightly fibrous to corky, up to 0.2 mm thick. Tubes concolorous with the pore surface, darker than the subiculum, corky, up to 0.3 mm long, with a distinct dark line between tubes and subiculum.

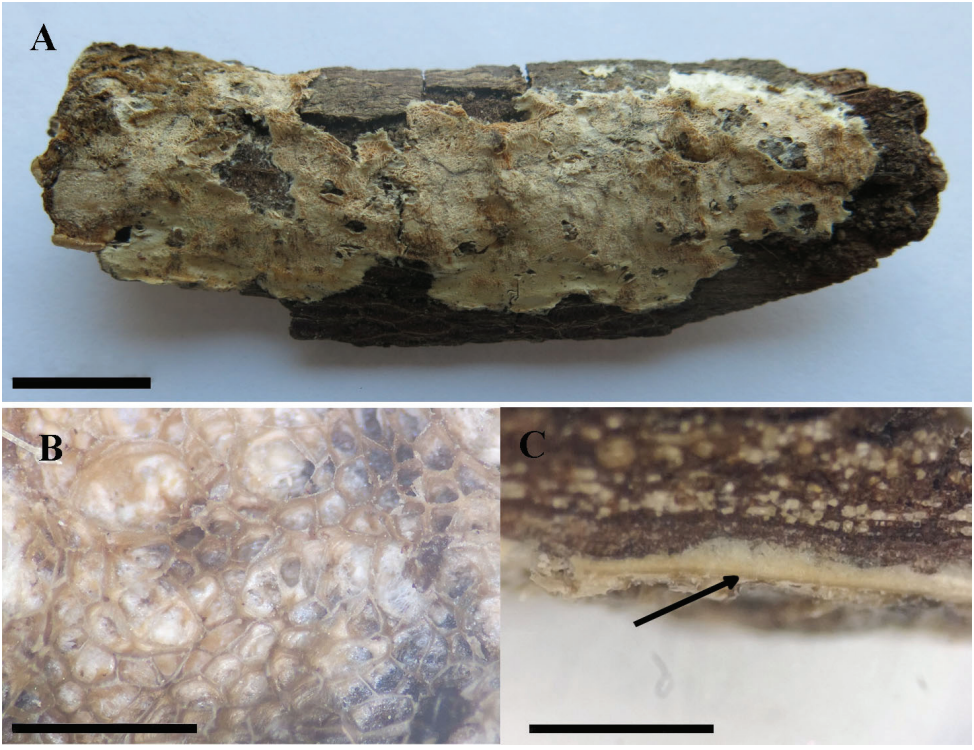

Figure 8. *Bjerkandera resupinata* (holotype, Y.C. Dai 16642) **A** basidiomata **B** poroid surface detail **C** a dark line between tubes and subiculum. Scale bars: 1 cm (**A**); 1 mm (**B, C**).

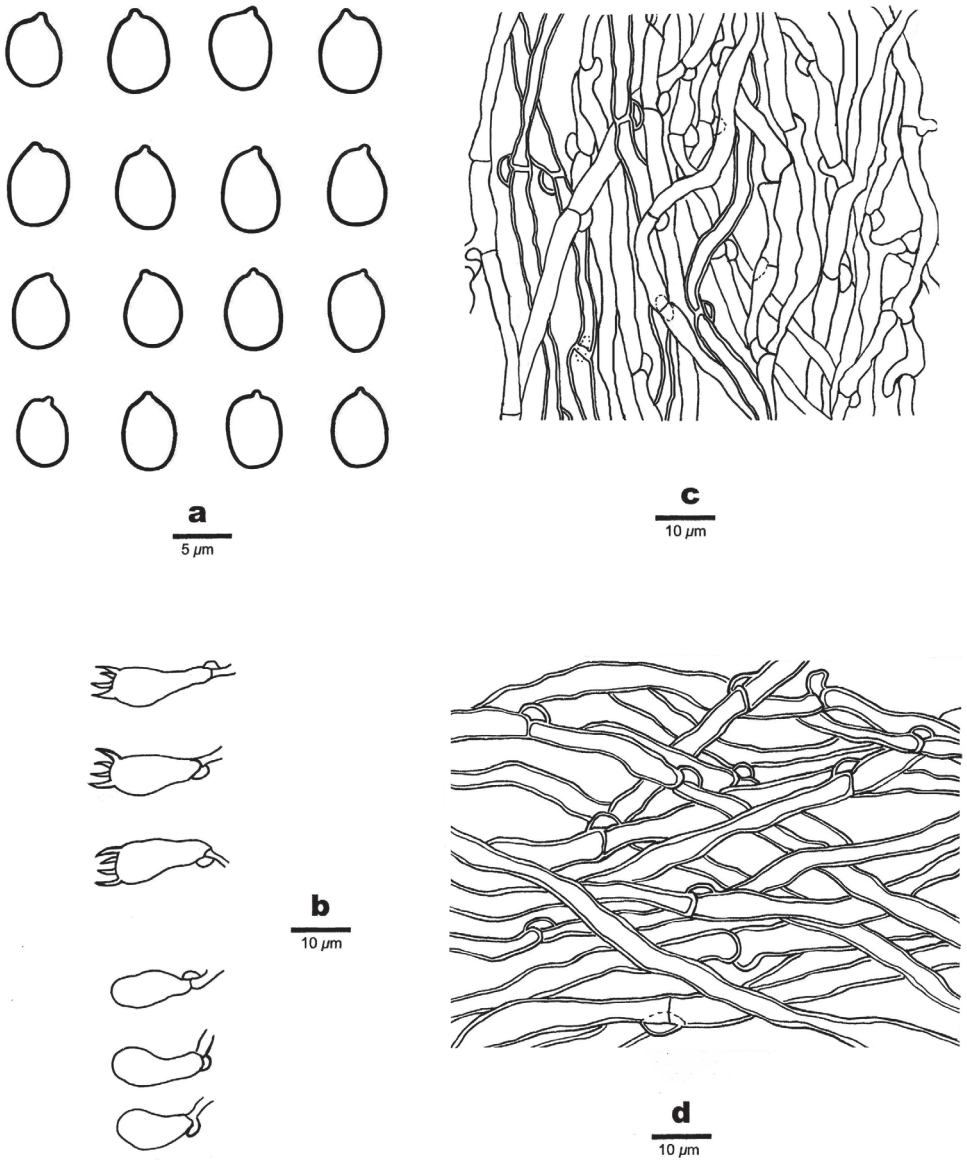

Figure 9. Microscopic structures of *Bjerkandera resupinata* (holotype, Y.C. Dai 16642) **a** basidiospores **b** basidia and basidioles **c** hyphae from trama **d** hyphae from subiculum.

Hyphal structure. Hyphal system monomitic; generative hyphae with clamp connections, smooth, hyaline to yellowish, CB+, IKI–; tissues becoming dark in KOH.

Subiculum. Generative hyphae thick-walled with a wide lumen, rarely branched, loosely interwoven, 4–5 μm in diam.

Tubes. Generative hyphae thin- to slightly thick-walled, frequently branched, loosely interwoven, 2.7–3.8 μm in diam. Cystidia and cystidioles absent. Basidia

Table 2. Morphological comparison of the currently accepted species in *Bjerkandera*.

	Basidiomata type	Pilei colour	Pore shape and number of pores	Poroid surface	Basidiospores size (µm)	Basidiospores shape	Reference
B. adusta	Pileate, effused-reflexed to resupinate	Cream to buff, then greyish to greyish-blue	Round to angular, 6–7/mm	Grey to black	4.5–6 × 2.5–3.5	Short-cylindrical to subellipsoid	Ryvarden and Melo 2017
B. albocinerea	Pileate to effused-reflexed	Sordid white to pale cream	Round, 8–11/mm	Dark brown grey to almost black when bruised	3.5–4.5 × 2–2.6	Oblong-ellipsoid to ellipsoid	Motato-Vásquez et al. 2020
B. atroalba	Pileate to effused-reflexed	White to cream, then grey	Round or more commonly angular, 2–5/mm	White to cream, then becoming dark	4–5 × 3–4	Narrowly ellipsoid to broadly ellipsoid	Westphalen et al. 2015
B. centroamericana	Pileate to effused-reflexed	White to cream, then brownish	Angular, 7–11/mm	Sordid white, then brown to black in bruised parts	4–5 × 3–4.5	Broadly ellipsoid to subglobose	Westphalen et al. 2015
B. ecuadorensis	Pileate	Pinkish-buff to buff	Round to angular, 7–9 /mm	Grey to dark-brown, then almost black in bruised parts	3.9–4.5 × 2.7–3	Ellipsoid	Present study
B. fulgida	Effused-reflexed	Pinkish buff to clay-buff	Round or sometimes angular, 6–8/mm	Clay-buff to pale brown, then dark brown in bruised parts	3.9–4.5 × 2.8–3.3	Ellipsoid to broadly ellipsoid	Present study
B. fumosa	Pileate to effused-reflexed	Buff to woody coloured	Round to angular 2–5/mm	Buff to isabelline	5.5–7 × 2.5–3.5	Short cylindrical	Ryvarden and Melo 2017
B. mikrofumosa	Effused-reflexed	Pale golden-brown	Angular, 7–9/mm	Pale to smoky brown, then dark grey in bruised parts	3.5–4.8 × 2.3–3	Ellipsoid	Motato-Vásquez et al. 2020
B. minispora	Pileate	Pinkish-buff to buff	Round to angular, 6–9/mm	Buff-yellow, ash-grey to pale brown, then almost black in bruised parts	3.1–4.2 × 2–2.8	Oblong-ellipsoid to ellipsoid	Present study
B. resupinata	Resupinate	–	Round to angular, 4–6/mm	Pinkish buff to pale brownish, then dark grey in bruised parts	4.5–6 × 3.2–4.1	Ellipsoid to broadly ellipsoid	Present study

clavate, with four sterigmata and a basal clamp connection, 14–16 × 5–6.5 µm; basidioles in shape similar to basidia, but smaller.

Basidiospores. Ellipsoid to broadly ellipsoid, hyaline, thin-walled, smooth, CB–, IKI–, 4.5–6(–6.2) × 3.2–4.1(–4.2) µm, L = 5.23 µm, W = 3.71 µm, Q = 1.40–1.42 (n = 60/2).

Additional specimen (paratype) examined. China. Yunnan Province, Tengchong County, Gaoligong Mts., fallen angiosperm branch, 24. X. 2009, B.K. Cui 8017 (BJFC006506).

Remarks. *Bjerkandera resupinata* is characterised by resupinate basidiomata, pinkish buff to pale brownish pore surface, clavate basidia, and ellipsoid to broadly ellipsoid basidiospores measuring 4.5–6 × 3.2–4.1 µm. *Ceriporiopsis umbrinescens* (Murrill) Ryvarden and *Bjerkandera resupinata* have resupinate basidiomata, pale buff to brownish pore surface, similar sterile margin, a monomitic hyphal structure, and almost the same size of basidiospores, but *C. umbrinescens* has bigger pores (2–4 per mm), unchanged pore surface when touched, and a dark line absent between tubes and subiculum (Murrill 1920; Domański 1963; Núñez and Ryvarden 2001; Zhao et al. 2015).

Additional specimens examined. ***Bjerkandera adusta*:** China. Heilongjiang Province, Heihe, Shengshan Nature Reserve, *Populus*, 26. VIII. 2014, Y. C. Dai 14516 (BJFC017794); Yunnan Province, Yongde County, Daxueshan Nature Reserve, rotten Angiosperm stump, 27. VIII. 2015, Y. C. Dai 15665 (BJFC019769); Gansu Province, Tianshui, Fangmatan Forest Park, fallen branch of *Populus*, 08. VIII. 2015, Y. C. Dai 15495 (BJFC019600). France. Lyons, *Abies*, 24. XI. 2012, Y. C. Dai 13201 (BJFC014065). Finland, Helsinki, Tamisto Nature Reserve, *Betula*, 4. XI. 2011, Y. C. Dai 12640 (BJFC012222). ***B. albocinerea*:** USA. CT, CAES Valley Lab, Dead log, 13. XII. 2015, Y. C. Dai 16411 (BJFC020499). ***B. fumosa*:** China. Chongqing, Jinfoshan Forest Park, dead angiosperm tree, 1. XI. 2019, Y. C. Dai 21100 (BJFC032759); Beijing, Chinese Academy of Sciences, living tree of *Diospyros*, Y. C. Dai 21087 (BJFC032746); Sichuan Province, Xiaojin County, Jiajin Mts., *Hippophae*, 17. X. 2012, B. K. Cui 10747 (BJFC013669). Finland, Helsinki, Tamisto Nature Reserve, *Populus*, 6. XI. 2011, Y. C. Dai 12474B (BJFC012257). ***B. mikrofumosa*:** Costa Rica. Monteverde, J. Vlasák Jr. JV 1707/10J-1; JV 1707/10J-2. ***B. centroamericana*:** Costa Rica, Carara Nature Reserve, J. Vlasák JV 1704/97. ***B. atroalba*:** Brazil. Recife, Charles Darwin Ecological Reserve, on angiosperm stump, Y. C. Dai 17457 (BJFC024988). ***Ceriporiopsis carnegieae*:** USA, Virgin Islands, St. John, on hard wood, J. Vlasák Jr. JV 0409/27-J. ***Ceriporiopsis* sp.:** Costa Rica. Arenal Mts., J. Vlasák Jr. JV 1512/13-J.

Key to the species of *Bjerkandera*

1	Basidiomata resupinate	***B. resupinata***
–	Basidiomata effused-reflexed to pileate	**2**
2	Pores < 5 per mm	**3**
–	Pores > 5 per mm	**4**
3	Pileal surface white to cream; basidiospores broadly ellipsoid	***B. atroalba***
–	Pileal surface buff to woody-coloured; basidiospores short cylindrical	***B. fumosa***
4	Pileal surface white to cream when fresh	**5**
–	Pileal surface buff to grey when fresh	**6**
5	Basidiospores subglobose to broadly ellipsoid	***B. centroamericana***
–	Basidiospores oblong-ellipsoid to ellipsoid	***B. albocinerea***
6	Crystals present among hymenium	**7**
–	Crystals absent among hymenium	**8**
7	Pileal margin dark brown when dry	***B. mikrofumosa***
–	Pileal margin buff when dry	***B. fulgida***
8	Basidiospores > 4.5 µm in length	***B. adusta***
–	Basidiospores < 4.5 µm in length	**9**
9	Basidiospores 3.1–4.2 × 2–2.8 µm, Q = 1.49–1.53	***B. minispora***
–	Basidiospores 3.9–4.5 × 2.7–3 µm, Q = 1.43	***B. ecuadorensis***

Discussion

Our phylogeny recovered *Bjerkandera* as a monophyletic genus, with ten species including the four new species – *Bjerkandera ecuadorensis*, *B. fulgida*, *B. minispora*, and *B. resupinata* – nested in the *Bjerkandera* clade (Fig. 1).

Bjerkandera ecuadorensis, *B. minispora*, *B. adusta*, *B. albocinerea*, and *B. fumosa* are phylogenetically related (Fig. 1). *B. adusta*, *B. albocinerea*, and *B. fumosa* form a group which is consistent with previous studies (Westphalen et al. 2015; Motato-Vásquez et al. 2020). The specimen we studied Dai 16411 from CT, USA and *Bjerkandera albocinerea* share cream to buff-yellow pileal surface when dry, dark brownish grey to black pore surface, round pores (8–11 per mm), and oblong-ellipsoid to ellipsoid basidiospores (3.5–4.5 × 2–2.5 μm). Also, there are two base pairs differences between them, which amounts to < 1% nucleotide differences in the ITS regions. So both specimens represent the same species. The type of *Bjerkandera albocinerea* and other specimens were collected from Brazil, but the specimen Dai 16411 from CT, USA, *B. albocinerea* has a wide distribution in America. Morphologically, *Bjerkandera albocinerea* is different from other four species by its white fresh pileal surface (Motato-Vásquez et al. 2020), and *B. minispora* can be distinguished from *B. ecuadorensis*, *B. adusta* and *B. fumosa* by smaller basidiospores (3.1–4.2 × 2–2.8 μm in *B. minispora*, 3.9–4.5 × 2.7–3 μm in *B. ecuadorensis*, and 4.5–6 × 2.5–3.5 μm in *B. adusta*, 5.5–7 × 2.5–3.5 μm in *B. fumosa*, Ryvarden and Melo 2017). *Bjerkandera fumosa* has the thicker context usually more than 6 mm, while the other two less than 6 mm (Ryvarden and Melo 2017). *Bjerkandera adusta* has short-cylindric to subellipsoid and bigger basidiospores (4.5–6 × 2.5–3.5 μm, Ryvarden and Melo 2017), which can differ from *B. ecuadorensis*. Also, there are 21 base pairs differences between *Bjerkandera ecuadorensis* and *B. minispora*, which amounts to > 2% nucleotide differences in the ITS regions.

Bjerkandera fulgida grouped with *B. resupinata* in a joint subclade, and these two species are closely related to *B. atroalba* (Rick) Westph. & Tomšovský, *B. centroamericana* Kout, Westph. & Tomšovský, and *B. mikrofumosa* Ryvarden with strong support (99/98/1.00). *Bjerkandera resupinata* has resupinate basidiomata, big pores and basidiospores, which can be distinguished from *B. fulgida* indeed. Also, there are eight base pairs differences between them, which amounts to 2% nucleotide differences in the ITS regions. *Bjerkandera atroalba*, *B. centroamericana* and *B. mikrofumosa* have a neotropical distribution (Westphalen et al. 2015; Motato-Vásquez et al. 2020), while *B. fulgida* and *B. resupinata* from tropical China are proved to nest in the group according to our phylogenetic study. Morphologically, *Bjerkandera resupinata* is a resupinate species, while basidiomata are effused-reflexed to pileate in *B. fulgida*, *B. atroalba*, *B. centroamericana*, and *B. mikrofumosa* (Westphalen et al. 2015; Motato-Vásquez et al. 2020). *Bjerkandera atroalba* and *B. centroamericana* differ from *B. fulgida* by their white pilei when fresh, sordid white to cream pore surface, and the presence of cystidioles (Westphalen et al. 2015). *B. mikrofumosa* differs from *B. fulgida* by its pale golden-brown pileal surface and pale to smoky brown pore surface (Motato-Vásquez et al. 2020). In addition, we

found *Ceriporiopsis umbrinescens* (Murrill) Ryvarden and *B. resupinata* have resupinate basidiomata, pale buff to brownish pore surface, similar sterile margin, a monomitic hyphal structure, and almost the same size of basidiospores, but *C. umbrinescens* has bigger pores (2–4 per mm) and unchanged pore surface when touched (Murrill 1920; Domański 1963; Núñez and Ryvarden 2001; Zhao et al. 2015).

In our phylogenetic analysis, *Ceriporiopsis carnegieae* (D.V. Baxter) Gilb. & Ryvarden is phylogenetically close to the genus *Bjerkandera*. *Ceriporiopsis* Domański is a polyphyletic genus, which is nested in the families Irpicaceae, Meruliaceae (the type species *C. gilvescens* (Bres.) Domański belongs to Meruliaceae), and Phanerochaetaceae (Justo et al. 2017). Meanwhile, *Ceriporiopsis carnegieae* resembles *Bjerkandera* by having a monomitic hyphal system, generative hyphae with abundant clamps, and oblong to short-cylindric basidiospores (Baxter 1941; Gilbertson and Ryvarden 1985). However, the former has basidiomata with sharp and pungent odor when fresh, unchanged pore surface when touched or bruised, and seem to lack any dark line between tubes and subiculum (Gilbertson and Ryvarden 1985). One specimen – JV1512–13J – from Costa Rica forms a sister group to the three sequences annotated as *Ceriporiopsis carnegieae*, and we treat this specimen as *Ceriporiopsis* sp. There is ongoing controversy regarding for the generic affiliation of *C. carnegieae* (Nobles 1965; Justo et al. 2017; Motato-Vásquez et al. 2020), because the black line is absent from *Ceriporiopsis carnegieae*. For the time being, we are reluctant to combine them in *Bjerkandera* although the two taxa are phylogenetically related. To solve this problem more specimens should be examined and analysed phylogenetically.

Beside the ten species of *Bjerkandera* in our phylogeny (Fig. 1), another three taxa – *Bjerkandera terebrans* (Berk. & M.A. Curtis) Murrill, *B. subsimulans* (Berk. et M. A. Curtis) Murrill and *B. amorpha* (Fr.) P. Karst. – were included in the genus. However, *Bjerkandera terebrans* was mentioned probably as a form of *B. fumosa* or variant of *Osteina obducta* (Berk.) Donk Because of its basidiomata with a stipe-like base (Murrill 1907; Zmitrovich et al. 2016). *B. subsimulans* has lobed and broadly sterile margin with a zone of appressed hairs, and angular irregular pores (1–3 per mm), which are in accord with the description of *Abortiporus biennis* (Bull.) Singer (Murrill 1907; Zmitrovich et al. 2016). *B. amorpha* has dimitic hyphal system and allantoid basidiospores that differ from *Bjerkandera*, so it is now *Skeletocutis amorpha* (Fr.) Kotl. & Pouzar (Kotlába and Pouzar 1958).

Tyromyces vivii Homble ex Ryvarden was described from Norway (Ryvarden et al. 2003), and later it was treated as a synonym of *B. fumosa* (Ryvarden and Melo 2017). The type material of *T. vivii* was analyzed, and it nested in *B. fumosa* (Fig. 1). We confirm this conclusion by molecular evidence.

Previously, the well-known *Bjerkandera adusta* and *B. fumosa* have been reported from the northern hemisphere and South America. However, the diversity of *Bjerkandera* was underestimated, *B. centroamericana*, *B. mikrofumosa* and *B. albocinerea* were recently described in the neotropics (Westphalen et al. 2015; Ryvarden 2016), and new species in our study have a distribution in the neotropics and tropical Asia. So, the genus has a wide distribution from boreal to tropical areas.

Acknowledgements

The research was supported by the National Natural Science Foundation of China (Project No. 31870007) and by the institutional support of the Academy Sciences of the Czech Republic RVO: 60077344. Special thanks are due to Josef Vlasák Jr. (USA) for forwarding specimens for our study.

References

Anonymous (1969) Flora of British fungi. Colour identification chart. Her Majesty's Stationery Office, London.

Baxter DV (1941) Some resupinate polypores from the region of the Great Lakes. 12. Papers of the Michigan Academy of Sciences 26: 107–131.

Binder M, Justo A, Riley R, Salamov A, López-Giráldez F, Sjökvist E, Copeland A, Foster B, Sun H, Larsson E, Larsson KH, Townsend J, Grigoriev IV, Hibbett DS (2013) Phylogenetic and phylogenomic overview of the Polyporales. Mycologia 105: 1350–1373. https://doi.org/10.3852/13-003

Corner EJH (1989) Ad Polyporaceas V. The genera *Albatrellus*, *Boletopsis*, *Coriolopsis* (dimitic), *Cristelloporia*, *Diacanthodes*, *Elmerina*, *Fomitopsis* (dimitic), *Gloeoporus*, *Grifola*, *Hapalopilus*, *Heterobasidion*, *Hydnopolyporus*, *Ischnoderma*, *Loweporus*, *Parmastomyces*, *Perenniporia*, *Pyrofomes*, *Steccherinum*, *Trechispora*, *Truncospora* and *Tyromyces*. Beihefte zur Nova Hedwigia 96: 1–218.

Cui BK, Li HJ, Ji X, Zhou JL, Song J, Si J, Yang ZL, Dai YC (2019) Species diversity, taxonomy and phylogeny of Polyporaceae (Basidiomycota) in China. Fungal Diversity 97: 137–302. https://doi.org/10.1007/s13225-019-00427-4

Domański S (1963) Dwa nowe rodzaje grzybów z grupy "*Poria* Pers. ex S.F. Grey". (Two new genera of fungi from group "*Poria* Pers. ex S.F. Grey"). Acta Societatis Botanicorum Poloniae 32: 731–739. https://doi.org/10.5586/asbp.1963.044

Floudas D, Hibbett DS (2015) Revisiting the taxonomy of *Phanerochaete* (Polyporales, Basidiomycota) using a four gene dataset and extensive ITS sampling. Fungal Biology 119: 679–719. https://doi.org/10.1016/j.funbio.2015.04.003

Gilbertson RL, Ryvarden L (1985) Some new combinations in Polyporaceae. Mycotaxon 22: 363–365.

Gilbertson RL, Ryvarden L (1986) North American polypores 1. *Abortiporus* – *Lindtneria*. Fungiflora, Oslo, 433 pp.

Hall TA (1999) BioEdit: a user-friendly biological sequence alignment editor and analysis program for Windows 95/98/NT. Nucleic Acids Symposium Series 41: 95–98.

Han ML, Chen YY, Shen LL, Song J, Vlasák J, Dai YC, Cui BK (2016) Taxonomy and phylogeny of the brown-rot fungi: *Fomitopsis* and its related genera. Fungal Diversity 80: 343–373. https://doi.org/10.1007/s13225-016-0364-y

Hopple JS, Vilgalys R (1999) Phylogenetic relationships in the mushroom genus *Coprinus* and dark-spored allies based on sequence data from the nuclear gene coding for the large

ribosomal subunit RNA: divergent domains, outgroups, and monophyly. Molecular Phylogenetics and Evolution 13: 1–19. https://doi.org/10.1006/mpev.1999.0634

Jung PE, Fong JJ, Park MS, Oh SY, Kim C, Lim YW (2014) Sequence validation for the identification of the white-rot fungi *Bjerkandera* in public sequence databases. Journal of Microbiology and Technology 24: 1313–1319. https://doi.org/10.4014/jmb.1404.04021

Jung PE, Lee H, Wu SH, Hattori T, Tomšovský M, Rajchenberg M, Zhou M, Lim YW (2018) Revision of the taxonomic status of the genus *Gloeoporus* (Polyporales, Basidiomycota) reveals two new species. Mycological Progress 17: 855–863. https://doi.org/10.1007/s11557-018-1400-y

Justo A, Miettinen O, Floudas D, Ortiz-Santana B, Sjökvist E, Lindner D, Nakasone K, Niemelä T, Larsson KH, Ryvarden L, Hibbett DS (2017) A revised family-level classification of the Polyporales (Basidiomycota). Fungal Biology 121: 798–824. https://doi.org/10.1016/j.funbio.2017.05.010

Katoh K, Standley DM (2013) MAFFT multiple sequence alignment software version 7: improvements in performance and usability. Molecular Phylogenetics and Evolution 30: 772–780. https://doi.org/10.1093/molbev/mst010

Kotlaba F, Pouzar Z (1964) Studie o bčlochoroši nazelenalém – A study of *Tyromyces pannocinctus* (Romell) comb. nov. Česká Mykologie 18: 65–76.

Miettinen O, Vlasák J, Rivoire B, Spirin V (2018) *Postia* caesia complex (Polyporales, Basidiomycota) in temperate Northern Hemisphere. Fungal Systematics and Evolution 1: 101–129. https://doi.org/10.3114/fuse.2018.01.05

Miller MA, Holder MT, Vos R, Midford PE, Liebowitz T, Chan L, Hoover P, Warnow T (2009) The CIPRES Portals. http://www.phylo.org/sub_sections/portal [Archived by WebCite(r) at] http://www.webcitation.org/5imQlJeQa

Motato-Vásquez V, Gugliotta AM, Rajchenberg M, Catania M, Urcelay C, Robledo G (2020) New insights on *Bjerkandera* (Phanerochaetaceae, Polyporales) in the Neotropics with description of *Bjerkandera albocinerea* based on morphological and molecular evidence. Plant Ecology and Evolution 153: 229–245. https://doi.org/10.5091/plecevo.2020.1667

Murrill WA (1907) (Agaricales) Polyporaceae. North American Flora 9: 1–71.

Murrill WA (1920) Light-colored resupinate polypores. 1. Mycologia 12: 77–92. https://doi.org/10.1080/00275514.1920.12016821

Nobles MK (1965) Cultural characters as a guide to the taxonomy and phylogeny of the Polyporaceae. Canadian Journal of Botany 36: 883–926. https://doi.org/10.1139/b58-071

Núñez M, Ryvarden L (2001) East Asian Polypores, Synopsis Fungorum 14, vol 2. Fungiflora, Oslo, Norway, 229–231.

Nylander JAA (2004) MrModeltest vol 2. Program distributed by the author. Evolutionary Biology Centre, Uppsala University.

Petersen JH (1996) The Danish Mycological Society's colour-chart. Foreningen til Svampekundskabens Fremme, Greve.

Pilát A (1937) 1. Polyporaceae. In: Kavina K, Pilát A (Eds) Atlas des Champignons de l'Europe. Tome 3. Prague.

Pouzar Z (1966) Studies in the taxonomy of the Polypores 2. Botanical Institute of the Czechoslovak Academy of Sciences. Pruhonice near Praha, 356–375. https://doi.org/10.1007/BF02854587

Ronquist F, Huelsenbeck JP (2003) MRBAYES 3: Bayesian phylogenetic inference under mixed models. Bioinformatics 19: 1572–1574. https://doi.org/10.1093/bioinformatics/btg180

Ryvarden L (1985) Type studies in the Polyporaceae 17. Species described by W.A. Murrill. Mycotaxon 23: 169–198.

Ryvarden L (1991) Genera of Polypores nomenclature and taxonomy. Synopsis Fungorum 5, Fungiflora, Oslo, 116 pp.

Ryvarden L (2016) Studies in Neotropical polypores 43 Some new species from tropical America. Synopsis Fungorum 35: 43–47.

Ryvarden L, Gilbertson RL (1993) European Polypores, Synopsis Fungorum 6, vol 1. Fungiflora, Oslo, 168–171.

Ryvarden L, Melo I (2017) Poroid fungi of Europe (2nd edn.). Synopsis Fungorum 37: 1–431.

Ryvarden L, Stokland L, Larsson KH (2003) A critical checklist of corticoid and poroid fungi of Norway. Synopsis Fungorum 17: 1–209.

Sayers EW, Cavanaugh M, Clark K, Pruitt KD, Schoch CL, Sherry ST, Karsch-Mizrachi I (2021) GenBank. Nucleic Acids Research 49: D92–D96. https://doi.org/10.1093/nar/gkaa1023

Shen LL, Wang M, Zhou JL, Xing JH, Cui BK, Dai YC (2019) Taxonomy and phylogeny of *Postia*. Multi-gene phylogeny and taxonomy of the brown-rot fungi: *Postia* (Polyporales, Basidiomycota) and related genera. Persoonia 42: 101–126. https://doi.org/10.3767/persoonia.2019.42.05

Sun YF, Costa-Rezende DH, Xing JH, Zhou JL, Zhang B, Gibertoni TB, Gates G, Glen M, Dai YC, Cui BK (2020) Multi-gene phylogeny and taxonomy of *Amauroderma* s.lat. (Ganodermataceae). Persoonia 44: 206–239. https://doi.org/10.3767/persoonia.2020.44.08

Swofford DL (2002) PAUP*: phylogenetic analysis using parsimony (*and other methods), version 4.0b10. Sinauer Associates, Sunderland, Massachusetts. https://doi.org/10.1002/0471650129.dob0522

Thompson JD, Gibson TJ, Plewniak F, Jeanmougin F, Higgins DG (1997) The Clustal_X windows interface: flexible strategies for multiple sequence alignment aided by quality analysis tools. Nucleic Acids Research 25: 4876–4882. https://doi.org/10.1093/nar/25.24.4876

Viktor P, Bálint D (2018) New systematic position of *Aurantiporus alborubescens* (Meruliaceae, Basidiomycota), a threatened old-growth forest polypore. Mycological Progress 17: 319–332. https://doi.org/10.1007/s11557-017-1356-3

Westphalen MC, Tomšovský M, Kout J, Gugliotta AM (2015) *Bjerkandera* in the Neotropics: phylogenetic and morphological relations of *Tyromyces atroalbus* and description of a new species. Mycological Progress 14: e100. https://doi.org/10.1007/s11557-015-1124-1

White TJ, Bruns T, Lee S, Taylor J (1990) Amplification and direct sequencing of fungal ribosomal RNA genes for phylogenetics. In: Innis MA, Gefand DH, Sninsky JJ, White JT (Eds) PCR Protocols: A Guide to Methods and Applications. Academic Press, San Diego, 315–322. https://doi.org/10.1016/B978-0-12-372180-8.50042-1

Zhao CL, Cui BK, Dai YC (2013) New species and phylogeny of *Perenniporia* based on morphological and molecular characters. Fungal Diversity 58: 47–60. https://doi.org/10.1007/s13225-012-0177-6

Zhao CL, Wu F, Liu HX, Dai YC (2015) A phylogenetic and taxonomic study on *Ceriporiopsis* s. str. (Polyporales) in China. Nova Hedwigia 101: 403–417. https://doi.org/10.1127/nova_hedwigia/2015/0282

Zhu L, Song J, Zhou JL, Si J, Cui BK (2019) Species diversity, phylogeny, divergence time and biogeography of the genus *Sanghuangporus* (Basidiomycota). Frontiers in Microbiology 10: e812. https://doi.org/10.3389/fmicb.2019.00812

Zmitrovich IV, Bondartseva MA, Vasilyev NP (2016) The Meruliaceae of Russia. I. *Bjerkandera*. Turczaninowia 19: 5–18. https://doi.org/10.14258/turczaninowia.19.1.1

MycoKeys 79: 173–192 (2021)
doi: 10.3897/mycokeys.79.60662
https://mycokeys.pensoft.net

RESEARCH ARTICLE

A peer-reviewed open-access journal
MycoKeys
Launched to accelerate biodiversity research

Morpho-molecular characterization of *Discosia ravennica* sp. nov. and a new host record for *Sporocadus rosigena*

Digvijayini Bundhun[1,2,3], Rajesh Jeewon[4], Indunil C. Senanayake[5,6], Erio Camporesi[7,8,9], Janith V. S. Aluthmuhandiram[2,10], Alvin M. C. Tang[11], Ji-Chuan Kang[1], Vishwakalyan Bhoyroo[12], Kevin D. Hyde[2,6]

1 *Engineering and Research Center for Southwest Bio-Pharmaceutical Resources of National Education Ministry of China, Guizhou University, Guiyang, Guizhou Province 550025, China* **2** *Center of Excellence in Fungal Research, Mae Fah Luang University, Chiang Rai, 57100, Thailand* **3** *Department of Entomology and Plant Pathology, Faculty of Agriculture, Chiang Mai University, Chiang Mai, 50200, Thailand* **4** *Department of Health Sciences, Faculty of Medicine and Health Sciences, University of Mauritius, Reduit, Mauritius* **5** *College of Life Science and Oceanography, Shenzhen University, 1068, Nanhai Avenue, Nanshan, Shenzhen, 518055, China* **6** *Innovative Institute of Plant Health, Zhongkai University of Agriculture and Engineering, Haizhu District, Guangzhou, 510225, China* **7** *A.M.B. Gruppo Micologico Forlivese "Antonio Cicognani", Via Roma, Forli, Italy* **8** *A.M.B. Circolo Micologico "Giovanni Carini", Brescia, Italy* **9** *Società per gli Studi Naturalistici della Romagna, Bagnacavallo (RA), Italy* **10** *Beijing Key Laboratory of Environment Friendly Management on Fruit Diseases and Pests in North China, Institute of Plant and Environment Protection, Beijing Academy of Agriculture and Forestry Sciences, Beijing, 100097, China* **11** *Division of Applied Science, College of International Education, Hong Kong Baptist University, Hong Kong SAR, China* **12** *Faculty of Agriculture, University of Mauritius, Reduit, Mauritius*

Corresponding author: Ji-Chuan Kang (jckang@gzu.edu.cn)

Academic editor: G. Rambold | Received 11 November 2020 | Accepted 29 March 2021 | Published 27 April 2021

Citation: Bundhun D, Jeewon R, Senanayake IC, Camporesi E, Aluthmuhandiram JVS, Tang AMC, Kang J-C, Bhoyroo V, Hyde KD (2021) Morpho-molecular characterization of *Discosia ravennica* sp. nov. and a new host record for *Sporocadus rosigena*. MycoKeys 79: 173–192. https://doi.org/10.3897/mycokeys.79.60662

Abstract

Collections of fungal samples from two dead leaf specimens from Italy were subjected to morphological examination and phylogenetic analyses. Two coelomycetous taxa belonging to two different genera in Xylariomycetidae, Sordariomycetes, namely *Discosia* and *Sporocadus*, were identified. The *Discosia* taxon is revealed as a new species and is herein introduced as *Discosia ravennica* **sp. nov.** while the *Sporocadus* taxon is identified as *Sporocadus rosigena*. Multi-locus phylogeny based on DNA sequence data of the large subunit (LSU) and internal transcribed spacer (ITS) of nuclear ribosomal genes, β-tubulin (*β-tub*) and

RNA polymerase II second largest subunit (*rpb2*) showed that *D. ravennica* is related to *D. neofraxinea* but it forms an independent lineage that supports its new species status. The new taxon also differs from other *Discosia* species by its unilocular to bilocular, superficial and applanate conidiomata with basal stroma composed of cells of *textura angularis*, elongate-ampulliform conidiogenous cells and conidia smaller in size. *Sporocadus rosigena* is here reported as a new host record from *Quercus ilex* from Italy. Descriptions, illustrations and molecular data for both species are provided in this paper.

Keywords
Amphisphaeriales, asexual morphs, new species, saprobes, taxonomy

Introduction

Members of the Sporocadaceae (Amphisphaeriales, Sordariomycetes) are generally appendage-bearing coelomycetes equally known as "pestalotioid fungi" (Tanaka et al. 2011; Liu et al. 2019). *Discosia* Lib. ex Durieu & Mont. and *Sporocadus* Corda are two genera in this family and they were shown to be phylogenetically linked as sister taxa (Jeewon et al. 2002; Maharachchikumbura et al. 2016).

After Libert (1837) established *Discosia*, it was re-studied by Subramanian and Reddy (1974) who designated *D. strobilina* Lib. ex Sacc. as lectotype for the genus (Nag Raj 1993; Tanaka et al. 2011). Later, when *Sphaeria artocreas* Tode was transferred to the genus and combined under *D. artocreas* (Tode) Fr., the latter was chosen as lectotype of the genus (Fries 1849; Vanev 1991). Morgan-Jones (1964) investigated both *D. artocreas* [same material examined by Fries (1849)] and *D. strobilina* and reported them as two different species. Subramanian and Reddy (1974) did not examine the type of *D. artocreas*, but the features of *D. strobilina* they observed did not match the same reported by Morgan-Jones (1964). The status of *D. artocreas* as type species of *Discosia*, therefore, has not been confirmed (Sutton 1980). Nevertheless, it is currently accepted as the type species of the genus (Crous et al. 2013; Index Fungorum, http://www.indexfungorum.org/Names/Names.asp). Recently, an epitype for *D. artocreas* was designated (Liu et al. 2019).

Delineation of *Discosia* taxa was earlier, primarily focused on morphological characteristics such as septation of the conidia, varying proportional lengths of the conidial cells and the conidium size (Subramanian and Reddy 1974; Sutton 1980; Vanev 1991, 1992, 1996; Nag Raj 1993). However, these similar morphological characters have been found to be overlapping for most *Discosia* species (Sutton 1977, 1980; Nag Raj 1993; Jeewon et al. 2002; Barber et al. 2011; Tanaka et al. 2011). Species of *Discosia* were earlier also divided into four sections based on the size, septation and pigmentation of the conidia (Subramanian and Reddy 1974). Later, six sections for the species were proposed based on the same conidial morphology (Vanev 1991). Acquisition of DNA sequence data for *Discosia* species followed by phylogenetic analyses have, however, shown that the concept of subdivision based on morphology alone has been inaccurate and that proper delineation of species must rely on both morphology and molecular phylogeny (Tanaka et al. 2011).

Sporocadus is a recently resurrected genus, characterized by integrated or discrete conidiogenous cells and generally 3-septate, ellipsoid, cylindrical or obovoid conidia which lack appendages (Liu et al. 2019). The genus was originally introduced to accommodate four species, including *S. herbarum* Corda, *S. georginae* Corda, *S. lichenicola* Corda and *S. maculans* Corda (Corda 1839). No type species for the genus was designated when these species were introduced. However, *S. lichenicola* was chosen as the lectotype by Hughes (1958). Although Wijayawardene et al. (2016) followed the synonymy of *Sporocadus* under *Seimatosporium* by Sutton (1975), Brockman (1976) and Nag Raj (1993) did not accept this. Recently, multi-loci phylogenetic analyses showed that *Sporocadus* and *Seimatosporium* are two separate genera, with the former genus usually accommodating taxa without appendages and epitypified by *S. lichenicola* (Liu et al. 2019).

Documenting fungal species, whether they are novel species or new records, is an important contribution to diversity, taxonomy and plant pathology. It is also imperative that these fungal taxa are studied as a number of them are recognized to be potential emerging plant pathogens and they can impact on disease management strategies (Dugan et al. 2009; Giraud et al. 2010; Ghelardini et al. 2016; Rodeva et al. 2016; Jayasiri et al. 2019; Jayawardena et al. 2020). The aim of this paper is to introduce a new *Discosia* species collected from Italy based on morphology supported by phylogenetic analyses of combined LSU, ITS, *β-tub* and *rpb2* sequence data. In addition, we report a new host record for a sporocadus-like taxon, identified as *Sporocadus rosigena*, isolated from *Quercus ilex* (Fagaceae) in Italy.

Materials and methods

Sample collection and isolation

Samples of plant materials bearing discosia-like and sporocadus-like fungi were collected from dead land leaves of *Pyrus* sp. and *Quercus ilex* in the provinces of Ravenna, Oriolo dei Fichi– Faenza and Forlì-Cesena, Fiumana di Predappio, Italy, respectively. They were brought to the laboratory in paper bags and labelled initially as IT 3632 and IT 3569. The specimens were then examined using a dissecting microscope (Motic SMZ-168).

Single-spore isolation was carried out as described in Senanayake et al. (2020). Conidia of the sporocadus-like taxon successfully germinated and were transferred aseptically to malt extract agar (MEA) plates. The cultures were incubated at 18 °C for 2–3 weeks with frequent observations to assess the colony color and other characters.

Morphological studies

Free-hand sections of conidiomata of the *Discosia* taxon were prepared to examine their morphological characters. The following structures were observed and measured: height, diameter, and shape of conidiomata, conidiomatal wall cell structure, shape and dimen-

sions of conidiophores and conidiogenous cells, length and width of conidia. Morphology of the representatives of the *Sporocadus* species was obtained from the culture and the morphological characters examined included conidiomata, conidiophores, conidiogenous cells and conidia. All the fungal characters were examined with a fluorescence microscope (Nikon Eclipse E600) and digital images were captured with a Nikon DS-U2 and Cannon 750D camera. All measurements were made using the Tarosoft (R) Image Frame Work software v.0.9.0.7. Images used for photo plates were processed with Adobe Photoshop CS6 v. 12.0 (Adobe Systems, USA).

Material deposition

The holotype of the newly described taxon herein was deposited in the Mae Fah Luang University Herbarium (MFLU), Chiang Rai, Thailand while the isotype at the Cryptogamic Herbarium, Kunming Institute of Botany Academia Sinica (HKAS), Chinese Academy of Sciences, Kunming, China. Herbarium specimen for *S. rosigena* was also deposited in MFLU while its living culture in Mae Fah Luang University Culture Collection (MFLUCC). Facesoffungi and MycoBank numbers are provided as described in Jayasiri et al. (2015) and MycoBank (http://www.MycoBank.org) respectively. Species concepts are discussed following Jeewon and Hyde (2016).

DNA extraction, PCR amplification and sequencing

Fresh mycelium from the culture of *S. rosigena* (MFLUCC 18-0387) scraped from the margin of colonies on MEA plates (incubated at room temperature for 4 weeks), and conidiomata of the new taxon (MFLU 18-0131) from natural substrate were used for DNA extraction. Around 20 conidiomata of the new taxon (MFLU 18-0131) were carefully picked from the sterilized material using a fine sterile needle, observed through a stereomicroscope and collected in a 1.5 ml micro-centrifuge tube for subsequent DNA extraction. Genomic DNA was extracted using Forensic DNA Kit (D3591-01, OMEGA bio-tek), following the manufacturer's instructions. The loci LSU, ITS, *β-tub* and *rpb2* were amplified using primers LR0R/LR5 (Vilgalys and Hester 1990; Rehner and Samuels 1994), ITS5/ITS4 (White et al. 1990; Ward and Adams 1998), BT-2a/BT-2b (Glass and Donaldson 1995) and fRPB2-5F/fRPB2-7cR (Liu et al. 1999; Sung et al. 2007) respectively. Polymerase Chain Reactions (PCR) were conducted in an Applied Biosystems C1000 Touch™ Thermal Cycler with the following PCR conditions for LSU, ITS, *β-tub* and *rpb2* regions: initial denaturation at 95 °C for 3 min followed by 34 cycles of denaturation at 95 °C for 30 s and 30 s of annealing and elongation at 72 °C for 1 min, and a final extension at 72 °C for 10 min. The annealing temperatures were 52 °C for LSU and 58 °C for ITS, *β-tub* and *rpb2*. The PCR reaction mixture, 25 µL in final volume, was composed of 0.3 µL of TaKaRa Ex-Taq DNA polymerase (TaKaRa, China), 2.5 µL of 10x Ex-Taq buffer (TaKaRa, China), 3.0 µL (2.5 µM) of dNTPs (TaKaRa, China), 1 µL of genomic DNA, 1 µL (0.4 µM) of each primer, and 16.2 µL of double-distilled H_2O. Sequencing of PCR products was carried out with the

same primers as mentioned above at the Beijing Biomed Gene Technology Co., Ltd, and Sangon Biotech, Shanghai China. The newly generated sequences were deposited in GenBank (Table 1).

Phylogenetic analyses

Newly generated sequences from LSU, ITS, *β-tub* and *rpb2* during this study (Table 1) were analyzed with other sequences obtained from GenBank along with recently published relevant phylogenies (Wanasinghe et al. 2018; Liu et al. 2019). Sequences for each locus (LSU, ITS, *β-tub* and *rpb2*) were aligned using MAFFT V.7.036 (http://mafft.cbrc.jp/alignment/server/; Katoh et al. 2019), with L-INS-i Iterative refinement methods and manually improved when necessary in BioEdit v. 7.0 (Hall 2004). Phylogenetic analyses of the aligned data were based on maximum likelihood (ML) and Bayesian inference (BI) analyses with details as outlined by Tang et al. (2007, 2009).

RAxML-HPC2 on XSEDE (v. 8.2.8) (Stamatakis et al. 2008; Stamatakis 2014) in the CIPRES Science Gateway platform (Miller et al. 2010) was used to generate the ML trees. Optimal ML tree search was conducted with 1000 separate runs, using the default algorithm of the program from a random starting tree for each run. The ultimate tree was selected among suboptimal trees from each run by comparing likelihood scores under the GTRGAMMA substitution model.

Bayesian analysis was executed in MrBayes v. 3. 1. 2 (Huelsenbeck and Ronquist 2001) through Markov Chain Monte Carlo (MCMC) sampling to calculate the posterior probabilities (PP) (Rannala and Yang 1996; Zhaxybayeva and Gogarten 2002). Partitioning of data was initially done by locus and then the parameters of the nucleotide substitution models for every partition were selected independently using MrModeltest v. 2.3 (Nylander 2004). Six Markov chains were run in parallel for 5M generations with trees being sampled every 1000th generation. The distribution of log-likelihood scores was examined to determine the stationary phase for each search and to decide whether additional runs were required to reach convergence, using the program Tracer 1.5 (Rambaut and Drummond 2007). Convergence was declared when the average standard deviation of split frequencies at the end of the total MCMC generations was at 0.01. First 20% of generated trees was discarded as burn-in and the remaining 80% was used to calculate PP of the majority rule consensus tree (Dissanayake et al. 2020). The resulting trees were viewed in FigTree v. 1.4.0 (Rambaut 2012) and annotated in Microsoft PowerPoint (2013). The final alignment was registered in TreeBASE under the submission ID: 27601.

Results

Phylogenetic analyses

The combined gene dataset (LSU, ITS, *β-tub* and *rpb2*) used to generate ML tree in Fig. 1 comprised 51 taxa including the newly generated sequences. *Pestalotiopsis hollandica* (CBS

Table 1. Taxa used in the phylogenetic analyses and corresponding GenBank accession numbers.

Taxa	Strain number	GenBank accession numbers			
		LSU	ITS	*β-tub*	*rpb2*
Discosia artocreas	CBS 124848^{T}	MH554213	MH553994	MH554662	MH554903
Discosia aff. *brasiliensis*	NRBC 104198	AB593706	AB594774	N/A	N/A
Discosia brasiliensis	MFLUCC 12-0429 = NTCL094-2	KF827436	KF827432	KF827469	KF827473
	MFLUCC 12-0431 = NTCL095	KF827437	KF827433	KF827470	KF827474
	MFLUCC 12-0435 = NTCL097-2	KF827438	KF827434	KF827471	KF827475
Discosia fagi	MFLU 14-0299A =IT-722A^{T}	KM678048	KM678040	N/A	N/A
	MFLU14-0299B = IT-722B	KM678047	KM678039	N/A	N/A
Discosia italica	MFLU 14-0298A = IT-712A^{T}	KM678045	KM678042	N/A	N/A
	MFLU 14-0298B = IT-712B	KM678046	KM678043	N/A	N/A
	MFLU14-0298C = IT-712C	KM678044	KM678041	N/A	N/A
Discosia macrozamiae	CPC 32109	MH327856	MH327820	MH327895	N/A
Discosia neofraxinea	MFLUCC 12-0670 = NTIT469	KF827439	KF827435	KF827472	KF827476
	MFLU 15-0375^{T}	KR072672	KR072673	N/A	N/A
Discosia pini	MAFF 410149	AB593708	AB594776	AB594174	N/A
Discosia aff. *pleurochaeta*	KT2192 = MAFF 242782	AB593714	AB594782	AB594180	N/A
	KT2179 = MAFF 242778	AB593709	AB594777	AB594175	N/A
	KT2188 = MAFF 242779	AB593713	AB594781	AB594179	N/A
Discosia pseudoartocreas	CBS 136438^{T}	KF777214	KF777161	MH554672	MH554913
Discosia querci	MFLUCC 16-0642^{T}	MG815830	MG815829	N/A	N/A
Discosia ravennica	**MFLU 18-0131^{T}**	**MT376617**	**MT376615**	**MT393594**	**MW468059**
Discosia rubi	CBS 143893^{T}	MH554334	MH554131	MH554804	MH555038
Discosia tricellularis	MAFF 237478	AB593730	AB594798	AB594189	N/A
Discosia tricellularis	NBRC 32705^{T}	AB593728	AB594796	AB594188	N/A
Discosia yakushimensis	MAFF 242774 = NBRC 104194^{T}	AB594796	AB594789	AB594187	N/A
Pestalotiopsis hollandica	CBS 265.33^{T}	AB594188	KM199328	KM199388	MH554936
Pseudopestalotiopsis cocos	CBS 272.29^{T}		NR_145246	KM199467	MH554938
Sporocadus biseptatus	CBS 110324 = MYC 754^{T}	MH554179	MH553956	MH554615	MH554853
Sporocadus cornicola	CBS 143889 = CPC 23235	MH554326	MH554121	MH554794	MH555029
	MFLUCC 14-0448^{T}	N/A	KU974967	N/A	N/A
Sporocadus cotini	CBS 139966 = MFLUCC 14-0623^{T}	MH554222	MH554003	MH554675	MH554916
Sporocadus incanus	CBS 123003^{T}	MH554210	MH553991	MH554659	MH554900
Sporocadus lichenicola	CBS 354.90 = NBRC 32677	MH554252	MH554035	MH554711	MH554948
	CPC 24528	MH554332	MH554127	MH554800	MH555036
	NBRC 32625 = IMI 079706^{T}	MH883646	MH883643	MH883645	MH883647
Sporocadus mali	CBS 446.70^{T}	MH554261	MH554049	MH554725	MH554960
Sporocadus microcyclus	CBS 424.95^{T}	MH554258	MH554045	MH554721	MH554956
	CBS 887.68 = NBRC 32680	MH554280	MH554068	MH554744	MH554981
Sporocadus multiseptatus	CBS 143899 = CPC 26606^{T}	MH554343	MH554141	MH554814	MH555047
Sporocadus rosarum	CBS 113832 = UPSC 2172	MH554189	MH553970	MH554629	MH554864
Sporocadus rosigena	CBS 116498	MH554200	MH553983	MH554642	MH554883
	CBS 129166 = MSCL 860	MH554215	MH553996	MH554665	MH554905
	CBS 182.50	MH554233	MH554013	MH554689	MH554926
	CBS 250.49	MH554245	MH554023	MH554699	MH554934
	CBS 466.96	MH554265	MH554052	MH554728	MH554965
	MFLU 16-0239^{T}	MG829069	MG828958	N/A	N/A
Sporocadus rosigena	**MFLUCC 18-0387**	**MT376616**	**MT376614**	**MT393595**	**N/A**
Sporocadus rotundatus	CBS 616.83^{T}	MH554273	MH554060	MH554737	MH554974

Taxa	Strain number	GenBank accession numbers			
		LSU	ITS	*β-tub*	*rpb2*
Sporocadus sorbi	MFLUCC 14-0469^{T}	KT281911	KT284774	N/A	N/A
	CBS 160.25	MH554229	MH554008	MH554684	MH554924
Sporocadus sp.	CBS 506.71	MH554268	MH554055	MH554731	MH554968
Sporocadus trimorphus	CBS 114203 = UPSC 2430^{T}	MH554196	MH553977	MH554636	MH554876

Abbreviations: **CBS**: Culture collection of the Westerdijk Fungal Biodiversity Institute, Utrecht, The Netherlands, **CPC**: Culture collection of Pedro Crous, housed at the Westerdijk Institute, **IMI**: International Mycological Institute, CABI-Bioscience, Egham, Bakeham Lane, United Kingdom, **MAFF**: Ministry of Agriculture, Forestry and Fisheries, Tsukuba, Ibaraki, Japan, **MFLU**: Mae Fah Luang University, Chiang Rai, Thailand, **MFLUCC**: Mae Fah Luang University Culture Collection, Chiang Rai, Thailand, **MSCL**: Microbial Strain Collection of Latvia, **NBRC**: Biological Resource Center, **UPSC**: Uppsala University Culture Collection of Fungi, Sweden. Types, ex-types and authentic strains are indicated with T. Newly generated sequences in this study are indicated in bold. "N/A" sequence is unavailable.

265.33) and *Pseudopestalotiopsis cocos* (CBS 272.29) were selected as outgroup. The ML tree topology was similar to the one of the BI consensus tree. The best scoring RAxML tree with final optimization had a likelihood value of -15179.071239. The matrix had 1020 distinct alignment patterns, with 24.74% of gaps and completely undetermined characters. Estimated base frequencies were as follows: A= 0.247496, C= 0.245307, G= 0.252993, T= 0.254204, with substitution rates AC= 1.621276, AG= 6.173475, AT= 1.526832, CG= 1.406021, CT= 9.022198, GT= 1.000000; gamma distribution shape parameter α= 0.158554 and Tree-length = 1.305620.

Discosia taxa were divided into two separate clades (A and B). Clade A, consisting of 3 strains of *Discosia*, grouped with and was sister to *Sporocadus* with strong statistical support (100% ML, 1.00 PP). Clade B, comprising 21 strains of *Discosia*, was basal to both *Sporocadus* and clade A with strong statistical support (100% ML, 1.00 PP). Our strain MFLU 18-0131 was positioned in clade A, basal to both strains of *D. neofraxinea* (MFLU 15-0375 and MFLUCC 12-0670 = NTIT469), forming an independent lineage with good statistical support (96% ML/ 1.00 PP).

All the *Sporocadus* species formed a monophyletic clade with strong statistical support (100% ML, 1.00 PP). The strain MFLUCC 18-0387 from this study clustered with the other existing *S. rosigena* strains with a bootstrap support of 91% ML and 0.98 PP (Fig. 1).

Taxonomy

Discosia ravennica **Bundhun, Jeewon, Camporesi, J.C. Kang & K.D. Hyde, sp. nov.**
MycoBank No: 837963
Facesoffungi Number: FoF07929
Figure 2

Etymology. The specific epithet *ravennica* refers to the province of Ravenna, where the fungus was collected.

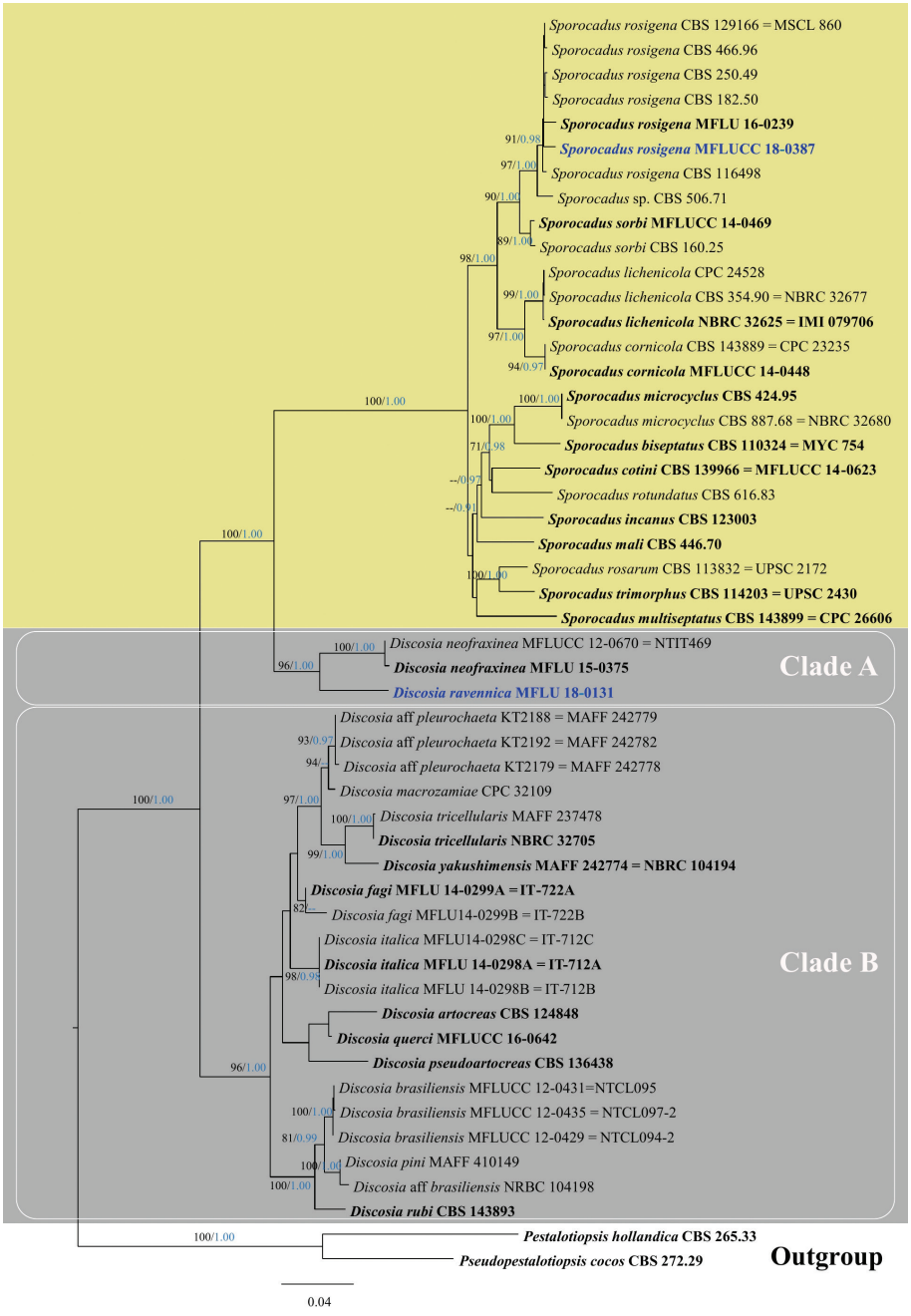

Figure 1. Phylogram generated from maximum likelihood (RAxML) based on analysis of a combined dataset of LSU, ITS, *β-tub* and *rpb2* sequence data. Bootstrap support values for ML equal to or greater than 70% (black) and Bayesian posterior probabilities (PP) equal to or greater than 0.90 (blue) are defined as ML/PP above or below the nodes. Type collections are in bold while the newly generated sequences are in blue bold type. The tree is rooted to *Pestalotiopsis hollandica* (CBS 265.33) and *Pseudopestalotiopsis cocos* (CBS 272.29). The scale bar represents the expected number of nucleotide substitutions per site.

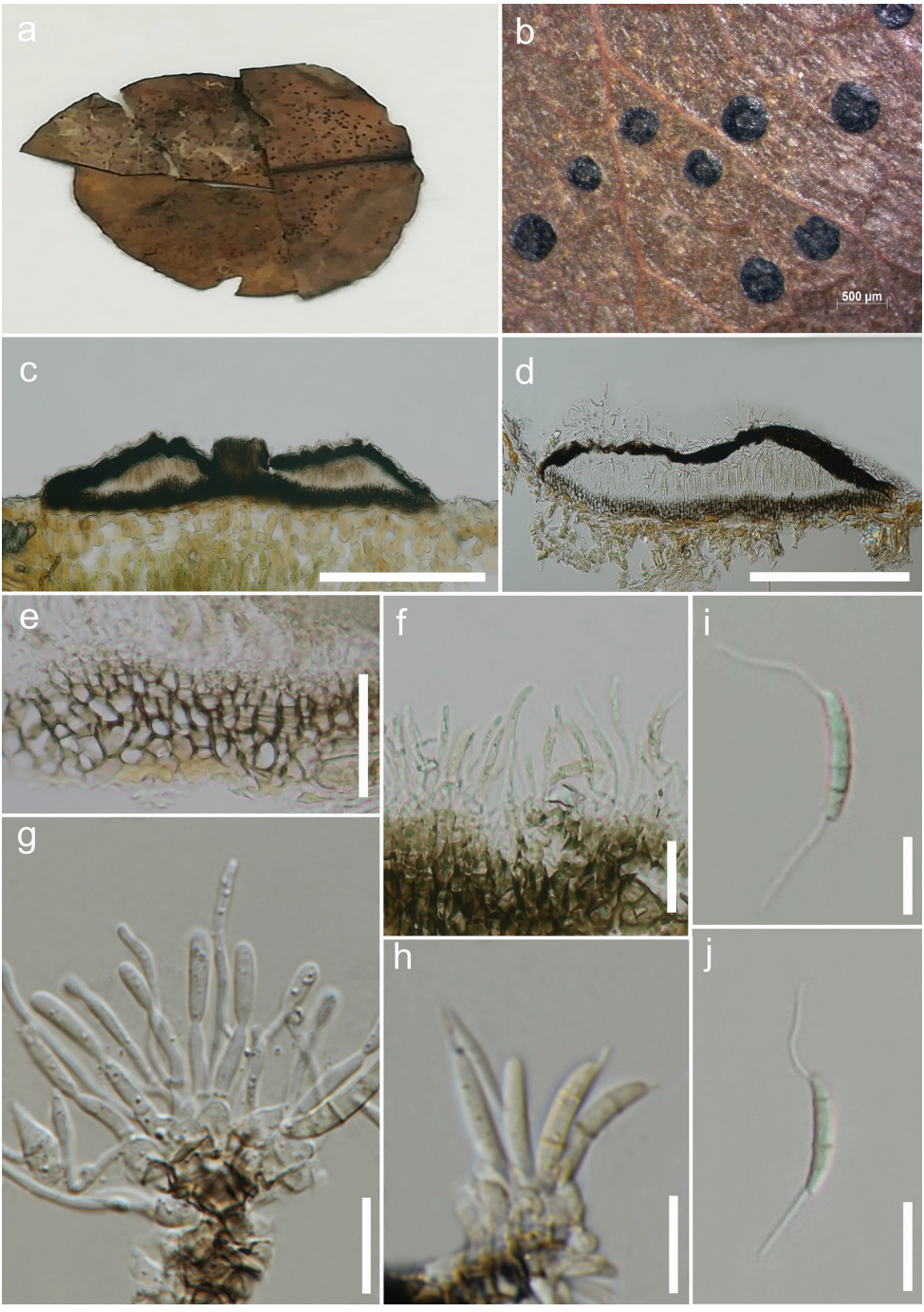

Figure 2. *Discosia ravennica* (MFLU 18-0131, holotype) **a** Herbarium specimen **b** Conidiomata on the host **c, d** Vertical sections of conidiomata **e** Conidioma wall at the base **f–h** Conidiogenous cells and developing conidia **i, j** Conidia. Scale bars: 500 µm (**b**); 200 µm (**c, d**); 10 µm (**e, g–j**); 20 µm (**f**).

Holotype. MFLU 18-0131

Description. *Saprobic* on leaves of *Pyrus* sp. ***Sexual morph*:** Undetermined. ***Asexual morph***: *Conidiomata* 45–70 µm high, 410–800 µm diam., stromatic, scattered to gregarious, superficial, rounded to unevenly outlined with complete margins, applanate, unilocular to bilocular, rugose, not glabrous, dull black, ostiolate. *Ostiole* 50–90 µm diam., circular to oval, opening to the exterior, central. *Conidiomatal wall* 10–20 µm thick at the base, dark brown in the outermost layer, comprising thick-walled cells of *textura angularis*, gradually becoming pale towards the inner layer; 10–20 µm thick near the apex, dark brown to black, made up of thick-walled cells of *textura epidermoidea*; interlocular wall composed of dark brown thick-walled cells of *textura prismatica*, becoming thin-walled and paler towards the outer layers. *Conidiophores* up to 40 µm high, originating from the innermost layer cells of the basal stroma, unbranched or at times branched, mostly 0–1-septate, rarely 2-septate or reduced to conidiogenous cells, cylindrical, hyaline, smooth. *Conidiogenous cells* 8–30 × 0.7–1.5 µm ($\overline{x}$ = 14.3 × 1.1 µm, n = 15), subcylindrical to elongate-ampuliform, hyaline, smooth-walled, holoblastic. *Conidia* 12–16 × 1.5–3 µm ($\overline{x}$ = 13.8 × 2.3 µm, n = 40) naviculate, to subcylindrical, narrow towards the base, straight or faintly curved, euseptate, mostly 3-septate, occasionally 2-septate, with septa thicker and darker than the periclinal wall, with cells unequal, hyaline to sub-hyaline, smooth-walled, without constriction at septa, bearing appendages on both apical and basal cells; basal cell 3–6 µm ($\overline{x}$ = 3.8 µm) long, narrowly obconic, with truncate base bearing a conspicuous dehiscence scar; 2 median cells, together 6–10 µm ($\overline{x}$ = 7.4 µm) long [second cell 4–6 µm ($\overline{x}$ = 5.0 µm) long, close to apical cell, almost twice the size of the third cell 2–4 µm ($\overline{x}$ = 3.0 µm) long, close to basal cell]; apical cell 3–5 µm ($\overline{x}$ = 3.6 µm) long, subconical with acute apex, hyaline at apex and sub-hyaline below; appendages tubular, faintly broad at the base, unbranched, flexuous; appendage on apical cell 5–17 µm ($\overline{x}$ = 10.1 µm) long, single, polar; appendage on basal cell 4–17 µm ($\overline{x}$ = 9.4 µm) long, single, inserted slightly above conidium base.

Material examined. ITALY. Province of Ravenna [RA], Oriolo dei Fichi– Faenza; on dead land leaves of *Pyrus* sp.; 24 Dec. 2017; Erio Camporesi; IT 3632 (MFLU 18-0131, ***holotype***; HKAS 104973, isotype).

Notes. In the present study, no culture could be obtained for *D. ravennica* despite several trials on various media including MEA, potato dextrose agar, corn meal agar or water agar at different incubation conditions, the reason for which the species was subjected to direct DNA extraction from conidiomata. *Discosia ravennica* is morphologically similar to *D. neofraxinea* in terms of superficial conidiomata, which are not glabrous and 3-septate conidia with cells of unequal length. It also closely resembles *D. fraxinea* (Schwein.) Nag Raj (1993) in having uni-to bi-locular applanate conidiomata and naviculate to subcylindrical 3-septate conidia with cells of unequal length. The new species, however, also differs from the latter two species as mentioned in Table 2.

Table 2. Features distinguishing *Discosia ravennica*, *D. fraxinea* and *D. neofraxinea*.

Features	***Discosia ravennica*** **(this study)**	***Discosia fraxinea*** **(Nag Raj 1993)**	***Discosia neofraxinea*** **(Senanayake et al. 2015)**
Host occurrence	Leaves of *Pyrus* sp.	*Amelanchier vulgaris, Crataegus* sp., *Fraxinus americana*, *Populus* sp., *Sorbus americana* and undetermined leaves	Leaves of *Fagus sylvatica*
Known distribution	Italy	Austria, France, Germany, U.S.A.	Italy
Conidiomata	Superficial	Erumpent	Superficial
Basal stroma	Composed of cells of *textura angularis*	Composed of cells of *textura prismatica*	Composed of cells of *textura prismatica*
Conidiogenous cells	8–30 × 0.7–1.5 µm Subcylindrical to elongate-ampuliform	7–40 × 1.5–2.5 µm Subcylindrical to langeniform or ampuliform	6–40 × 1–2 µm Cylindrical
Conidia	12–16 × 1.5–3 µm ($\overline{x}$ = 13.8 × 2.3 µm)	12.5–19 × 2.5–3.5 µm ($\overline{x}$ = 16.2 × 3 µm)	15–18 × 2.5–3.5 µm ($\overline{x}$ = 16 × 3 µm)

Sporocadus rosigena **F. Liu, L. Cai & Crous, in Liu, Bonthond, Groenewald, Cai & Crous, Stud. Mycol. 92: 402 (2018)**

Facesoffungi number: FoF07930

Figure 3

≡ *Seimatosporium rosicola* Wanas., Goonas., Camporesi, & K.D. Hyde, in Wanasinghe et al., Fungal Diversity 193 (2018)

Description. *Saprobic* on *Quercus ilex* L. ***Sexual morph*****:** Illustrated in Wanasinghe et al. (2018). ***Asexual morph*****:** *Conidiomata* (on host) 115–145 µm diam., 70–130 µm high, acervular, solitary to aggregated, semi-immersed, black; (on MEA) 50–70 µm diam., acervular, solitary to aggregated, erumpent, black. *Conidiophores* (on MEA) cylindrical, branched, hyaline, smooth, up to 30 µm long. *Conidiogenous cells* (on MEA) 7–18 × 2–3 µm ($\overline{x}$ = 10.1 × 2.1 µm, n = 20) cylindrical, enteroblastic, annellidic, integrated or discrete, hyaline, determinate, smooth. *Conidia* (on MEA) 12–15 × (3–) 5–7 µm ($\overline{x}$ = 13.5 × 5.4 µm, n = 47), obovoid, ellipsoid, broad fusiform or subcylindrical, straight or curved, hyaline when immature, pale to moderate brown at maturity, with 3 transverse, thick, darker septa, rarely constricted at the septa, often obtuse at both ends, or well rounded, smooth-walled, no appendage or sheath; basal cell obconic with a truncate base, pale brown or hyaline, thin-walled, 1–2.5 µm long ($\overline{x}$ = 2 µm); two median cells doliiform, hyaline or pale brown, turning brown at maturity, together 5–7 µm long ($\overline{x}$ = 6.1 µm), second cell from the base 1–3 µm long ($\overline{x}$ = 2.5 µm), third cell from the base 1.4–4 µm long ($\overline{x}$ = 2.6 µm); apical cell conical with obtuse or rounded apex, concolorous with the median cells, 1.8–3.5 µm long ($\overline{x}$ = 2.5 µm).

Culture characteristics. Colonies on MEA reaching 2–3 cm diam. after 11 days at 18 °C in darkness, filamentous, circular, flat with entire margin, white from above, reverse pale yellow.

Material examined. ITALY. Province of Forlì-Cesena, Fiumana di Predappio; on dead land leaf of *Quercus ilex* L. (Fagaceae); 20 Nov. 2017; Erio Camporesi; IT 3569 (MFLU 17-2803); living culture MFLUCC 18-0387.

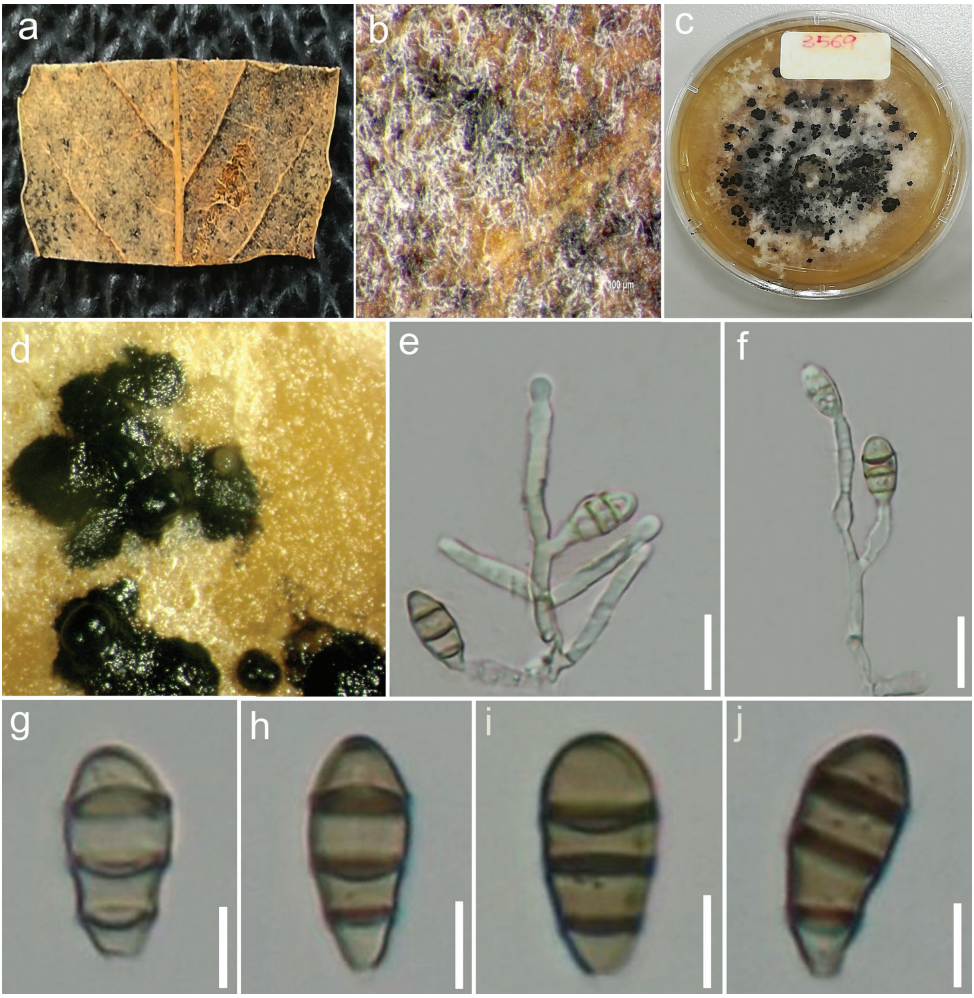

Figure 3. *Sporocadus rosigena* (MFLU 17-2803) **a** Leaf of *Quercus ilex* L **b** Close-up of conidiomata on host **c** Upper view of colony on MEA **d** Conidiomata in culture (MFLUCC 18-0387) **e, f** Different stages of conidiogenesis (MFLUCC 18-0387) **g–j** Conidia (MFLUCC 18-0387). Scale bars: 10 μm (**e, f**); 5 μm (**g–j**).

Notes. *Sporocadus rosigena* from the present study shares similar morphology with the other *S. rosigena* strains in having almost obovoid, ellipsoid or fusiform to subcylindrical conidia (Wanasinghe et al. 2018; Liu et al. 2019). Pairwise comparison of DNA sequence data of the isolate MFLUCC 18-0387 with the other strains of *S. rosigena* revealed very minor differences and thus, the strain MFLUCC 18-0387 is considered as *S. rosigena*.

Discussion

Discosia ravennica sp. nov. forms an independent lineage, basal to the two strains of *D. neofraxinea* (96% ML/ 1.00 PP) (Fig. 1). It is different from *D. neofraxinea* in its unilocular to bilocular, applanate conidiomata along with elongate-ampulliform conidiogenous cells and conidia smaller in size (Table 2). With regard to DNA sequence data comparison, *D. ravennica* differs from both strains of *D. neofraxinea* (MFLU 15-0375 and MFLUCC 12-0670 = NTIT469) in having 14 out of 531 (2.6 %) and 8 out of 512 (1.6%) different base pairs (bp) in the ITS alignments respectively. Moreover, 13 bp out of 229 (5.7%) and 82 bp out of 832 (9.9%) differences in the *ß-tub* and *rpb2* alignments respectively can be observed between *D. ravennica* and *D. neofraxinea* (MFLUCC 12-0670 = NTIT469). Sequence data of *ß-tub* and *rpb2* are not available for the strain of *D. neofraxinea* (MFLU 15-0375) in GenBank and hence could not be compared. Similarly, no molecular data for *D. fraxinea* are accessible in GenBank, following which the new species, *D. ravennica*, has been delineated based on morphology (Table 2). The 5.7% and 9.9% differences in nucleotides in *ß-tub* and *rpb2* respectively may acceptably support the establishment of a new species (Jeewon and Hyde 2016). Following this assumption along with the above-mentioned morphological differences and high statistical support, *D. ravennica* is herein established as a new species.

A peculiar finding from our DNA sequence analyses is the placement of *D. neofraxinea* and *D. ravennica*. Both of them constitute a strongly supported independent clade (clade A) basal to species of *Sporocadus*. One might argue that given their distinct phylogenetic nature, a new genus accommodating these two species might be a possibility. However, in this particular scenario, we would rather take a more conservative and lumping taxonomic approach and maintain the latter two species in *Discosia*. The reasons we would advocate are that there is a lot of morphological resemblance between members of clades A and B. For instance, when we compare *D. neofraxinea* and *D. ravennica* (clade A) with the type species, *D. artocreas* (clade B), they all have stromatic conidiomata, conidiophores which arise from the upper cell layer of the basal stroma, and hyaline to sub-hyaline, usually 3-septate conidia bearing two appendages (Nag Raj 1993; Senanayake et al. 2015; Liu et al. 2019). The main difference is that *D. neofraxinea* and *D. ravennica* have the third cell of their conidia from the base longer than the second cell while *D. artocreas* has the second cell of its conidia from the base longer than the third cell (Nag Raj 1993) or both median cells of almost equal length (Liu et al. 2019). However, this distinctive characteristic is not sufficient enough for the establishment of a new genus. It might be that the genus is paraphyletic, but until more species are recovered and analyzed to provide further taxonomic insights, we refrain from making any taxonomic amendments. It might also be possible that there is a need to establish species complexes given the wide intraspecies variation as we have seen in other genera such as *Phyllosticta* (Norphanphoun et al. 2020).

The second recovered species from this study, *Sporocadus rosigena*, clusters with other *S. rosigena* strains in a well-supported clade (91% ML / 0.98 PP) in our 4-gene phylogeny (Fig. 1). The latter shows similar topology to the 5-gene phylogeny reported

by Liu et al. (2019). *Sporocadus rosigena* has earlier been reported as saprobic or endophytic on species of *Rosa*, *Rubus*, *Pyrus* (Rosaceae), *Rhododendron* (Ericaceae) and *Vitis* (Vitaceae) (Wanasinghe et al. 2018; Liu et al. 2019). In this study, the species was found from *Quercus ilex* (Fagaceae) and is therefore introduced as a new host record. Different fungi have equally been reported from *Quercus ilex* in Italy; for instance, the genera *Alternaria* (Lunghini et al. 2013), *Beltrania* (Pirozynski 1963), *Endothia* (Spaulding 1961), *Monochaetia* (Nag Raj 1993), *Neognomoniopsis* (Crous et al. 2019), *Pestalotia* (Nag Raj 1993), *Xylaria* and *Zygosporium* (Lunghini et al. 2013), indicating a broad diversity of fungi on the same host. All *Sporocadus* species in their asexual stage possess 3-septate, obovoid, fusoid to cylindrical conidia, which do not have any appendage. The only exceptions are *S. trimorphus* and *S. rosarum*, which are known to produce conidia both with and without appendages (Liu et al. 2019).

Fungal diversity and classification are always ever-changing and require an ongoing assessment (Hyde and Soytong 2008; Jeewon et al. 2017). This becomes especially essential in cases where taxa are described from genera which usually accommodate pathogens. *Discosia*, for instance, is known to comprise the plant pathogen *D. yakushimensis* which causes leaf spots on plants such as *Symplocos prunifolia* (Tanaka et al. 2011). Identifying novel species in a genus may also potentially imply the discovery of emerging pathogens which can cause damage to crops of economic importance (Jayawardena et al. 2019a, 2019b). Evolutionary relationships and ecological roles of fungi have been reported to be intricately linked to the emergence of new species (Zhang et al. 2008; Hyde et al. 2020). However, such phenomena also extend to the recognition of existing species from new hosts, as is the case for *S. rosigena* in the present study. Documenting records from new hosts has become useful repertoires for mycologists who aim to understand evolution of fungi, host jumping, expanding host diversity and adaptations to different environmental conditions (Hyde et al. 2020). These are equally important for proper quarantine measures, whereby potential pathogens or species known to have a wide host diversity are to be closely monitored with a view to avoid unintentional disturbance to a specific environment (Cai et al. 2011).

Acknowledgements

This work was funded by grants of the National Natural Science Foundation of China (NSFC Grants Nos. 31670027 & 31460011) and the Open Research Foundation of the Key Laboratory (Engineering Center) of National Education Ministry at Guizhou University (Grant no. GZUKEY 20160705). Mae Fah Luang University, the Center of Excellence in Fungal Research and the Mushroom Research Foundation, Thailand, are acknowledged for the support provided for research. Rajesh Jeewon is grateful to the University of Mauritius and Mae Fah Luang University for enabling research collaboration. Digvijayini Bundhun thanks Yuanpin Xiao, RS Jayawardena and CS Bhunjun for their help and suggestions. All authors thank Shaun Pennycook for checking the nomenclature of the new taxon.

References

Barber PA, Crous PW, Groenewald JZ, Pascoe IG, Keane P (2011) Reassessing *Vermisporium* (Amphisphaeriaceae), a genus of foliar pathogens of eucalypts. Persoonia 27: 90–118. https://doi.org/10.3767/003158511X617381

Brockmann I (1976) Untersuchungen über die Gattung *Discostroma* Clements (Ascomycetes). Sydowia 28: 275–338.

Cai L, Giraud T, Zhang N, Begerow D, Cai GH, Shivas RG (2011) The evolution of species concepts and species recognition criteria in plant pathogenic fungi. Fungal Diversity 50: 121–133. https://doi.org/10.1007/s13225-011-0127-8

Corda AC (1839) Icones fungorum hucusque cognitorum 3: 1–55.

Crous PW, Wingfield MJ, Guarro J, Cheewangkoon R, van der Bank M, Swart WJ, Stchigel AM, Cano-Lira JF, Roux J, Madrid H, Damm U, Wood AR, Shuttleworth LA, Hodges CS, Munster M, de Jesús Yáñez-Morales M, Zúñiga-Estrada L, Cruywagen EM, de Hoog GS, Silvera C, Najafzadeh J, Davison EM, Davison PJN, Barrett MD, Barrett RL, Manamgoda DS, Minnis AM, Kleczewski NM, Flory SL, Castlebury LA, Clay K, Hyde KD, Maússe-Sitoe SND, Chen S, Lechat C, Hairaud M, Lesage-Meessen L, Pawłowska J, Wilk M, Sliwińska-Wyrzychowska A, Mętrak M, Wrzosek M, Pavlic-Zupanc D, Maleme HM, Slippers B, Mac Cormack WP, Archuby DI, Grünwald NJ, Tellería MT, Dueñas M, Martín MP, Marincowitz S, de Beer ZW, Perez CA, Gené J, Marin-Felix Y, Groenewald JZ (2013) Fungal Planet description sheets: 154–213. Persoonia 31: 188–296. https://doi.org/10.3767/003158513X675925

Crous PW, Carnegie AJ, Wingfield MJ, Sharma R, Mughini G, Noordeloos ME, Santini A, Shouche YS, Bezerra JDP, Dima B, Guarnaccia V, Imrefi I, Jurjević Ž, Knapp DG, Kovács GM, Magistà D, Perrone G, Rämä T, Rebriev YA, Shivas RG, Singh SM, Souza-Motta CM, Thangavel R, Adhapure NN, Alexandrova AV, Alfenas AC, Alfenas RF, Alvarado P, Alves AL, Andrade DA, Andrade JP, Barbosa RN, Barili A, Barnes CW, Baseia IG, Bellanger JM, Berlanas C, Bessette AE, Bessette AR, Biketova AY, Bomfim FS, Brandrud TE, Bransgrove K, Brito ACQ, CanoLira JF, Cantillo T, Cavalcanti AD, Cheewangkoon R, Chikowski RS, Conforto C, Cordeiro TRL, Craine JD, Cruz R, Damm U, de Oliveira RJV, de Souza JT, de Souza HG, Dearnaley JDW, Dimitrov RA, Dovana F, Erhard A, EsteveRaventós F, Félix CR, Ferisin G, Fernandes RA, Ferreira RJ, Ferro LO, Figueiredo CN, Frank JL, Freire KTLS, García D, Gené J, Gęsiorska A, Giberton TB, Gondra RAG, Gouliamova DE, Gramaje D, Guard F, Gusmão LFP, Haitook S, Hirooka Y, Houbraken J, Hubka V, Inamdar A, Iturriaga T, Iturrieta-González I, Jadan M, Jiang N, Justo A, Kachalkin AV, Kapitonov VI, Karadelev M, Karakehian J, Kasuya T, Kautmanová I, Kruse J, Kušan I, Kuznetsova TA, Landell MF, Larsson KH, Lee HB, Lima DX, Lira CRS, Machado AR, Madrid H, Magalhães OMC, Majerova H, Malysheva EF, Mapperson RR, Marbach PAS, Martín MP, Martín-Sanz A, Matočec N, McTaggart AR, Mello JF, Melo RFR, Mešić A, Michereff SJ, Miller AN, Minoshima A, Molinero-Ruiz L, Morozova OV, Mosoh D, Nabe M, Naik R, Nara K, Nascimento SS, Neves RP, Olariaga I, Oliveira RL, Oliveira TGL, Ono T, Ordoñez ME, Ottoni A de M, Paiva LM, Pancorbo F, Pant B, Pawłowska J, Peterson SW, Raudabaugh DB, Rodríguez-Andrade E, Rubio E, Rusevska K, Santiago

ALCMA, Santos ACS, Santos C, Sazanova NA, Shah S, Sharma J, Silva BDB, Siquier JL, Sonawane MS, Stchige AM, Svetasheva T, Tamakeaw N, Telleria MT, Tiago PV, Tian CM, Tkalčec Z, Tomashevskaya MA, Truong HH, Vecherskii MV, Visagie CM, Vizzini A, Yilmaz N, Zmitrovich IV, Zvyagina EA, Boekhout T, Kehlet T, Læssøe T, Groenewald JZ (2019) Fungal planet description sheets: 868–950. Persoonia 42: 291–473. https://doi.org/10.3767/persoonia.2019.42.11

Dissanayake AJ, Bhunjun CS, Maharachchikumbura SSN, Liu JK (2020) Applied aspects of methods to infer phylogenetic relationships amongst fungi. Mycosphere 11: 2652–2676. https://doi.org/10.5943/mycosphere/11/1/18

Dugan FM, Glawe DA, Attanayake RN, Chen W (2009) The importance of reporting new host-fungus records for ornamental and regional crops. Plant Health Progress 10: 34. https://doi.org/10.1094/PHP-2009-0512-01-RV

Fries EM (1849) Summa Vegetabilium Scandinaviae. Sectio posterior. Typographia Academica, Uppsala, 259–572.

Ghelardini L, Pepori AL, Luchi N, Capretti P, Santini A (2016) Drivers of emerging fungal diseases of forest trees. Forest Ecology and Management 381: 235–246. doi:10.1016/j.foreco.2016.09.032

Giraud T, Gladieux P, Gavrilets S (2010) Linking the emergence of fungal plant diseases with ecological speciation. Trends in Ecology & Evolution 25: 387–395. http://dx.doi.org/10.1016/j.tree.2010.03.006

Glass NL, Donaldson GC (1995) Development of primer sets designed for use with the PCR to amplify conserved genes from filamentous ascomycetes. Applied and Environmental Microbiology 61: 1323–1330. https://doi.org/10.1128/AEM.61.4.1323-1330.1995

Hall TA (2004) BioEdit Sequence Alignment Editor 7.0. 1. Carlsbad, CA, USA: Isis Pharmaceuticals.

Huelsenbeck JP, Ronquist F (2001) MRBAYES: Bayesian inference of phylogenetic trees. Bioinformatics 17: 754–755. https://doi.org/10.1093/bioinformatics/17.8.754

Hughes SJ (1958) Revisiones hyphomycetum aliquot cum appendice de nominibus rejiciendis. Canadian Journal of Botany 36: 727–836. https://doi.org/10.1139/b58-067

Hyde KD, Soytong K (2008) The fungal endophyte dilemma. Fungal Diversity 33: 163–173.

Hyde KD, de Silva NI, Jeewon R, Bhat DJ, Phookamsak R, Doilom M, Boonmee S, Jayawardena RS, Maharachchikumbura SSN, Senanayake IC, Manawasinghe IS, Liu NG, Abeywickrama PD, Chaiwan N, Karunarathna A, Pem D, Lin CG, Sysouphanthong P, Luo ZL, Wei DP, Wanasinghe DN, Norphanphoun C, Tennakoon DS, Samarakoon MC, Jayasiri SC, Jiang HB, Zeng XY, Li JF, Wijesinghe SN, Devadatha B, Goonasekara ID, Brahmanage RS, Yang EF, Aluthmuhandiram JVS, Dayarathne MC, Marasinghe DS, Li WJ, Dissanayake LS, Dong W, Huanraluek N, Lumyong S, Liu JK, Karunarathna SC, Jones EBG, Al-Sadi AM, Xu JC, Harishchandra D, Sarma VV, Bulgakov T (2020) AJOM new records and collections of fungi: 1–100. Asian Journal of Mycology 3: 22–294. http://doi.org/10.5943/ajom/3/1/3

Jayasiri SC, Hyde KD, Ariyawansa HA, Bhat J, Buyck B, Cai L, Dai YC, Abd-Elsalam KA, Ertz D, Hidayat I, Jeewon R, Jones EBG, Bahkali AH, Karunarathna SC, Liu JK, Luangsa-ard JJ, Lumbsch HT, Maharachchikumbura SSN, McKenzie EHC, Moncalvo JM, Ghobad-

Nejhad M, Nilsson H, Pang KL, Pereira OL, Phillips AJL, Raspé O, Rollins AW, Romero AI, Etayo J, Selçuk F, Stephenson SL, Suetrong S, Taylor JE, Tsui CKM, Vizzini A, Abdel-Wahab MA, Wen TC, Boonmee S, Dai DQ, Daranagama DA, Dissanayake AJ, Ekanayaka AH, Fryar SC, Hongsanan S, Jayawardena RS, Li WJ, Perera RH, Phookamsak R, de Silva NI, Thambugala KM, Tian Q, Wijayawardene NN, Zhao RL, Zhao Q, Kang JC, Promputtha I (2015) The Faces of Fungi database: fungal names linked with morphology, phylogeny and human impacts. Fungal Diversity 74: 3–18. https://doi.org/10.1007/s13225-015-0351-8

Jayasiri SC, Hyde KD, Jones EBG, McKenzie EHC, Jeewon R, Phillips AJL, Bhat DJ, Wanasinghe DN, Liu JK, Lu YZ, Kang JC, Xu J, Karunarathna SC (2019) Diversity, morphology and molecular phylogeny of Dothideomycetes on decaying wild seed pods and fruits. Mycosphere 10: 1–186. https://doi.org/10.5943/mycosphere/10/1/1

Jayawardena RS, Hyde KD, Jeewon R, Ghobad-Nejhad M, Wanasinghe DN, Liu NG, Phillips AJL, Oliveira-Filho JRC, da Silva GA, Gibertoni TB, Abeywikrama P, Carris LM, Chethana KWT, Dissanayake AJ, Hongsanan S, Jayasiri SC, McTaggart AR, Perera RH, Phutthacharoen K, Savchenko KG, Shivas RG, Thongklang N, Dong W, Wei D, Wijayawardena NN, Kang JC (2019a) One stop shop II: taxonomic update with molecular phylogeny for important phytopathogenic genera: 26–50. Fungal Diversity 94: 41–129. https://doi.org/10.1007/s13225-019-00418-5

Jayawardena RS, Hyde KD, McKenzie EH, Jeewon R, Phillips AJL, Perera RH, de Silva NI, Maharachchikumbura SSN, Samarakoon MC, Ekanayake AH, Tennakoon DS, Dissanayake AJ, Norphanphoun C, Lin C, Manawasinghe IS, Tian Q, Brahmanage R, Chomnunti P, Hongsanan S, Jayasiri SC, Halleen F, Bhunjun CS, Karunarathna A, Wang Y (2019b) One stop shop III: taxonomic update with molecular phylogeny for important phytopathogenic genera: 51–75. Fungal Diversity 98: 77–160. https://doi.org/10.1007/s13225-019-00433-6

Jayawardena RS, Hyde KD, Chen YJ, Papp V, Palla B, Papp D, Bhunjun CS, Hurdeal VG, Senwanna C, Manawasinghe IS, Harischandra DL, Gautam AK, Avasthi S, Chuankid B, Goonasekara ID, Hongsanan S, Zeng XY, Liyanage KK, Liu NG, Karunarathna A, Hapuarachchi KK, Luangharn T, Raspé O, Brahmanage R, Doilom M, Lee HB, Mei L, Jeewon R, Huanraluek N, Chaiwan N, Stadler M, Wang Y (2020) One stop shop IV: taxonomic update with molecular phylogeny for important phytopathogenic genera: 76–100 (2020). Fungal Diversity 103: 87–218. https://doi.org/10.1007/s13225-020-00460-8

Jeewon R, Hyde KD (2016) Establishing species boundaries and new taxa among fungi: recommendations to resolve taxonomic ambiguities. Mycosphere 7: 1669–1677. https://doi.org/10.5943/mycosphere/7/11/4

Jeewon R, Liew EC, Hyde KD (2002) Phylogenetic relationships of *Pestalotiopsis* and allied genera inferred from ribosomal DNA sequences and morphological characters. Molecular Phylogenetics and Evolution 25: 378–392. https://doi.org/10.1016/S1055-7903(02)00422-0

Jeewon R, Wanasinghe DN, Rampadaruth S, Puchooa D, Zhou LG, Liu AR, Wang HK (2017) Nomenclatural and identification pitfalls of endophytic mycota based on DNA sequence analyses of ribosomal and protein genes phylogenetic markers: A taxonomic dead end?. Mycosphere 8: 1802–1817. https://doi.org/10.5943/mycosphere/8/10/7

Katoh K, Rozewicki J, Yamada KD (2019) MAFFT online service: multiple sequence alignment, interactive sequence choice and visualization. Briefings in Bioinformatics 20: 1160–1166. https://doi.org/10.1093/bib/bbx108

Libert MA (1837) Plantae Cryptogamae, quas in Arduenna collegit. Fasc. 4: 301–400.

Liu F, Bonthond G, Groenewald JZ, Cai L, Crous PW (2019) Sporocadaceae, a family of coelomycetous fungi with appendage-bearing conidia. Studies in Mycology 92: 287–415. https://doi.org/10.1016/j.simyco.2018.11.001

Liu YJ, Whelen S, Hall BD (1999) Phylogenetic relationships among ascomycetes: evidence from an RNA polymerase II subunit. Molecular Biology and Evolution 16: 1799–1808. https://doi.org/10.1093/oxfordjournals.molbev.a026092

Lunghini D, Granito VM, Di Lonardo DP, Maggi O, Persiani AM (2013) Fungal diversity of saprotrophic litter fungi in a Mediterranean maquis environment. Mycologia 105: 1499–1515. https://doi.org/10.3852/13-103

Maharachchikumbura SSN, Hyde KD, Jones EBG, McKenzie EHC, Bhat JD, Dayarathne MC, Huang SK, Norphanphoun C, Senanayake IC, Perera RH, Jayawardena RS, Daranagama DA, Konta S, Goonasekara ID, Zhuang WY, Jeewon R, Phillips AJL, Abdel-Wahab MA, Al-Sadi AM, Bahkali AH, Boonmee S, Boonyuen N, Cheewangkoon R, Dissanayake AJ, Kang J, Li QR, Liu JK, Liu XZ, Liu ZY, Luangsa-ard JJ, Pang KL, Phookamsak R, Promputtha I, Suetrong S, Stadler M, Wen T, Wijayawardene NN (2016) Families of Sordariomycetes. Fungal Diversity 79: 1–317. https://doi.org/10.1007/s13225-016-0369-6

Miller MA, Pfeiffer W, Schwartz T (2010) Creating the CIPRES Science Gateway for inference of large phylogenetic trees. In: Gateway Computing Environments Workshop (GCE). Ieee, 1–8 pp. https://doi.org/10.1109/GCE.2010.5676129 [Accessed on 28 September 2020]

Morgan-Jones G (1964) Taxonomic and biological studies in the Coelomycetes. PhD thesis, Nottingham, United Kingdom: University of Nottingham.

Nag Raj TR (1993) Coelomycetous anamorphs with appendage-bearing conidia. Mycologue Publications, Waterloo, Canada, 1101 pp.

Norphanphoun C, Hongsanan S, Gentekaki E, Chen YJ, Kuo CH, Hyde KD (2020) Differentiation of species complexes in *Phyllosticta* enables better species resolution. Mycosphere 11: 2542–2628. https://doi.org/10.5943/mycosphere/11/1/16

Nylander JAA (2004) MrModeltest v2. Program distributed by the author. Evolutionary Biology Centre, Uppsala University.

Pirozynski KA (1963) *Beltrania* and related genera. Mycological Paper 90: 1–37.

Rambaut A (2012) FigTree v. 1.4. Molecular evolution, phylogenetics and epidemiology. Edinburgh, UK: University of Edinburgh, Institute of Evolutionary Biology. Available from: http://tree.bio.ed.ac.uk/software/figtree/ (Accessed on 30 September 2020).

Rambaut A, Drummond AJ (2007) Tracer v1, 4. Available from: http://beast.bio.ed.ac.uk/Tracer (Accessed on 10 October 2020).

Rannala B, Yang Z (1996) Probability distribution of molecular evolutionary trees: a new method of phylogenetic inference. Journal of Molecular Evolution 43: 304–311. https://doi.org/10.1007/BF02338839

Rehner SA, Samuels GJ (1994) Taxonomy and phylogeny of *Gliocladium* analysed from nuclear large subunit ribosomal DNA sequences. Mycological Research 98: 625–634. https://doi.org/10.1016/S0953-7562(09)80409-7

Rodeva R, Gabler J, Machowicz-Stefaniak Z, Kačergius A, Zimowska B, Zalewska E, Stoyanova Z (2016) CPL 1: New, emerging and re-emerging fungal diseases on medicinal and aromatic plants in European domain. Julius-Kühn-Archiv 453: 33–39.

Senanayake IC, Rathnayaka AR, Marasinghe DS, Calabon MS, Gentekaki E, Lee HB, Hurdeal VG, Pem D, Dissanayake LS, Wijesinghe SN, Bundhun D, Nguyen TT, Goonasekara ID, Abeywickrama PD,Bhunjun CS,Jayawardena RS, Wanasinghe DN,Jeewon R,Bhat DJ, Xiang MM (2020) Morphological approaches in studying fungi: collection, examination, isolation, sporulation and preservation. Mycosphere 11: 2678–2754. https://doi.org/10.5943/mycosphere/11/1/20

Senanayake IC, Maharachchikumbura SS, Hyde KD, Bhat JD, Jones EBG, McKenzie EH, Dai DQ, Daranagama DA, Dayarathne MC, Goonasekara ID, Konta S, Li WJ, Shang QJ, Stadler M, Wijayawardene NN, Xiao YP, Norphanphoun C, Li Q, Liu XZ, Bahkali AH, Kang JC, Wang Y, Wen TC, Wendt L, Xu JC, Camporesi E (2015) Towards unraveling relationships in Xylariomycetidae (Sordariomycetes). Fungal Diversity 73: 73–144. https://doi.org/10.1007/s13225-015-0340-y

Spaulding P (1961) Foreign Diseases of Forest Trees of the World. U.S.D.A. Agriculture Handbook 197: 1–361.

Stamatakis A (2014) RAxML version 8: a tool for phylogenetic analysis and post-analysis of large phylogenies. Bioinformatics 30: 1312–1313. https://doi.org/10.1093/bioinformatics/btu033

Stamatakis A, Hoover P, Rougement J (2008) A rapid bootstrap algorithm for the RAxML web servers. Systemic Biology 57: 758–771. https://doi.org/10.1080/10635150802429642

Subramanian CV, Reddy KRC (1974) The genus *Discosia*. I, Taxonomy. Kavaka 2: 57–89.

Sung GH, Sung JM, Hywel-Jones NL, Spatafora JW (2007) A multigene phylogeny of Clavicipitaceae (Ascomycota, Fungi): identification of localized incongruence using a combinational bootstrap approach. Molecular Phylogenetics and Evolution 44: 1204–1223. https://doi.org/10.1016/j.ympev.2007.03.011

Sutton BC (1975) Coelomycetes V. Coryneum. Mycological Papers 138: 1–224.

Sutton BC (1977) Coelomycetes. VI. Nomenclature of generic names proposed for coelomycetes. Mycological Papers 141: 1–253.

Sutton BC (1980) The Coelomycetes-Fungi imperfecti with pycnidia, acervuli and stromata. Commonwealth Mycological Institute, Kew, UK, 496 pp.

Tanaka K, Endo M, Hirayama K, Okane I, Hosoya T, Sato T (2011) Phylogeny of *Discosia* and *Seimatosporium*, and introduction of *Adisciso* and *Immersidiscosia* genera nova. Persoonia 26: 85–98. https://doi.org/10.3767/003158511X576666

Tang AM, Jeewon R, Hyde KD (2007) Phylogenetic utility of protein (RPB2, β-tubulin) and ribosomal (LSU, SSU) gene sequences in the systematics of Sordariomycetes (Ascomycota, Fungi). Antonie Van Leeuwenhoek. 91: 327. https://doi.org/10.1007/s10482-006-9120-8

Tang AM, Jeewon R, Hyde KD (2009) A re-evaluation of the evolutionary relationships within the Xylariaceae based on ribosomal and protein-coding gene sequences. Fungal Diversity 34: 127–155.

Vanev SG (1991) Species conception and sections delimitation of genus *Discosia*. Mycotaxon 41: 387–396.

Vanev SG (1992) Comparative morphological studies of *Discosia artocreas* and *Discosia faginea*. Mycotaxon XLIV: 461–470.

Vanev SG (1996) Fungi of the genus *Discosia* (Deuteromycotina) in the Mediterranean area. Bocconea 5: 351–357.

Vilgalys R, Hester M (1990) Rapid genetic identification and mapping of enzymatically amplified ribosomal DNA from several *Cryptococcus* species. Journal of Bacteriology 172: 4238–4246. https://doi.org/10.1128/JB.172.8.4238-4246.1990

Wanasinghe DN, Phukhamsakda C, Hyde KD, Jeewon R, Lee HB, Jones EBG, Tibpromma S, Tennakoon DS, Dissanayake AJ, Jayasiri SC, Gafforov Y, Camporesi E, Bulgakov TS, Ekanayake AH, Perera RH, Samarakoon MC, Goonasekara ID, Mapook A, Li WJ, Senanayake IC, Li J, Norphanphoun C, Doilom M, Bahkali AH, Xu J, Mortimer PE, Tibell L, Tibell S, Karunarathna SC (2018) Fungal diversity notes 709–839: taxonomic and phylogenetic contributions to fungal taxa with an emphasis on fungi on Rosaceae. Fungal Diversity 89: 1–236. https://doi.org/10.1007/s13225-018-0395-7

Ward E, Adams MJ (1998) Analysis of ribosomal DNA sequences of *Polymyxa* species and related fungi and the development of genus- and species-specific PCR primers. Mycological Ressearch 102: 965–974. https://doi.org/10.1017/S0953756297005881

White TJ, Bruns T, Lee SJ, Taylor JW (1990) Amplification and direct sequencing of fungal ribosomal RNA genes for phylogenetics. In PCR Protocols; Elsevier: Amsterdam, The Netherlands, 315–322. https://doi.org/10.1016/B978-0-12-372180-8.50042-1

Wijayawardene NN, Hyde KD, Wanasinghe DN, Papizadeh M, Goonasekara ID, Camporesi E, Bhat DJ, McKenzie EHC, Phillips AJL, Diederich P, Tanaka K, Li WJ, Tangthirasunun N, Phookamsak R, Dai DQ, Dissanayake AJ, Weerakoon G, Maharachchikumbura SSN, Hashimoto A, Matsumura M, Bahkali AH, Wang Y (2016) Taxonomy and phylogeny of dematiaceous coelomycetes. Fungal Diversity 77: 1–316. https://doi.org/10.1007/s13225-016-0360-2

Zhang Y, Jeewon R, Fournier J, Hyde KD (2008) Multi-gene phylogeny and morphotaxonomy of *Amniculicola lignicola*: novel freshwater fungus from France and its relationships to the Pleosporales. Mycological Research 112: 1186–1194. https://doi.org/10.1016/j.mycres.2008.04.004

Zhaxybayeva O, Gogarten JP (2002) Bootstrap, Bayesian probability and maximum likelihood mapping: exploring new tools for comparative genome analyses. BMC Genomics 3: 1–15. https://doi.org/10.1186/1471-2164-3-4